

General Disclaimer

One or more of the Following Statements may affect this Document

- This document has been reproduced from the best copy furnished by the organizational source. It is being released in the interest of making available as much information as possible.
- This document may contain data, which exceeds the sheet parameters. It was furnished in this condition by the organizational source and is the best copy available.
- This document may contain tone-on-tone or color graphs, charts and/or pictures, which have been reproduced in black and white.
- This document is paginated as submitted by the original source.
- Portions of this document are not fully legible due to the historical nature of some of the material. However, it is the best reproduction available from the original submission.



(NASA-CR-152427) RADAR SYSTEMS FOR THE
WATER RESOURCES MISSION. VOLUME 4:
APPENDICES E-I Final Report (Kansas Univ.
Center for Research, Inc.) 279 p
HC A13/MF A01

N77-16424

CSCI 08B G3/43 13294
Unclass

Radar Systems for the Water
Resources Mission - Final Report
RSL Technical Report 295-3
VOL. IV
Appendices E - I



THE UNIVERSITY OF KANSAS CENTER FOR RESEARCH, INC.

2291 Irving Hill Drive—Campus West Lawrence, Kansas 66045



THE UNIVERSITY OF KANSAS SPACE TECHNOLOGY CENTER
Raymond Nichols Hall

2291 Irving Hill Drive—Campus West Lawrence, Kansas 66045

Telephone:

RADAR SYSTEMS FOR THE WATER RESOURCES MISSION
FINAL REPORT

Remote Sensing Laboratory
RSL Technical Report 295-3
Volume IV
(same as Volume II, TR 291-2, "Radar Systems
for Near-Polar Observations - Final Study
Report," Contract NAS 5-22325).

R. K. Moore
J. P. Claassen
R. L. Erickson
R. K. T. Fong
B. C. Hanson
M. J. Koinen
S. B. McMillan
S. K. Parashar

June, 1976

Supported by:

NATIONAL AERONAUTICS AND SPACE ADMINISTRATION
Goddard Space Flight Center
Greenbelt, Maryland 20771

CONTRACT NAS 5-22384

Technical Monitor: Dr. James Shiue

CRES

REMOTE SENSING LABORATORY

VOLUME IV TABLE OF CONTENTS

- APPENDIX E, RSL TR 295-1, "A Short Study of a Scanning SAR for Hydrological Monitoring on a Global Basis," by John Claassen, (September, 1975).
- APPENDIX F, RSL TM 295-7, "Comb Filter Theory for Use in a Scanning Synthetic Aperture Radar Signal Processor (SCANSAR)," by Mark Komen (March, 1976).
- APPENDIX G, RSL TR 295-2, "Detailed System Design for the Scanning Synthetic-Aperture Radar (SCANSAR) Using Comb-Filter Range-Offset Processing," by Mark Komen, (July, 1976).
- APPENDIX H, RSL TM 295-2, "A Review of Swath-Widening Techniques," by Stan McMillan, (January, 1976).
- APPENDIX I, RSL TM 295-3, "Synthetic Aperture Radar and Digital Processing," by Stan McMillan, (September, 1975). [Discussion of Gerchberg correlation processor].
- APPENDIX J, RSL TM 295-4, "Methods to Vary Elevation Look Angle and Antenna Beam Pointing Requirements for Spacecraft SAR," by Richard K. T. Fong, (January, 1976).
- APPENDIX K, RSL TM 295-8, "Effects of Different Scan Angles on Ambiguity-Versus-Beamwidth Limitations for SCANSAR," by Richard K. T. Fong, (April, 1976).
- APPENDIX L, TM 295-9, "Focussed Synthetic Aperture Technique Using FFT," by Rod Erickson, (July, 1976, revised edition); 1st printing by Richard K. T. Fong (April, 1976).
- APPENDIX M, RSL TM 295-10, "Use of a Multi-Look Unfocussed SAR Processor on Spacecraft," by Richard K. T. Fong and Rodney L. Erickson, (June, 1976, revised edition); 1st printing by Fong (April, 1976).
- APPENDIX N, TM 291-8, "Development of Single-Sideband SAR Radar Technique," by Richard K. T. Fong, (May, 1976).

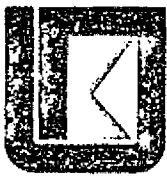
APPENDIX O, RSL TM 291-1, "State of the Art Radar System Parameters,"
by Rod Erickson, (August, 1975).

APPENDIX P, RSL TM 291-3, "State of the Art Integrated-Circuit Hardware
for Synthetic Aperture Radar Processing," by Rod Erickson,
(June, 1976, revised edition); 1st printing November, 1975.

APPENDIX Q, RSL TM 291-7, "Evaluation of the Fresnel Zone-Plate Processor
For Applications in Spaceborne Synthetic Aperture Radar,"
by Rod Erickson, (June, 1976).

APPENDIX R, RSL TM 295-12, "Hardware and Power Requirements of a SCANSAR
Correlation Processor," by Rod Erickson, (July, 1976).

APPENDIX E
RSL TECHNICAL REPORT 295-3
VOLUME IV



THE UNIVERSITY OF KANSAS SPACE TECHNOLOGY LABORATORIES

2291 Irving Hill Dr. — Campus West Lawrence, Kansas 66044

Telephone:

A SHORT STUDY OF A SCANNING SAR FOR HY-
DROLOGICAL MONITORING ON A GLOBAL
BASIS

John P. Claassen

RSL Technical Report 295-1
Remote Sensing Laboratory

September, 1975

Supported by:

NATIONAL AERONAUTICS AND SPACE ADMINISTRATION
Goddard Space Flight Center
Greenbelt, Maryland 20771

CONTRACT NAS 5-22384

ABSTRACT

The ambiguity problem in synthetic-aperture radars for spacecraft use constrains their application in usual form to relatively narrow swathwidths. Monitoring hydrological and other parameters that require frequent and timely observations indicates the need for much wider swath widths. In this report the use of a scanning antenna beam for a synthetic aperture system is examined as a solution to this problem. When the resolution required is modest, the radar need not use all the time the beam is passing a given point on the ground to build a synthetic aperture, so time is available to scan the beam to other positions and build several images at different ranges. The result is that the scanning synthetic-aperture radar (SCANSAR) can achieve swathwidths of well over 100 km with modest antenna size.

Design considerations for a SCANSAR for hydrologic parameter observation are presented here. Because of the high sensitivity to soil moisture at angles of incidence near vertical, a 7 to 22° swath is considered for that application. For snow and ice monitoring a 22 - 37° scan is used. Frequencies from X-band to L-band were used in the design studies, but the proposed system operates in C-band at 4.75 GHz. It achieves an azimuth resolution of about 50 meters at all angles, with a range resolution varying from 150 meters at 7° to 31 meters at 37° . The antenna requires an aperture of 3×4.16 meters, and the average transmitter power is under 2 watts.

The system uses recursive filters implemented with shift registers to achieve on-board processing. This serial approach seems quite feasible to implement with relatively simple state-of-the-art components in small enough quantity that their cost and power consumption will not be excessive. The result is an output that requires only about 4 megabits/second for telemetry.

Gray-scale resolution is not as good as required for the final analysis, but can be improved by combining cells on the ground.

A SHORT STUDY OF A SCANNING SAR FOR HYDROLOGICAL MONITORING ON A GLOBAL BASIS

John P. Claassen

I. Introduction

Intensive interest has recently been indicated in orbiting synthetic aperture radars (SARS) for various global applications. In some applications it is highly desirable to provide expansive coverage on each orbit. A casual examination of the theory indicates that coverage by a SAR is severely limited by the interaction between doppler and range ambiguities. Pulse coding schemes have been proposed to overcome the limitation. However, when high resolution is not necessary, it is conceivable that a radar can synthesize images over a wide swath by scanning to and dwelling on successive cross-track image cells as illustrated in Figure 1. An image is synthesized while the radar dwells on each cell. If the dwell time is sufficiently short (but not too short) and the angular scanning sufficiently rapid, continuous coverage on a wide swath can be realized.

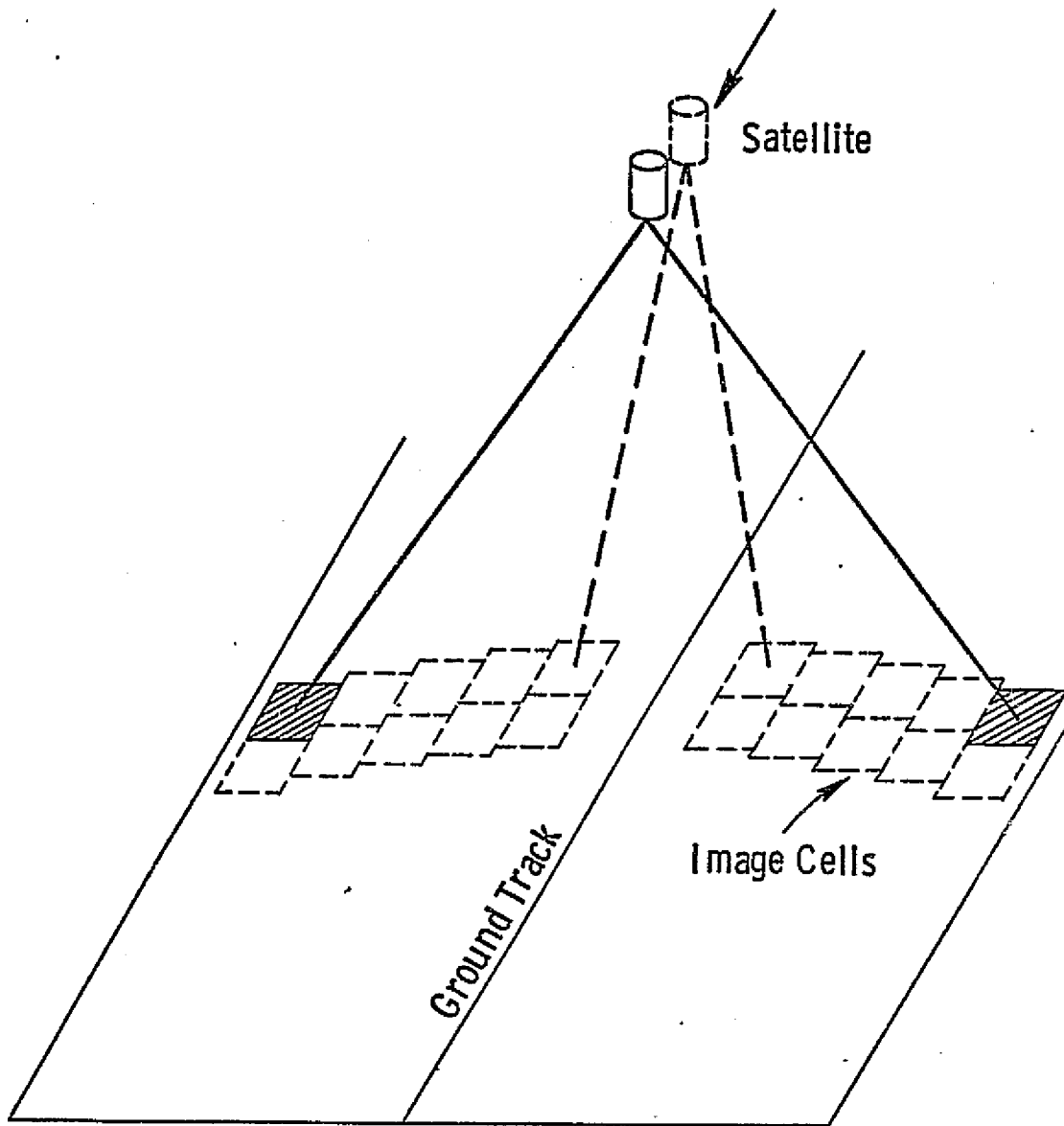
It is the objective of this report to demonstrate the feasibility of such a scanning SAR for a hydrological application requiring moderate resolution. In particular, the theory of a scanning SAR is developed. The theory was incorporated into a computer design program (SCANSAR) and several computer design cases suitable for monitoring soil moisture are reported. Additional design cases are archived in Appendix A while SCANSAR is documented in Appendix B.

On the basis of these design studies a scanning SAR system suitable for hydrological monitoring is proposed and described. A design objective in proposing the system was to realize a simple and relatively inexpensive SAR. A simple on-board processor is proposed. The relaxed resolution requirement and advancements in LSI electronic technology should enable one to realize a simple analog digital processor as proposed here to synthesize image elements on-board the spacecraft. The realization of an on-board processor reduces the required telemetry channel capacity and the ground based processing significantly.

II. System Theory and Design

A. Introduction

A synthetic aperture radar creates an image by preserving both the range and azimuthal histories as it linearly scans a scene. High azimuthal resolution images



Pictorial concept of a scanning SAR.

are achieved by tracking the Doppler (or phase) history of a target for the entire scan through the beam. To adequately preserve that Doppler record, the radar must sample returns from the target at a rate at least twice the Doppler bandwidth F_d . As a consequence the pulse repetition frequency PRF must satisfy

$$\text{PRF} \geq 2 F_d \quad (1)$$

On the other hand to avoid range ambiguities, the PRF period must be greater than the time for two successive pulses to arrive at the radar simultaneously from the near and far edges of the illuminated area. This is usually expressed as

$$\text{PRF} < \frac{c}{2 \Delta R} \quad (2)$$

where ΔR is the slant range across the illuminated area and c is the velocity of propagation.

As a result of (1) and (2), we require

$$\frac{c}{2 \Delta R} > \text{PRF} \geq 2 F_d \quad (3)$$

Now for a narrow beam it is easily shown that the slant range is given by

$$\Delta R = Z_o B_H \tan \theta_o / \cos \theta_o \quad (4)$$

where

$$B_H = \lambda / H = \text{beam width in the elevation plane}$$

$$Z_o = \text{altitude of the SAR}$$

$$\theta_o = \text{beam pointing angle}$$

$$H = \text{aperture height}$$

With little loss in generality a planar earth as shown in Figure 2 will be assumed.

From the above it is evident that

$$B_H < \frac{c \cos \theta_o}{4 F_d Z_o \tan \theta_o} \quad (5)$$

ie., the beamwidth in the elevation plane is limited by the doppler band. Now, since the azimuthal resolution r_a for a fully focused system is related to the total doppler bandwidth by

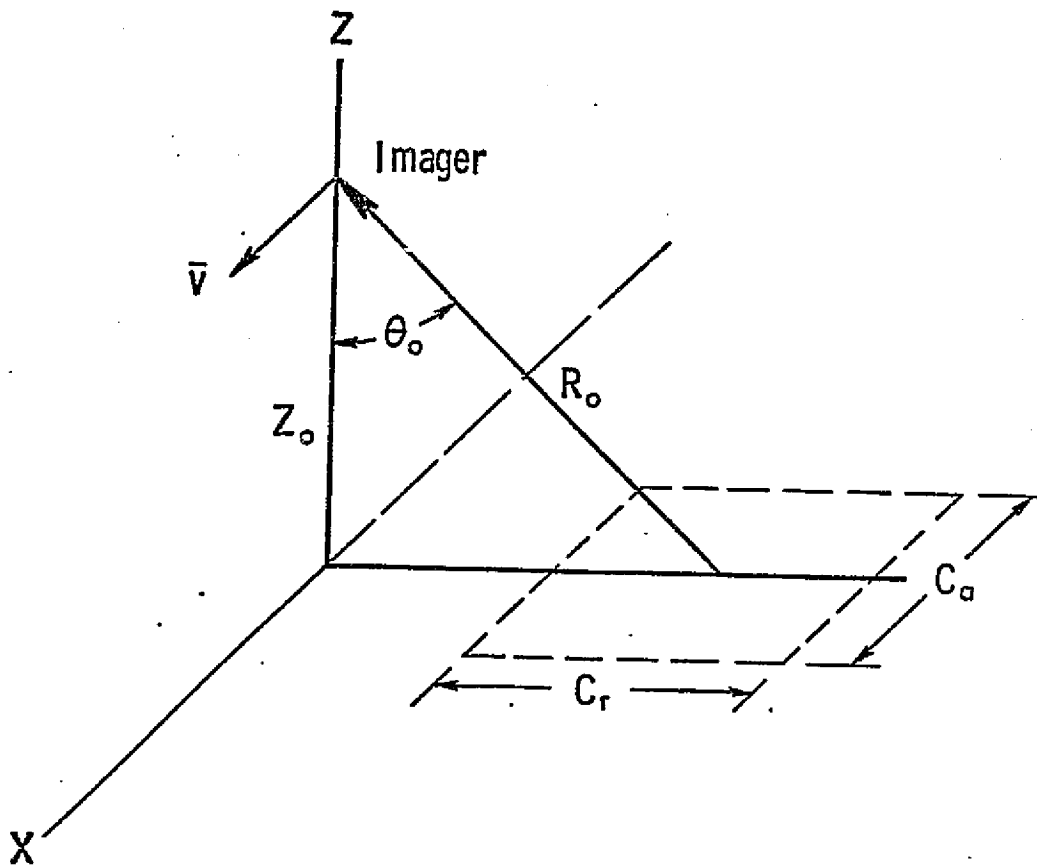


Figure 2. SAR geometry.

$$r_a = v_g / F_d \quad (6)$$

where v_g is the ground velocity of the imager, it is clear that

$$B_H \leq \frac{c r_a \cos \theta_o}{4 v_g Z_o \tan \theta_o} \quad (7)$$

It is observed that the beamwidth in the elevation plane is proportional to the desired azimuth resolution. When the range resolution r_r is to be comparable to the azimuth resolution r_a , the images must invariably point at moderate or large incident angles to avoid excessive RF bandwidths. At a pointing angle of 45° , for example, the beamwidth requirement becomes

$$B_H < 4.9^\circ \quad (8)$$

when

$$\begin{aligned} r_a &= 5 \text{ meters} \\ v_g &= 7.2 \text{ km/sec} \\ Z_o &= 435 \text{ km} \end{aligned}$$

The corresponding maximum cross-track coverage, given by

$$C_r = Z_o B_H \cos \theta_o \quad (9)$$

is only 72.7 km.

To provide more coverage per orbit one may employ partially focused or unfocused systems at the sacrifice of azimuthal resolution. If one further sacrifices to some degree multiple looks on the same resolution cell it is conceivable that sufficient time may be available to slew the radar beam over various image cells over a wide swath while synthesizing images on each cell. Indeed as the following sections show such a scanning SAR can be realized. A design theory is presented and various design realizations of interest are illustrated.

B. A Design Theory for a Scanning Radar.

1. Azimuth Resolution and the Basic Concept.

Suppose that cross-track coverage is desired between incident angles θ_1 and θ_2 as illustrated in Figure 3.* Further suppose that the radar operates at wavelength λ , has an antenna length L , and orbits at an altitude Z_o with a ground velocity v_g . If an azimuth resolution r_{a1} is required in the near image cell, a tracking bandwidth (not the total bandwidth) of

* Again a planar earth is assumed with little loss of design accuracy

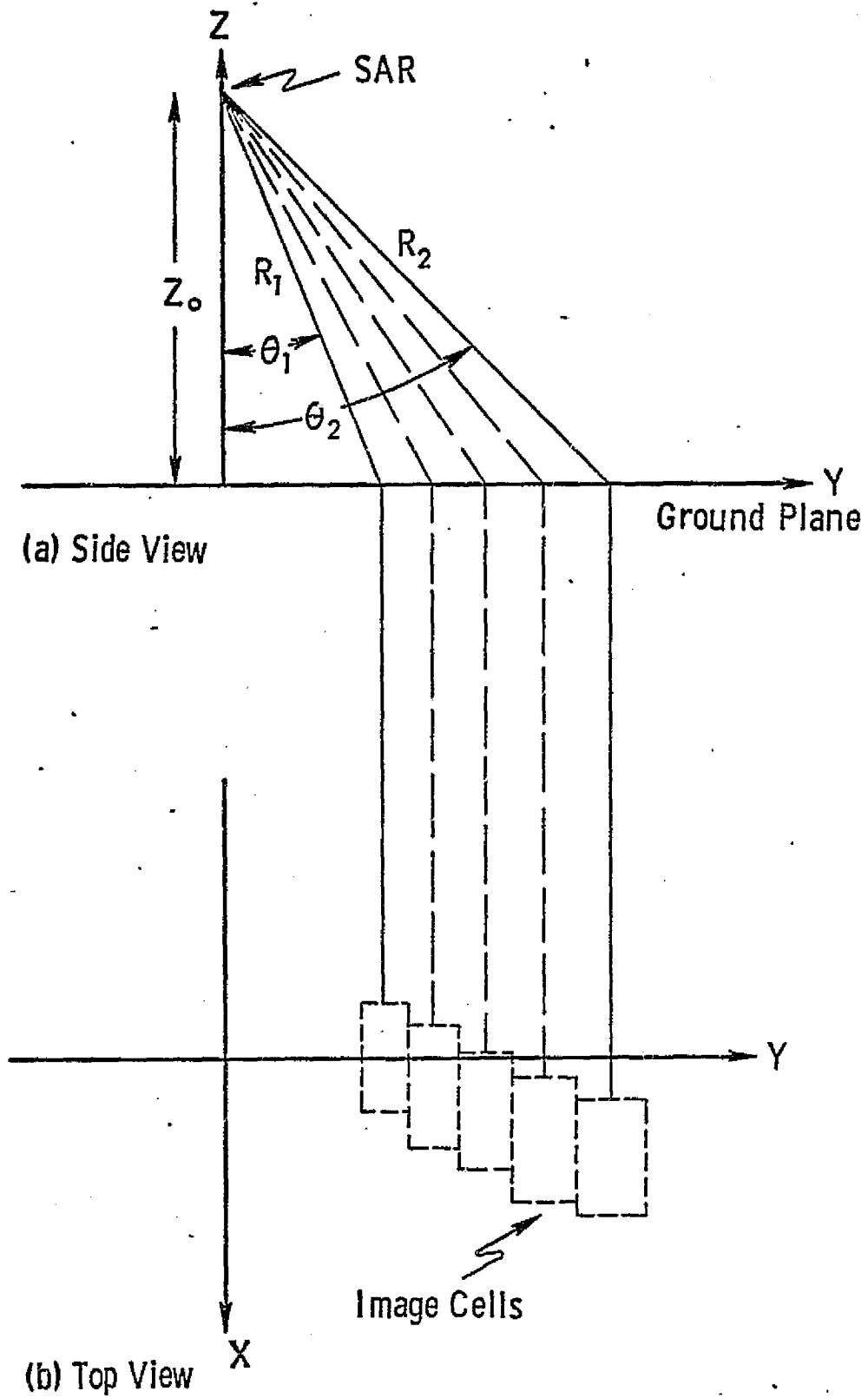


Figure 3. Geometry for a scanning SAR.

$$\Delta f_d = \frac{2 v_g}{\lambda} \frac{r_{a1}}{R_1} \quad (10)$$

is required where R_1 is the radar range to the nearest image cell.

To observe a response from this filter a target in this doppler bandwidth must be tracked for

$$\tau_d = 1/\Delta f_d \quad (11)$$

seconds. It is clear that we require

$$r_{a1} \geq \frac{L}{2} \quad (12)$$

for a realizable design, since $\frac{L}{2}$ is the resolution limit for the fully focused case. If $\frac{L}{2} < r_{a1} < \sqrt{\frac{\lambda R_1}{2}}$ a tracking filter must be employed. On the otherhand, if

$$r_{a1} \geq \sqrt{\frac{\lambda R_1}{2}} \quad (13)$$

then an unfocused design is specified. In the latter case a resolution, given by

$$r_a = \sqrt{\frac{\lambda R_1}{2}} \quad (14)$$

is obtained simply by doppler beam sharpening of the illuminated area with stationary filters.

Regardless of whether tracking or stationary filters are employed, when the total doppler bandwidth is given by

$$F_d = 2 v_g / L \quad (15)$$

the number of azimuthal filters required to obtain the desired azimuth resolution is given by

$$N_a = 2 F_d / f_d \quad (16)$$

Now with an aperture length of L the width of the nearest cell of the antenna beam will be given by

$$C_x = \frac{\lambda}{L} R_1 \quad (17)$$

For continuous coverage on adjacent scans we therefore require that the angular scan be limited to a time

$$T_s = C_x (\theta_1) / v_g \quad (18)$$

ie., the time for the imager to pass the closest cell.

2. Tracking Filters

The function of the azimuthal tracking filters may be understood in the context of matched filtering as usually applied to synthetic aperture radars. The signal from a point scatterer as observed by an imager can be represented by a time varying phasor

$$s(t) = a(x, y, z, t) \exp [j\omega_0 (t - 2r/c)] \quad (19)$$

where ω_0 is the rf frequency of the radar, r is the range (time varying) from the imager to the target and $a(x, y, z)$ is a complex amplitude associated with the target reflectivity, the transmitted power and spatial losses ($\frac{1}{4\pi r^2}$ dependence). When the beam is narrow the distance r may be approximated by

$$r = \sqrt{r_0^2 + x^2}$$

or

$$\cong r_0 + \frac{x^2}{2r_0} \quad (20)$$

where r_0 is the minimum slant range and x is the along-track displacement to the target. When it is noted that

$$x = v_g t \quad (21)$$

and when a constant phase factor is absorbed in $a(x, y, z, t)$, the return signal may be written as

$$s(t) = a(x, y, z, t) \exp [j\omega_0 (t - v_g^2 t^2 / r_0 c)] \quad (22)$$

The quadratic phase factor describes the azimuthal chirp history. A filter matched to this signal might remove the chirp and integrate the energy in the de-chirped signal.

This action can be realized by the technique shown in Figure 4. The return signal is de-chirped by product modulating with $\cos (w_1 + w_0 v_g^2 t / r_0 c) t$, removing the upper sideband and coherently integrating successive return pulses with a delay line filter. The coherent integrator is tuned to radian frequency $w_0 - w_1$ by adjusting the phase shift so that

$$\Phi = (w_0 - w_1) \tau_r - 2\pi k \quad (23)$$

where k is the largest integer dividing $w_0 - w_1$ and $\tau_r = 1/\text{PRF}$ [1]. In the above it is assumed that $w_0 > w_1$ and that w_1 is greater than half the rf bandwidth.

The inhibit and sample gate interrupts the integration after G_p pulses and directs the result to the output. In a fully focused system the integration is performed during the entire period when the target is in the beam. In an unfocused system the chirping modulator is discarded and the delay filter is tuned to a particular doppler strip whose bandwidth is given by

$$f_d = v_g / r_a \quad (24)$$

where $r_a = \sqrt{\frac{\lambda R}{2}}$. The integration time is restricted to r_a / v_g as opposed to $N_a r_a / v_g$ for the fully focused case. The semi-focused case integrates for periods between these limits.

The output of the integrator contains a part or all the range history for an azimuthal element of width r_a depending on the integration time. In the case of a fully focused system, the filter is tuned to the slant range r_0 . Other range elements drift through the filter without integrating, so only one range element integrates coherently. Therefore a tracking filter must be provided for each range-element as well as azimuthal element. For the unfocused case the integration time is sufficiently short that the range history in an entire azimuthal doppler strip is available at the output of the coherent integrator. The required number of filters is therefore N_a . For the partially focused case additional filters to cover the range dimension may be required depending on the integration time, wavelength and view angle.

The number of additional filters may be established from the following geometrical considerations. Suppose that the integration period is $1/\Delta f_d$. During this period the spacecraft will have moved a distance

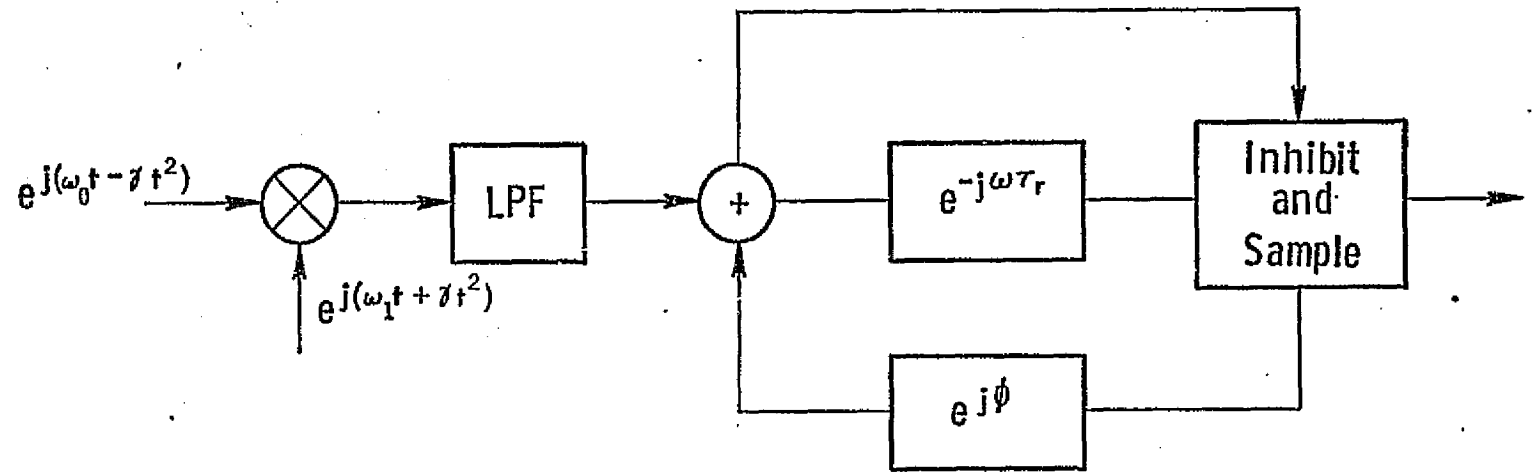


Figure 4. Matched filter for SAR.

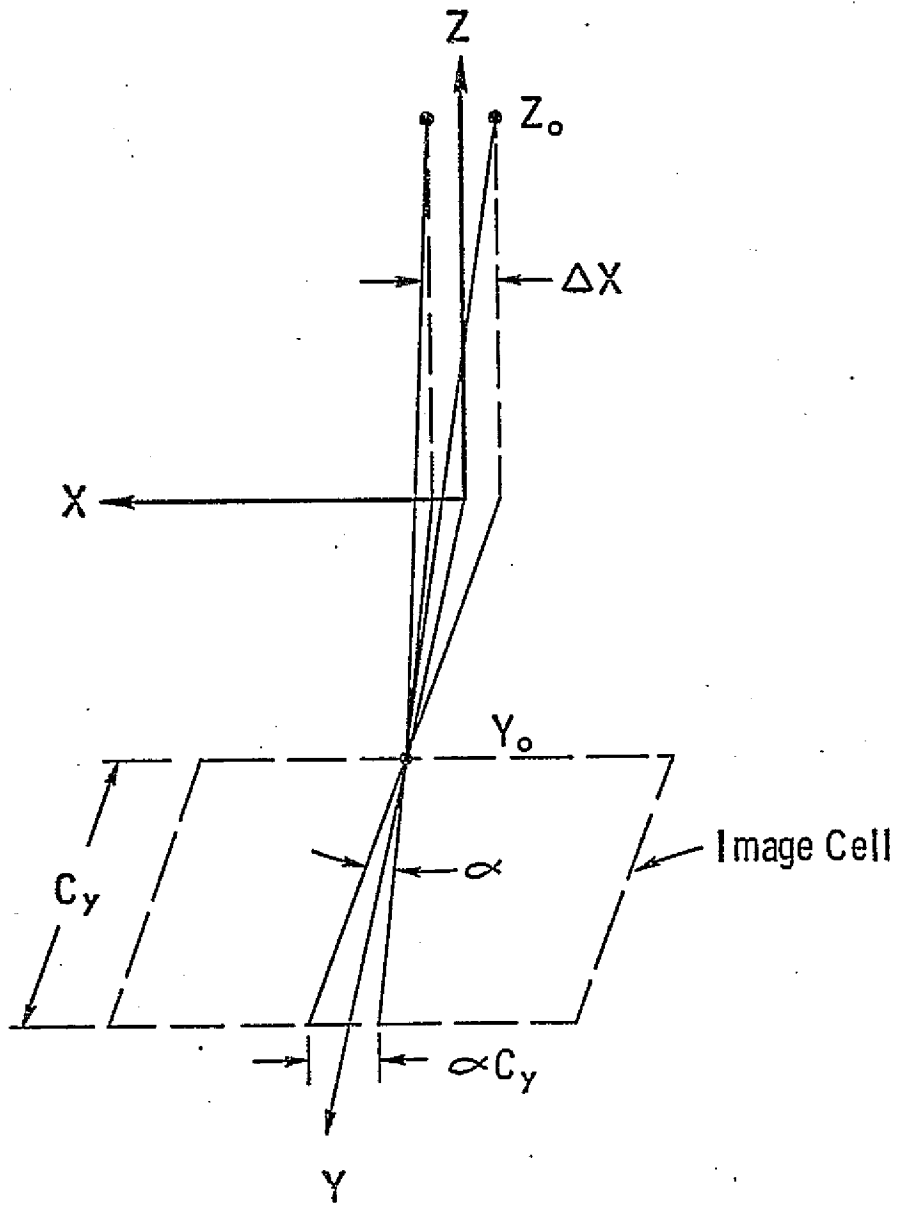


Figure 5. Range de-focusing geometry.

$$\Delta x = v_g \frac{1}{\Delta f_d} \quad (25)$$

(See Figure 5). If we consider that the filter is tuned to the near edge of the image cell then during the integration period the filter will have scanned an angle of α on the ground to keep the near edge in focus. In doing so the filter will have attempted to integrate the targets on the far edge subtended by α . If C_y is the length of the image cell, then the distance traversed on the far edge will be given by αC_y . If $\alpha C_y < r_a$, then the entire azimuthal strip will have remained essentially in focus. On the other hand, if $\alpha C_y > r_a$ then additional filters are required in range. If

$$\alpha C_y = N_r r_a \quad (26)$$

where N_r is an integer, then the number of filters in range is given by N_r . The total number of filters is given by

$$N_f = N_r N_a \quad (27)$$

Although not obvious from the above, N_r is dependent on view angle; the near image cells require more filters in range than far image cells.

3. Aperture Height and Related Parameter

If a range guard band factor of 2 is chosen, the PRF is specified as

$$\text{PRF} = c/4 \Delta R_2 \quad (28)$$

where ΔR_2 is the slant range across the farthest image cell. Substituting (4), we may write

$$\text{PRF} = \frac{c \cos \theta_2}{4 z_o B_H \tan \theta_2} \quad (29)$$

If we conservatively sample the total Doppler bandwidth such that

$$\text{PRF} = 2.5 F_d \quad (30)$$

then using (28) and (29) from above we can specify

$$B_H = \frac{c}{10 R_2 F_d \tan \theta_2} \quad (31)$$

or
$$H = \frac{\lambda}{B_H} = \frac{10 z_o F_d \tan \theta_2}{c \cos \theta_2} = \frac{10 z_o F_d \tan \theta_2}{F_o \cos \theta_2} \quad (32)$$

where $R_2 = Z/\cos\theta_2$ has been used. The necessary aperture height has thus been established.

The PRF will be governed by the farthest image cell, i.e.,

$$\text{PRF} = c/4 \Delta R_2 \quad (33)$$

where

$$\Delta R_2 = B_H R_2 \tan\theta_2 \quad (34)$$

(See Figure 2).

With the above parameters we are in a position to compute several others. The processing gain, assuming the full RF band will be processed, will be given by

$$G_p = \text{PRF}/\Delta f_d \quad (35)$$

where $1/\Delta f_d$ is the integration time. The number of scan cells between θ_1 and θ_2 is given by

$$N_c = (\theta_2 - \theta_1) / B_H \quad (36)$$

and the dwell time on each cell by

$$T_c = T_s / N_c \quad (37)$$

If $T_c < \frac{1}{\Delta f_d}$, then there is insufficient time to build a subaperture with the desired resolution. In this case either the azimuthal resolution must be relaxed or the angular coverage $\theta_2 - \theta_1$ shortened. If $T_c \geq 1/\Delta f_d$, the design may proceed. If $T_c \geq 2/\Delta f_d$, multiple looks on the same azimuthal strip are possible when many parallel subapertures are simultaneously synthesized across the beam. The number of multiple looks will be given by

$$D_f = T_c \Delta f_d \quad (38)$$

The multiple looks can be used to reduce the speckle inherent in coherently constructed images.

Finally with aperture height specified it is noted that coverage in the range dimension for a particular look angle is given by

$$C_r = B_H Z / \cos\theta \quad (39)$$

4. Range Resolution and the RF Bandwidth.

If a range resolution of r_r is required by the design, the RF bandwidth will be given by

$$BW = c/2r_r \sin \theta_1 \quad (40)$$

where θ_1 is the smallest pointing angle. The pulse duration is therefore

$$\tau_p = 1/BW \quad (41)$$

Note that, if pulse compression is used, this is the width of the compressed pulse.

5. Power Requirement

To compute the transmit power requirement, we note that the peak return power W_{rp} from a single resolution cell is given by

$$W_{rp} = \frac{W_{tp} A^2 \sigma^o r_r r_a}{4 \pi \lambda^2 R^4 L} \quad (42)$$

where

- W_{tp} = peak transmitter power
- A = effective aperture of antenna
- σ^o = scattering coefficient
- R = range to cell
- L = Loss factor

Since the tracking filter is a matched filter, it is appropriate to define the signal to noise ratio in terms of the peak power to the mean-squared noise. The peak signal power in relation to this signal-to-noise ratio is therefore given by

$$W_{rp} = F k T BW (S/N)/G_p \quad (43)$$

where

- F = receiver noise figure
- k = Boltzmann's constant
- T = receiver input noise temperature
- BW = rf bandwidth
- G_p = match-filtered processing gain

The peak transmitter power is related to the average transmitter power by

$$W_{tp} = \frac{BW}{PRF} W_{ta} \quad (44)$$

The required transmitter power is therefore

$$W_{ta} = \frac{4\pi \lambda^2 R^4 L F k T (S/N) PRF}{G_p A^2 \sigma^{\circ} r_a r_r} \quad (45)$$

In view of a typical scattering characteristic, the transmit power will be governed by the minimum σ° at the largest view angle θ_2 . A conservative estimate of σ° would include the Rayleigh characteristic of the return in computing W_{ta} . These considerations were, however, discarded within the time frame of this study.

6. Telemetry Channel Capacity

If σ_{\max}° and σ_{\min}° are, respectively, the maximum and minimum scattering coefficients anticipated in the interval (θ_2, θ_1) , then the bit requirement N_b is given by

$$2^{N_b} = \frac{\sigma_{\max}^{\circ}}{3.01 \sigma_{\min}^{\circ}} \quad (47)$$

if we presume a gray-scale resolution equal the minimum σ° . If a N bit word is transmitted for each resolution cell, then the total number of bits per scan cell is given by

$$B_c = N_b C_r C_a / r_r r_a \quad (48)$$

and the required channel capacity by

$$C_c = B_c / T_c \quad \text{bits/sec} \quad (49)$$

Error recovery codes, calibration parameters and control words would increase the bit rate slightly.

If the number of levels is specified in terms of a fractional gray scale resolution (constant resolution in dB), the derivation is somewhat different. For this case logarithmic encoding is required. The number of levels needed is then

$$N_L = \frac{\sigma_{\max}^{\circ} \text{ (dB)} - \sigma_{\min}^{\circ} \text{ (dB)}}{r_g \text{ (dB)}} \quad (50)$$

where r_g is the gray-scale fractional resolution. The number of bits required per resolution cell is therefore

$$N_b = \log_2 N_L \quad (51)$$

The required channel capacity is given by (48) and (49), with (51) used instead of (47). The computer outputs presented here are based on use of (47) rather than (51), but use of the criterion expressed in (50) will result in an easily applied multiplier.

C. Computer Aided Design Study

A computerized design program was based on the above design theory. The coding appears in Appendix A. The program, with the aid of the above text and the comments integral to the program, make the program largely self-explanatory.

With the assistance of the computer program various scanning SAR designs were considered. Parametric studies were primarily based on the span of angles (θ_2, θ_1), operating wavelength λ , aperture length L and resolution specifications. In all cases a spacecraft ground velocity of 7.2 km/sec and an altitude of 435 km were assumed. The transmit power was based on readily available scattering data, a loss factor of 7dB, a signal to noise ratio of 3dB (for the smallest σ^0), an aperture efficiency of 75%, and a receiver input noise temperature of 300°K. The loss factor is based on 3dB attenuation between the transmitter and antenna and on a 1dB two way atmospheric loss. These values are believed to be conservative. Noise figures were based on conservative estimates depending on wavelength. The results of all design cases considered are tabulated in Appendix B.

The parametric studies considered scans between 7° and 22° and between 22° and 37°. The angular span about the smaller angles was chosen since it is known that the sensitivity to soil moisture is greatest at small angles of incidence [2]. The span across moderate angles was examined as an alternative which also may intuitively be useful for hydrology studies of snow covered mountainous terrain and for surveying arctic ice*. Frequencies of 9., 4.75, 3.75 and 1.4 GHz were investigated. The central two frequencies are considered near optimum for soil moisture detection when the ground is covered with vegetation [3]. For the above combination of angles and frequencies, various aperture lengths from 1 to 10 meters, depending on frequency, were considered. Moderate resolutions from 50 to 150 meters were specified in the design cases. Results of these studies are summarized in Table IV.

* The time span of this study did not permit the author to search for measurements in these categories. Other reports in this series examine these problems.

An examination of the cases in Appendix A indicates the following observations:

1. Increased coverage is indeed feasible with a scanning SAR, e.g., 125 km coverage for small angles of incidence as opposed to 15 km for a non-scanning SAR.
2. All design cases were achieved with a very modest transmitter power requirement. For example, most cases of interest indicated powers in the neighborhood of a watt (four watts when Rayleigh fading is included).
3. As a result of the modest resolutions specified and on-board processing anticipated in the design very nominal telemetry channel capacities are required.
4. At small incident angles, range resolutions less than 150 meters require large RF bandwidths with prohibitive sampling rates for the processor. The tracking filter bit capacity to integrate the range history, for example, must be excessively high to achieve the desired bit resolution.
5. The number of tracking filters is inversely proportional to the antenna length, proportional to wavelength and inversely proportional to the azimuth resolution.
6. It is also apparent that the number of independent looks can be increased by sacrificing resolution or swath width (or both).
7. The total number of filters increases with decreasing frequency for the same antenna length. The reader will note from Appendix B, that the antenna length was increased to 10 meters and the swath width decreased to 10° at $\lambda = .214$ in attempt to decrease the number of filters.

When choosing an imager suitable for soil moisture detection, one must consider designs at $\lambda = 0.063$ and 0.08 meters over the small view angles. Also, recent studies [4] indicate that 50 meter resolution is a minimal resolution to define field boundaries. Yet as observed above, 50 meter resolution in the range dimension is difficult to achieve at the small incident angles without undue complexity in the tracking filters. As a compromise it is proposed that 150 meter resolution in the range dimension be accepted at the smallest view angle and a 50 meter resolution in the azimuthal dimension over the entire swath. Since the total number of filters is smaller at $\lambda = 0.063$, considerations will be focused on that wavelength and an aperture length of 3 meters. It is interesting to note that the antenna is nearly square and would also serve as a suitable radiometer antenna should one consider a

composite sensor. The chosen design case is shown in Table I. The upper third of the table discloses the input design parameters as apply to the smallest and largest pointing angle (first and second row). The remainder of the table discloses the computed design values. The entries are defined in Table II. From the computed range resolutions it is apparent that the range resolution improves with pointing angle and achieves a value of 48.80 meters at the outer image cell. If the aperture height were increased to 4.17 meters the same system could also optionally scan the angular region between 22° and 37° with a nominal 50 x 50 meter resolution over the entire swath as Table III indicates. It is noted that four independent looks are achieved between 7° and 22° and two independent looks between 22° and 37° .

TABLE I RECOMMENDED DESIGN FOR COVERAGE
BETWEEN 7 AND 22 DEGREES

PAW DESIGN PARAMETERS

PARAMETERS	VALUES	UNITS
ANGLE SPAN	7.00	22.00 DEG
AZ RES	50.00	M
RA RES	150.00	M
LAMBDA	0.063	M
GRD VEL	7.2	KM/SEC
ALTITUDE	435.0	KM
APER LENGTH	3.0	M
APER EFF	75.0	PERCENT
LOSS FACTOR	7.0	DB
SIGMAX	12.00	2.00 DB
SIGMIN	-4.00	-8.00 DB
NOISE FIG	6.0	DB
REC TEMP	300.0	DEG K
SIG/NOISE	3.00	DB

COMPUTED SYSTEM PARAMETERS

SYSTEM TYPE:	SEMI-FOCUSED	
APER HEIGHT	1.92	M
XMIT PWR	0.14	1.35 WATTS
PRF	12.00	KHZ
FD	4.80	KHZ
RF BW	8.2	MHZ
PROC GAIN	463	
NCAP	4	
NCA	1	1
NO. OF FIL	185	
CHAN CAP	0.78	2.76 MBITS/SEC

COVERAGE AND RESOLUTION

SWATH	137.96	KM
CELLS/SCAN	8	
CELL WIDTH	9.26	9.91 KM
CELL LENGTH	14.56	16.68 KM
SCAN TIME	1.29	SEC
TIME/CELL	0.161	SEC
AZ RES	50.00	M
RA RES	150.00	M

TABLE II
DEFINITION OF SYMBOLS

APER	=	aperture
AZ	=	azimuth
XMIT PWR	=	transmit power
FD	=	total doppler bandwidth
RF BW	=	rf bandwidth
PROC	=	processing
NCAP	=	no. of multiple looks on the same azimuthal strip
NCA	=	no. of filters in range
No. of FIL	=	number of filters in azimuth
CHAN CAP	=	Channel capacity
RES	=	resolution

Note: Total number of filters is given by $NCA \times \text{No. of filters.}$

TABLE III A DESIGN COMPATIBLE WITH THAT OF
TABLE I BUT OPERATING BETWEEN 22 AND 37 DEGREES

RAW DESIGN PARAMETERS

PARAMETERS	VALUES		UNITS
ANGLE SPAN	22.00	37.00	DEG
LAMBDA	0.063		M
APER LENGTH	3.0		M
AZ RES	50.00		M
RA RES	50.00		M
GRD VEL	7.2		KM/SEC
ALTITUDE	435.0		KM
APER EFF	75.0		PERCENT
LOSS FACTOR	7.0		DB
NOISE FIG	5.0		DB
SIG/NOISE	3.00		DB
REC TEMP	300.0		DEG K
SIGMAX	2.00	-2.00	DB
SIGMIN	-8.00	-12.00	DB

COMPUTED SYSTEM PARAMETERS

SYSTEM TYPE:	SEMI-FOCUSED		
APER HEIGHT	4.16		M
XMIT PWR	0.22	1.41	WATTS
PRF	12.00		KHZ
FD	4.80		KHZ
RF BW	8.0		MHZ
PROC GAIN	496		
NCRP	2		
NCA	1	1	
NO. OF FIL	198		
CHAN CAP	1.89	4.08	NBITS/SEC

COVERAGE AND RESOLUTION

SWATH	161.09		KM
CELLS/SCAN	17		
CELL WIDTH	9.91	11.51	KM
CELL LENGTH	7.71	10.39	KM
SCAN TIME	1.38		SEC
TIME/CELL	0.081		SEC
AZ RES	50.00	58.05	M
RA RES	50.00	31.12	M

TABLE IV SUMMARY OF DESIGN CASES
IN APPENDIX A

X Band - 3.13 cm <u>7-22°</u>									
APERTURE Length - Height (M) (M)	Swath (KM)	r _R (M)	r _A (M)	# Ind. Looks	P _T (W)	# FIL	RF BW (MHz)	TM CAP (MB/S)	
1	3.03	128	50-16	50-54	4	39	292	25	9.5
			150-49	50-54	4	13	292	8.2	3.2
			150-49	88-95	7	13	165	8.2	1.8
3	1.01	138	50-16	50-54	4	39	97	25	9.5
			150-49	50-54	4	13	97	8.2	3.2
			150-49	88-95	7	13	55	8.2	1.8
6	0.50	154	50-16	50-54	4	39	98	25	9.5
			150-49	50-54	4	13	98	8.2	3.2
			150-49	88-95	7	13	28	8.2	1.8
<u>22-37°</u>									
1	6.6	155	50-31	50-59	2	13	312	8.0	5.0
			150-93	50-58	2	5	312	2.7	1.7
			150-93	95-111	4	4	164	2.7	0.9
3	2.19	161	50-31	50-58	2	13	104	8.0	4.9
			150-93	50-58	2	5	104	2.7	1.6
			150-93	95-111	4	4	52	2.7	0.9

TABLE IV (CONT.)

C-Band - 6.3 cm 7-22°

APERTURE Length - Height		Swath	r _R	r _A	# Ind. Looks	P _T	# FIL	RF BW	TM CAP
3	1.9	138	50-16	50-54	4	3	185	25	8.3
			150-49	50-54	4	1.4	185	8.2	2.8
			150-49	122-131	10	1.1	76	8.2	1.1
6	1.0	154	50-16	50-54	4	3	372	25	8.3
			150-49	50-54	4	1.4	372	8.2	2.8
			150-49	122-131	10	1.1	38	8.2	1.1

22-37°

3	4.2	161	50-31	50-58	2	1.4	198	8.0	4.1
			150-93	50-58	2	0.5	198	2.7	1.4
			150-93	131-153	5	0.5	75	2.7	0.5
6	2.1	170	50-31	50-58	2	1.4	99	8.0	4.3
			150-93	50-58	2	0.5	99	2.7	1.4
			150-93	131-153	5	0.5	38	2.7	0.6

TABLE IV (CONT.)

S-Band - 8.0 cm <u>7-22°</u>									
APERTURE					# Ind.		#	RF	TM
Length	Height	Swath	r _R	r _R	Looks	P _T	FIL	BW	CAP
3	2.4	138	50-16	50-54	4	4	468	25	7.1
			150-49	50-54	4	1.4	468	8.2	2.4
			150-49	137-147	11	1.4	85	8.2	0.9
6	1.2	154	50-16	50-54	4	4	585	25	7.1
			150-49	50-54	4	1.4	585	8.2	2.4
			150-49	137-147	11	1.3	43	8.2	0.9
<u>22-37°</u>									
3	5.25	161	50-31	50-58	2	2.2	250	8.0	4.9
			150-93	50-58	2	0.5	250	2.7	1.6
			150-93	148-171	6	0.5	85	2.7	0.6
6	2.6	170	50-31	50-58	2	1.4	125	8.0	5.2
			150-93	50-58	2	0.5	125	2.7	1.7
			150-93	148-171	5	0.5	42	2.7	0.6
L-Band - 21.4 cm <u>10-20°</u>									
6	2.9	117	150-76	50-52	8	0.3	3150	5.8	1.0
10	1.7	140	150-76	50-52	10	0.3	3969	5.8	0.8
<u>20-30°</u>									
6	5.0	116	150-103	50-54	4	0.3	1650	2.9	1.0
10	3.0	131	150-103	50-54	5	0.3	594	2.9	0.8

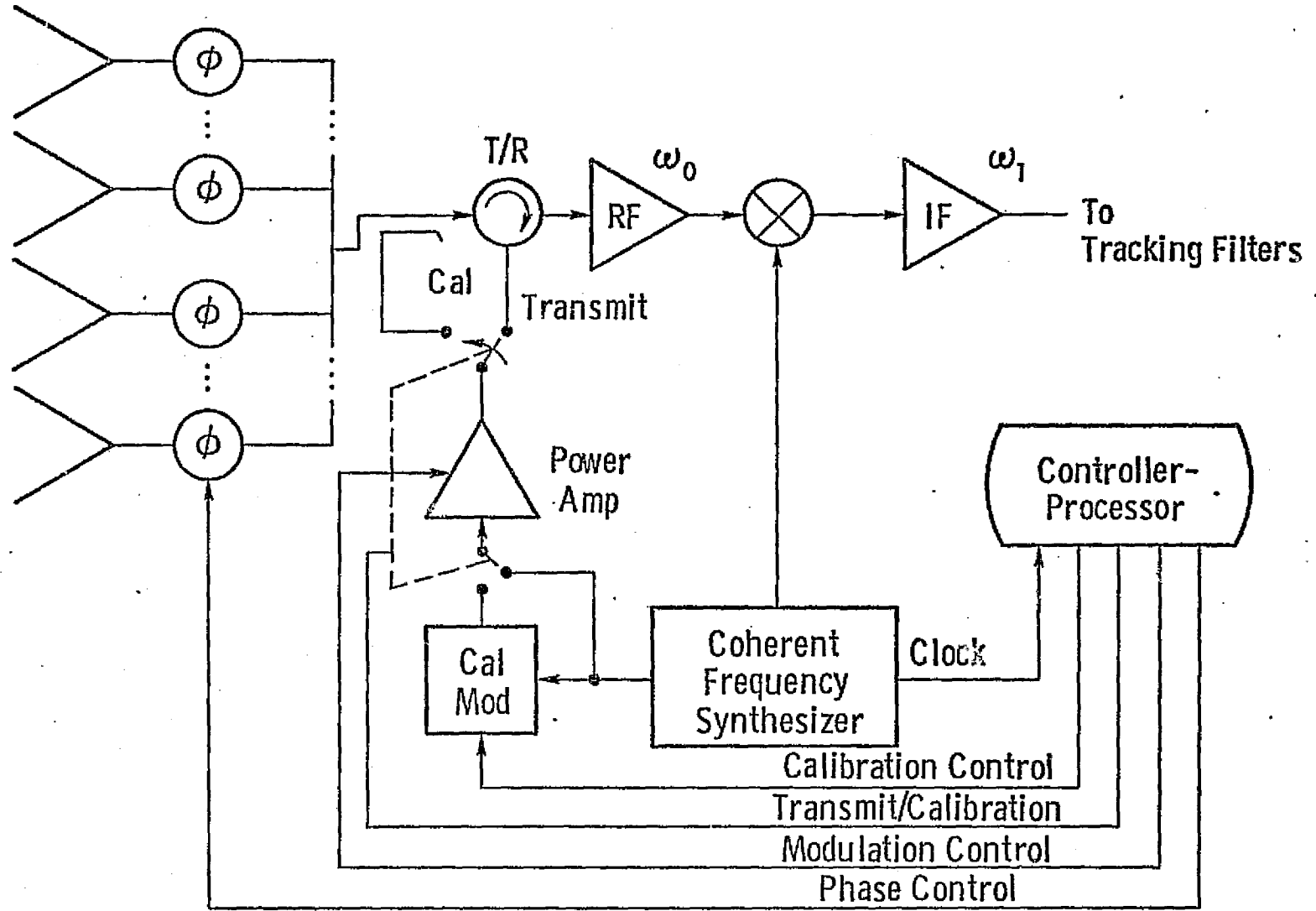


Figure 6. Transmitter and receiver for scanning SAR.

III. Proposed System Design

To achieve the design objective of 250 km coverage it is proposed that two scanning SARs be operated simultaneously. Each SAR would scan one side of the ground track providing coverage between 7° and 22° (could reduce to 20°) and would have the design characteristics specified in Table I. To scan in angle rapidly it is necessary that a controllable phase array be employed. It is preferable to use a vertically polarized array since the power requirement would not be as great. If possible the same array would cover both sides of the track. The frequency assigned to each system would be separated by several RF bandwidths (8.2 megahertz) to provide isolation between the left and right processors. Each scanning SAR would have its own receiver as well as processor; however, the transmitter (and antenna) could be time-shared by both. If two processors are allocated per side, it is conceivable to operate at two frequencies on each side to realize another four independent looks on each resolution cell.

The transmitter - receiver section of one of the SARs is illustrated in Figure 6. The controller commands the phased array to point at the appropriate image cell. The transmitter-modulator transmits G_p pulses where G_p is the processing gain. The RF and IF chain amplifies the return while retaining coherence.

The output of the IF amplifier is fed to a set of parallel tracking filters each assigned to a different azimuth-range strip. Figure 7 illustrates one filter and post processor channel. The controller initializes the transmit cycle on the basis of the chirp frequency and controls the chirp rate in accord with the spacecraft ground speed. The product modulator dechirps the incoming signal, the LPF discards the upper modulation product. The clutter tracker follows the center frequency in the channel and adjusts the mean frequency of the de-chirp oscillator so as to account for changes in the center of the doppler return frequency as induced by beam squinting. The dechirp oscillators in the other channel should be replicas of one another except that the chirps will be off-set from one another. As a consequence the chirp oscillators need not be duplicated for each channel. As the signal is de-chirped, the pulses are coherently integrated by the delay line filter. The filter may be digital or discrete time analog devices to avoid drift in the delay time. The processor would provide the clock frequency for the filter. The phase shift θ_1 is set to integrate w_2 and its harmonics. After G_p pulses the integration is interrupted and the range history is dumped. The

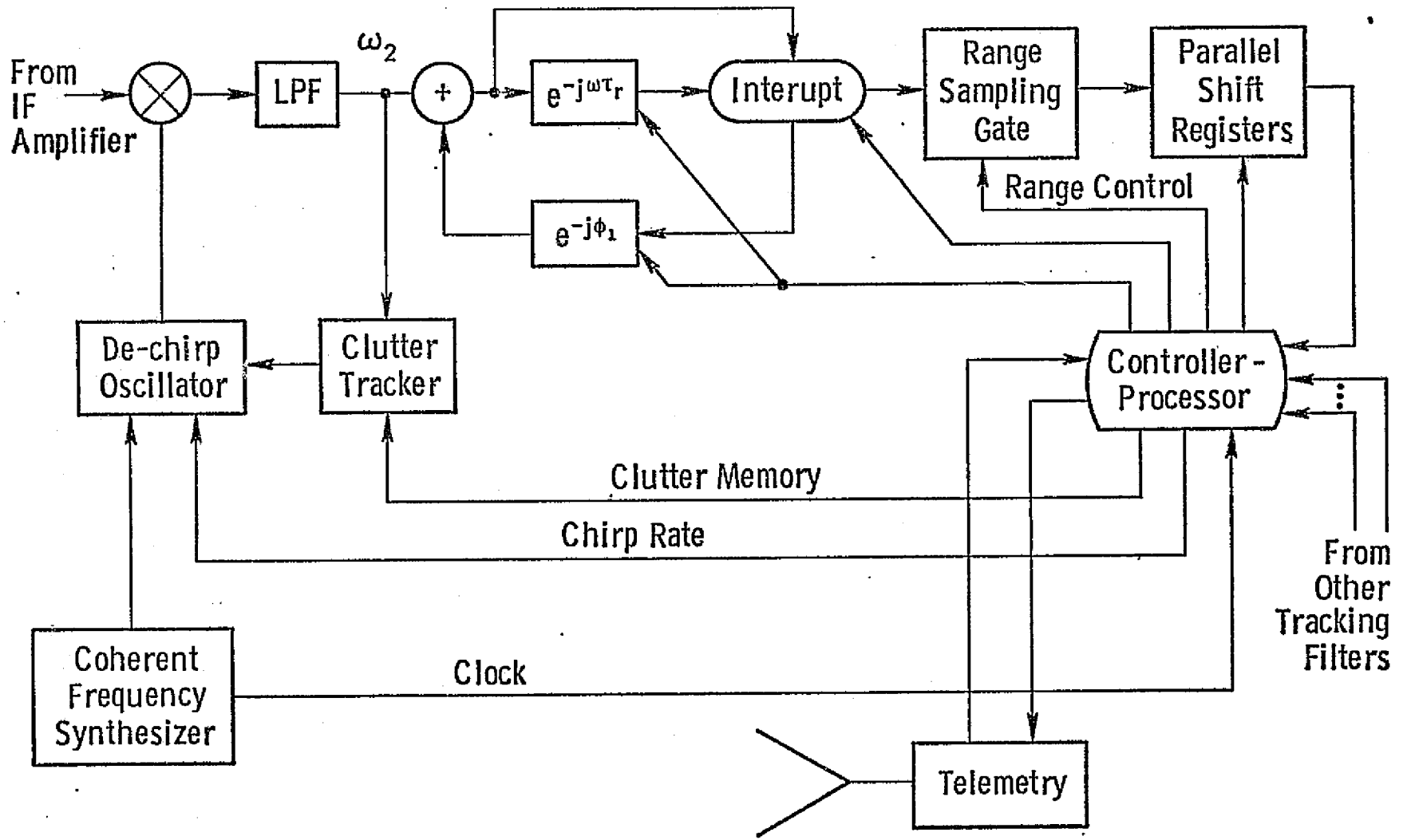


Figure 7. Tracking filters with post processor.

range history is then sampled under control of the processor and stored in a set of parallel shift registers. The controller then initiates a new cycle. In the mean time the processor stores and clears the contents of the shift register. The contents are squared and added to previous looks on the same azimuthal-range strip. Once the multiple looks are completed, the array scans to a new angle and the cycle is initiated on a new image cell. The averaged data is then passed to the telemetry stream. The processor must retain memory of the azimuth off-set between looks at the same pointing angle. This memory is transferred to the clutter-tracker for the proper azimuth off-set compensation.

IV. Conclusions and Recommendations

This short system study has developed a design procedure for a scanning synthetic aperture radar. With this design procedure it was shown by way of many examples (Appendix B) that when the resolution is relaxed sufficiently increased swath width coverage can be realized as compared to a fixed angle SAR operating in nominally the same angular band. Specifically at small incident angles a scanning SAR can provide coverage in the vicinity of 140 km as opposed to a fixed angle coverage of nominally 15 to 30 km. A method of on-board processing which should be realizable with today's technology [5], [6] was proposed. The design cases show that the complexity of the processor decreases with increasing frequency for a given aperture length.

A particular design suitable for soil moisture monitoring was proposed. A double sided scanning SAR providing coverage at near optimum angles and frequency was shown to offer a total swath width of 270 km. Half the coverage occurs on each side of the ground track between 7° and 22° . The design based on an azimuth resolution of 50 meters, a minimum range resolution of 150 meters and a 3 by 1.9 meter antenna was achieved with a total of 370 tracking filters in the post processor, a modest transmitter power of 2.70 watts and a telemetry channel capacity of 5.50 megabits/second.* The range resolution improved to 49 meters at the farthest image cell.

In preparing this design study the author uncovered certain problems that within this time frame remain unresolved in his own mind. The literature available to him indicates they have been solved, although the techniques were not disclosed. First it is known that the clutter lock or tracker has long been implemented aboard aircraft. The specific implementation method, however, was not uncovered during this study. It

* This figure could be reduced if on-board storage is provided.

is recommended that the technique be developed from the literature and adapted to this design. The transmitter power should be reassessed on the basis of the clutter lock S/N ratio requirement. Secondly, in the review of the literature on delay line filters it was not clear how the phase advance is implemented accurately. A cursory examination showed that small phase shift increments are required between adjacent tracking filters. The means by which this is implemented and controlled is not clear. This problem should also be resolved.

REFERENCES

- [1] Bickel, H. J., "Spectrum Analysis with Delay Line Filters," IRE Wescon Convention Record, Part 8, pp. 59-67, 1959.
- [2] Ulaby, F.T. and P.P. Batlivala, "The Effects of Surface Roughness on Radar Sensitivity to Soil Moisture," URSI Meeting, University of Illinois, June 3-5, 1975.
- [3] Ulaby, F.T., Private Communication, University of Kansas Remote Sensing Laboratory.
- [4] Hardy, N., Private Communication, University of Kansas Remote Sensing Laboratory.
- [5] Gershberg, R., "Synthetic Aperture Radar and Digital Processing," University of Kansas Center for Research, Inc., CRES Technical Report 177-10, Supported under NASA Contract NAS 9-19261, September 1970.
- [6] Kirk, J.C. Jr., "A Discussion of Digital Processing in Synthetic Aperture Radars," IEEE Transactions on Aerospace and Electronic Systems, Vol. AES - 11, No. 3, pp. 326-336, May 1975.

Appendix A
DESIGN CASES FOR A SCANNING SAR

SUMMARY TABLE 1

RAW DESIGN PARAMETERS

PARAMETERS		VALUES	UNITS
ANGLE SPAN	7.00	22.00	DEG
AZ RES	50.00		M
RA RES	50.00		M
LAMBDA	0.033		M
GRD VEL	7.2		KM/SEC
ALTITUDE	435.0		KM
APER LENGTH	1.0		M
APER EFF	75.0		PERCENT
LOSS FACTOR	7.0		DB
SIGMAX	8.00	-1.00	DB
SIGMIN	-10.00	-15.00	DB
NOISE FIG	6.0		DB
REC TEMP	300.0		DEG K
SIG/NOISE	3.00		DB

COMPUTED SYSTEM PARAMETERS

SYSTEM TYPE: SEMI-FOCUSED			
APER HEIGHT	3.03		M
XMIT PWR	3.24	38.60	WATTS
PRF	36.00		KHZ
FD	14.40		KHZ
RF BW	24.6		MHZ
PRDC GAIN	730		
NCAF	4		
NCA	1	1	
NO. OF FIL	292		
CHAN CAP	2.68	9.45	MBITS/SEC

COVERAGE AND RESOLUTION

SWATH	127.55		KM
CELLS/SCAN	24		
CELL WIDTH	14.59	15.62	KM
CELL LENGTH	4.85	5.56	KM
SCAN TIME	2.03		SEC
TIME/CELL	0.084		SEC
AZ RES	50.00	53.52	M
RA RES	50.00	16.27	M

REPRODUCIBILITY OF
ORIGINAL PAGE IS POOR

SUMMARY TABLE 2

RAW DESIGN PARAMETERS

PARAMETERS	VALUES	UNITS
ANGLE SPAN	7.00	22.00 DEG
LAMBDA	0.033	M
APER LENGTH	1.0	M
AZ RES	50.00	M
RA RES	150.00	M
GRD VEL	7.2	KM/SEC
ALTITUDE	435.0	KM
APER EFF	75.0	PERCENT
LOSS FACTOR	7.0	DB
NOISE FIG	6.0	DB
SIG/NOISE	3.00	DB
REC TEMP	300.0	DEG K
SIGMAX	8.00	-1.00 DB
SIGMIN	-10.00	-15.00 DB

COMPUTED SYSTEM PARAMETERS

SYSTEM TYPE: SEMI-FOCUSED		
APER HEIGHT	3.03	M
XMIT PWR	1.08	12.87 WATTS
PRF	36.00	KHZ
FD	14.40	KHZ
RF BW	8.2	MHZ
PROC GAIN	730	
NCFP	4	
NCA	1	1
NO. OF FIL	292	
CHAN CAP	0.89	3.15 MBITS/SEC

COVERAGE AND RESOLUTION

SWATH	127.55	KM
CELLS/SCAN	24	
CELL WIDTH	14.59	15.62 KM
CELL LENGTH	4.85	5.56 KM
SCAN TIME	2.03	SEC
TIME/CELL	0.084	SEC
AZ RES	50.00	M
RA RES	150.00	M

SUMMARY TABLE 3

RAW DESIGN PARAMETERS

PARAMETERS	VALUES	UNITS
ANGLE SPAN	7.00	22.00 DEG
AZ RES	88.38	M
RA RES	150.00	M
LAMBDA	0.033	M
GRD VEL	7.2	KM/SEC
ALTITUDE	435.0	KM
APER LENGTH	1.0	M
APER EFF	75.0	PERCENT
LOSS FACTOR	7.0	DB
SIGMAX	8.00	-1.00 DB
SIGMIN	-10.00	-15.00 DB
NOISE FIG	6.0	DB
REC TEMP	300.0	DEG K
SIG/NOISE	3.00	DB

COMPUTED SYSTEM PARAMETERS

SYSTEM TYPE: UNFOCUSED		
APER HEIGHT	3.03	M
XMIT PWR	1.08	12.87 WATTS
PRF	36.00	KHZ
FD	14.40	KHZ
RF BW	8.2	MHZ
PROC GAIN	413	
NCAP	7	
NCA	1	1
NO. OF FIL	165	
CHAN CAP	0.51	1.78 MBITS/SEC

COVERAGE AND RESOLUTION

SWATH	127.55	KM
CELLS/SCAN	24	
CELL WIDTH	14.59	15.62 KM
CELL LENGTH	4.85	5.56 KM
SCAN TIME	2.03	SEC
TIME/CELL	0.084	SEC
AZ RES	88.38	M
RA RES	150.00	48.80 M

SUMMARY TABLE 4

RAW DESIGN PARAMETERS

PARAMETERS		VALUES	UNITS
ANGLE SPAN	7.00	22.00	DEG
AZ RES	50.00		M
RA RES	50.00		M
LAMBDA	0.033		M
GRD VEL	7.2		KM/SEC
ALTITUDE	435.0		KM
APER LENGTH	3.0		M
APER EFF	75.0		PERCENT
LOSS FACTOR	7.0		DB
SIGMAX	8.00	-1.00	DB
SIGMIN	-10.00	-15.00	DB
NOISE FIG	6.0		DB
REC TEMP	300.0		DEG K
SIG/NOISE	3.00		DB

COMPUTED SYSTEM PARAMETERS

SYSTEM TYPE: SEMI-FOCUSED			
APER HEIGHT	1.01		M
XMIT PWR	3.24	38.66	WATTS
PRF	12.00		KHZ
FD	4.80		KHZ
RF BW	24.6		MHZ
PROC GAIN	243		
MDAP	4		
NCA	1	1	
NO. OF FIL	97		
CHAN CAP	2.68	9.45	MBITS/SEC

COVERAGE AND RESOLUTION

SWATH	137.96		KM
CELLS/SCAN	8		
CELL WIDTH	4.86	5.21	KM
CELL LENGTH	14.56	16.68	KM
SCAN TIME	0.68		SEC
TIME/CELL	0.084		SEC
AZ RES	50.00	53.52	M
RA RES	50.00	16.27	M

SUMMARY TABLE 5

RAW DESIGN PARAMETERS

PARAMETERS	VALUES	UNITS
ANGLE SPAN	7.00	22.00 DEG
LAMBDA	0.033	M
APER LENGTH	3.0	M
AZ RES	50.00	M
RA RES	150.00	M
GRD VEL	7.2	KM/SEC
ALTITUDE	435.0	KM
APER EFF	75.0	PERCENT
LOSS FACTOR	7.0	DB
NOISE FIG	6.0	DB
SIG/NOISE	3.00	DB
REC TEMP	300.0	DEG K
SIGMAX	8.00	-1.00 DB
SIGMIN	-10.00	-15.00 DB

COMPUTED SYSTEM PARAMETERS

SYSTEM TYPE: SEMI-FOCUSED		
APER HEIGHT	1.01	M
XMIT PWR	1.08	12.89 WATTS
PRF	12.00	KHZ
FD	4.80	KHZ
RF BW	8.2	MHZ
PROC GAIN	243	
NCRP	4	
MCA	1	1
NO. OF FIL	97	
CHAN CAP	0.89	3.15 MBITS/SEC

COVERAGE AND RESOLUTION

SWATH	137.96	KM
CELLS/SCAN	8	
CELL WIDTH	4.86	5.21 KM
CELL LENGTH	14.56	16.68 KM
SCAN TIME	0.68	SEC
TIME/CELL	0.084	SEC
AZ RES	50.00	53.52 M
RA RES	150.00	48.80 M

SUMMARY TABLE 6

RAW DESIGN PARAMETERS

PARAMETERS	VALUES	UNITS
ANGLE SPAN	7.00	22.00 DEG
AZ RES	88.38	M
RA RES	150.00	M
LAMBDA	0.033	M
GRD VEL	7.2	KM/SEC
ALTITUDE	435.0	KM
APER LENGTH	3.0	M
APER EFF	75.0	PERCENT
LOSS FACTOR	7.0	DB
SIGMAX	8.00	-1.00 DB
SIGMIN	-10.00	-15.00 DB
NOISE FIG	6.0	DB
REC TEMP	300.0	DEG K
SIG/NOISE	3.00	DB

COMPUTED SYSTEM PARAMETERS

SYSTEM TYPE: UNFOCUSED		
APER HEIGHT	1.01	M
XMIT PWR	1.08	12.84 WATTS
PRF	12.00	KHZ
FD	4.80	KHZ
RF BW	8.2	MHZ
PROC GAIN	138	
NCAP	7	
NCA	1	
NO. OF FIL	55	
CHAN CAP	0.51	1.78 MBITS/SEC

COVERAGE AND RESOLUTION

SWATH	137.96	KM
CELLS/SCAN	8	
CELL WIDTH	4.86	5.21 KM
CELL LENGTH	14.56	16.68 KM
SCAN TIME	0.68	SEC
TIME/CELL	0.084	SEC
AZ RES	88.38	94.61 M
RA RES	150.00	48.80 M

SUMMARY TABLE 7

RAW DESIGN PARAMETERS

PARAMETERS		VALUES	UNITS
ANGLE SPAN	7.00	22.00	DEG
AZ RES	50.00		M
RA RES	50.00		M
LAMBDA	0.033		M
GRD VEL	7.2		KM/SEC
ALTITUDE	435.0		KM
APER LENGTH	6.0		M
APER EFF	75.0		PERCENT
LOSS FACTOR	7.0		DB
SIGMAX	8.00	-1.00	DB
SIGMIN	-10.00	-15.00	DB
NOISE FIG	6.0		DB
REC TEMP	300.0		DEG K
SIG/NOISE	3.00		DB

COMPUTED SYSTEM PARAMETERS

SYSTEM TYPE: SEMI-FOCUSED			
APER HEIGHT	0.50		M
XMIT PWR	3.23	38.50	WATTS
PRF	6.00		KHZ
FD	2.40		KHZ
RF BW	24.6		MHZ
PROC GAIN	122		
NCAF	4		
NCA	2	1	
NO. OF FIL	49		
CHAN CAP	2.68	9.45	MBITS/SEC

COVERAGE AND RESOLUTION

SWATH	153.58		KM
CELLS/SCAN	4		
CELL WIDTH	2.43	2.60	KM
CELL LENGTH	29.12	33.37	KM
SCAN TIME	0.34		SEC
TIME/CELL	0.084		SEC
AZ RES	50.00	53.52	M
RA RES	50.00	16.27	M

SUMMARY TABLE 8

RAW DESIGN PARAMETERS

PARAMETERS	VALUES	UNITS
ANGLE SPAN	7.00	22.00 DEG
LAMBDA	0.033	M
APER LENGTH	6.0	M
AZ RES	50.00	M
RA RES	150.00	M
GRD VEL	7.2	KM/SEC
ALTITUDE	435.0	KM
APER EFF	75.0	PERCENT
LOSS FACTOR	7.0	DB
NOISE FIG	6.0	DB
SIG/NOISE	3.00	DB
REC TEMP	300.0	DEG K
SIGMAX	8.00	-1.00 DB
SIGMIN	-10.00	-15.00 DB

COMPUTED SYSTEM PARAMETERS

SYSTEM TYPE: SEMI-FOCUSED

APER HEIGHT	0.50	M
XMIT PWR	1.08	12.83 WATTS
PRF	6.00	KHZ
FD	2.40	KHZ
RF BW	8.2	MHZ
PROC GAIN	122	
NCRP	4	
NCA	2	1
NO. OF FIL	49	
CHAN CAP	0.89	3.15 MBITS/SEC

COVERAGE AND RESOLUTION

SWATH	153.58	KM
CELLS/SCAN	4	
CELL WIDTH	2.43	2.60 KM
CELL LENGTH	29.12	33.37 KM
SCAN TIME	0.34	SEC
TIME/CELL	0.084	SEC
AZ RES	50.00	53.52 M
RA RES	150.00	48.80 M

SUMMARY TABLE 9

RAW DESIGN PARAMETERS

PARAMETERS		VALUES	UNITS
ANGLE SPAN	7.00	22.00	DEG
AZ RES	88.38		M
RA RES	150.00		M
LAMBDA	0.033		M
GRD VEL	7.2		KM/SEC
ALTITUDE	435.0		KM
APER LENGTH	6.0		M
APER EFF	75.0		PERCENT
LOSS FACTOR	7.0		DB
SIGMAX	8.00	-1.00	DB
SIGMIN	-10.00	-15.00	DB
NOISE FIG	6.0		DB
REC TEMP	300.0		DEG K
SIG/NOISE	3.00		DB

COMPUTED SYSTEM PARAMETERS

SYSTEM TYPE: UNFOCUSED			
APER HEIGHT	0.50		M
XMIT PWR	1.08	12.84	WATTS
PRF	6.00		KHZ
FD	2.40		KHZ
RF BW	8.2		MHZ
PROC GAIN	69		
NCAP	7		
NCA	1	1	
NO. OF FIL	28		
CHAN CAP	0.51	1.78	MBITS/SEC

COVERAGE AND RESOLUTION

SWATH	153.58		KM
CELLS/SCAN	4		
CELL WIDTH	2.43	2.60	KM
CELL LENGTH	29.12	33.37	KM
SCAN TIME	0.34		SEC
TIME/CELL	0.084		SEC
AZ RES	88.38	94.61	M
RA RES	150.00	48.80	M

SUMMARY TABLE 10

RAW DESIGN PARAMETERS

PARAMETERS	VALUES		UNITS
ANGLE SPAN	22.00	37.00	DEG
LAMBDA	0.033		M
APER LENGTH	1.0		M
AZ RES	50.00		M
RA RES	50.00		M
GRD VEL	7.2		KM/SEC
ALTITUDE	435.0		KM
APER EFF	75.0		PERCENT
LOSS FACTOR	7.0		DB
NOISE FIG	6.0		DB
SIG/NOISE	3.00		DB
REC TEMP	300.0		DEG K
SIGMAX	-1.00	-5.00	DB
SIGMIN	-15.00	-18.00	DB

COMPUTED SYSTEM PARAMETERS

SYSTEM TYPE: SEMI-FOCUSED			
APER HEIGHT	6.56		M
XMIT PWR	2.68	13.44	WATTS
PRF	38.00		KHZ
FD	14.40		KHZ
RF BW	8.0		MHZ
PROC GAIN	781		
NCAF	2		
NCA	1	1	
NO. OF FIL	312		
CHAN CAP	2.31	5.00	MBITS/SEC

COVERAGE AND RESOLUTION

SWATH	155.06		KM
CELLS/SCAN	52		
CELL WIDTH	15.62	18.14	KM
CELL LENGTH	2.57	3.46	KM
SCAN TIME	2.17		SEC
TIME/CELL	0.042		SEC
AZ RES	50.00	58.05	M
RA RES	50.00	31.12	M

SUMMARY TABLE II

RAW DESIGN PARAMETERS

PARAMETERS	VALUES		UNITS
ANGLE SPAN	22.00	37.00	DEG
LAMBDA	0.033		M
APER LENGTH	1.0		M
AZ RES	50.00		M
RA RES	150.00		M
GRD VEL	7.2		KM/SEC
ALTITUDE	435.0		KM
APER EFF	75.0		PERCENT
LOSS FACTOR	7.0		DB
NOISE FIG	6.0		DB
SIG/NOISE	3.00		DB
REC TEMP	300.0		DEG K
SIGMAX	-1.00	-5.00	DB
SIGMIN	-15.00	-18.00	DB

COMPUTED SYSTEM PARAMETERS

SYSTEM TYPE: SEMI-FOCUSED			
APER HEIGHT	6.56		M
XMIT PWR	0.89	4.48	WATTS
PRF	36.00		KHZ
FD	14.40		KHZ
RF BW	2.7		MHZ
PROC GAIN	781		
NCP	2		
NCR	1	1	
NO. OF FIL	312		
CHAN CAP	0.77	1.67	MBITS/SEC

COVERAGE AND RESOLUTION

SWATH	155.06		KM
CELLS/SCAN	52		
CELL WIDTH	15.62	18.14	KM
CELL LENGTH	2.57	3.46	KM
SCAN TIME	2.17		SEC
TIME/CELL	0.042		SEC
AZ RES	50.00	58.05	M
RA RES	150.00	93.37	M

SUMMARY TABLE 12

RAW DESIGN PARAMETERS

PARAMETERS	VALUES		UNITS
ANGLE SPAN	22.00	37.00	DEG
LAMBDA	0.033		M
APER LENGTH	1.0		M
AZ RES	95.27		M
RA RES	150.00		M
GRD VEL	7.2		KM/SEC
ALTITUDE	435.0		KM
APER EFF	75.0		PERCENT
LOSS FACTOR	7.0		DB
NOISE FIG	6.0		DB
SIG/NOISE	3.00		DB
REC TEMP	300.0		DEG K
SIGMAX	-1.00	-5.00	DB
SIGMIN	-15.00	-18.00	DB

COMPUTED SYSTEM PARAMETERS

SYSTEM TYPE: UNFOCUSED			
APER HEIGHT	6.57		M
XMIT PWR	0.89	4.48	WATTS
PRF	36.00		KHZ
FD	14.40		KHZ
RF BW	2.7		MHZ
PROC GAIN	410		
NCAP	4		
NCA	1	1	
NO. OF FIL	164		
CHAN CAP	0.40	0.87	MBITS/SEC

COVERAGE AND RESOLUTION

SWATH	155.06		KM
CELLS/SCAN	52		
CELL WIDTH	15.64	18.15	KM
CELL LENGTH	2.57	3.46	KM
SCAN TIME	2.17		SEC
TIME/CELL	0.042		SEC
AZ RES	95.27	110.61	M
RA RES	150.00	93.37	M

SUMMARY TABLE 13

RAW DESIGN PARAMETERS

PARAMETERS	VALUES		UNITS
ANGLE SPAN	22.00	37.00	DEG
LAMBDA	0.033		M
APER LENGTH	3.0		M
AZ RES	50.00		M
RA RES	50.00		M
GRD VEL	7.2		KM/SEC
ALTITUDE	435.0		KM
APER EFF	75.0		PERCENT
LOSS FACTOR	7.0		DB
NOISE FIG	6.0		DB
SIG/NOISE	3.00		DB
REC TEMP	300.0		DEG K
SIGMAX	-1.00	-5.00	DB
SIGMIN	-15.00	-18.00	DB

COMPUTED SYSTEM PARAMETERS

SYSTEM TYPE: SEMI-FOCUSED			
APER HEIGHT	2.19		M
XMIT PWR	2.68	13.46	WATTS
PRF	12.00		KHZ
FD	4.80		KHZ
RF BW	8.0		MHZ
PROC GAIN	260		
NCRP	2		
NCA	1	1	
NO. OF FIL	104		
CHAN CAP	2.26	4.90	MBITS/SEC

COVERAGE AND RESOLUTION

SWATH	161.09		KM
CELLS/SCAN	17		
CELL WIDTH	5.21	6.05	KM
CELL LENGTH	7.71	10.39	KM
SCAN TIME	0.72		SEC
TIME/CELL	0.043		SEC
AZ RES	50.00	58.05	M
RA RES	50.00	31.12	M

SUMMARY TABLE 14

RAW DESIGN PARAMETERS

PARAMETERS	VALUES	UNITS
ANGLE SPAN	22.00	37.00 DEG
LAMBDA	0.033	M
APER LENGTH	3.0	M
AZ RES	50.00	M
RA RES	150.00	M
GRD VEL	7.2	KM/SEC
ALTITUDE	435.0	KM
APER EFF	75.0	PERCENT
LOSS FACTOR	7.0	DB
NOISE FIG	6.0	DB
SIG/NOISE	3.00	DB
REC TEMP	300.0	DEG K
SIGMAX	-1.00	DB
SIGMIN	-15.00	-18.00 DB

COMPUTED SYSTEM PARAMETERS

PARAMETERS	VALUES	UNITS
SYSTEM TYPE:	SEMI-FOCUSED	
APER HEIGHT	2.19	M
XMIT PWR	0.89	4.49 WATTS
PRF	12.00	KHZ
FD	4.80	KHZ
RF BW	2.7	MHZ
PROC GAIN	260	
NCAP	2	
NCA	1	1
NO. OF FIL	104	
CHAN CAP	0.75	1.63 MBITS/SEC

COVERAGE AND RESOLUTION

PARAMETERS	VALUES	UNITS
SWATH	161.09	KM
CELLS/SCAN	17	
CELL WIDTH	5.21	6.05 KM
CELL LENGTH	7.71	10.39 KM
SCAN TIME	0.72	SEC
TIME/CELL	0.043	SEC
AZ RES	50.00	58.05 M
RA RES	150.00	93.37 M

SUMMARY TABLE 15

RAW DESIGN PARAMETERS

PARAMETERS	VALUES	UNITS
ANGLE SPAN	22.00	37.00 DEG
LAMBDA	0.033	M
APER LENGTH	3.0	M
AZ RES	95.23	M
RA RES	150.00	M
GRD VEL	7.2	KM/SEC
ALTITUDE	435.0	KM
APER EFF	75.0	PERCENT
LOSS FACTOR	7.0	DB
NOISE FIG	6.0	DB
SIG/NOISE	3.00	DB
REC TEMP	300.0	DEG K
SIGMAX	-1.00	-5.00 DB
SIGMIN	-15.00	-18.00 DB

COMPUTED SYSTEM PARAMETERS

SYSTEM TYPE: UNFOCUSED		
APER HEIGHT	2.19	M
XMIT PWR	0.89	4.47 WATTS
PRF	12.00	KHZ
FD	4.80	KHZ
RF BW	2.7	MHZ
PROC GAIN	137	
NCAP	4	
NCA	1	1
NO. OF FIL	55	
CHAN CAP	0.40	0.86 MBITS/SEC

COVERAGE AND RESOLUTION

SWATH	161.09	KM
CELLS/SCAN	17	
CELL WIDTH	5.21	6.05 KM
CELL LENGTH	7.71	10.39 KM
SCAN TIME	0.72	SEC
TIME/CELL	0.043	SEC
AZ RES	95.23	110.56 M
RA RES	150.00	93.37 M

SUMMARY TABLE 16

RAW DESIGN PARAMETERS

PARAMETERS		VALUES	UNITS
ANGLE SPAN	7.00	22.00	DEG
AZ RES	50.00		M
RA RES	50.00		M
LAMBDA	0.063		M
GRD VEL	7.2		KM/SEC
ALTITUDE	435.0		KM
APER LENGTH	3.0		M
APER EFF	75.0		PERCENT
LOSS FACTOR	7.0		DB
SIGMAX	12.00	2.00	DB
SIGMIN	-4.00	-8.00	DB
NOISE FIG	5.0		DB
REC TEMP	300.0		DEG K
SIG/NOISE	3.00		DB

COMPUTED SYSTEM PARAMETERS

SYSTEM TYPE: SEMI-FOCUSED			
APER HEIGHT	1.92		M
XMIT PWR	0.34	3.22	WATTS
PRF	12.00		KHZ
FD	4.80		KHZ
RF BW	24.6		MHZ
PROC GAIN	463		
NCAP	4		
NCA	1	1	
NO. OF FIL	185		
CHAN CAP	2.35	8.27	MBITS/SEC

COVERAGE AND RESOLUTION

SWATH	137.96		KM
CELLS/SCAN	8		
CELL WIDTH	9.26	9.91	KM
CELL LENGTH	14.56	16.68	KM
SCAN TIME	1.29		SEC
TIME/CELL	0.161		SEC
AZ RES	50.00	53.52	M
RA RES	50.00	16.27	M

SUMMARY TABLE 17

RAW DESIGN PARAMETERS

PARAMETERS	VALUES	UNITS
ANGLE SPAN	7.00	22.00 DEG
AZ RES	50.00	M
RA RES	150.00	M
LAMBDA	0.063	M
GRD VEL	7.2	KM/SEC
ALTITUDE	435.0	KM
APER LENGTH	3.0	M
APER EFF	75.0	PERCENT
LOSS FACTOR	7.0	DB
SIGMAX	12.00	DB
SIGMIN	-4.00	-8.00 DB
NOISE FIG	6.0	DB
REC TEMP	300.0	DEG K
SIG/NOISE	3.00	DB

COMPUTED SYSTEM PARAMETERS

SYSTEM TYPE: SEMI-FOCUSED		
APER HEIGHT	1.92	M
XMIT PWR	0.14	1.35 WATTS
PRF	12.00	KHZ
FD	4.80	KHZ
RF BW	8.2	MHZ
PROC GAIN	463	
NCAP	4	
NCA	1	1
NO. OF FIL	185	
CHAN CAP	0.78	2.76 MBITS/SEC

COVERAGE AND RESOLUTION

SWATH	137.96	KM
CELLS/SCAN	8	
CELL WIDTH	9.26	9.91 KM
CELL LENGTH	14.56	16.68 KM
SCAN TIME	1.29	SEC
TIME/CELL	0.161	SEC
AZ RES	50.00	53.52 M
RA RES	150.00	48.80 M

SUMMARY TABLE 18

RAW DESIGN PARAMETERS

PARAMETERS	VALUES	UNITS
COVERAGE	7.00	DEG
AZ RES	121.95	M
RA RES	150.00	M
LAMBDA	0.063	M
GRD VEL	7.2	KM/SEC
ALTITUDE	435.0	KM
APER LENGTH	3.0	M
APER EFF	75.0	PERCENT
LOSS FACTOR	7.0	DB
SIGMAX	12.00	DB
SIGMIN	-4.00	DB
NOISE FIG	5.0	DB
REC TEMP	300.0	DEG K
SIG/NOISE	3.00	DB

COMPUTED SYSTEM PARAMETERS

SYSTEM TYPE: UNFOCUSED		
APER HEIGHT	1.92	M
XMIT PWR	0.11	1.07 WATTS
PRF	12.00	KHZ
FD	4.80	KHZ
RF BW	8.2	MHZ
PROC GAIN	190	
NCAF	10	
NCA	1	1
NO. OF FIL	76	
CHAN CAP	0.32	1.13 MBITS/SEC

COVERAGE AND RESOLUTION

SWATH	137.96	KM
CELLS/SCAN	8	
CELL WIDTH	9.26	9.91 KM
CELL LENGTH	14.56	16.68 KM
SCAN TIME	1.29	SEC
TIME/CELL	0.161	SEC
AZ RES	121.95	130.55 M
RA RES	150.00	48.80 M

SUMMARY TABLE 19

RAW DESIGN PARAMETERS

PARAMETERS		VALUES	UNITS
ANGLE SPAN	7.00	22.00	DEG
AZ RES	50.00		M
RA RES	50.00		M
LAMBDA	0.063		M
GRD VEL	7.2		KM/SEC
ALTITUDE	435.0		KM
APER LENGTH	6.0		M
APER EFF	75.0		PERCENT
LOSS FACTOR	7.0		DB
SIGMAX	12.00	2.00	DB
SIGMIN	-4.00	-8.00	DB
NOISE FIG	5.0		DB
REC TEMP	300.0		DEG K
SIG/NOISE	3.00		DB

COMPUTED SYSTEM PARAMETERS

SYSTEM TYPE: SEMI-FOCUSED			
APER HEIGHT	0.96		M
XMIT PWR	0.34	3.21	WATTS
PRF	6.00		KHZ
FD	2.40		KHZ
RF BW	24.6		MHZ
PROC GAIN	232		
NCAP	4		
NCA	4	1	
NO. OF FIL	93		
CHAN CAP	2.35	8.27	MBITS/SEC

COVERAGE AND RESOLUTION

SWATH	153.58		KM
CELLS/SCAN	4		
CELL WIDTH	4.63	4.96	KM
CELL LENGTH	29.12	33.37	KM
SCAN TIME	0.64		SEC
TIME/CELL	0.161		SEC
AZ RES	50.00	53.52	M
RA RES	50.00	16.27	M

SUMMARY TABLE 20

RAW DESIGN PARAMETERS

PARAMETERS	VALUES	UNITS
ANGLE SPAN	7.00	22.00 DEG
LAMBDA	0.063	M
APER LENGTH	6.0	M
AZ RES	50.00	M
RA RES	150.00	M
GRD VEL	7.2	KM/SEC
ALTITUDE	435.0	KM
APER EFF	75.0	PERCENT
LOSS FACTOR	7.0	DB
NOISE FIG	6.0	DB
SIG/NOISE	3.00	DB
REC TEMP	300.0	DEG K
SIGMAX	12.00	DB
SIGMIN	-4.00	DB

COMPUTED SYSTEM PARAMETERS

PARAMETERS	VALUES	UNITS
SYSTEM TYPE:	SEMI-FOCUSED	
APER HEIGHT	0.96	M
XMIT PWR	0.14	1.35 WATTS
PRF	6.00	KHZ
FD	2.40	KHZ
RF BW	8.2	MHZ
PROC GAIN	232	
NCAP	4	
NCA	4	1
NO. OF FIL	93	
CHAN CAP	0.78	2.76 MBITS/SEC

COVERAGE AND RESOLUTION

PARAMETERS	VALUES	UNITS
SWATH	153.58	KM
CELLS/SCAN	4	
CELL WIDTH	4.63	4.96 KM
CELL LENGTH	29.12	33.37 KM
SCAN TIME	0.64	SEC
TIME/CELL	0.161	SEC
AZ RES	50.00	53.52 M
RA RES	150.00	48.80 M

SUMMARY TABLE 21

RAW DESIGN PARAMETERS

PARAMETERS	VALUES	UNITS
ANGLE SPAN	7.00	22.00 DEG
AZ RES	121.95	M
RA RES	150.00	M
LAMBDA	0.063	M
GRD VEL	7.2	KM/SEC
ALTITUDE	435.0	KM
APER LENGTH	6.0	M
APER EFF	75.0	PERCENT
LOSS FACTOR	7.0	DB
SIGMAX	12.00	2.00 DB
SIGMIN	-4.00	-8.00 DB
NOISE FIG	5.0	DB
REC TEMP	300.0	DEG K
SIG/NOISE	3.00	DB

COMPUTED SYSTEM PARAMETERS

SYSTEM TYPE: UNFOCUSED		
APER HEIGHT	0.96	M
XMIT PWR	0.11	1.07 WATTS
PRF	6.00	KHZ
FD	2.40	KHZ
RF BW	8.2	MHZ
PROC GAIN	95	
NCAF	10	
NCA	1	1
NO. OF FIL	38	
CHAN CAP	0.32	1.13 MBITS/SEC

COVERAGE AND RESOLUTION

SWATH	153.58	KM
CELLS/SCAN	4	
CELL WIDTH	4.63	4.96 KM
CELL LENGTH	29.12	33.37 KM
SCAN TIME	0.64	SEC
TIME/CELL	0.161	SEC
AZ RES	121.95	130.55 M
RA RES	150.00	48.80 M

SUMMARY TABLE 22

RAW DESIGN PARAMETERS

PARAMETERS	VALUES		UNITS
ANGLE SPAN	22.00	37.00	DEG
LAMBDA	0.063		M
APER LENGTH	3.0		M
AZ RES	50.00		M
RA RES	50.00		M
GRD VEL	7.2		KM/SEC
ALTITUDE	435.0		KM
APER EFF	75.0		PERCENT
LOSS FACTOR	7.0		DB
NOISE FIG	5.0		DB
SIG/NOISE	3.00		DB
REC TEMP	300.0		DEG K
SIGMAX	2.00	-2.00	DB
SIGMIN	-3.00	-12.00	DB

COMPUTED SYSTEM PARAMETERS

SYSTEM TYPE: SEMI-FOCUSED			
APER HEIGHT	4.16		M
XMIT PWR	0.22	1.41	WATTS
PRF	12.00		KHZ
FD	4.80		KHZ
RF BW	8.0		MHZ
PROC GAIN	496		
NCAP	2		
NCA	1	1	
NO. OF FIL	198		
CHAN CAP	1.89	4.02	MBITS/SEC

COVERAGE AND RESOLUTION

SWATH	161.09		KM
CELLS/SCAN	17		
CELL WIDTH	9.91	11.51	KM
CELL LENGTH	7.71	10.39	KM
SCAN TIME	1.38		SEC
TIME/CELL	0.081		SEC
AZ RES	50.00	58.05	M
RA RES	50.00	31.12	M

SUMMARY TABLE 23

RAW DESIGN PARAMETERS

PARAMETERS	VALUES	UNITS
ANGLE SPAN	22.00 37.00	DEG
LAMBDA	0.063	M
APER LENGTH	3.0	M
AZ RES	50.00	M
RA RES	150.00	M
GRD VEL	7.2	KM/SEC
ALTITUDE	435.0	KM
APER EFF	75.0	PERCENT
LOSS FACTOR	7.0	DB
NOISE FIG	5.0	DB
SIG/NOISE	3.00	DB
REC TEMP	300.0	DEG K
SIGMAX	2.00 -2.00	DB
SIGMIN	-8.00 -12.00	DB

COMPUTED SYSTEM PARAMETERS

SYSTEM TYPE: SEMI-FOCUSED		
APER HEIGHT	4.16	M
XMIT PWR	0.07 0.47	WATTS
PRF	12.00	KHZ
FD	4.80	KHZ
RF BW	2.7	MHZ
PROC GAIN	496	
NCAP	2	
NCA	1 1	
NO. OF FIL	198	
CHAN CAP	0.63 1.36	MBITS/SEC

COVERAGE AND RESOLUTION

SWATH	161.09	KM
CELLS/SCAN	17	
CELL WIDTH	9.91 11.51	KM
CELL LENGTH	7.71 10.39	KM
SCAN TIME	1.38	SEC
TIME/CELL	0.081	SEC
AZ RES	50.00 58.05	M
RA RES	150.00 93.37	M

SUMMARY TABLE 24

RAW DESIGN PARAMETERS

PARAMETERS	VALUES		UNITS
ANGLE SPAN	22.00	37.00	DEG
LAMBDA	0.063		M
APER LENGTH	3.0		M
AZ RES	131.40		M
RA RES	150.00		M
GRD VEL	7.2		KM/SEC
ALTITUDE	435.0		KM
APER EFF	75.0		PERCENT
LOSS FACTOR	7.0		DB
NOISE FIG	5.0		DB
SIG/NOISE	3.00		DB
REC TEMP	300.0		DEG K
SIGMAX	2.00	-2.00	DB
SIGMIN	-8.00	-12.00	DB

COMPUTED SYSTEM PARAMETERS

SYSTEM TYPE: UNFOCUSED			
APER HEIGHT	4.16		M
XMIT PWR	0.07	0.47	WATTS
PRF	12.00		KHZ
FD	4.80		KHZ
RF BW	2.7		MHZ
PROC GAIN	189		
NCAP	5		
NCA	1	1	
NO. OF FIL	75		
CHAN CAP	0.24	0.52	MBITS/SEC

COVERAGE AND RESOLUTION

SWATH	161.09		KM
CELLS/SCAN	17		
CELL WIDTH	9.91	11.51	KM
CELL LENGTH	7.71	10.39	KM
SCAN TIME	1.38		SEC
TIME/CELL	0.081		SEC
AZ RES	131.40	152.55	M
RA RES	150.00	93.37	M

SUMMARY TABLE 25

RAW DESIGN PARAMETERS

PARAMETERS	VALUES	UNITS
ANGLE SPAN	22.00	37.00 DEG
LAMBDA	0.063	M
APER LENGTH	6.0	M
AZ RES	50.00	M
RA RES	50.00	M
GRD VEL	7.2	KM/SEC
ALTITUDE	435.0	KM
APER EFF	75.0	PERCENT
LOSS FACTOR	7.0	DB
NOISE FIG	5.0	DB
SIG/NOISE	3.00	DB
REC TEMP	300.0	DEG K
SIGMAX	2.00	-2.00 DB
SIGMIN	-8.00	-12.00 DB

COMPUTED SYSTEM PARAMETERS

SYSTEM TYPE: SEMI-FOCUSED		
APER HEIGHT	2.08	M
XMIT PWR	0.22	1.41 WATTS
PRF	6.00	KHZ
FD	2.40	KHZ
RF BW	8.0	MHZ
PROC GAIN	248	
NCAP	2	
NCA	1	1
NO. OF FIL	99	
CHAN CAP	2.00	4.32 MBITS/SEC

COVERAGE AND RESOLUTION

SWATH	170.14	KM
CELLS/SCAN	9	
CELL WIDTH	4.96	5.76 KM
CELL LENGTH	15.41	20.77 KM
SCAN TIME	0.69	SEC
TIME/CELL	0.077	SEC
AZ RES	50.00	58.05 M
RA RES	50.00	31.12 M

SUMMARY TABLE 26

RAW DESIGN PARAMETERS

PARAMETERS	VALUES		UNITS
ANGLE SPAN	22.00	37.00	DEG
LAMBDA	0.063		M
APER LENGTH	6.0		M
AZ RES	50.00		M
RA RES	150.00		M
GRD VEL	7.2		KM/SEC
ALTITUDE	435.0		KM
APER EFF	75.0		PERCENT
LOSS FACTOR	7.0		DB
NOISE FIG	5.0		DB
SIG/NOISE	3.00		DB
REC TEMP	300.0		DEG K
SIGMAX	2.00	-2.00	DB
SIGMIN	-8.00	-12.00	DB

COMPUTED SYSTEM PARAMETERS

SYSTEM TYPE: SEMI-FOCUSED

APER HEIGHT	2.08		M
XMIT PWR	0.07	0.47	WATTS
PRF	6.00		KHZ
FD	2.40		KHZ
RF BW	2.7		MHZ
PROC GAIN	248		
NCAP	2		
NCA	1	1	
NO. OF FIL	99		
CHAN CAP	0.67	1.44	MBITS/SEC

COVERAGE AND RESOLUTION

SWATH	170.14		KM
CELLS/SCAN	9		
CELL WIDTH	4.96	5.76	KM
CELL LENGTH	15.41	20.77	KM
SCAN TIME	0.69		SEC
TIME/CELL	0.077		SEC
AZ RES	50.00	58.05	M
RA RES	150.00	93.37	M

SUMMARY TABLE 27

RAW DESIGN PARAMETERS

PARAMETERS	VALUES		UNITS
ANGLE SPAN	22.00	37.00	DEG
LAMBDA	0.063		M
APER LENGTH	6.0		M
AZ RES	131.40		M
RA RES	150.00		M
GRD VEL	7.2		KM/SEC
ALTITUDE	435.0		KM
APER EFF	75.0		PERCENT
LOSS FACTOR	7.0		DB
NOISE FIG	5.0		DB
SIG/NOISE	3.00		DB
REC TEMP	300.0		DEG K
SIGMAX	2.00	-2.00	DB
SIGMIN	-8.00	-12.00	DB

COMPUTED SYSTEM PARAMETERS

SYSTEM TYPE: UNFOCUSED			
APER HEIGHT	2.08		M
XMIT PWR	0.07	0.47	WATTS
PRF	6.00		KHZ
FD	2.40		KHZ
RF BW	2.7		MHZ
PROC GAIN	94		
NCAP	5		
NCA	1	1	
NO. OF FIL	38		
CHAN CAP	0.25	0.55	MBITS/SEC

COVERAGE AND RESOLUTION

SWATH	170.14		KM
CELLS/SCAN	9		
CELL WIDTH	4.96	5.76	KM
CELL LENGTH	15.41	20.77	KM
SCAN TIME	0.69		SEC
TIME/CELL	0.077		SEC
AZ RES	131.40	152.55	M
RA RES	150.00	93.37	M

SUMMARY TABLE 28

RAW DESIGN PARAMETERS

PARAMETERS	VALUES	UNITS
COVERAGE	7.00	22.00 DEG
AZ RES	50.00	M
RA RES	50.00	M
LAMBDA	0.080	M
GRD VEL	7.2	KM/SEC
ALTITUDE	435.0	KM
APER LENGTH	3.0	M
APER EFF	75.0	PERCENT
LOSS FACTOR	7.0	DB
SIGMAX	5.00	3.00 DB
SIGMIN	-5.00	-12.00 DB
NOISE FIG	3.0	DB
REC TEMP	300.0	DEG K
SIG/NOISE	3.00	DB

COMPUTED SYSTEM PARAMETERS

SYSTEM TYPE: SEMI-FOCUSED		
APER HEIGHT	2.43	M
XMIT PWR	0.21	4.04 WATTS
PRF	12.00	KHZ
FD	4.80	KHZ
RF BW	24.6	MHZ
PROC GAIN	584	
NCAP	4	
NCA	2	1
NO. OF FIL	234	
CHAN CAP	2.01	7.09 MBITS/SEC

COVERAGE AND RESOLUTION

SWATH	137.96	KM
CELLS/SCAN	8	
CELL WIDTH	11.69	12.51 KM
CELL LENGTH	14.56	16.68 KM
SCAN TIME	1.62	SEC
TIME/CELL	0.203	SEC
AZ RES	50.00	53.52 M
RA RES	50.00	16.27 M

SUMMARY TABLE 29

RAW DESIGN PARAMETERS

PARAMETERS	VALUES	UNITS
ANGLE SPAN	7.00	22.00 DEG
LAMBDA	0.080	M
APER LENGTH	3.0	M
AZ RES	50.00	M
RA RES	150.00	M
GRD VEL	7.2	KM/SEC
ALTITUDE	435.0	KM
APER EFF	75.0	PERCENT
LOSS FACTOR	7.0	DB
NOISE FIG	3.0	DB
SIG/NOISE	3.00	DB
REC TEMP	300.0	DEG K
SIGMAX	5.00	3.00 DB
SIGMIN	-5.00	-12.00 DB

COMPUTED SYSTEM PARAMETERS

SYSTEM TYPE:	SEMI-FOCUSED	
APER HEIGHT	2.43	M
XMIT PWR	0.07	1.35 WATTS
PRF	12.00	KHZ
FD	4.80	KHZ
RF BW	8.2	MHZ
PRDC GAIN	584	
NCAP	4	
NCA	2	1
NO. OF FIL	234	
CHAN CAP	0.67	2.36 MBITS/SEC

COVERAGE AND RESOLUTION

SWATH	137.96	KM
CELLS/SCAN	8	
CELL WIDTH	11.69	12.51 KM
CELL LENGTH	14.56	16.68 KM
SCAN TIME	1.62	SEC
TIME/CELL	0.203	SEC
AZ RES	50.00	53.52 M
RA RES	150.00	48.80 M

SUMMARY TABLE 30

RAW DESIGN PARAMETERS

PARAMETERS	VALUES	UNITS
ANGLE SPAN	7.00	22.00 DEG
AZ RES	136.99	M
RA RES	150.00	M
LAMBDA	0.080	M
GRD VEL	7.2	KM/SEC
ALTITUDE	435.0	KM
APER LENGTH	3.0	M
APER EFF	75.0	PERCENT
LOSS FACTOR	7.0	DB
SIGMAX	5.00	3.00 DB
SIGMIN	-5.00	-12.00 DB
NOISE FIG	3.0	DB
REC TEMP	300.0	DEG K
SIG/NOISE	3.00	DB

COMPUTED SYSTEM PARAMETERS

SYSTEM TYPE: UNFOCUSED		
APER HEIGHT	2.43	M
XMIT PWR	0.07	1.35 WATTS
PRF	12.00	KHZ
FD	4.80	KHZ
RF BW	8.2	MHZ
PROC GAIN	213	
NCAP	11	
NCA	1	1
NO. OF FIL	85	
CHAN CAP	0.24	0.86 MBITS/SEC

COVERAGE AND RESOLUTION

SMATH	137.96	KM
CELLS/SCAN	8	
CELL WIDTH	11.69	12.51 KM
CELL LENGTH	14.56	16.68 KM
SCAN TIME	1.62	SEC
TIME/CELL	0.203	SEC
AZ RES	136.99	146.65 M
RA RES	150.00	48.80 M

SUMMARY TABLE 31

RAW DESIGN PARAMETERS

PARAMETERS	VALUES	UNITS
COVERAGE	7.00	22.00 DEG
AZ RES	50.00	M
RA RES	50.00	M
LAMBDA	0.080	M
GRD VEL	7.2	KM/SEC
ALTITUDE	435.0	KM
APER LENGTH	6.0	M
APER EFF	75.0	PERCENT
LOSS FACTOR	7.0	DB
SIGMAX	5.00	3.00 DB
SIGMIN	-5.00	-12.00 DB
NOISE FIG	3.0	DB
REC TEMP	300.0	DEG K
SIG/NOISE	3.00	DB

COMPUTED SYSTEM PARAMETERS

SYSTEM TYPE:	SEMI-FOCUSED	
APER HEIGHT	1.21	M
XMIT PWR	0.21	4.04 WATTS
PRF	6.00	KHZ
FD	2.40	KHZ
RF BW	24.6	MHZ
PREC GAIN	292	
NCAP	4	
NCA	5	1
NO. OF FIL	117	
CHAN CAP	2.01	7.09 MBITS/SEC

COVERAGE AND RESOLUTION

SWATH	153.58	KM
CELLS/SCAN	4	
CELL WIDTH	5.84	6.26 KM
CELL LENGTH	29.12	33.37 KM
SCAN TIME	0.81	SEC
TIME/CELL	0.203	SEC
AZ RES	50.00	53.52 M
RA RES	50.00	16.27 M

SUMMARY TABLE 32

RAW DESIGN PARAMETERS

PARAMETERS	VALUES	UNITS
ANGLE SPAN	7.00	22.00 DEG
LAMBDA	0.080	M
APER LENGTH	6.0	M
AZ RES	50.00	M
RA RES	150.00	M
GRD VEL	7.2	KM/SEC
ALTITUDE	435.0	KM
APER EFF	75.0	PERCENT
LOSS FACTOR	7.0	DB
NOISE FIG	3.0	DB
SIG/NOISE	3.00	DB
REC TEMP	300.0	DEG K
SIGMAX	5.00	DB
SIGMIN	-5.00	-12.00 DB

COMPUTED SYSTEM PARAMETERS

SYSTEM TYPE: SEMI-FOCUSED		
APER HEIGHT	1.21	M
XMIT PWR	0.07	1.35 WATTS
PRF	6.00	KHZ
FD	2.40	KHZ
RF BW	8.2	MHZ
PROC GAIN	292	
NCAP	4	
NCA	5	1
NO. OF FIL	117	
CHAN CAP	0.67	2.36 MBITS/SEC

COVERAGE AND RESOLUTION

SWATH	153.58	KM
CELLS/SCAN	4	
CELL WIDTH	5.84	6.26 KM
CELL LENGTH	29.12	33.37 KM
SCAN TIME	0.81	SEC
TIME/CELL	0.203	SEC
AZ RES	50.00	53.52 M
RA RES	150.00	48.80 M

SUMMARY TABLE 33

RAW DESIGN PARAMETERS

PARAMETERS	VALUES	UNITS
ANGLE SPAN	7.00	22.00 DEG
AZ RES	136.99	M
RA RES	150.00	M
LAMBDA	0.080	M
GRD VEL	7.2	KM/SEC
ALTITUDE	435.0	KM
APER LENGTH	6.0	M
APER EFF	75.0	PERCENT
LOSS FACTOR	7.0	DB
SIGMAX	5.00	3.00 DB
SIGMIN	-5.00	-12.00 DB
NOISE FIG	3.0	DB
REC TEMP	300.0	DEG K
SIG/NOISE	3.00	DB

COMPUTED SYSTEM PARAMETERS

PARAMETERS	VALUES	UNITS
SYSTEM TYPE: UNFOCUSED		
APER HEIGHT	1.21	M
XMIT PWR	0.07	1.34 WATTS
PRF	6.00	KHZ
FB	2.40	KHZ
RF BW	8.2	MHZ
PROC GAIN	107	
NCAF	11	
NCA	1	1
NO. OF FIL	4	
CHAN CAP	0.24	0.86 MBITS/SEC

COVERAGE AND RESOLUTION

PARAMETERS	VALUES	UNITS
SWATH	133.58	KM
CELLS/SCAN	4	
CELL WIDTH	5.84	6.26 KM
CELL LENGTH	29.12	33.37 KM
SCAN TIME	0.81	SEC
TIME/CELL	0.203	SEC
AZ RES	136.99	146.65 M
RA RES	150.00	48.80 M

SUMMARY TABLE 34

RAW DESIGN PARAMETERS

PARAMETERS	VALUES		UNITS
ANGLE SPAN	22.00	37.00	DEG
LAMBDA	0.080		M
APER LENGTH	3.0		M
AZ RES	50.00		M
RA RES	50.00		M
GRD VEL	7.2		KM/SEC
ALTITUDE	435.0		KM
APER EFF	75.0		PERCENT
LOSS FACTOR	7.0		DB
NOISE FIG	5.0		DB
SIG/NOISE	3.00		DB
REC TEMP	300.0		DEG K
SIGMAX	3.00	0.	DB
SIGMIN	-12.00	-15.00	DB

COMPUTED SYSTEM PARAMETERS

SYSTEM TYPE: SEMI-FOCUSED			
APER HEIGHT	5.25		M
XMIT PWR	0.44	2.23	WATTS
PRF	12.00		KHZ
FD	4.80		KHZ
RF BW	8.0		MHZ
PROC GAIN	626		
NCAP	2		
NCA	1	1	
NO. OF FIL	250		
CHAN CAP	2.26	4.90	MBITS/SEC

COVERAGE AND RESOLUTION

SWATH	161.09		KM
CELLS/SCAN	17		
CELL WIDTH	12.51	14.52	KM
CELL LENGTH	7.71	10.39	KM
SCAN TIME	1.74		SEC
TIME/CELL	0.102		SEC
AZ RES	50.00	58.05	M
RA RES	50.00	31.12	M

SUMMARY TABLE 35

RAW DESIGN PARAMETERS

PARAMETERS	VALUES	UNITS
ANGLE SPAN	22.00	37.00 DEG
LAMBDA	0.080	M
APER LENGTH	3.0	M
AZ RES	50.00	M
RA RES	150.00	M
GRD VEL	7.2	KM/SEC
ALTITUDE	435.0	KM
APER EFF	75.0	PERCENT
LOSS FACTOR	7.0	DB
NOISE FIG	3.0	DB
SIG/NOISE	3.00	DB
REC TEMP	300.0	DEG K
SIGMAX	3.00	DB
SIGMIN	-12.00	-15.00 DB

COMPUTED SYSTEM PARAMETERS

SYSTEM TYPE: SEMI-FOCUSED		
APER HEIGHT	5.25	M
XMIT PWR	0.09	0.47 WATTS
PRF	12.00	KHZ
FD	4.80	KHZ
RF BW	2.7	MHZ
PROC GAIN	626	
NCAP	2	
NCA	1	1
NO. OF FIL	250	
CHAN CAP	0.75	1.63 MBITS/SEC

COVERAGE AND RESOLUTION

SWATH	161.09	KM
CELLS/SCAN	17	
CELL WIDTH	12.51	14.52 KM
CELL LENGTH	7.71	10.39 KM
SCAN TIME	1.74	SEC
TIME/CELL	0.102	SEC
AZ RES	50.00	58.05 M
RA RES	150.00	93.37 M

SUMMARY TABLE 36

RAW DESIGN PARAMETERS

PARAMETERS	VALUES		UNITS
ANGLE SPAN	22.00	37.00	DEG
LAMBDA	0.080		M
APER LENGTH	3.0		M
AZ RES	147.60		M
RA RES	150.00		M
GRD VEL	7.2		KM/SEC
ALTITUDE	435.0		KM
APER EFF	75.0		PERCENT
LOSS FACTOR	7.0		DB
NOISE FIG	3.0		DB
SIG/NOISE	3.00		DB
REC TEMP	300.0		DEG K
SIGMAX	3.00	0.	DB
SIGMIN	-12.00	-15.00	DB

COMPUTED SYSTEM PARAMETERS

SYSTEM TYPE: UNFOCUSED

APER HEIGHT	5.25		M
XMIT PWR	0.09	0.47	WATTS
PRF	12.00		KHZ
FD	4.80		KHZ
RF BW	2.7		MHZ
PROC GAIN	212		
NCAP	6		
NCA	1	1	
NO. OF FIL	85		
CHAN CAP	0.26	0.55	MBITS/SEC

COVERAGE AND RESOLUTION

SWATH	161.09		KM
CELLS/SCAN	17		
CELL WIDTH	12.51	14.52	KM
CELL LENGTH	7.71	10.39	KM
SCAN TIME	1.74		SEC
TIME/CELL	0.102		SEC
AZ RES	147.60	171.36	M
RA RES	150.00	93.37	M

SUMMARY TABLE 37

RAW DESIGN PARAMETERS

PARAMETERS	VALUES		UNITS
ANGLE SPAN	22.00	37.00	DEG
LAMBDA	0.080		M
APER LENGTH	6.0		M
AZ RES	50.00		M
RA RES	50.00		M
GRD VEL	7.2		KM/SEC
ALTITUDE	435.0		KM
APER EFF	75.0		PERCENT
LOSS FACTOR	7.0		DB
NOISE FIG	3.0		DB
SIG/NOISE	3.00		DB
REC TEMP	300.0		DEG K
SIGMAX	3.00	0.	DB
SIGMIN	-12.00	-15.00	DB

COMPUTED SYSTEM PARAMETERS

SYSTEM TYPE: SEMI-FOCUSED			
APER HEIGHT	2.63		M
XMIT PWR	0.28	1.40	WATTS
PRF	6.00		KHZ
FD	2.40		KHZ
RF BW	8.0		MHZ
PROC GAIN	313		
NCAP	2		
NCA	1	1	
NO. OF FIL	125		
CHAN CAP	2.40	5.19	MBITS/SEC

COVERAGE AND RESOLUTION

SWATH	170.14		KM
CELLS/SCAN	9		
CELL WIDTH	6.26	7.26	KM
CELL LENGTH	15.41	20.77	KM
SCAN TIME	0.87		SEC
TIME/CELL	0.097		SEC
AZ RES	50.00	58.05	M
RA RES	50.00	31.12	M

SUMMARY TABLE 38

RAW DESIGN PARAMETERS

PARAMETERS	VALUES		UNITS
ANGLE SPAN	22.00	37.00	DEG
LAMBDA	0.080		M
APER LENGTH	6.0		M
AZ RES	50.00		M
RA RES	150.00		M
GRD VEL	7.2		KM/SEC
ALTITUDE	435.0		KM
APER EFF	75.0		PERCENT
LOSS FACTOR	7.0		DB
NOISE FIG	3.0		DB
SIG/NOISE	3.00		DB
REC TEMP	300.0		DEG K
SIGMAX	3.00	0.	DB
SIGMIN	-12.00	-15.00	DB

COMPUTED SYSTEM PARAMETERS

SYSTEM TYPE: SEMI-FOCUSED			
APER HEIGHT	2.63		M
XMIT PWR	0.09	0.47	WATTS
PRF	6.00		KHZ
FD	2.40		KHZ
RF BW	2.7		MHZ
PROC GAIN	313		
NCAP	2		
NCA	1	1	
NO. OF FIL	125		
CHAN CAP	0.80	1.73	MBITS/SEC

COVERAGE AND RESOLUTION

SWATH	170.14		KM
CELLS/SCAN	9		
CELL WIDTH	6.26	7.26	KM
CELL LENGTH	15.41	20.77	KM
SCAN TIME	0.87		SEC
TIME/CELL	0.097		SEC
AZ RES	50.00	58.05	M
RA RES	150.00	93.37	M

SUMMARY TABLE 39

RAW DESIGN PARAMETERS

PARAMETERS		VALUES	UNITS
ANGLE SPAN	22.00	37.00	DEG
LAMBDA	0.080		M
APER LENGTH	6.0		M
AZ RES	147.60		M
RA RES	150.00		M
GRD VEL	7.2		KM/SEC
ALTITUDE	435.0		KM
APER EFF	75.0		PERCENT
LOSS FACTOR	7.0		DB
NOISE FIG	3.0		DB
SIG/NOISE	3.00		DB
REC TEMP	300.0		DEG K
SIGMAX	3.00	0.	DB
SIGMIN	-12.00	-15.00	DB

COMPUTED SYSTEM PARAMETERS

SYSTEM TYPE: UNFOCUSED			
APER HEIGHT	2.63		M
XMIT PWR	0.09	0.47	WATTS
PRF	6.00		KHZ
FD	2.40		KHZ
RF BW	2.7		MHZ
PROC GAIN	106		
NCAP	5		
NCA	1	1	
NO. OF FIL	42		
CHAN CAP	0.27	0.59	MBITS/SEC

COVERAGE AND RESOLUTION

SWATH	170.14		KM
CELLS/SCAN	9		
CELL WIDTH	6.26	7.26	KM
CELL LENGTH	15.41	20.77	KM
SCAN TIME	0.87		SEC
TIME/CELL	0.097		SEC
AZ RES	147.60	171.36	M
RA RES	150.00	93.37	M

SUMMARY TABLE 40

RAW DESIGN PARAMETERS

PARAMETERS	VALUES	UNITS
ANGLE SPAN	10.00 20.00	DEG
LAMBDA	0.214	M
APER LENGTH	6.0	M
AZ RES	50.00	M
RA RES	150.00	M
GRD VEL	7.2	KM/SEC
ALTITUDE	435.0	KM
APER EFF	75.0	PERCENT
LOSS FACTOR	7.0	DB
NOISE FIG	3.0	DB
SIG/NOISE	3.00	DB
REC TEMP	300.0	DEG K
SIGMAX	12.00 5.00	DB
SIGNIN	-5.00 -10.00	DB

COMPUTED SYSTEM PARAMETERS

SYSTEM TYPE: SEMI-FOCUSED		
APER HEIGHT	2.88	M
XMIT PWR	0.03 0.25	WATTS
PRF	6.00	KHZ
FD	2.40	KHZ
RF BW	5.8	MHZ
PROC GAIN	788	
NCAP	8	
NCA	10 6	
NO. OF FIL	315	
CHAN CAP	0.45 0.97	MBITS/SEC

COVERAGE AND RESOLUTION

SWATH	116.54	KM
CELLS/SCAN	2	
CELL WIDTH	15.75 16.51	KM
CELL LENGTH	33.28 36.55	KM
SCAN TIME	2.19	SEC
TIME/CELL	1.094	SEC
AZ RES	50.00 52.40	M
RA RES	150.00 76.16	M

SUMMARY TABLE 41

RAW DESIGN PARAMETERS

PARAMETERS	VALUES	UNITS
ANGLE SPAN	10.00 20.00	DEG
LAMBDA	0.214	M
APER LENGTH	10.0	M
AZ RES	50.00	M
RA RES	150.00	M
GRD VEL	7.2	KM/SEC
ALTITUDE	435.0	KM
APER EFF	75.0	PERCENT
LOSS FACTOR	7.0	DB
NOISE FIG	3.0	DB
SIG/NOISE	3.00	DB
REC TEMP	300.0	DEG K
SIGMAX	12.00 5.00	DB
SIGMIN	-5.00 -10.00	DB

COMPUTED SYSTEM PARAMETERS

SYSTEM TYPE: SEMI-FOCUSED

APER HEIGHT	1.73	M
XMIT PWR	0.03 0.25	WATTS
PRF	3.60	KHZ
FD	1.44	KHZ
RF BW	5.8	MHZ
PRDC GAIN	473	
NCAF	10	
NCA	21 3	
NO. OF FIL	189	
CHAN CAP	0.37 0.81	MBITS/SEC

COVERAGE AND RESOLUTION

SWATH	139.81	KM
CELLS/SCAN	1	
CELL WIDTH	9.45 9.91	KM
CELL LENGTH	55.46 60.91	KM
SCAN TIME	1.31	SEC
TIME/CELL	1.313	SEC
AZ RES	50.00 52.40	M
RA RES	150.00 76.16	M

SUMMARY TABLE 42

RAW DESIGN PARAMETERS

PARAMETERS	VALUES	UNITS
ANGLE SPAN	20.00 30.00	DEG
LAMBDA	0.214	M
APER LENGTH	6.0	M
AZ RES	50.00	M
RA RES	150.00	M
GRD VEL	7.2	KM/SEC
ALTITUDE	435.0	KM
APER EFF	75.0	PERCENT
LOSS FACTOR	7.0	DB
NOISE FIG	3.0	DB
SIG/NOISE	3.00	DB
REC TEMP	300.0	DEG K
SIGMAX	5.00 2.00	DB
SIGMIN	-10.00 -15.00	DB

COMPUTED SYSTEM PARAMETERS

SYSTEM TYPE: SEMI-FOCUSED		
APER HEIGHT	4.96	M
XMIT PWR	0.04 0.25	WATTS
PRF	6.00	KHZ
FD	2.40	KHZ
RF BW	2.9	MHZ
PROC GAIN	826	
NCAP	4	
NCA	5 2	
NO. OF FIL	330	
CHAN CAP	0.57 0.98	MBITS/SEC

COVERAGE AND RESOLUTION

SWATH	115.94	KM
CELLS/SCAN	4	
CELL WIDTH	16.51 17.92	KM
CELL LENGTH	21.23 25.00	KM
SCAN TIME	2.29	SEC
TIME/CELL	0.573	SEC
AZ RES	50.00 54.25	M
RA RES	150.00 102.61	M

SUMMARY TABLE 43

RAW DESIGN PARAMETERS

PARAMETERS	VALUES	UNITS
ANGLE SPAN	20.00 30.00	DEG
LAMBDA	0.214	M
APER LENGTH	10.0	M
AZ RES	50.00	M
RA RES	150.00	M
GRD VEL	7.2	KM/SEC
ALTITUDE	435.0	KM
APER EFF	75.0	PERCENT
LOSS FACTOR	7.0	DB
NOISE FIG	3.0	DB
SIG/NOISE	3.00	DB
REC TEMP	300.0	DEG K
SIGMAX	5.00 2.00	DB
SIGMIN	-10.00 -15.00	DB

COMPUTED SYSTEM PARAMETERS

SYSTEM TYPE: SEMI-FOCUSED

APER HEIGHT	2.98	M
XMIT PWR	0.04 0.25	WATTS
PRF	3.60	KHZ
FD	1.44	KHZ
RF BW	2.9	MHZ
PROC GAIN	495	
NCAP	5	
NCA	3	1
NO. OF FIL	198	
CHAN CAP	0.48 0.82	MBITS/SEC

COVERAGE AND RESOLUTION

SWATH	131.35	KM
CELLS/SCAN	2	
CELL WIDTH	9.91 10.75	KM
CELL LENGTH	35.39 41.67	KM
SCAN TIME	1.38	SEC
TIME/CELL	0.688	SEC
AZ RES	50.00 54.25	M
RA RES	150.00 102.61	M

APPENDIX B

COMPUTERIZED DESIGN PROGRAM FOR THE SCANNING SAR

(SCANSAR)

```

0010CSCANSAR      DESIGN OF A SCANNING SAR
0020C              THIS PROGRAM WAS PREPARED BY
0030C
0040C              JOHN P. CLASSEN
0050C
0060      DIMENSION THETAD(2), THETAR(2), SIGMAX(2), RA(2),
0070      & RR(2), CC(2), WT(2), TYPE(4), GP(2), GA(2), R(2),
0080      & SIGMIN(2)
0090      REAL NF, KT, LOSS, K
0100      DATA C, DEG, YES, PI, TYPE, THOUS, K, JJ/
0110      & 3.0E08, 0.0174532925, 'YES', 3.141925,
0120      & 'UNFOCU', 'SED', 'SEMI-F', 'DCUSED', 1000.0, 1.38E-23,
0130      & 0177177077040/
0140C      ARITHMETIC ASSIGNMENT STATEMENT
0150      TAN(X) = SIN(X)/COS(X)
0160C      SPPRESS CAPRIAGE RETURNS ON READS
0170      CALL FPARAM(3, JJ)
0180C      INPUT PARAMETERS(GEOMETRY)
0190 10 WRITE(6,1000)
0200 1000 FORMAT(////1X, 'DESIGN OF A SCANNING SAR HAVING',
0210      & ' INPUT DESIGN PARAMETERS AS FOLLOWS: '//
0220      & 'APERTURE LENGTH (M) ')
0230      READ(5,1001) AL
0240 1001 FORMAT(F8.2)
0250      WRITE(6,1002)
0260 1002 FORMAT(1X, 'OPERATING WAVELENGTH (M) ')
0270      READ(5,1001) WL
0280      WRITE(6,1003)
0290 1003 FORMAT(1X, 'MIN AND MAX VIEW ANGLES (DEG) ')
0300      READ(5,1008) THETAD
0310 1008 FORMAT(2F8.2)
0320      WRITE(6,1004)
0330 1004 FORMAT(1X, 'AZIMUTH RESOLUTION (M) ')

                                0340      READ(5,1001) RA(1)

0350      WRITE(6,1005)
0360 1005 FORMAT(1X, 'RANGE RESOLUTION (M) ')
0370      READ(5,1001) RR(1)
0380      WRITE(6,1006)
0390 1006 FORMAT(1X, 'GROUND VELOCITY (KM/SEC) ')
0400      READ(5,1001) VGP
0410      WRITE(6,1007)
0420 1007 FORMAT(1X, 'SPACECRAFT ALTITUDE (KM) ')
0430      READ(5,1001) ZP

```

Figure B-1a. Fortran Listing for SCANSAR.

```

0440C          SCALE VARIABLES
0450          VG = VGP*THOUS
0460          Z = ZP*THOUS
0470C          UNFOCUSED PRESUMPTION
0480          ITYPE = 1
0490C          COMPUTE MAX AND MIN RANGE
0500          DO 20 I=1,2
0510          THETAR(I) = THETAD(I)*DEG
0520          R(I) = Z/COS(THETAR(I))
0530          20 CONTINUE
0540C          FULLY FOCUSED LIMITATION
0550          RAFF = AL/2.0
0560          IF(RAFF .LT. RA(1)) GO TO 30
0570          WRITE(6,2000)
0580          2000 FORMAT(1X,'INADEQUATE APERTURE LENGTH TO',
0590          & 'ACHIEVE RESOLUTION. INPUT DATA AGAIN!')
0600          GO TO 10
0610C          UNFOCUSED LIMITATION
0620          30 RAUF = SQRT(WL*R(2)/2.0)
0630C          ESTABLISH SYSTEM TYPE
0640          IF(RAUF .LT. RA(1)) GO TO 40
0650C          PARTIALLY OR FULLY FOCUSED SYSTEM REQUIRED
0660          DFD = 2.0*VG*RA(1)/R(1)/WL
0670          RA(2) = DFD*WL*R(2)/2.0*VG
0680          ITYPE = 3
0690          GO TO 45
0700          40 RA(1) = RAUF
0710C          UNFOCUSED SYSTEM REQUIRED
0720          DFD = 2.0*VG*RA(1)/R(1)/WL
0730          RA(2) = DFD*WL*R(2)/2.0*VG
0740C          APERTURE HEIGHT TO SATISFY DOPPLER SAMPLING
0750C          REQUIREMENT
0760          45 FD = 2.0*VG/AL
0770          NFILT = FD/DFD + 0.5
0780          AH = 10.0*FD*R(2)*TAN(THETAR(2))*WL/C
0790C          CHECK WITH DESIGNER
0800          WRITE(6,3000) AH
0810          3000 FORMAT(1X,'THE APERTURE HEIGHT IS',F6.2,' M.',
0820          & ' DO YOU WISH TO INCREASE THE HEIGHT')
0830          READ(5,3001) ANS
0840          3001 FORMAT(A3)
0850          IF(ANS .NE. YES) GO TO 70
0860          50 READ(5,1001) AHNEW

```

Figure 8-1b. Fortran Listing for SCANSAR.

```

0870      IF (AHNEW .GT. AH) GO TO 60
0880      WRITE(6,3002)
0890 3002  FORMAT(1X,'NEW APERTURE HEIGHT MUST BE LARGER THAN',
0900      & ' THE OLD. TRY AGAIN!')
0910      GO TO 50
0920 60   AH = AHNEW
0930 70   BETAH = WL/AH
0940C      COVERAGE PARAMETERS
0950      NCELL = (THETAR(2)-THETAR(1))/BETAH + 0.5
0960      BETAL = WL/AL
0970      DO 80 I = 1,2
0980      GR(I) = P(I)*BETAL/THOUS
0990      GR(I) = R(I)*BETAH/COS(THETAR(I))/THOUS
1000 80   CONTINUE
1010      SWATH = (R(2)*SIN(THETAR(2))-R(1)*SIN(THETAR(1)))/THOUS +
1020      & (GR(2) + GR(1))/2.0
1030C      TIMING
1040      TSLEW = GR(1)/VG*THOUS
1050      TCELL = TSLEW/NCELL
1060      IF(TCELL .GT. 1.0/DFD) GO TO 85
1070      WRITE(6,3003)
1080 3003  FORMAT(//1X,'INSUFFICIENT TIME TO ACHIEVE RESOLUTION:',
1090      & ' TRY AGAIN')
1100      GO TO 10
1110C      PULSE REPETITION FREQUENCY
1120 85   DELR = BETAH*P(2)*TAN(THETAR(2))
1130      PRF = C/(4.0+DELR)
1140C      RANGE RESOLUTION
1150      DR = RR(1)*SIN(THETAR(1))
1160      RR(2) = DR/SIN(THETAR(2))
1170C      BANDWIDTH REQUIRED
1180      BW = C/2.0/DR/THOUS**2
1190C      PROCESSING GAIN
1200      NGP = PRF/DFD + 0.5
1210C      NO. OF CELLS AVAILABLE FOR AVERAGING
1220      NCAP = TCELL*DFD + 0.5
1230C      NO. OF CELL AVERAGABLE BEFORE
1240C      DEFocusing IN AZIMUTH
1250      Y = Z*TAN(THETAR(2) - BETAH/2.0)
1260      DELY = -Y + Z*TAN(THETAR(2) + BETAH/2.0)
1270      DELX = VG/DFD
1280      BETA = 2.0*ATAN(DELY/2.0/Y)
1290      NCA = RA(2)/BETA/DELY + 0.5

```

Figure B-1c. Fortran Listing for SCANSAR.

```

1300C          INPUT POWER PARAMETERS
1310          WRITE(6,4000)
1320 4000  FORMAT(1X,'LOSS FACTOR (DB)')
1330          READ(5,1001) LOSS
1340          WRITE(6,4002)
1350 4002  FORMAT(1X,'NOISE FIGURE (DB)')
1360          READ(5,1001) NF
1370          WRITE(6,4003)
1380 4003  FORMAT(1X,'SIGNAL/NOISE (DB)')
1390          READ(5,1001) SN
1400          WRITE(6,4004)
1410 4004  FORMAT(1X,'MAX SCATTERING COEFFICIENTS (DB)')
1420          READ(5,1008) SIGMAX
1430          WRITE(6,4007)
1440 4007  FORMAT(1X,'MIN SCATTERING COEFFICIENTS (DB)')
1450          READ(5,1008) SIGMIN
1460          WRITE(6,4005)
1470 4005  FORMAT(1X,'APERTURE EFF (PERCENT)')
1480          READ(5,1001) AEFF
1490          AEFF = AEFF/100.0
1500          WRITE(6,4006)
1510 4006  FORMAT(1X,'RECEIVER INPUT TEMPERATURE (DEG K)')
1520          READ(5,1001) TEMP
1530C          COMPUTE TRANSMITTER POWER AND CHANNEL CAPACITY
1540          FACTOR = 4.0*PI*WL**2*10.0**((LOSS+NF+SN)/10.0)*PRF*K*TEMP
1550C          NO. OF BITS PER CELL
1560          NBITS = (SIGMAX(1)-SIGMIN(2))/3.0103 + 0.5
1570          DO 90 I = 1,2
1580          WT(I) = FACTOR*P(I)**4/(10.0**((SIGMIN(I)/10.0)*RA(I)+RR(I)+NGP*
1590          & (AL*AH+AEFF)**2)
1600          CC(I) = GR(I)*GA(I)/(RA(I)+RR(I))*NBITS/TCELL
1610          90  CONTINUE
1620C          LIST SYSTEM DESIGN PARAMETERS
1630          WRITE(6,5000) THETA0, WL, AL, RA(1), RR(1),
1640          & VGP, ZP, AEFF*100.0, LOSS, NF, SN, TEMP, SIGMAX, SIGMIN
1650 5000  FORMAT(///20X,'SUMMARY TABLE',1X,'RAW DESIGN PARAMETERS'///
1660          & 1X,'PARAMETERS'17X,'VALUES',10X,'UNITS'///
1670          & 1X,'ANGLE SPAN',4X, 2(F10.2,5X),'DEG'//
1680          & 1X,'LAMBDA',8X,F10.3,20X,'M'//
1690          & 1X,'APER LENGTH',3X,F10.1,20X,'M'//
1700          & 1X,'AZ RES',8X,F10.2,20X,'M'//
1710          & 1X,'RA RES',8X,F10.2,20X,'M'//
1720          & 1X,'GRD VEL',7X,F10.1,20X,'KM/SEC'//
1730          & 1X,'ALTITUDE',6X,F10.1,20X,'KM'//
1740          & 1X,'APER EFF',6X,F10.1,20X,'PERCENT'//
1750          & 1X,'LOSS FACTOR',3X,F10.1,20X,'DB'//
1760          & 1X,'NOISE FIG',5X,F10.1,20X,'DB'//

```

Figure B-1d. Fortran Listing for SCANSAR.

```

1770      & 1X,'SIG/NOISE',5X,F10.2,20X,'DB'//
1780      & 1X,'REC TEMP',6X,F10.1,20X,'DEG K'//
1790      & 1X,'SIGMAX',8X,2(F10.2,5X),'DB'//
1800      & 1X,'SIGMIN',8X,2(F10.2,5X),'DB'///
1810C      COMPUTED PARAMETERS
1820      WRITE(6,5001) TYPE(ITYPE),TYPE(ITYPE+1),RH, WT,
1830      & PRF/THOUS, FD/THOUS, BW, NGP, NCAP, NCA, NFILT, CC
1840 5001  FORMAT(1X,'COMPUTED SYSTEM PARAMETERS'//
1850      & 1X,'SYSTEM TYPE:',2X,2A6/
1860      & 1X,'APER HEIGHT',3X,F10.2,20X,'M'//
1870      & 1X,'XMIT PWR',6X,2(F10.2,5X),'WATTS'//
1880      & 1X,'PRF',11X,F10.2,20X,'KHZ'//
1890      & 1X,'FD',12X,F10.2,20X,'KHZ'//
1900      & 1X,'RF BW',9X,F10.1,20X,'MHZ'//
1910      & 1X,'PPDC GAIN',5X,I10/
1920      & 1X,'NCAP',10X,I10/
1930      & 1X,'NCA',11X,I10/
1940      & 1X,'NO. OF FIL',4X,I10/
1950      & 1X,'CHAN CAP',6X,2(F10.2,5X),'MBITS/SEC'////
1960      WRITE(6,5002) SWATH, NCELL, GA, GP, TSLEW, TCELL, RA, PR
1970 5002  FORMAT(1X,'COVERAGE AND RESOLUTION'//
1980      & 1X,'SWATH',9X,F10.2,20X,'KM'//
1990      & 1X,'CELLS/SCAN',4X,I10/
2000      & 1X,'CELL WIDTH',4X,2(F10.2,5X),'KM'//
2010      & 1X,'CELL LENGTH',3X,2(F10.2,5X),'KM'//
2020      & 1X,'SCAN TIME',5X,F10.2,20X,'SEC'//
2030      & 1X,'TIME/CELL',5X,F10.3,20X,'SEC'//
2040      & 1X,'AZ RES',8X,2(F10.2,5X),'M'//
2050      & 1X,'RA RES',8X,2(F10.2,5X),'M'////
2060      & 1X,'WANT TO DESIGN ANOTHER ONE'//
2070      READ(5,3001) ANS
2080      IF(ANS .EQ. YES) GO TO 10
2090      WRITE(6,9000)
2100 9000  FORMAT(//1X,'VERY INTERESTING!', ' AUFWIEDERSEHEN'//)
2110      STOP
2120      END

```

Figure B-1e. Fortran Listing for SCANSAR.

APPENDIX F
RSL TECHNICAL REPORT 295-3
VOLUME IV



THE UNIVERSITY OF KANSAS SPACE TECHNOLOGY CENTER

Raymond Nichols Hall

2291 Irving Hill Drive—Campus West Lawrence, Kansas 66045

Telephone:

COMB FILTER THEORY FOR USE IN A SCANNING SYNTHETIC
APERTURE RADAR SIGNAL PROCESSOR (SCANSAR)

Remote Sensing Laboratory
RSL Technical Memorandum 295-7

Mark Komen

March, 1976

Supported by:

NATIONAL AERONAUTICS AND SPACE ADMINISTRATION
Goddard Space Flight Center
Greenbelt, Maryland 20771

CONTRACT NAS 5-22384



REMOTE SENSING LABORATORY

TABLE OF CONTENTS

	<u>Page</u>
ABSTRACT	ii
1.0 INTRODUCTION	1
2.0 THE COMB FILTER PROCESSOR	1
3.0 ANALYSIS OF A COMB FILTER DELAY LINE	2
4.0 ULTIMATE USE IN THE SAR PROCESSOR	7
REFERENCES	10

LIST OF FIGURES

Figure 1	Comb filter passbands showing carrier and its sidebands (zero phase shift).	8
2	Comb filter passbands phase-shifted to account for Doppler shifting.	8
3	A comb filter delay line.	8
4	A simplified comb filter delay line.	9
5	$\sin nx/\sin x$ comb response centered on the harmonics of the received pulse.	9
6	Representation of comb filter Doppler band coverage.	9

ABSTRACT

A great deal of interest has been shown in the development of a spaceborne synthetic aperture radar capable of wide-swath coverage. Although digital processors are presently quite popular, analog processors offer a means for processing radar images on-board and in real time. The processor discussed herein is based on the idea of comb filters implemented by recursive use of delay lines. In this form, the various range elements are processed sequentially as a signal circulates around a delay line and is added to the incoming signal. No memory is required for the individual signal elements as in processors that first accumulate all the elements required for the synthetic apertures for a bank of range cells and then process them in a batch mode. The resulting reduction in processor size, complexity, and power consumption makes the comb filter processor concept an attractive possibility for use in a spaceborne system.

COMB FILTER THEORY FOR USE IN A SCANNING SYNTHETIC APERTURE RADAR SIGNAL PROCESSOR (SCANSAR)

Mark Komen

1.0 INTRODUCTION

A real-time spaceborne synthetic-aperture radar could provide the wide-swath coverage necessary for the water resources and sea ice missions, and other missions requiring frequent imaging. With a relatively modest resolution, the radar has enough time to build many images of areas on the ground and can scan its beam to look at areas at different ranges.

Basically, SAR data processing involves correlating chirp waveforms generated by varying Doppler shifts as the radar travels past targets on the ground. Today, digital processing of SAR data has become widely used thanks to its speed, capacity, reliability, and cost effectiveness. Obviously, a satellite-borne processor must be compact and fast enough to provide data in real time. Although digital processors have the necessary speed, their large memory requirements and the subsequently large number of operations involved make them questionable candidates for modest-resolution radars when considering power consumption and spacecraft size constraints.

A very credible alternative to the digital processor is a serial analog processor using comb filters to process the returns from different azimuth elements (range elements at a given azimuth being processed sequentially). The comb filter has a set of passbands spaced as the Fourier components of the received pulse, thereby permitting narrow-band Doppler filtering while retaining the wideband characteristic of the pulse train necessary to retain range resolution. This memorandum concerns itself with an analytical description of the theory behind a comb filter processor.

2.0 THE COMB FILTER PROCESSOR

The great advantage of this type of processor is that it sequentially processes the data as it is received from the ground thus tremendously decreasing the amount of data storage space needed by the digital processor. The comb-filter processor is described in analog terms, but could be implemented digitally.

If the integration time necessary to yield a required azimuth resolution is T and if the system pulse repetition frequency is F , then the number of pulses transmitted (and received) by the system during building of each synthetic aperture is given by

$$N = TF$$

In other words, the ground is illuminated by N pulses and by integrating these N returns, an image is constructed. In the comb filter, each return is delayed by the repetition period and summed with the next incoming return, this cycle being repeated until all N pulses have been added together. Only signals having the proper period add each time, the others drifting in and out of phase during integration.

The comb filter passbands are spaced such that they align with the Fourier components of the received pulse as in Figure 1. However, the effect of Doppler shift is to introduce an offset in the spectral components, so the comb filters must be phase-shifted by this same amount per Figure 2. The system then is composed of a set of comb filters, each tuned to accommodate the Doppler shifts from a different azimuth element such that the entire range of Doppler frequencies over an observed area on the ground is within the total passband of the processor.

As shown in Figure 3, a comb filter consists of a delay device, a tunable phase shifter, and a weighting amplifier. The delay device samples the first return and holds it for the proper period, the phase-shifter tunes the filter for the desired Doppler shift, and the weighting amplifier is used to reduce sidelobes in the $\sin X/X$ character of the comb teeth. After the proper number of received pulses has been integrated by the filter, the resulting composite waveform is then fed into a buffer for temporary storage.

3.0 ANALYSIS OF A COMB FILTER DELAY LINE

To examine what happens analytically during processing, refer to Figure 4 for a simplified version of the comb filter delay line. A pulse enters through the switch into a delay device where it is delayed for one repetition period. The delayed pulse is then phase-shifted and added to the next incoming pulse entering via the switch.

For pulses circulating the loop at some frequency w_n , the value of the output after N trips through is given by

$$\begin{aligned} & \sum a_n \cos w_n t \\ & + \sum a_n \cos [w_n (t - T) + \phi] \\ & + \sum a_n \cos [w_n (t - 2T) + 2\phi] \\ & + \quad \quad \quad \vdots \\ & + \sum a_n \cos [w_n (t - NT) + N\phi] \end{aligned}$$

where T is a variable time delay and ϕ is a constant phase shift. It is desired to set a value for ϕ such that all cosine ($w_n t$) terms will add in phase. ϕ must be less than 2π .

Examine the expression for an entering pulse and one that has been through the loop (both at frequency w_n):

$$a_n \cos w_n t + a_n \cos (w_n t + \phi - w_n T)$$

For these quantities to add in phase

$$\phi - w_n T = -2\pi r$$

where r is some integer.

Therefore,

$$w_n = \frac{\phi + 2\pi r}{T}$$

Now looking at the expression for a pulse at frequency w_n having been through the loop twice

$$\cos (w_n t + 2\phi - 2w_n T)$$

It can be seen that

$$2(-\phi + w_n T) = 2\pi s$$

To add in phase with the other pulses (s is an integer)

$$w_n = \frac{\phi + \pi s}{T}$$

Where $r = 2s$, the two equations for w_n are identical.

It has been shown that

$$w_n T - \phi = 2\pi r$$

Looking at the next harmonic w_{n+1}

$$\begin{aligned} w_{n+1} T - \phi &= 2\pi (r+1) \\ w_{n+1} &= \frac{\phi + 2\pi (r+1)}{T} \end{aligned}$$

Noting that $w_0 = \frac{2\pi}{T}$ where w_0 is the pulse repetition frequency

$$\begin{aligned} w_{n+1} &= \frac{\phi}{T} + (n+1) w_0 \\ w_n &= \frac{\phi}{T} + n w_0 \quad \text{where } n = r \end{aligned}$$

From this result, it can be seen that a constant phase shift introduced at some frequency w_n will appear in all the harmonics of that frequency.

At this point, suppose a small drift from w_n is introduced

$$w = w_n + \delta_n$$

Rewriting the circulation expression for N trips through the loop:

$$\begin{aligned} & a_n \cos (w_n + \delta_n) t \\ & + a_n \cos [(w_n + \delta_n) (t - T) + \phi] \\ & + a_n \cos [(w_n + \delta_n) (t - 2T) + 2\phi] \\ & + \quad \vdots \\ & + a_n \cos [(w_n + \delta_n) (t - iT) + i\phi] \\ & + \quad \vdots \\ & + a_n \cos [(w_n + \delta_n) (t - NT) + N\phi] . \end{aligned}$$

Examining the expression after one trip through the loop by opening the brackets

$$\begin{aligned} (w_n + \delta_n) (t - T) + \phi &= w_n t + \delta_n t - w_n T - \delta_n T + \phi \\ w_n T &= \phi + n w_0 T \end{aligned}$$

from before, and

$$\omega_0 T = 2\pi \quad \text{or}$$

$$n \omega_0 T = 2n\pi .$$

Hence,

$$\omega_n T = \phi + 2n\pi .$$

However, phases differing by multiples of 2π can be ignored, so

$$\omega_n T = \phi \quad \text{and}$$

$$\begin{aligned} (\omega_n + \delta_n)(t - T) + \phi &= \omega_n t + \delta_n t - \phi - \delta_n T + \phi \\ &= \omega_n t + \delta_n(t - T) \end{aligned}$$

Expanding the brackets for the i^{th} trip through the loop

$$\begin{aligned} (\omega_n + \delta_n)(t - iT) + i\phi &= \omega_n t - i\omega_n T + \delta_n t - i\delta_n T + i\phi \\ &= \omega_n t - i(\phi + 2\pi n) + \delta_n t - i\delta_n T + i\phi \\ &= \omega_n t + \delta_n(t - iT) \end{aligned}$$

Rewriting the circulation expression up to the I^{th} iteration as exponentials

$$\sum_n \sum_i a_{ni} e^{j\omega_n t} e^{j\delta(t - iT)}$$

If $a_{ni} = a_n$ for all i

$$\sum_n a_n e^{j(\omega_n + \delta_n)t} \sum_i e^{-ji\delta_n T}$$

Recognizing the second summation as the sum of a geometric series of the form

$$\sum_i r^i = \frac{1 - r^I}{1 - r} ,$$

the expression becomes

$$\sum_n a_n e^{j(\omega_n + \delta_n)t} \left(\frac{1 - e^{-jI\delta_n T}}{1 - e^{-j\delta_n T}} \right)$$

Manipulating the quantity in the parentheses and using Euler's formula, the final form of the expression is

$$\sum_n a_n e^{j(w_n + \delta_n)t} \left(\frac{\sin \frac{IT\delta}{2}}{\sin \frac{T\delta}{2}} \right) e^{j \frac{(I-1) T\delta}{2}}$$

Note that $\sum_n a_n e^{j(w_n + \delta_n)t}$ represents the original signal w_n with the δ_n offset. The $e^{j \frac{(I-1) T\delta}{2}}$ term can be neglected since T and δ are both small quantities. The $\sin nx / \sin x$ expression shows the comb response. There will be a maximum where

$$\sin \frac{T\delta}{2} = 0$$

or where

$$\frac{T\delta}{2} = m\pi$$

For small $\frac{T\delta}{2}$,

$$\frac{\sin \frac{IT\delta}{2}}{\sin \frac{T\delta}{2}} = \frac{IT\delta}{2} = I$$

Therefore, there will be a peak of height I where

$$\delta = \frac{2m\pi}{T} = \omega_0 m$$

See Figure 5.

From this, it can be seen that regardless of the modulating signal, as long as the pulse repetition frequency is the same, there will be an offset δ where there is a drift δ_n from w_n , and a consequent reduction in amplitude.

Introducing the weighting amplifier with gain K as originally shown in Figure 3 will modify the circulation expression which now becomes

$$\sum_n a_n e^{j(w_n + \delta_n)t} \prod_i K_i e^{-j i \delta_n T}$$

for the i^{th} trip through the loop where K_i is the amplifier gain function. Standard methods in antenna and filter design can be used to establish weights $[K_i]$ that give desired sidelobe suppression, with the usual widening of the main response.

4.0 ULTIMATE USE IN THE SAR PROCESSOR

As stated previously, the SAR processor must separate out returns from different azimuth elements. This is accomplished by setting up a bank of comb filters, each tuned to a different Doppler frequency such that the bandwidth of the entire banks is at least equal to the expected Doppler bandwidth of returns from the ground. As the satellite moves at its given velocity, the shift will also change at some given rate. Therefore, the returns from a target on the ground will appear in several of the filters as the satellite travels. Figure 6 illustrates the Doppler band coverage. The purpose of each comb filter is to separate these different Dopplers from different along-track elements.

Since the Doppler shift for any point target decreases linearly in frequency with time as the radar passes the target, the processor must take this into account. This can be done either of two ways: (1) change the phase shift in the comb filter feedback path to track the varying Doppler shift; or (2) convert the varying frequency to a fixed frequency by beating the incoming signal with an appropriate reference frequency varying at the same rate as the signal from a point target.

Mechanization of the serial processor is the subject of other reports in this series.

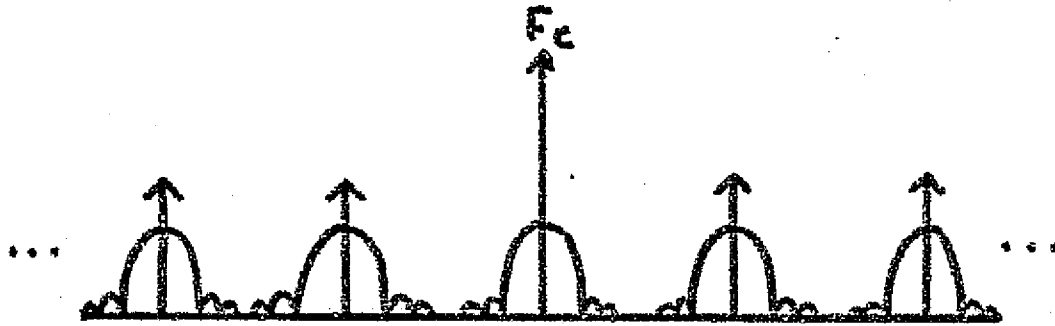


Figure 1. Comb filter passbands showing carrier and its side-bands (zero phase shift).

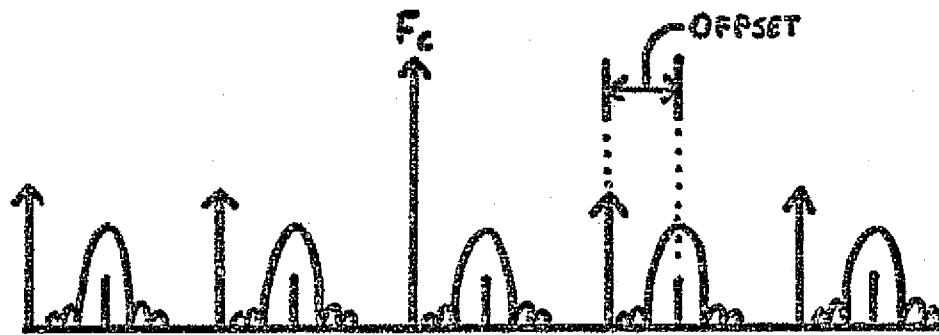


Figure 2. Comb filter passbands phase-shifted to account for Doppler shifting.

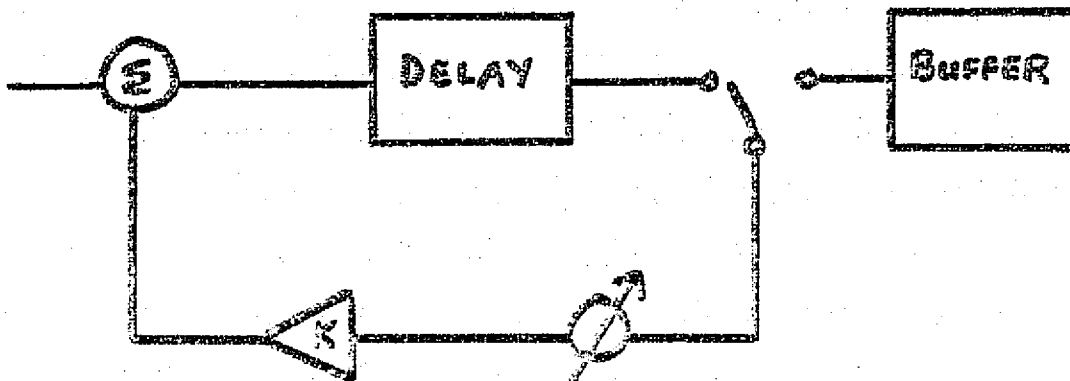


Figure 3. A comb filter delay line.

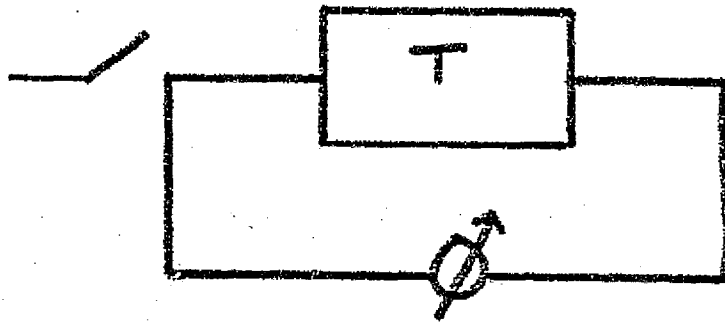


Figure 4. A simplified comb filter delay line.

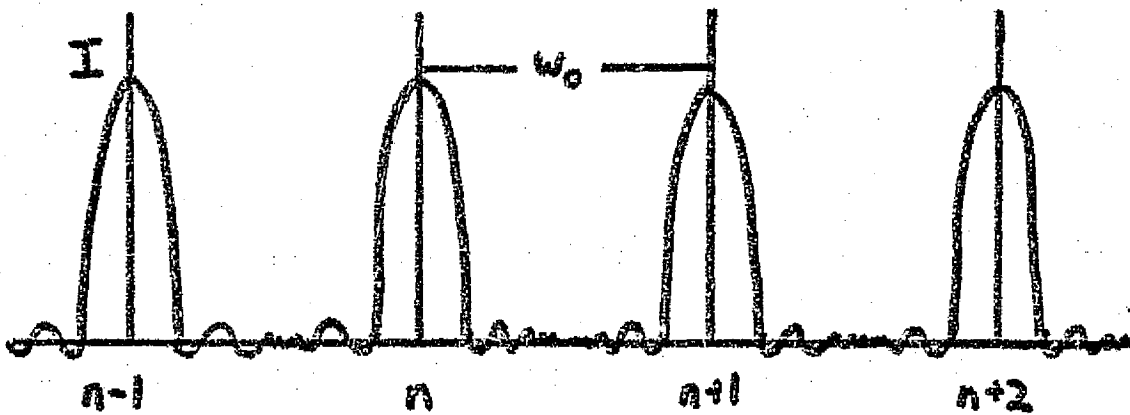


Figure 5. $\sin nx / \sin x$ comb response centered on the harmonics of the received pulse.

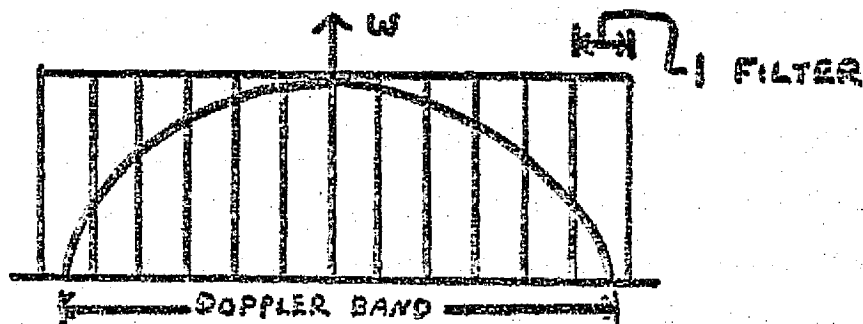


Figure 6. Representation of comb filter Doppler band coverage.

REFERENCES

1. Bickel, H. J., "Spectrum Analysis With Delay Line Filters," IRE Wescon Convention Record, Part 8, pp. 59-67, 1959.
2. Claassen, J. P., "A Short Study of a Scanning SAR For Hydrological Monitoring on a Global Basis," RSL Technical Report 295-1, University of Kansas Center for Research, Inc., September 1975.
3. Dome, George, Private Communication, University of Kansas Remote Sensing Laboratory.
4. McMillan, S., "Synthetic Aperture Radar and Digital Processing," RSL Technical Memorandum 295-3, University of Kansas Center for Research, Inc., September 1975.
5. Westinghouse Electric Corporation, "Final Report Spaceborne SAR Pilot Study," Systems Development Division, Baltimore, MD., April 11, 1974.

APPENDIX G
RSL TECHNICAL REPORT 295-3
VOLUME IV



THE UNIVERSITY OF KANSAS SPACE TECHNOLOGY CENTER
Raymond Nichols Hall

2291 Irving Hill Drive—Campus West Lawrence, Kansas 66045

Telephone:

DETAILED SYSTEMS DESIGN FOR THE SCANNING
SYNTHETIC-APERTURE RADAR (SCANSAR)
USING COMB FILTER RANGE-OFFSET PROCESSING

Remote Sensing Laboratory
RSL Technical Report 295-3

Mark J. Komen

July, 1976

Supported by:

NATIONAL AERONAUTICS AND SPACE ADMINISTRATION
Goddard Space Flight Center
Greenbelt, Maryland 20771

CONTRACT NAS 5-22384



ABSTRACT

With modest resolution requirements, a spacecraft synthetic aperture radar system can be developed which is capable of wide swath coverage. This is achieved by scanning the antenna beam outward in range to dwell on successive areas on the ground (scan or image cells). This scanning synthetic aperture radar (SCANSAR) can utilize the extra observation time brought about by this resolution to take several looks at areas on the ground and improve image interpretability.

The SCANSAR system discussed herein utilizes a comb filter approach to analog processing implemented by the use of serial analog memories as recursive delay lines. By this method, the various range elements are processed sequentially as a signal circulates around the delay line and is added to the incoming signal, thereby eliminating memory requirements for individual signal elements. Furthermore, the use of low power CMOS devices in the processor makes for small power consumption.

The angular swath coverages for the SCANSAR design are 6.7 to 22.5° to sense soil moisture and 22.1 to 37° for ice monitoring. Total swaths are 128.8 km and 150.2 km respectively. Azimuth resolution is 50 m in both swaths with the range resolution varying from 150 m at angles near the satellite track to 33 m at the far angles. The average transmitter power is approximately 15 watts and the total power consumption for a single-sided SCANSAR processor is around 200 watts.

TABLE OF CONTENTS

	<u>Page</u>
ABSTRACT	ii
1.0 THE SCANSAR CONCEPT	1
1.1 INTRODUCTION	1
1.2 COVERAGE LIMITATIONS	1
1.3 SCANSAR DESIGN THEORY	5
1.4 INTERPRETABILITY CONSIDERATIONS	11
2.0 SYSTEM PARAMETERS	16
2.1 INTRODUCTION	16
2.2 PARAMETER SELECTION	16
2.3 CONCLUSIONS	17
3.0 RADAR SYSTEM AND ANTENNA	22
3.1 INTRODUCTION	22
3.2 PULSE COMPRESSION TECHNIQUES	22
3.2.1 Linear FM	22
3.2.2 Phase-coding	23
3.3 RECOMMENDED HARDWARE	26
3.3.1 Power Output Amplifier	26
3.3.2 Receiver Front-End	26
3.4 ANTENNA CONSIDERATIONS	27

	<u>Page</u>
4.0 PROCESSOR	28
4.1 INTRODUCTION	28
4.2 COMB FILTER CONCEPTS	28
4.3 DESIGN CONSIDERATIONS	31
4.3.1 PRF Diversity	31
4.3.2 Doppler Slope	36
4.4 SYSTEM DESIGN	40
4.4.1 The Scanning Local Oscillator (SLO)	44
a. SLO by Phase Shifting	44
b. SLO by Balanced Modulators	46
4.4.2 Divider Network	58
4.4.3 The Filter Channel	58
a. Serial Analog Memories	60
b. Phase-Shifter	61
c. Weighting	63
d. Gain Stabilization	67
e. Channel Summing Point	67
4.5 DETECTION AND BUFFERING	70
4.6 TIMING AND CONTROL	74
4.7 ALTERNATIVE PROCESSOR CONFIGURATION	74
4.8 EDGE EFFECTS	76
4.9 SUMMING THE LOOKS	82
5.0 MOTION COMPENSATION	83

	<u>Page</u>
6.0 POWER AND SIZE	86
6.1 POWER CONSUMPTION	86
6.2 SIZE	91
7.0 CONCLUSIONS AND RECOMMENDATIONS	94
APPENDIX A	95
APPENDIX B	101
APPENDIX C	103
APPENDIX D	129
APPENDIX E	133
REFERENCES	136

LIST OF FIGURES

	<u>Page</u>
Figure 1 Pictorial concept of a scanning SAR.	2
2 SAR geometry.	4
3 Satellite isodops (top view).	7
4 Image cell isodops.	7
5 Pixel size.	13
6a The S&L volume.	13
6b	13
7 A chirp generator and decoder using SAW dispersive delay lines.	24
8 A pulse $N\tau$ seconds long expressed in a binary phase code.	
9 A phase-coded receiver.	25
10 Comb filter passbands showing carrier and its sidebands (zero phase shift).	30
11 Comb filter passbands phase-shifted to account for Doppler shifting.	30
12 A comb filter delay line.	30
13 Doppler slope geometry.	38
14 RF to IF frequency translation showing RF bandwidth.	42
15 RF bandwidth on 5 MHz filter channel carrier showing Doppler spread.	42
16 Representation of comb filter coverage of Doppler spread.	42
17 Basic processor.	43
18a Mixer Input.	43
18b Mixer Output.	43
19 SLO.	47

	<u>Page</u>
Figure 20	SLO using balanced modulators. 56
21	Reference chirp generator. 57
22	A comb-filter channel. 59
23	Parallel channel SAM banks. 62
24	All-pass phase shift network. 65
25	Gain stabilization circuit. 68
26	Channel summing point. 69
27	Detector-low pass filter circuit. 71
28	Buffer output system. 71
29	Detailed buffer output system. 72
30	An alternative filter channel arrangement. 75
31	Scan cell slide over 6 looks. 78
32	Components of the 1677.6 m slide 79
33	5 scan cells showing slides. 79
34	Starting points of cells relative to cell 1. 80
35	Cell overlap in azimuth 81
36	Motion compensation circuit using balanced modulation. 85
37	Number of filter channels vs. aperture length. 90
38	Filter channel power consumption vs. aperture length. 93

1.0 THE SCANSAR CONCEPT

1.1 INTRODUCTION

The SCANSAR concept was born out of a need to provide wide swath coverage with special regard to the water resources and sea ice missions (and other missions requiring frequent imaging). However, SAR coverage is limited by the interaction between Doppler (azimuth) and range ambiguities. Fully focussed fine-resolution systems suffer these coverage deficiencies. If fine resolution could be sacrificed for somewhat more modest resolution the radar would have time to achieve the wide-swath coverage desired by scanning to and dwelling on successive cross-track image cells (see Figure 1). With the proper resolution, the radar may have enough time to take several "looks" at each image cell, allowing for averaging and thereby enhancing the interpretability of the radar image.

1.2 COVERAGE LIMITATIONS

To adequately preserve the Doppler history of a target, the Nyquist sampling theorem states that for azimuth-offset the radar must sample the target returns with at least twice the Doppler bandwidth, F_d .

$$PRF \geq 2 \cdot F_d$$

However, Harger (1970) states that for range-offset SAR systems, a sampling rate equal to the Doppler bandwidth is acceptable. Oversampling by 50%, the PRF inequality becomes

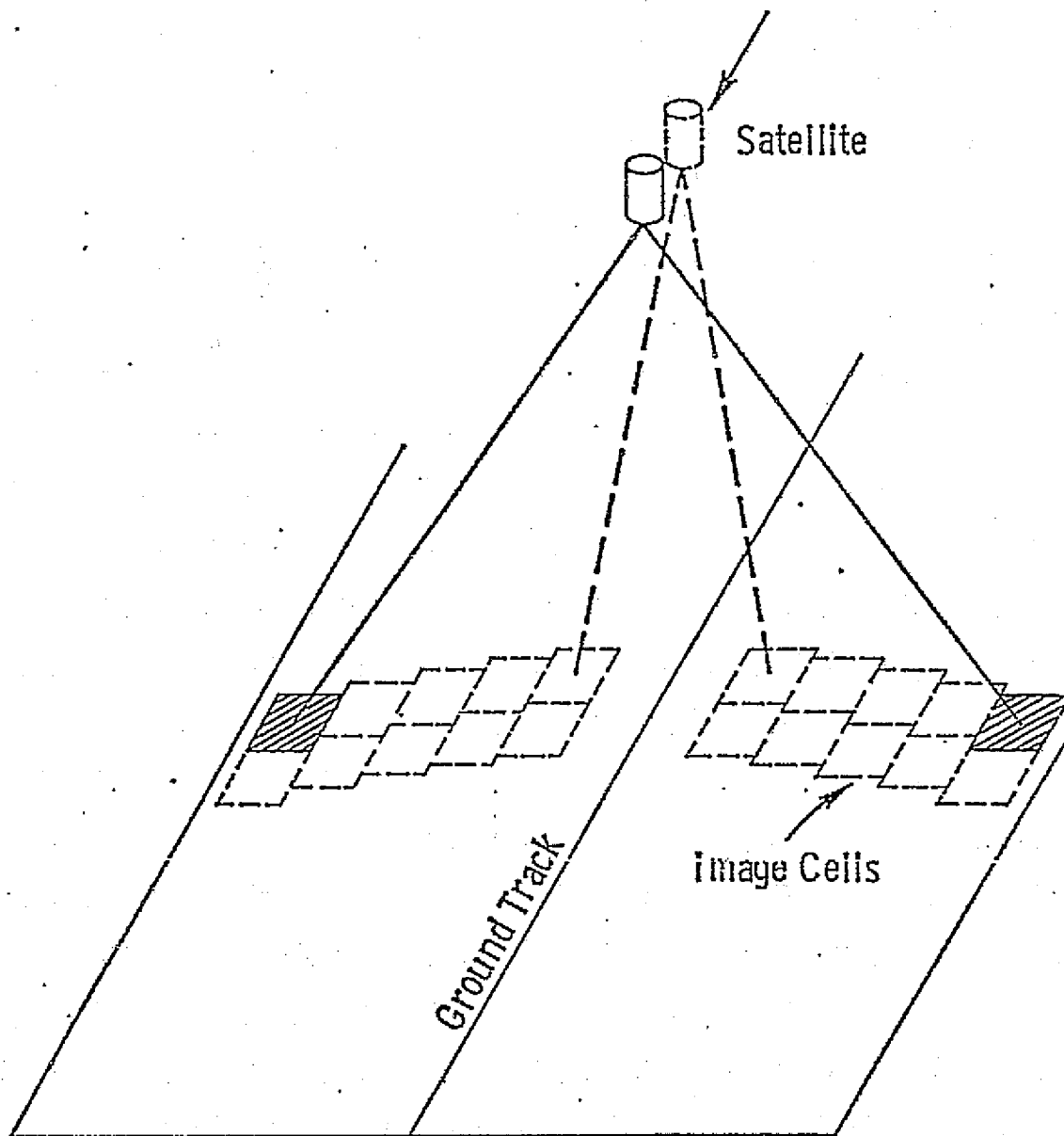
$$PRF \geq 1.5 F_d = 1.5 \left(\frac{2 Vg}{L} \right)$$

where Vg = satellite ground velocity

L = physical length of the antenna.

For a fully-focussed SAR, the azimuth resolution for an antenna of length L is

$$r_a = \frac{L}{2}$$



REPRODUCIBILITY OF THE
ORIGINAL PAGE IS POOR

Figure 1. Pictorial concept of a scanning SAR.

Hence,

$$\text{PRF} \geq \frac{1.5 Vg}{r_a}$$

For a satellite at an altitude Z_o , with a beamwidth B_h , whose antenna is looking at its farthest look angle θ , illuminating a cross-track distance L on the ground, as in Figure 2, to guarantee that the n^{th} pulse reflected from $R_1 + \Delta R$ reaches the receiver before the arrival of the $(n+1)^{\text{th}}$ pulse reflected from R_1 ,

$$\Delta T > \frac{2\Delta R}{c}$$

where $\Delta T = \frac{1}{\text{PRF}}$.

Choosing a range guard band of 2,

$$\text{PRF} < \frac{c}{4\Delta R}$$

Therefore to avoid ambiguities in range and azimuth it is required that

$$\frac{1.5 Vg}{r_a} < \text{PRF} < \frac{c}{4\Delta R}$$

Or

$$\frac{\Delta R}{r_a} < \frac{c}{6Vg}$$

From Figure 2

$$\Delta R = B_h R \tan \theta .$$

Since $R = \frac{Z_o}{\cos \theta}$, assuming plane-earth geometry for simplicity,

$$\Delta R = \frac{B_h Z_o \tan \theta}{\cos \theta} .$$

Substituting into the ambiguity inequality,

$$\frac{Z_o B_h \tan \theta}{r_a \cos \theta} < \frac{c}{6Vg}$$

$$B_h < \frac{c r_a \cos \theta}{6Vg Z_o \tan \theta}$$

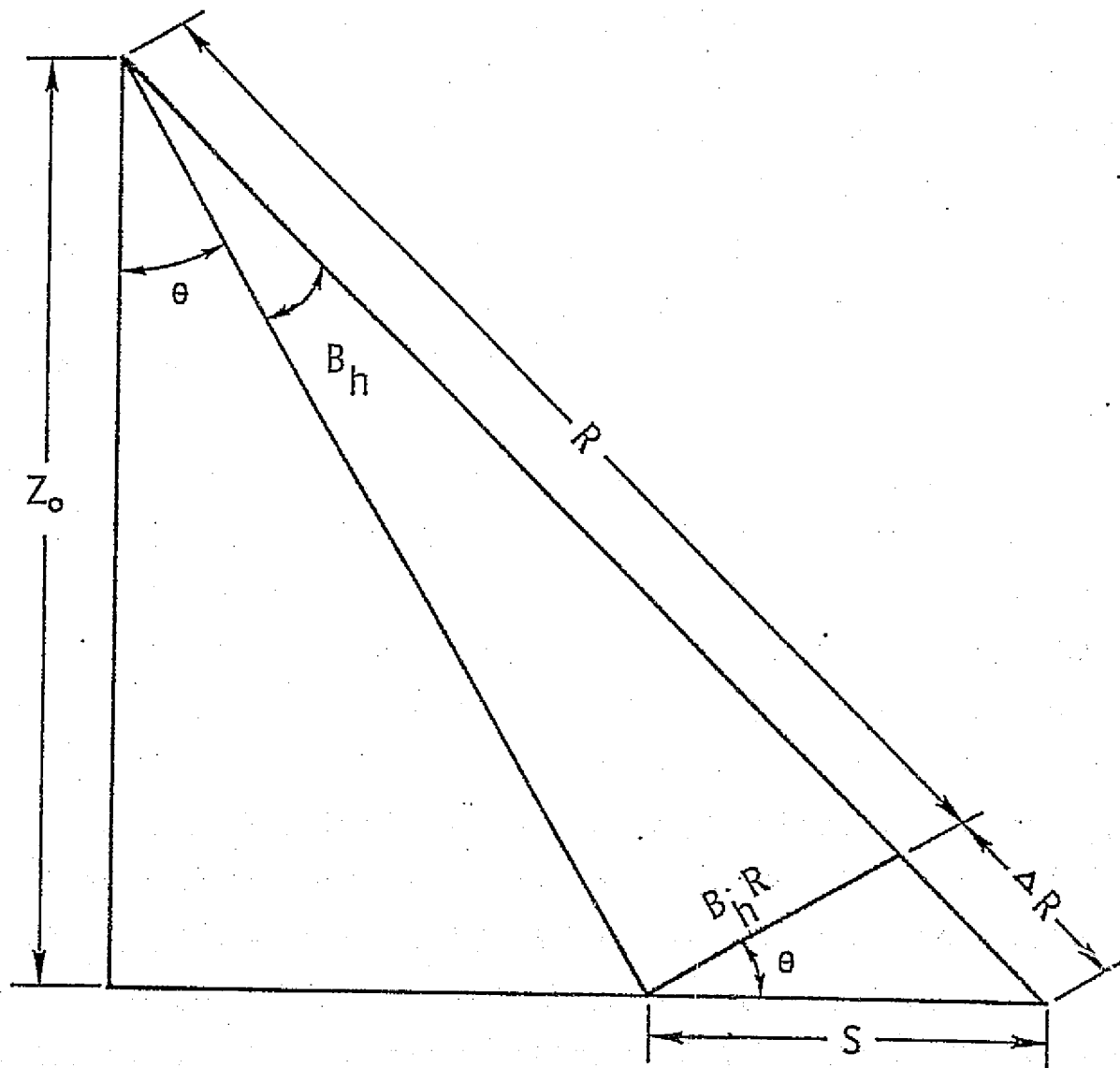


Figure 2. SAR geometry.

From this equation, it can be seen that the elevation beamwidth is proportional to the azimuth resolution, and since azimuth resolution

$$r_a = \frac{Vg}{F_d}$$

for a fully focussed system, B_h is inversely proportional to the Doppler bandwidth. The cross-track coverage (swath) is then given by

$$S = \frac{B_h Z_o}{\cos^2 \theta}$$

If a very fine resolution is used, r_a is small, B_h will be small, and correspondingly, the swath will be small.

The tracking bandwidth is

$$\Delta f_d = \frac{2Vg r_a}{\lambda R}$$

where λ is the wavelength and R is the slant range to the nearest image cell. To observe a response from a tracking filter with this bandwidth, the integration time is

$$\tau_d = \frac{1}{\Delta f_d}$$

Again, with a fine resolution system, Δf_d will be small and τ_d will be large. By sacrificing azimuth resolution, the coverage can be increased and since integration time is inversely proportional to azimuth resolution, time will be available at the expense of the number of independent looks averaged, to scan the radar beam over various image cells over a wide swath. This is the basic concept behind SCANSAR.

1.3 SCANSAR DESIGN THEORY

Claassen discusses the fine points of the SCANSAR design theory in his paper (1975) which is the source for many of the equations used in this section.

For a fully focussed SAR, the azimuth resolution limit is equal to

half the physical length of the antenna. For an unfocussed system, the azimuth resolution is a function of the operating wavelength and the slant range to the image cell observed. Semi-focussed systems are between these two extremes:

$$\frac{L}{2} < r_{a_1} < \sqrt{\frac{\lambda R_1}{2}}$$

where

L = physical length of the antenna

λ = operating wavelength

r_{a_1} = azimuth resolution at the nearest image cell

R_1 = slant range to the nearest image cell.

In this resolution range, tracking filters (or their equivalent) must be employed. The number of filters depends on the total Doppler bandwidth F_d

$$F_d = \frac{2Vg}{L}$$

and the number of filters is given by

$$N_a = \frac{F_d}{\Delta F_d}$$

where Δf_d is the tracking bandwidth discussed earlier. It would be appropriate at this point to discuss the tracking filter concept.

The isodops in the region broad side to the satellite and perpendicular to the satellite track are hyperbolas as in Figure 3 for flat terrain. In the region near the cross-track direction and for relatively narrow beamwidths in both azimuth and elevation, these isodops are closely approximated by parallel straight lines parallel to the zero isodop. This is shown for an image cell in Figure 4. The tracking filters can then be thought of as forming slightly displaced synthetic beams, each filter Δf_d Hz wide, integrating returns from a different azimuth strip. As the satellite moves, the Doppler frequencies for each cell will shift and the filters must be able to track the change. Comb filters will be used to track the time varying Doppler frequencies in the proposed design and will be

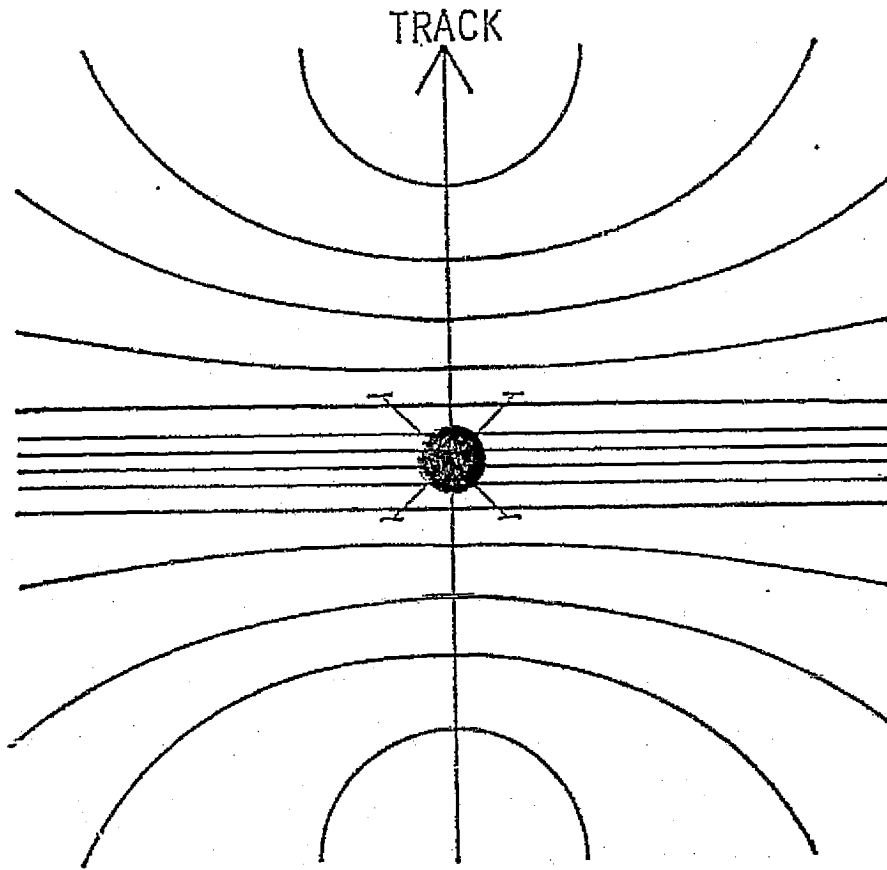


Figure 3. Satellite isodops (top view)

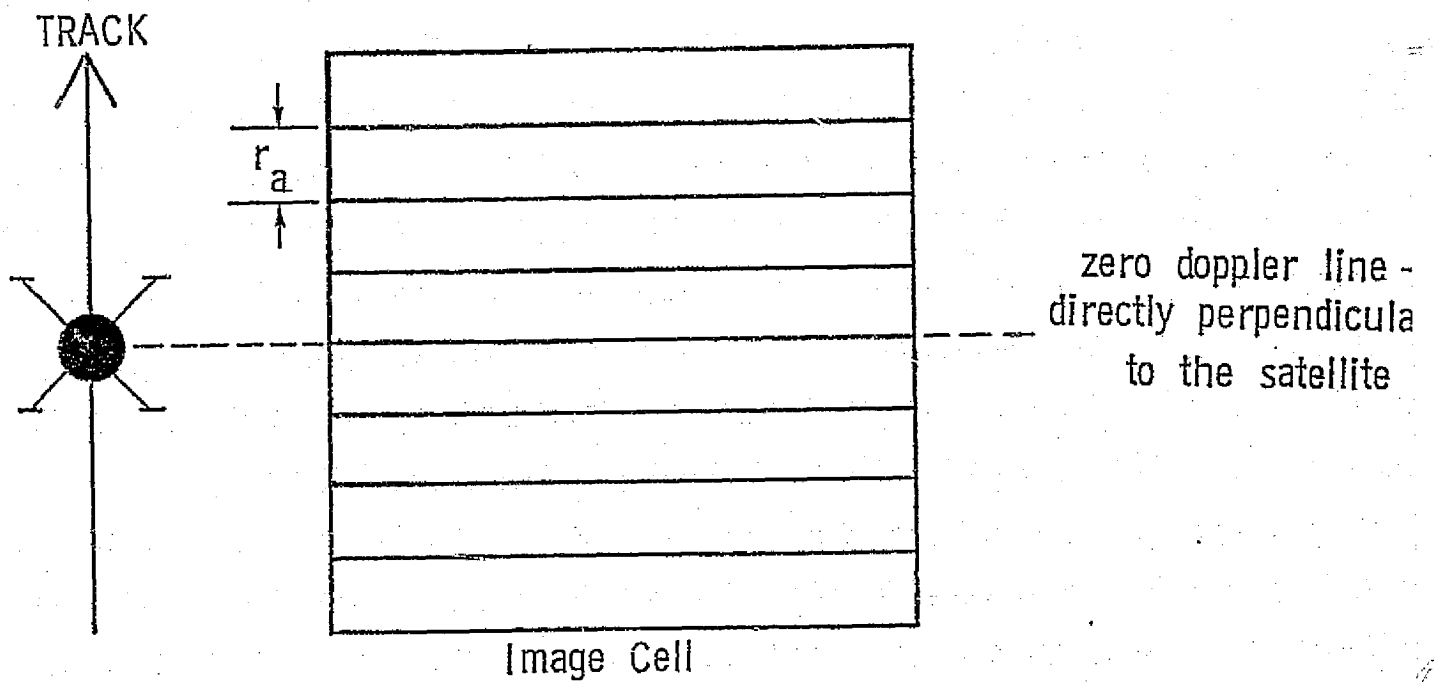


Figure 4. Image cell isodops.

discussed in section 4.

Since the antenna scans, the number of cross-track scan or image cells (not pixels or resolution cells) in a swath is

$$N_{\text{cell}} = (\theta_2 - \theta_1) / B_h$$

where θ_2 and θ_1 are the inner and outer look angles over which the beam is scanned.

Referring again to Figure 2, the azimuthal width of the image cell nearest the satellite track is

$$GA_1 = B_h R_1 = \frac{B_h Z_0}{\cos \theta_1}$$

Therefore for continuous coverage, the total time to scan over the range of look angles is

$$T_{\text{SLEW}} = \frac{GA_1(\theta)}{V_g}$$

where GA_1 is the azimuthal width of the image cell closest to the satellite track, and the aperture is constrained to fit this cell.

Hence, the time available to look at each image cell is

$$T_{\text{CELL}} = \frac{T_{\text{SLEW}}}{N_{\text{CELL}}}$$

T_{CELL} must be greater than or equal to $\frac{1}{\Delta f_d}$ to achieve the integration time for the azimuth resolution at each subaperture. If $T_{\text{CELL}} \geq \frac{2}{\Delta f_d}$, there is time to take 2 or more looks at each image cell before scanning to the next one. The number of looks is

$$N_{\text{LOOKS}} = T_{\text{CELL}} \cdot \Delta f_d$$

The PRF was set according to the range to the farthest image cell with a guard band of 2

$$\text{PRF} = \frac{C}{4\Delta R}$$

and,

$$\Delta R = \frac{Z_0 B_h \tan \theta_2}{\cos \theta_2}$$

where θ_2 is the largest look angle.

Substituting,

$$\text{PRF} = \frac{c \cos \theta_2}{4Z_0 B_h \tan \theta_2}$$

Sampling the total Doppler bandwidth such that

$$\text{PRF} = 1.5 F_d$$

$$B_h = \frac{c \cos \theta_2}{6Z_0 F_d \tan \theta_2}$$

The aperture height H is given approximately by

$$H = \frac{\lambda}{B_h}$$

Noting that $F_0 = \frac{c}{\lambda}$,

$$H = \frac{6 Z_0 F_d \tan \theta_2}{F_0 \cos \theta_2}$$

where F_0 = carrier frequency.

If the ground-range resolution r_r is specified in the design, the RF bandwidth will be given by

$$\text{BW} = \frac{c}{2 r_r \sin \theta_1}$$

where θ_1 is the smallest pointing angle. The unchirped pulse length is then

$$\tau_p = \frac{1}{\text{BW}}$$

To compute the transmit power requirement, it is noted that the peak return power W_{rp} from a single pixel (resolution cell) is

$$W_{rp} = \frac{W_{tp} A^2 \sigma^0 r_r r_a}{4\pi \lambda^2 R^4 L_f}$$

where

W_{tp} = peak transmitter power

A = effective aperture of antenna

σ° = scattering coefficient

R = range to cell

L_f = loss factor

The peak signal power in relation to the signal-to-noise ratio is

$$W_{rp} = \frac{F k T BW (S/N)}{G_p}$$

where

F = receiver noise figure

k = Boltzmann's constant

T = receiver input noise temperature

BW = RF bandwidth

G_p = tracking filter processing gain

$G_p = \frac{PRF}{\Delta f_d}$ and can be thought of as the number of pulses integrated necessary to achieve the desired resolution.

The peak transmitter power is related to the average transmitter power by

$$W_{tp} = \frac{BW}{PRF} W_{ta}$$

Therefore, the required transmitter average power is

$$W_{ta} = \frac{4\pi \lambda^2 R^4 L F k T (S/N) PRF}{G_p A^2 \sigma^\circ r_a r_r}$$

If σ_{max}° and σ_{min}° are the maximum and minimum scattering coefficients expected in the interval (θ_2, θ_1) , the telemetry bit requirement N_b is

$$N_b = \frac{\sigma_{max}^\circ}{3.01 \sigma_{min}^\circ}$$

presuming a gray scale resolution equal to the minimum σ° . If an N bit

word is transmitted for each resolution cell, the total number of bits per scan cell is

$$B_c = \frac{N_b (GR_1) (GA_1)}{r_r r_a}$$

where

- GR_1 = length of image cell nearest satellite track
- GA_1 = width of the image cell nearest satellite track
- r_r = range resolution
- r_a = azimuth resolution.

The required channel capacity is then,

$$C_c = \frac{B_c}{T_c} \text{ bits/sec.}$$

1.4 INTERPRETABILITY CONSIDERATIONS

The interpretability of images is strongly affected by pixel size and by the degree to which speckle hides differences between pixels. There are two considerations in choosing the spatial resolution (pixel size) alone. Bandwidth is related to ground-range resolution by

$$BW = \frac{c}{2 r_r \sin \theta}$$

as discussed in section 1.3. At small look angles, the bandwidth becomes quite large, in spite of modest ground range resolutions. Secondly, if large azimuth resolutions are chosen, fewer filters are required and the complexity of the processor is reduced.

According to Moore (1976), interpretability I is related to resolution by

$$I = I_0 e^{-V/V_c}$$

where V = a volume descriptive of the resolution

V_c = an effective volume characteristic of the features to be interpreted.

The volume V , also known as the spatial gray-level volume (SGL) can be expressed as

$$V = r_a r_r r_g$$

where

r_a = pixel azimuth resolution

r_r = pixel range resolution

r_g = gray-level resolution.

Moore defines gray-level resolution for square-law detection as

$$r_{gN} = \frac{W_{N90}}{W_{N10}}$$

where

W_{N90} = power level below which 90% of the fading signals lie with N independent samples averaged

W_{N10} = level below which 10% of the signals lie with N independent samples averaged.

This ratio is then a measure of the ratio of signal powers that bound 80% of the expected received levels; or in terms of picture quality, this ratio is that within which 80% of the brightness levels are found. For a Rayleigh-fading signal (coherent reception, no averaging) $r_{gN} = 21.9$ while for a photograph (where thousands of independent samples are averaged by the panchromatic nature of light), $r_{gN} = 1$.

The potential resolution of the system using the full bandwidth for range resolution is r_{ao} by r_{ro} . Averaging signals from several cells results in a larger cell as in Figure 5. In this case 15 smaller cells have been averaged. Synthetic aperture systems may first process the 15 smaller pixels and add them together later or use subaperture processing in azimuth. r_{ao} would be the resolution limit for the fully focussed SAR, $\frac{L}{2}$ where L is the physical length of the antenna.

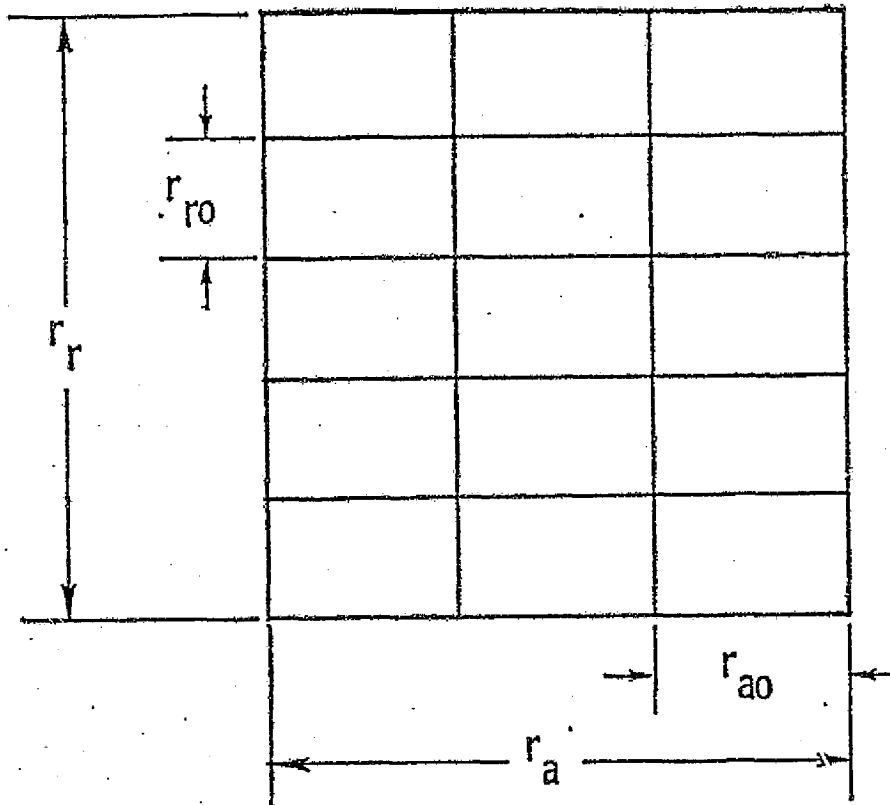


Figure 5. Pixel size.

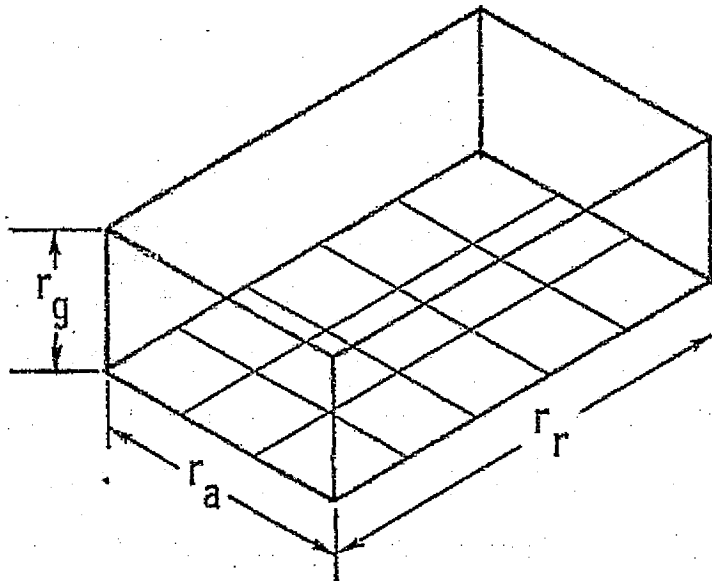


Figure 6a. The SGL volume.

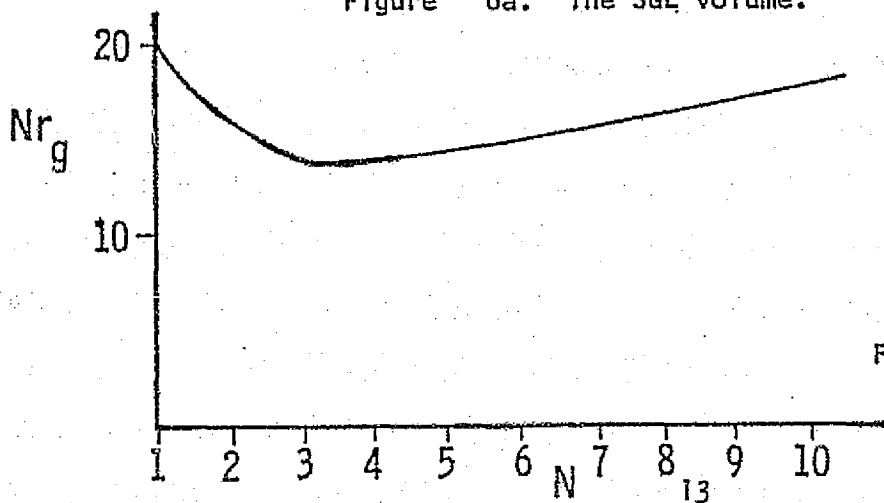


Figure 6b.

Figure 6a shows the resolution volume. Rewriting the SGL volume as

$$V = r_r [r_{ao} (N)] [r_g (N)]$$

where

$$r_a = r_{ao} N$$

allows for better observation of the inter-relation of the three quantities r_a , r_r , and r_g . This definition of V states that the interpretability is dependent on the area of the pixel and not just its linear dimension.

The minimum volume (best effective resolution) occurs where $N r_g (N)$ is a minimum, if r_r is fixed. $r_g (N)$ decreases rapidly as N goes from 1 to a small number, and then it decreases more slowly. The product $N r_g (N)$ is plotted in Figure 6b, where the minimum is shown to lie between $N = 2$ and $N = 3$. Since the picture quality is better for $N = 3$ than for $N = 2$, and since effective resolution is equivalent, $N = 3$ gives optimum results for visual interpretation. For quantitative measurement of scattering coefficient, $N = 3$ results in excessive uncertainty and some resolution must be sacrificed by making N larger to improve the precision of the measurement.

Regarding SCANSAR, and thinking of N as the number of looks per pixel in each scan cell, the tradeoffs between azimuth resolution and interpretability become apparent. The number of looks N_L is given by

$$N_L = \frac{T_{cell}}{\tau} = (T_{cell}) (\Delta f_d)$$

where

T_{cell} = dwell time on each image cell

Δf_d = tracking bandwidth

τ = integration time necessary to achieve the desired azimuth resolution.

The tracking bandwidth is directly proportional to the azimuth resolution. For fine resolutions, Δf_d is small and therefore the number of looks is small (and the number of filters needed to process the Doppler bandwidth)

is large). For somewhat worse resolutions, Δf_d is larger, the number of looks increases, and the interpretability goes up until $N = 3$. Obviously very coarse azimuth resolutions are unwanted due to their low information yield.

2.0 SYSTEM PARAMETERS

2.1 INTRODUCTION

The relationships discussed in 1.3 were compiled by Claassen into a computer design program entitled "SCANSAR". This program has since been modified somewhat and an updated listing can be found in Appendix A.

2.2 PARAMETER SELECTION

Two swaths determined by two look angle spans were chosen in order to accommodate both the sea ice and different parts of the water resources missions. An angular span of 7° - 22° was chosen since according to Ulaby (1976), the sensitivity to soil moisture is greatest at small angles of incidence. A 22° - 37° span was chosen for studies of snow-covered terrain, standing water, glaciers, lake ice, icebergs and sea ice. Although several candidates for operating wavelength were considered, 0.063 m (\sim 4.75 GHz) was chosen for two reasons. First, 4.75 GHz is considered a near-optimum frequency for viewing soil moistures when the ground is covered with vegetation (Ulaby, 1976). Second, the number of tracking filters is proportional to wavelength and 0.063 m was the smaller wavelength relative to other possible selections.

The aperture length was selected at 3 meters, the spacecraft altitude at 435 km, and the spacecraft ground velocity at 7.2 km/sec. 50 meters was chosen for the azimuth resolution, but at small incidence angles, 50 meter range resolution involves excessive bandwidth. Hence, 150 m range resolution was decided on for the inner edge of the near swath (7° - 22° angle range) and 50 m by 50 m was used in the far swath (22° - 37° angle range). The transmit power was based on readily available scattering data, a loss factor of 7 dB (3 dB one-way attenuation between antenna and transmitter and 1 dB 2-way atmospheric loss), a signal-to-noise ratio of 3 dB (for the smallest σ°), an aperture efficiency of 75%, and a receiver input noise temperature of 300° K.

The program is set up such that the angles input as the view angles are, in reality, the pointing angles. Hence, the actual range of illumination is somewhat larger due to the beamwidth of the antenna (which is assumed constant over the swath). A problem that has arisen from time to time is that of gaps appearing between the image cells at adjacent view angles. Since the beamwidth is a function of aperture height, which is a function of the largest look angle in the swath, this angle must be chosen with care. A good assumption to start with would be allowing the actual inner and outer edges of the swath illuminated by the extremes of the beamwidth at the inner and outer pointing angles to be $7^\circ - 22^\circ$ or $22^\circ - 37^\circ$ and increasing the number of cells in the swath by 1. Using this criterion, the actual input angles were 8.4° and 20.8° for the near swath (actual coverage from 6.7° to 22.4°) and 22.0° and 36.2° for the far swath (actual coverage from 22.1° to 36.9°). Computer runs for the two swaths follow. The "transmit power" number is the average. The processor gain can be thought of as the number of pulses integrated to achieve the desired resolution. The number of filter banks is the number needed for the processor to keep the Doppler shifts from ground targets in focus over the swath. The scan time is the total time for the antenna to scan over all the image cells in the swath. The time per cell is the amount of time the antenna dwells on each image cell.

2.3 CONCLUSIONS

In examining the system parameters and coverage output listings, several comments can be made. A relatively small antenna 3 meters by 2.4 meters could handle the system requirements. The average transmit power is a modest 15 watts in the far swath. 6 looks are obtained in the near swath, 3 in the far. Although the number of filters is fairly large, only one bank is needed for each swath, a filter bank being related to the radar's ability to track the Doppler returns over the swath, which is discussed in more detail in Section 4.0. Perhaps most important, the scanning SAR was able to provide coverage of 130 to 150 km compared with fixed angle coverage of only 15 to 30 km. Thus, for soil moisture obser-

vation, a scanning SAR looking out both sides of the satellite track could offer a total swath width of 260 km with a 50 m azimuth resolution. At a near optimum frequency of 4.75 GHz, using two 3 by 1.07 m antennas and 370 tracking filters, a transmitter power of 27 watts and a telemetry channel of 4.8 megabits/second are required.

DESIGN OF A SCANNING SAR HAVING INPUT DESIGN PARAMETERS AS FOLLOWS:

APERTURE LENGTH (M)? 3.0
 OPERATING WAVELENGTH (M)? 0.063
 MIN AND MAX VIEW ANGLES (DEG)? 8.40;20.80
 AZIMUTH RESOLUTION (M)? 50.00
 RANGE RESOLUTION (M)? 150.00
 GROUND VELOCITY (KM/SEC)? 7.2
 SPACECRAFT ALTITUDE (KM)? 435.0
 THE APERTURE HEIGHT IS 1.07 M. DO YOU WISH TO INCREASE THE HEIGHT? NO
 LOSS FACTOR (DB)? 7.0
 NOISE FIGURE (DB)? 6.0
 SIGNAL/NOISE (DB)? 3.00
 MAX SCATTERING COEFFICIENTS (DB)? 12.00;2.00
 MIN SCATTERING COEFFICIENTS (DB)? -4.00;-8.00
 APERTURE EFF (PERCENT)? 75.0
 RECEIVER INPUT TEMPERATURE (DEG K)? 300.0

SUMMARY TABLE

RAW DESIGN PARAMETERS

PARAMETERS	VALUES	UNITS
ANGLE SPAN	8.40 20.80	DEG
LAMBDA	0.063	M
APER LENGTH	3.0	M
AZ RES	50.00	M
RA RES	150.00	M
GRD VEL	7.2	KM/SEC
ALTITUDE	435.0	KM
APER EFF	75.0	PERCENT
LOSS FACTOR	7.0	DB
NOISE FIG	6.0	DB
SIG/NOISE	3.00	DB
REC TEMP	300.0	DEG K
SIGMAX	12.00 2.00	DB
SIGMIN	-4.00 -8.00	DB

COMPUTED SYSTEM PARAMETERS

SYSTEM TYPE:	SEMI-FOCUSED		
APER HEIGHT	1.07		M
XMIT PWR	1.85	13.39	WATTS
PRF	7.20		KHZ
FD	4.80		KHZ
RF BW	6.8		MHZ
PROC GAIN	277		
LOOKS	6		
FILTER BANKS	1		
FILTERS/BANK	185		
CHAN CAP	0.88	2.40	MBITS/SEC

COVERAGE AND RESOLUTION

SWATH	128.77		KM
CELLS/SCAN	5		
CELL WIDTH	9.23	9.77	KM
CELL LENGTH	26.19	29.33	KM
SCAN TIME	1.28		SEC
TIME/CELL	0.257		SEC
AZ RES	50.00	52.91	M
RA RES	150.00	19 61.71	M

DESIGN OF A SCANNING SAR HAVING INPUT DESIGN PARAMETERS AS FOLLOWS:

APERTURE LENGTH (M)? 3.0
 OPERATING WAVELENGTH (M)? 0.063
 MIN AND MAX VIEW ANGLES (DEG)? 22.90,36.20
 AZIMUTH RESOLUTION (M)? 50.00
 RANGE RESOLUTION (M)? 50.00
 GROUND VELOCITY (KM/SEC)? 7.2
 SPACECRAFT ALTITUDE (KM)? 435.0
 THE APERTURE HEIGHT IS 2.39 M. DO YOU WISH TO INCREASE THE HEIGHT? NO
 LOSS FACTOR (DB)? 7.0
 NOISE FIGURE (DB)? 5.0
 SIGNAL/NOISE (DB)? 3.00
 MAX SCATTERING COEFFICIENTS (DB)? 2.00,-2.00
 MIN SCATTERING COEFFICIENTS (DB)? -8.00,-12.00
 APERTURE EFF (PERCENT)? 75.0
 RECEIVER INPUT TEMPERATURE (DEG K)? 300.0

SUMMARY TABLE

RAW DESIGN PARAMETERS

PARAMETERS	VALUES	UNITS
ANGLE SPAN	22.90 36.20	DEG
LAMBDA	0.063	M
APER LENGTH	3.0	M
AZ RES	50.00	M
RA RES	50.00	M
GRD VEL	7.2	KM/SEC
ALTITUDE	435.0	KM
APER EFF	75.0	PERCENT
LOSS FACTOR	7.0	DB
NOISE FIG	5.0	DB
SIG/NOISE	3.00	DB
REC TEMP	300.0	DEG K
SIGMAX	2.00	DB
SIGMIN	-8.00 -12.00	DB

COMPUTED SYSTEM PARAMETERS

SYSTEM TYPE:	SEMI-FOCUSED		
APER HEIGHT	2.39		M
XMIT PWR	2.76	15.64	WATTS
PRF	7.20		KHZ
FD	4.80		KHZ
RF BW	7.7		MHZ
PRDC GAIN	297		
LOOKS	3		
FILTER BANKS	1		
FILTERS/BANK	198		
CHAN CAP	1.95	3.85	MBITS/SEC

COVERAGE AND RESOLUTION

SWATH	150.21		KM
CELLS/SCAN	10		
CELL WIDTH	9.92	11.32	KM
CELL LENGTH	13.53	17.64	KM
SCAN TIME	1.38		SEC
TIME/CELL	0.138		SEC
AZ RES	50.00	20 57.08	M
RA RES	50.00	32.94	M

DEFINITION OF SYMBOLS

APER = aperture
AZ = azimuth
XMIT PWR = average transmit power
 F_D = total Doppler bandwidth
RF BW = RF bandwidth
PROC = processing
CHAN CAP = channel capacity
RES = resolution

3.0 RADAR SYSTEM AND ANTENNA

3.1 INTRODUCTION

Based on the parameters discussed in section 2.0, the transmitted pulse length τ is the reciprocal of the RF bandwidth (6.8 MHz for the near swath) and the PRF is 7200 Hz. The duty cycle is defined as the ratio of the time the transmitter is pulsed to the interpulse period or

$$D = \frac{\tau}{T}$$

where $T = \frac{1}{\text{PRF}}$.

Using the above numbers, $D = .106\%$. The transmitter average and peak powers are related by the duty cycle as

$$W_{\text{av}} = D \cdot W_{\text{peak}}$$

If W_{av} is 15 watts, then the peak power is 14.2 KW. This very high peak power can be reduced by using chirp techniques to expand the transmitted pulse and increase the duty cycle. Using a 100 to 1 chirp, the transmitted pulse length becomes 14.7 microseconds, the duty cycle becomes 10.6%, and the peak power becomes a more modest 142 watts.

3.2 PULSE COMPRESSION TECHNIQUES

Although many pulse compression techniques have been developed, passive linear FM and active phase coded implementations are the most widely used. Either implementation could be used in the SCANSAR design.

3.2.1 Linear FM

The linear FM or chirp waveform is relatively easy to generate and because of its ease of implementation it has become one of the most popular pulse compression techniques. Two classes of devices are used in generating and processing chirp waveforms: 1) ultrasonic devices in which an electrical signal is converted to a sonic wave and back, and 2) electrical devices that use the dispersive characteristics of elec-

trical networks. Many types of devices exist in both classes, however, one of the best developed technologies is found in the area of dispersive delay lines which belongs to the ultrasonic class - specifically, the surface acoustic wave (SAW) delay line.

SAW dispersive delay lines use an input and output array of electrodes on the same surface of a piezoelectric plate (nondispersive medium) to create a linear delay-vs.-frequency characteristic. If an electric signal is applied to the electrodes, a surface wave is generated; conversely a surface wave applied to the electrodes will induce a voltage across them. The delay-vs.-frequency behavior is determined by the electrode spacing, which can effect an up or down-chip depending on the orientation. Figure 7 is a block diagram illustrating the use of a SAW delay line chirp generator and decoder. Here, a signal is down-chirped, mixed up to some carrier frequency and transmitted. The received signal is then mixed down to some intermediate frequency (typically 30-500 MHz) and up-chirped. In practice, the same dispersive delay line may be used for both the transmitted and received signals. Several manufacturers including Plessey and Andersen Laboratories offer product lines with SAW dispersive delay line pulse-compression ratios as high as 625.

3.2.2 Phase-coding

Phase coded waveforms differ from linear FM in that the pulse is divided into several sub-pulses, each of equal length and a particular phase. The phase is selected in accordance with a phase code. Binary coding, the most popular, consists of a sequence of 1s and 0s or +1s and -1s, the phase of the transmitted signal alternating between 0° and 180° in accordance with the sequence as in Figure 8. The compression ratio is equal to the number of subpulses in the waveform.

A special class of binary codes, the Barker codes, are considered optimum in the sense that the peak of the autocorrelation function is N and the sidelobe magnitude less than or equal to one, where N is the number of elements in the code. At present, Barker codes are known only

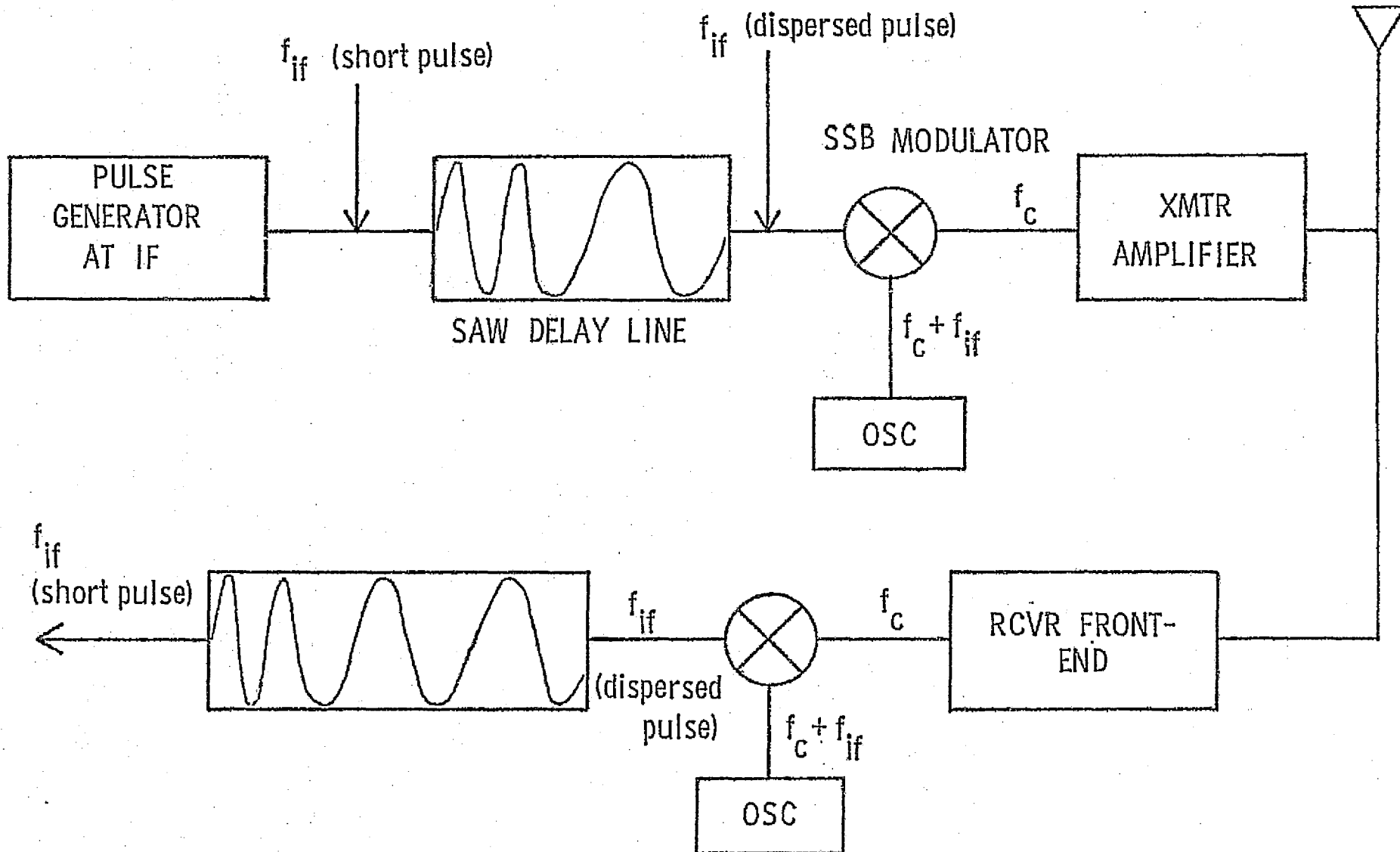


Figure 7. A chirp generator and decoder using SAW dispersive delay lines.

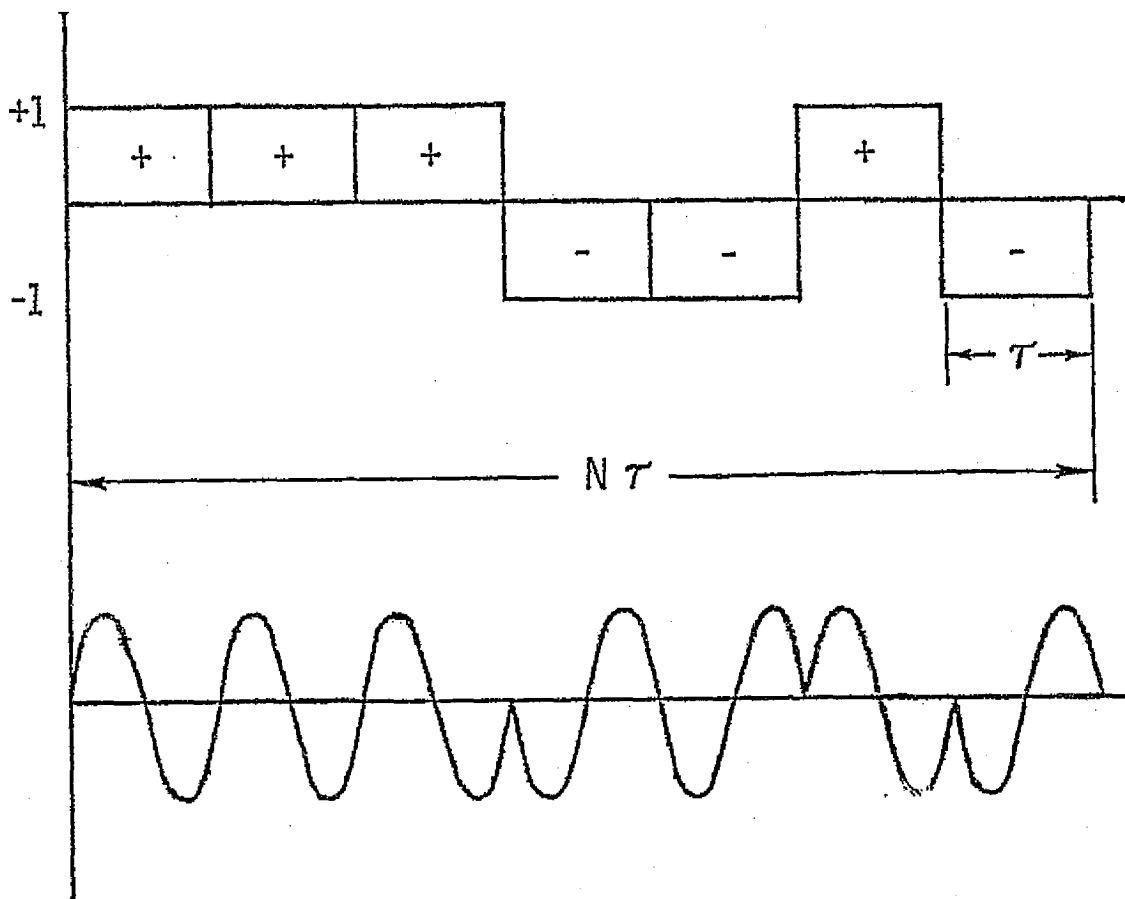


Figure 8. A pulse $N\tau$ seconds long expressed in a binary phase code.

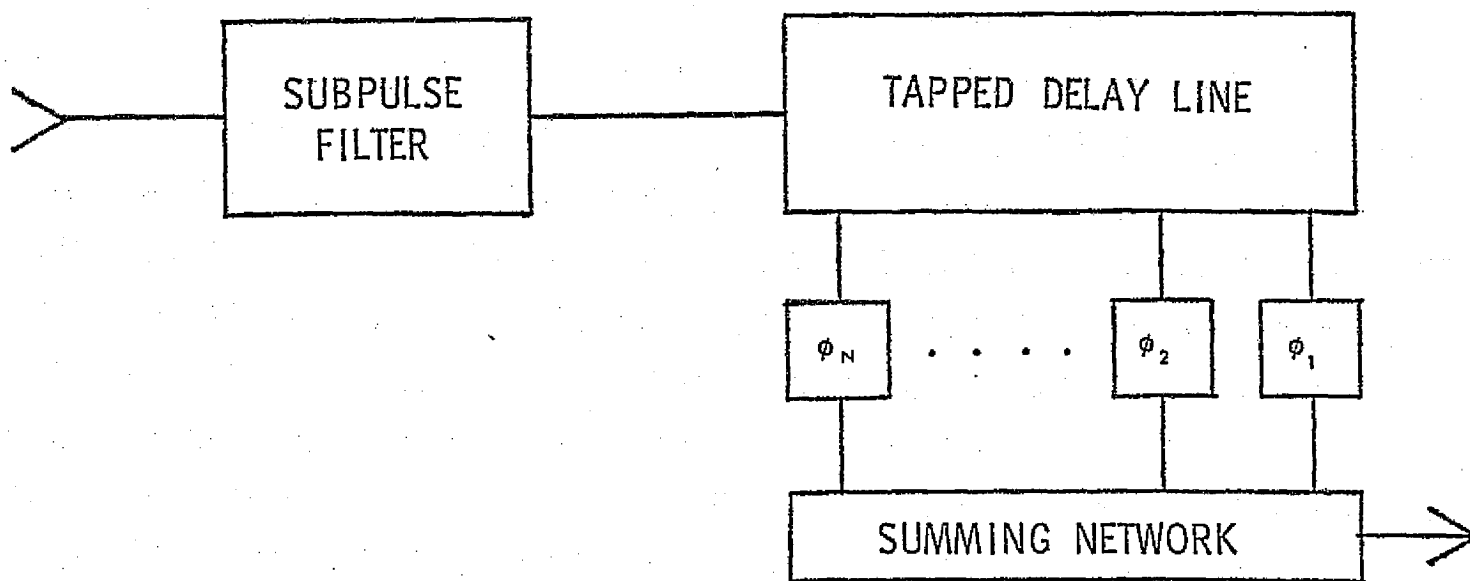


Figure 9. A phase-coded receiver.

up to a compression ratio as high as 13. Longer phase codes can, of course, be used for greater pulse-compression ratios. They are not optimum in the Barker-code sense, but codes with reasonable sidelobes exist and can be used.

A matched-filter receiver for phase coded waveforms is given in Figure 9. The received signal is passed through a bandpass filter matched to the subpulse width and applied to a tapped delay line. The taps are spaced at intervals of the subpulse width; the phase shift at each tap being 0° or 180° in accordance with the phase code.

3.3 RECOMMENDED HARDWARE

3.3.1 Power Output Amplifier

The selection of the power output amplifier may be made from three candidates: the travelling-wave tube (TWT) the klystron, and the solid state amplifier (SSA). At 4.8 GHz, the SSA, although ideal in many ways is limited in its maximum power output to a peak power on the order of 100 watts. The klystron stability is as good or better than the TWT but it suffers from a lack of bandwidth. The recommended TWT has the best overall bandwidth and efficiency (single stage efficiency running at about 25%). The TWT also has an excellent track record concerning its use on spacecraft. The Hughes family of space-qualified TWT's can boast over 800,000 hours of failure-free life-test and space operation. See Erickson (1975) for more detail concerning power output amplifiers.

3.3.2 Receiver Front-End

Perhaps the single most important consideration amongst receivers is noise. Possible choices for the low noise amplifier (LNA) are the parametric amplifier, the transistor amplifier, and the tunnel-diode amplifier (TDA). According to Erickson (1975), these three amplifiers have noise figures at 5 GHz of approximately 0.5 dB, 2.3 dB, and 4.5 dB respectively. With a total noise figure of 5 dB for SCANSAR, the TDA

can be rejected immediately. Of the paramp and the transistor amplifier, the latter can claim high reliability, large dynamic range, high power output, non-critical power supply, and low weight. With advancing technology the noise figure of the transistor amplifier may be reduced even further, so it would make an excellent choice for the SCANSAR LNA.

3.4 ANTENNA CONSIDERATIONS

Considering the aperture height at the maximum range in the far swath, a 3 meter by 3 meter electronically scanned antenna could handle the SCANSAR system requirements. Two antennas would be used for a double-sided SAR. Electronic scanning is desirable in that a minimum amount of time (1 to 3 microseconds) is spent changing pointing angles. Fong (1976) considers other benefits to electronic scanning including computer operation and reliability. The nominal pointing angle for each swath should be the farthest one. In the computer design, a constant beamwidth was assumed over each swath. In reality, the beamwidth is inversely proportional to the tangent of the pointing angle so the beamwidth increases with decreasing angle. For purposes of coverage, therefore, it would be desirable to set the beamwidth according to the farthest pointing angle and scan the beam inwards towards the satellite.

Another alternative antenna structure is a parabolic reflector with multiple, off-axis, feeds. The number of feeds required is 5 or 10 depending on the swath to be observed. Total scan is about 30° , so pointing at 22° would allow a scan of $\pm 15^\circ$. Since the feed for such an antenna need be off-axis by only half the scan angle, feeds need only occupy space $\pm 7.5^\circ$ from the "horizontal" axis of the antenna. Such an antenna might well be significantly less expensive than a scanned array, particularly in view of the extensive experience with reflector antennas on communication satellites.

Before reflector antennas can be considered as real candidates for SCANSAR, a thorough study should be made of the effect of aperture blockage on sidelobes and consequently on ambiguities.

4.0 PROCESSOR

4.1 INTRODUCTION

Although digital SAR processors are presently quite popular, analog processors offer another means for processing radar images on-board and in real time. The recommended processor uses comb filters implemented by recursive use of analog shift registers.

In this form, the various range elements are processed sequentially as a signal circulates around a delay element and is added to the incoming signal. The comb-filter has a set of passbands spaced as the Fourier components of the received pulse, permitting narrow band Doppler filtering while retaining the wideband characteristic of the pulse necessary to retain range resolution. An obvious benefit to using this type of processor is that the amount of storage necessary to process the returns is considerably less than those processors which batch process the range cells, since here no memory is required for individual signal elements.

4.2 COMB FILTER CONCEPTS

SAR data processing involves correlating chirp waveforms generated by varying Doppler shifts as the radar travels past targets on the ground. If the integration time necessary to yield a required azimuth resolution is T and if the system PRF is F , then the number of pulses, N , integrated during the building of each synthetic aperture is

$$N = TF.$$

In a comb filter, each return is delayed by the repetition period and summed with the next incoming return, this cycle being repeated until all N pulses have been added together. Only signals having the proper period add each time, the others drift in and out of phase during integration.

The comb-filter pass bands are spaced such that they align with the Fourier components of the received pulse as in Figure 10. The effect of Doppler shift is to introduce an offset in the spectral components, so the comb-filter must be phase shifted by this amount as in

Figure 11. The system, then is composed of a set of comb-filters, each tuned to accommodate the Doppler shifts from a particular azimuth element such that the entire range of Doppler frequencies over an observed area on the ground is within the total passband of the processor.

As shown in Figure 12, a comb filter consists of a delay device, a tunable phase shifter, and a weighting amplifier. The delay device samples the first return and holds it for the proper period, the phase shifter tunes the filter for the desired Doppler shift and the weighting amplifier is used to reduce the sidelobes in the $\sin x/x$ character of the comb teeth. After the proper number of pulses is integrated by the filter, the composite waveform is fed into a buffer for temporary storage. 198 filters per side are used to facilitate both swaths.

According to Komen (1976) in order for pulses from the same azimuthal strip to add in phase,

$$\phi - W_n T = -2\pi r$$

where

ϕ = phase shift to tune each filter channel

W_n = IF frequency of the returns

$$T = \frac{1}{\text{PRF}}$$

r = some integer.

Since $W_n = nW_0$ where $W_0 = \frac{2\pi}{T}$,

$$W_n = \frac{\phi}{T} + nW_0$$

$$W_{n+1} = \frac{\phi}{T} + (n+1)W_0$$

where W_n and W_{n+1} are harmonics of W_0 . These two equations show that a constant phase shift ϕ introduced at some frequency W_n will appear in all the harmonics of that frequency.

The expression for the pulses circulating the loop ℓ times can be written as

$$\sum_n a_n e^{j(W_n + \delta_n)t} \sum_i e^{-j\delta_n t}$$

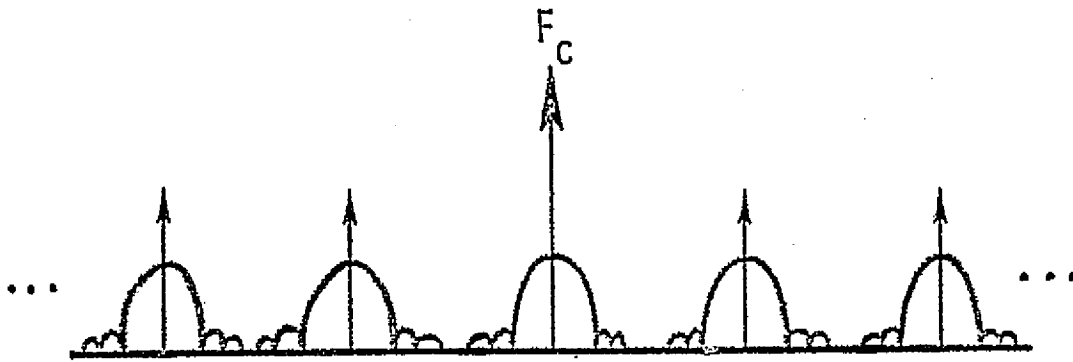


Figure 10. Comb filter passbands showing carrier and its side-bands (zero phase shift).

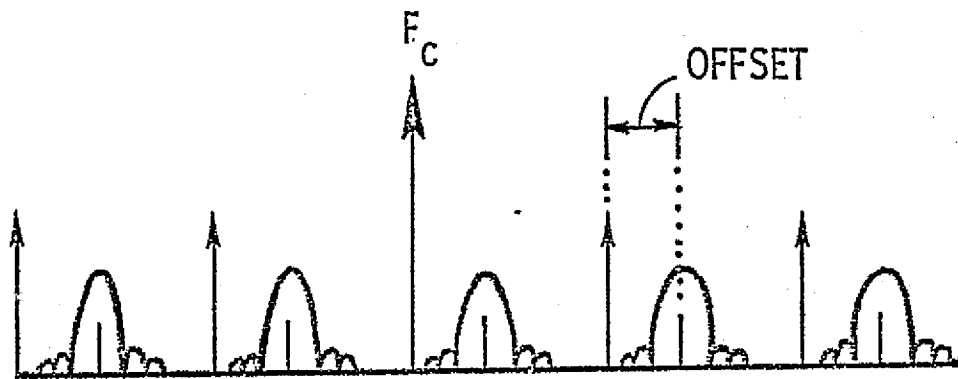


Figure 11. Comb filter passbands phase-shifted to account for Doppler shifting.

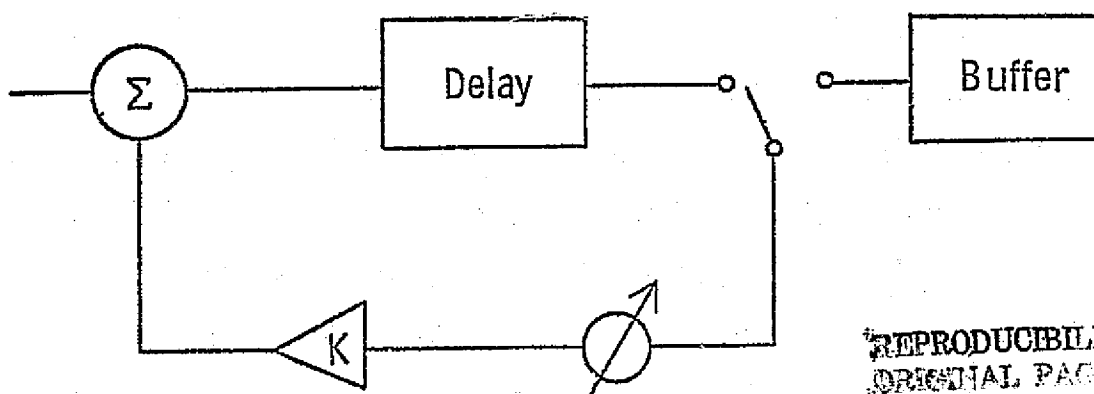


Figure 12. A comb filter delay line.

REPRODUCIBILITY OF
ORIGINAL PAGE

where δ_n is a small offset from W_n .

Rewriting, the expression becomes

$$\sum_n a_n e^{j(W_n + \delta_n)t} \left(\frac{\sin \frac{\ell T \delta_n}{2}}{\sin \frac{T \delta_n}{2}} \right) e^{\frac{j(\ell-1)T \delta_n}{2}}$$

It is noted that $\sum_n a_n e^{j(W_n + \delta_n)t}$ represents the original signal W_n with the δ_n offset. The $\sin nx/\sin x$ expression shows the comb response. As δ_n is small, the last factor can be neglected.

Introducing the weighting amplifier with gain K , the circulation expression becomes

$$\sum_n a_n e^{j(W_n + \delta_n)t} \sum_i K_i e^{-j i \delta_n T}$$

Standard methods in antenna and filter design can be used to establish weights (K_i) that give the desired sidelobe suppression with the usual widening of the main response.

Since the Doppler shift for any point target decreases linearly in frequency with time as the radar passes the target, the processor must take this into account. The SCANSAR system converts this varying frequency to a fixed frequency by beating the incoming signal with an appropriate reference function varying at the same rate as the signal from the point target. As the satellite moves, the ground returns will shift in frequency but after beating with the proper swept local oscillator signal, the return from each azimuth remains fixed. Implementation of the comb-filter follows.

4.3 DESIGN CONSIDERATIONS

4.3.1 PRF Diversity

The tracking bandwidth Δf_d , the integration time τ , the beamwidth

B_h , and the pulse width τ_p are listed below.

	Δf_d (Hz)	τ (sec)	B_h ($^\circ$)	τ_p (sec)
Near Swath	26.0	0.03846	3.376	$.147 \times 10^{-6}$
Far Swath	24.2	0.04132	1.513	$.130 \times 10^{-6}$

Assuming the beamwidth constant, the actual total angular coverage for each scan position for both swaths is listed in Table 1.

In examining the actual angular coverage at each scan position, an interesting problem arises. The beam energy will strike the near edge of each image cell before it strikes the far edge. Since the range R is a function of known angles, the actual times the returns arrive at the antenna can be determined by

$$T = \frac{2R}{c}$$

where c = speed of light.

The transmitter will send out pulses every $\frac{1}{\text{PRF}}$ seconds. After K pulses, the returns will begin arriving at the antenna at an interval of every $\frac{1}{\text{PRF}}$ seconds. Upon closer examination of the transmit and receive times it can be observed that at certain pointing angles, the returns will arrive during the time the transmitter is supposed to be transmitting.

For example, Table 2 lists the actual times a pulse will return from the inner and outer edges of each scan cell (the HP-25 calculator program which generated the data for this Table can be found in Appendix B), neglecting transmit pulse length. Table 3A shows the pulse transmit times at a PRF of 7200 Hz. It is observed that a pulse is being transmitted while the returns from near swath scan cell 4 and far swath cells 2, 6, 8, and 10 are being received at the antenna. This highly undesirable condition can be readily resolved by studying other PRFs that satisfy the ambiguity relationships and selecting one to use as an alternative at the selected pointing angles. A PRF of 7050 Hz was chosen and as Table 3B shows, the problem is solved for the aforementioned scan positions. This means that slightly fewer pulses are integrated. The

TABLE 1.

NEAR SWATH

<u>Scan Position</u>	<u>Beam Near Edge</u>	<u>Antenna Pointing Angle</u>	<u>Beam Far Edge</u>
1	6.712°	8.400°	10.088°
2	9.812°	11.500°	13.188°
3	12.912°	14.600°	16.288°
4	16.012°	17.700°	19.388°
5	19.112°	20.800°	22.488°

FAR SWATH

<u>Scan Position</u>	<u>Beam Near Edge</u>	<u>Antenna Pointing Angle</u>	<u>Beam Far Edge</u>
1	22.144°	22.900°	23.657°
2	23.622°	24.378°	25.135°
3	25.100°	25.856°	26.613°
4	26.577°	27.333°	28.089°
5	28.055°	28.811°	29.568°
6	29.533°	30.289°	31.046°
7	31.011°	31.767°	32.524°
8	32.488°	33.244°	34.001°
9	33.966°	34.722°	35.479°
10	35.444°	36.200°	36.957°

TABLE 2:
NEAR SWATH

Scan Cell	Time From Inner Edge	Time From Outer Edge	Pulse Length
1	2.92001 msec	2.94554 msec	25.52 msec
2	2.94305	2.97855	35.50
3	2.97523	3.02126	46.03
4	3.01705	3.07434	57.29
5	3.06917	3.13867	69.49

FAR SWATH

Scan Cell	Time From Inner Edge	Time From Outer Edge	Pulse Length
1	3.13094 msec	3.16606 msec	35.12 msec
2	3.16522	3.20332	38.11
3	3.20241	3.24366	41.25
4	3.24264	3.28717	44.54
5	3.28613	3.33721	48.08
6	3.33306	3.38487	51.81
7	3.38363	3.43942	55.79
8	3.43804	3.49807	60.03
9	3.49663	3.56122	64.58
10	3.55967	3.62914	69.47

TABLE 3A.

PRF = 7200 Hz

<u>Pulse Number</u>	<u>Transmit Time</u>
21	2.77778 msec
22	2.91667
23	3.05556
24	3.19444
25	3.33333
26	3.47222
27	3.61111
28	3.75000

TABLE 3B.

PRF = 7050 Hz

<u>Pulse Number</u>	<u>Transmit Time</u>
21	2.83688 msec
22	2.97872
23	3.12057
24	3.26241
25	3.40426
26	3.54610
27	3.68794
28	3.82979

number of pulses integrated in each swath for each PRF is listed below.

	<u>PRF = 7200 Hz</u>	<u>7050 Hz</u>
Near Swath	276	271
Far Swath	297	291

It should be noted that in section 2, the computer listing for the near swath shows the process gain as 277. However, in rounding the tracking filter bandwidth Δf_d to 26.0 Hz, the process gain reduces to 276 and the processor is designed around this number.

The PRF assignment for each scan cell of each swath is as follows:

	<u>PRF = 7200 Hz</u>	<u>7050 Hz</u>
Near Swath	1, 2, 3, 5	4
Far Swath	1, 3, 4, 5, 7, 9	2, 6, 8, 10

The PRF diversity does complicate the processor to some extent but it can be handled easily enough.

4.3.2 Doppler Slope

The SAR processor must correlate chirp waveforms generated by the varying Doppler shifts as the radar travels past targets on the ground. The SCANSAR system accomplishes this by beating these waveforms with some reference function varying at the same rate as the Doppler shifts. The result is a set of fixed frequencies which can be processed by the proper comb-filter channel. It is then necessary to determine just how much the Doppler shifts will change during the time it takes for one look.

From the Westinghouse report ("Final Report - Spaceborne SAR Pilot Study", 1974), the instantaneous Doppler frequency and FM slope are directly proportional to range rate (velocity) and range acceleration, respectively,

$$f_d = \frac{-2R}{\lambda}$$

and

$$f_d' = \frac{-2\dot{R}}{\lambda}$$

Figure 13 shows how these quantities are related to inertial or flight parameters. Triangle XYR forms a plane where X is the component of the distance from the antenna center to the target in the direction of the velocity vector. Y is the distance from the antenna center to the X plane (earth's surface) orthogonal to X while R is the distance from the antenna center to a target located along the X-axis. Hence,

$$R^2 = X^2 + Y^2.$$

Taking the time derivative of both sides,

$$\dot{R}R = X\dot{X} + Y\dot{Y}.$$

However, $\dot{Y} = 0$ since V and X are parallel and the satellite is assumed to be flying a straight path. Therefore,

$$\dot{R} = \frac{X\dot{X}}{R} = -V \cos \alpha = -V_R$$

where

V = spacecraft velocity

V_R = component of spacecraft velocity along the line of sight to the target (LOS)

α = angle between the velocity vector and the LOS to the target.

Then,

$$f_d = \frac{2V}{\lambda} \cos \alpha = \frac{2V_R}{\lambda}$$

Differentiating again with respect to time,

$$\dot{R}^2 + R\ddot{R} = \dot{X}^2 + X\ddot{X} + \dot{Y}^2 + Y\ddot{Y}$$

$$\ddot{R} = \frac{\dot{X}^2 - R^2}{R} + \frac{X\ddot{X}}{R} + \frac{\dot{Y}^2}{R} + \frac{Y\ddot{Y}}{R}$$

Since $\dot{Y} = 0$ and substituting for \dot{R} ,

$$\begin{aligned} \ddot{R} &= \frac{V^2 (1 - \cos^2 \alpha)}{R} + \ddot{X} \cos \alpha + \ddot{Y} \sin \alpha \\ &= \frac{V^2 \sin^2 \alpha}{R} + \ddot{X} \cos \alpha + \ddot{Y} \sin \alpha \end{aligned}$$

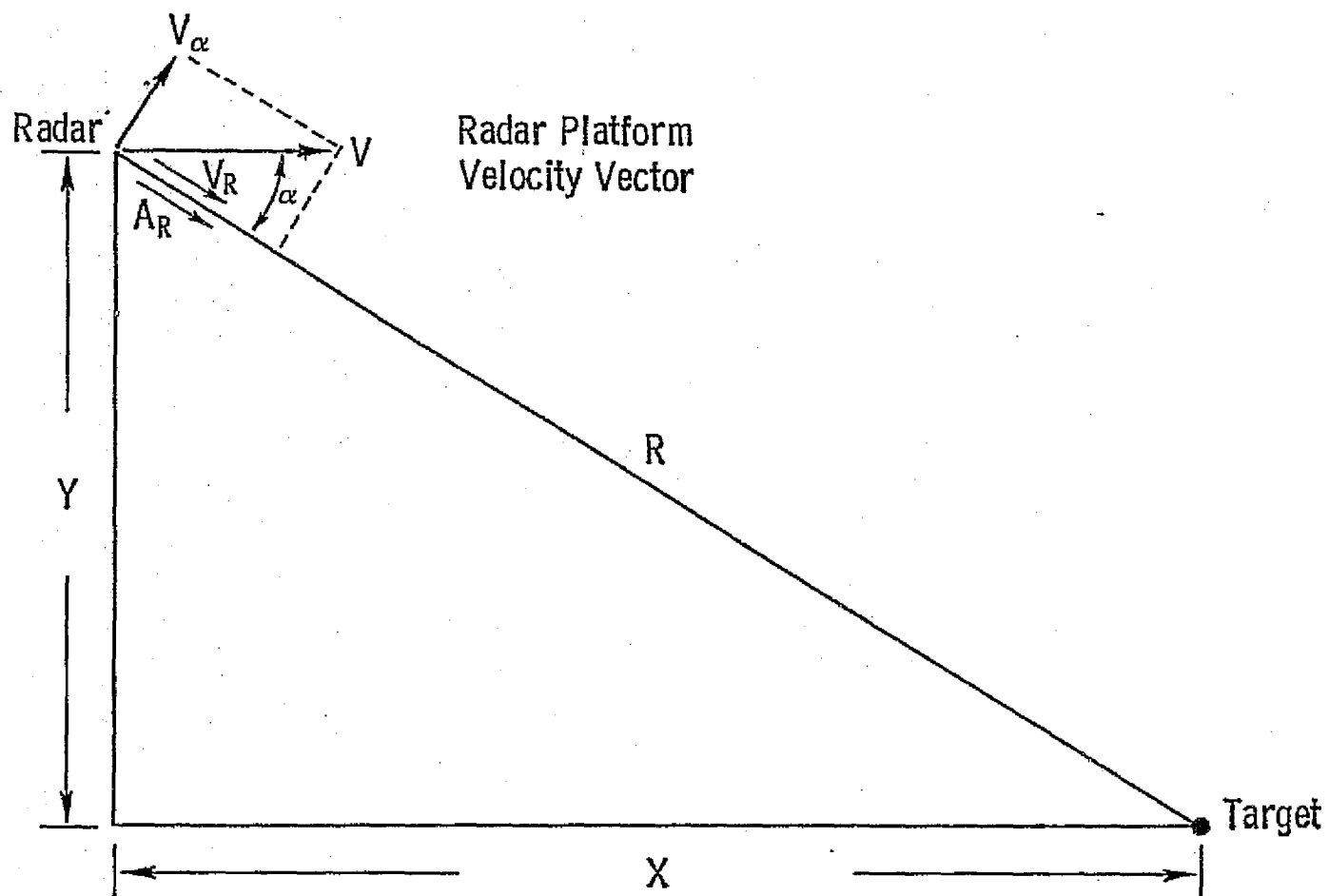


Figure 13. Doppler slope geometry.

or,

$$\ddot{R} = \frac{V_a^2}{R} - a_r$$

where

$V_a = V \sin \alpha =$ spacecraft velocity component perpendicular to LOS

$a_r =$ component of acceleration along LOS.

Thus, the Doppler FM slope is

$$\left| \dot{f}_d \right| = \frac{-2}{\lambda} \left[\frac{V_a^2}{R} - a_r \right]$$

For a constant velocity and a side looking radar,

$$\dot{f}_d = \frac{2 V_g^2}{\lambda R} \text{ Hz/sec}$$

where

$V_g =$ satellite ground velocity

$\lambda =$ wavelength

$R =$ range to the swath

To observe the Doppler shifts over the swath, the range R is considered to the swath inner edge, center, and outer edge.

The total change for one look is

$$\Delta f = \dot{f}_d (R) \tau$$

where $\tau =$ integration time for one look.

If the total change over the swath is less than the tracking bandwidth

$$\Delta f (R_i) - \Delta f (R_o) \leq \Delta f_d$$

where

$R_i =$ Range to swath inner edge

$R_o =$ Range to swath outer edge,

the range elements remain "in focus". If this condition is satisfied, one bank of filters will be able to process the returns. Setting the reference function to vary as Doppler frequency changes in the center of

the swath will enable the inner and outer edges to remain in focus. The reference function could vary on a per-pulse basis tuned to the swath center Δf_{pc} or

$$\Delta f_{pc} = \frac{\Delta f (R_c)}{N}$$

where

N = number of pulses integrated

R_c = range to swath center.

A summary is given for both swaths in Table 4.

4.4 SYSTEM DESIGN

The radar system will transmit and receive at 4.75 GHz. The incoming signal will be mixed down to 60 MHz and then to 5 MHz for use in the filter channels. Figure 14 shows the frequency translation and the RF bandwidth of the returns.

A better picture of what is to happen can be seen by expanding Figure 14 in the 5 MHz region and showing the comb of spectral components over the 6.8 MHz bandwidth of the near swath as in Figure 15. The 4.8 kHz spread about each spectral line is the Doppler frequency spread. In order to sample the return information properly, the processor sampling frequency must be at least twice the highest frequency over the bandwidth or, at least 16.8 MHz. Expanding this figure about the center frequency as in Figure 16 shows the individual filter positioning over the Doppler band. 198 filters will cover the Doppler returns from both swaths. Only 185 of these are needed for the near swath.

The basic processor for the SCANSAR is shown in Figure 17. The processing system takes the range-offset coherent video signals from the radar system, preprocesses them with a scanning local oscillator, comb-filters simultaneously observed banks of azimuth elements and delivers the processed pixels to the telemetry system for transmission back to earth. Examination of the subsystems follows.

TABLE 4.

	Near Swath	Far Swath
$f_d^* (R_i)$	3757.32 Hz/sec	3504.20 Hz/sec
$f_d^* (R_c)$	3656.39 Hz/sec	3273.10 Hz/sec
$f_d^* (R_o)$	3496.58 Hz/sec	3023.15 Hz/sec
$\Delta f (R_c)$	140.62 Hz	135.25 Hz
Δf (swath)	10.03 Hz	19.87 Hz
Δf_{pc} (PRF = 7200)	.509 Hz/pulse	.455 Hz/pulse
Δf_{pc} (PRF = 7050)	.519 Hz/pulse	.465 Hz/pulse

$\Delta f_d^* (R)$ = Doppler slope to the swath inner edge, center, and outer edge

$\Delta f (R_c)$ = total Doppler frequency change over one look at the swath center range

Δf (swath) = change in total Doppler frequency over the swath

Δf_{pc} (PRF) = change of reference function on a per-pulse basis tuned to the swath center

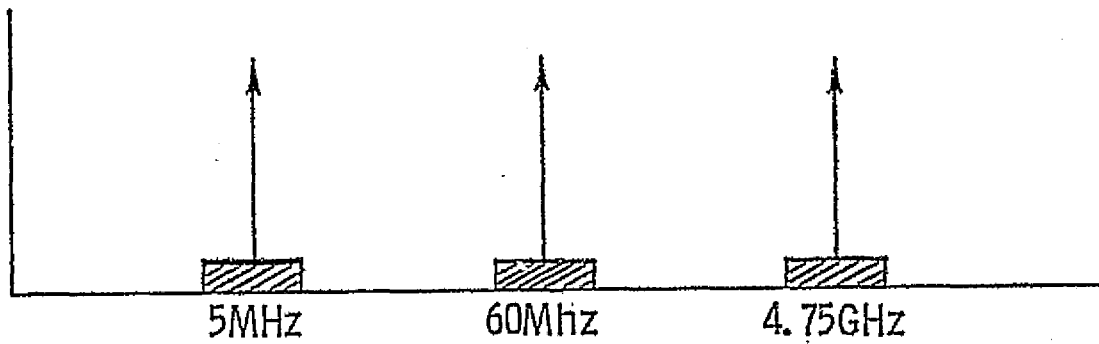


Figure 14. RF to IF frequency translation showing RF bandwidth.

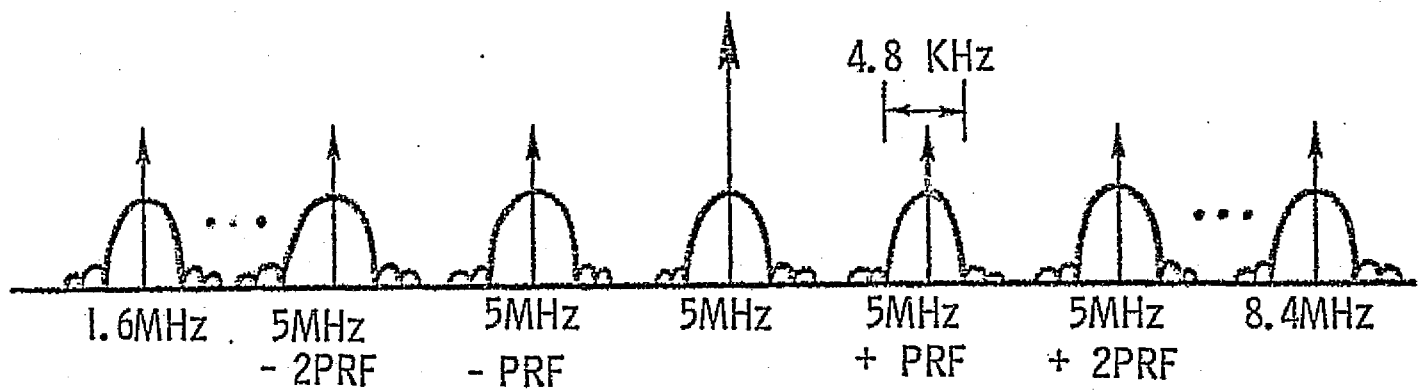


Figure 15. RF bandwidth on 5 MHz filter channel carrier showing Doppler spread.

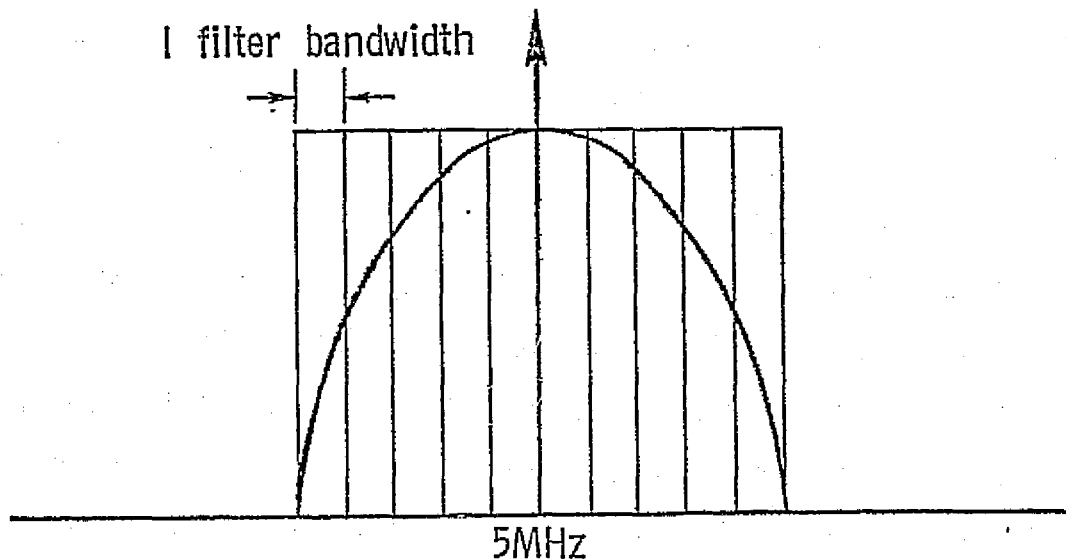


Figure 16. Representation of comb filter coverage of Doppler spread.

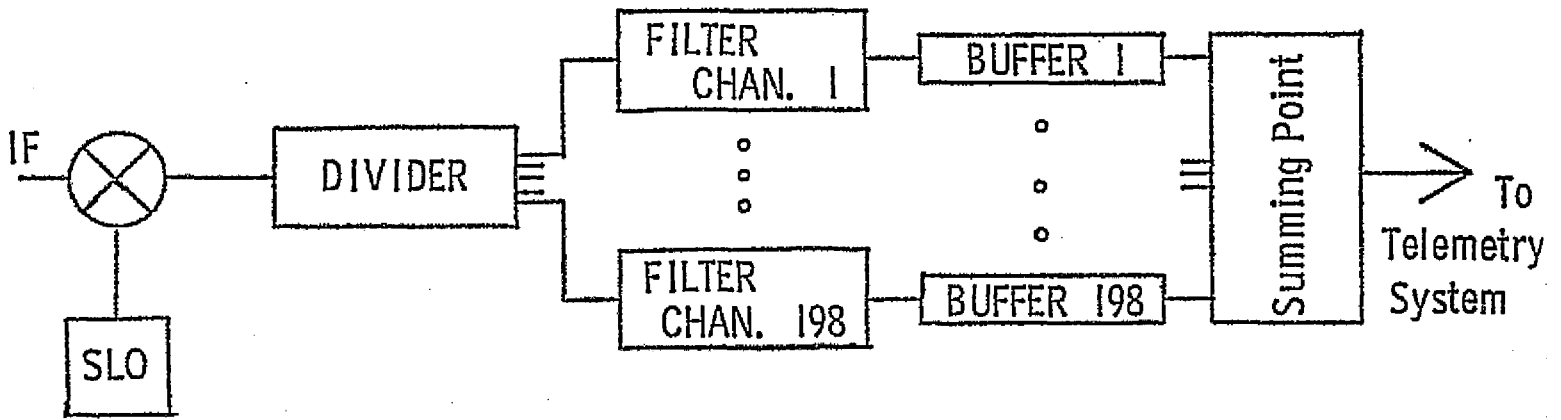


Figure 17. Basic processor.

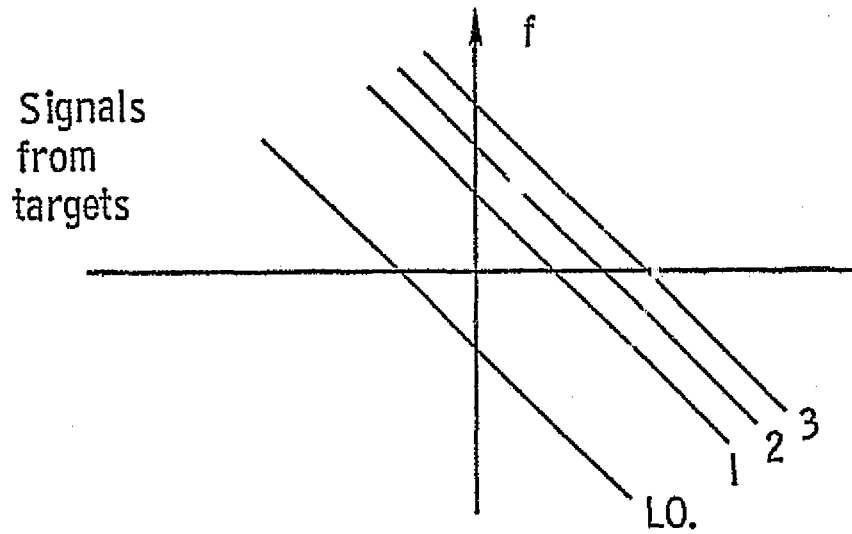


Figure 18a. Mixer Input.

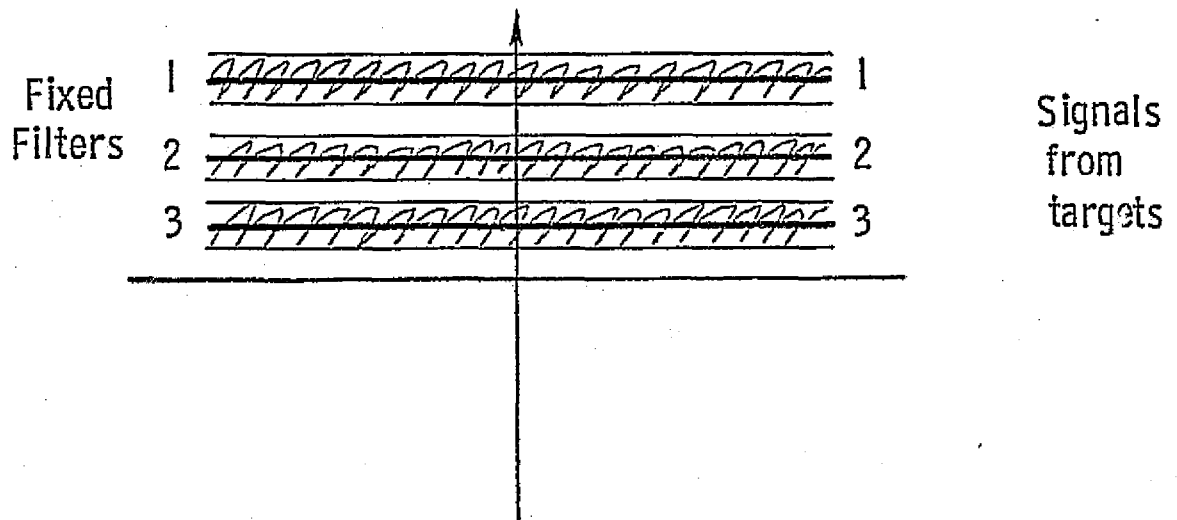


Figure 18b.. Mixer Output.

4.4.1 The Scanning Local Oscillator (SLO)

The SLO must provide a signal whose frequency varies at the same rate as the Doppler shift change for a given pixel so the mixer output for each pixel is a constant frequency as in Figure 18. In the figure, the Doppler frequency shifts from three point targets of adjacent along-track pixels are shown to be linearly decreasing functions of time. Mixing with the SLO yields a set of constant frequencies which can be filtered with fixed filters in the channel bank.

The SLO can be implemented by considering that the Doppler slope is known and the change of Doppler frequency has been calculated on a per-pulse basis in section 4.3. One method would be phase-shifting the SLO at certain increments after a specified number of pulses has been received to produce the desired frequency shift. Another would be using balanced modulators.

a. SLO by Phase Shifting

Frequency w is defined as the change of phase ϕ with time or,

$$\phi = \int w dt$$

Since it is desired to change the frequency with time,

$$\phi = \int (w \pm \Delta w) dt$$

where Δw is the total change in Doppler frequency during one look. As shown earlier, the total Doppler shift is given by

$$\Delta w = at$$

where

a = Doppler slope

t = time for one look.

Integrating,

$$\phi = wt \pm \frac{1}{2} at^2$$

where $\frac{1}{2} at^2$ is the total phase shift during one look.

Substituting,

$$\frac{1}{2} at^2 = \frac{1}{2} \Delta wt$$

$$\phi = \frac{2\pi \Delta ft}{2} \times \frac{180^\circ}{\pi} = 180^\circ \Delta ft$$

Using the numbers from Table 4 of the preceding section,

$$\phi \text{ (Total, Near Swath)} = 973^\circ$$

$$\phi \text{ (Total, Far Swath)} = 1006^\circ$$

The phase shift $\Delta\phi$ between any two returning pulses t_n and t_{n+1} is

$$\begin{aligned}\Delta\phi &= \frac{1}{2} at_{n+1}^2 - \frac{1}{2} at_n^2 \\ &= \frac{1}{2} a (t_{n+1}^2 - t_n^2) \\ &= \frac{1}{2} a (t_{n+1} + t_n) (t_{n+1} - t_n)\end{aligned}$$

Recognizing the last term as the repetition rate ($\frac{1}{\text{PRF}}$),

$$\Delta\phi = \frac{a}{\text{PRF}} \left(\frac{t_{n+1} + t_n}{2} \right)$$

where the term in parentheses is the actual average time coordinate for 2 adjacent pulses, T_{avg}

$$\Delta\phi \text{ (degrees)} = \frac{360^\circ a}{\text{PRF}} T_{\text{avg}}$$

Since there are two PRFs and a Doppler Slope (a) for each swath, this equation can be rewritten as

$$\Delta\phi \text{ (degrees)} = K T$$

where

$$K = \frac{360^\circ a}{\text{PRF}}$$

Values of K for each PRF and swath are listed below.

	<u>PRF = 7200 Hz</u>	<u>7050 Hz</u>
Near Swath	182.81950	186.70928
Far Swath	163.65950	167.14162

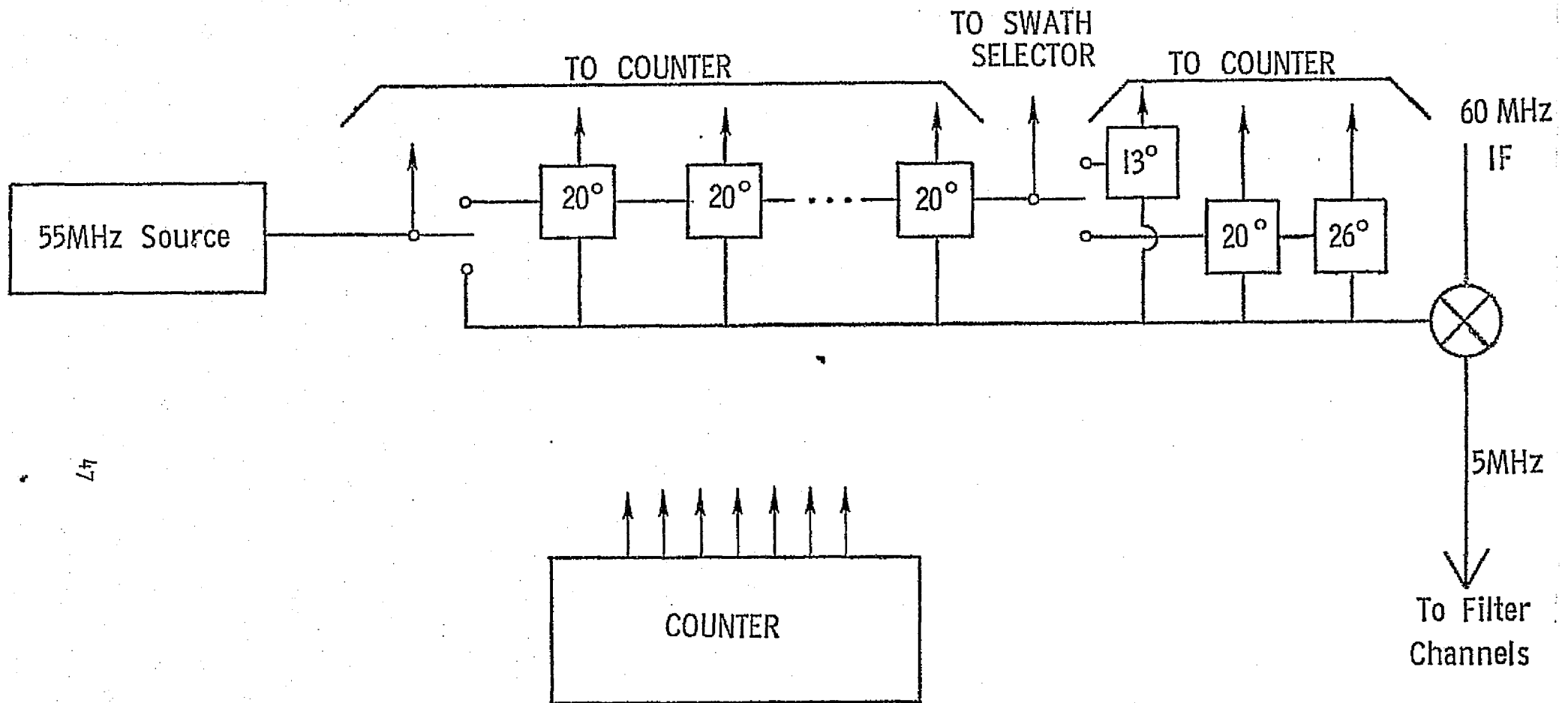
A FORTRAN computer program (see Appendix C) was written which calculates the phase shift necessary for each returning pulse. It would be more feasible to introduce a phase shift every X degrees instead of for every pulse. Since it is desired that the frequency decrease with time, the phase shifting process will proceed faster with earlier pulses than with later ones.

Tables 5 A, B, C and D show the results of introducing a phase shift every 20°. These results were obtained by taking the computer output listings in Appendix C, starting from the last pulse, calling it pulse 1 and working backwards. As can be seen, the earlier arriving pulses are grouped in 3s and 4s while later on, 10 pulses are grouped per 20° phase shift. The groupings were keyed on the 7200 Hz PRFs for each swath with these same groupings used for the 7050 Hz PRF.

SLO system operation proceeds as follows. The 60 MHz IF will be mixed with the 55 MHz SLO signal to place the return on a 5 MHz carrier. The counter will count the proper number of pulses and will switch in the proper amount of phase-shift such that after all the pulses for one look have returned, there will have been a cumulative phase-shift of 973° or 1006° depending on the swath. 49 lumped-constant phase shifters are needed for the near swath, 50 for the far, as in Figure 19. The average error over 1 look is essentially zero and the largest error after a given phase-shift is approximately 20° which amounts to about 3 Hz of Doppler shift. Future studies could attempt to optimize the error for each PRF.

b. SLO by Balanced Modulators

The use of balanced modulators is actually a single sideband technique which involves mixing two signals and getting out one of the two sidebands. This method is especially useful where the sidebands are close in frequency to the input signals. This system involves two subsystems: a chirp reference generator and the mixer. The basic configuration is shown in Figure 20.



47

Figure 19. SLO

TABLE 5A

NEAR SWATH PRF = 7200

Returning Pulses	Pulses Shifted	Total Actual Phase Shift	Total Using 20° Increments
1-3	3	20.99°	20°
4-6	3	41.75°	40°
7-9	3	62.28°	60°
10-12	3	82.58°	80°
13-15	3	102.65°	100°
16-18	3	122.49°	120°
19-21	3	142.11°	140°
22-24	3	161.49°	160°
25-27	3	180.65°	180°
28-30	3	199.58°	200°
31-33	3	218.28°	220°
34-36	3	236.75°	240°
37-39	3	255.00°	260°
40-42	3	273.01°	280°
43-45	3	290.80°	300°
46-48	3	308.36°	320°
49-52	4	331.42°	340°
53-56	4	354.06°	360°
57-60	4	376.30°	380°
61-64	4	398.14°	400°
65-68	4	419.57°	420°
69-72	4	440.59°	440°
73-76	4	461.21°	460°
77-80	4	481.42°	480°
81-84	4	501.50°	500°
85-88	4	520.62°	520°
89-92	4	539.62°	540°
93-96	4	558.20°	560°
97-100	4	576.38°	580°
101-104	4	494.16°	600°

NEAR SWATH PRF = 7200 (CONT.)

Returning Pulses	Pulses Shifted	Total Actual Phase Shift	Total Using 20° Increments
105-108	4	611.53°	620°
109-112	4	628.49°	640°
113-117	5	649.12°	660°
118-122	5	669.12°	680°
123-127	5	688.48°	700°
128-133	6	710.78°	720°
134-139	6	737.36°	740°
140-145	6	752.92°	760°
146-152	7	775.76°	780°
153-159	7	797.36°	800°
160-166	7	817.71°	820°
167-173	7	836.31°	840°
174-180	7	854.68°	860°
181-188	8	873.57°	880°
189-197	9	892.88°	900°
198-207	10	911.93°	920°
208-222	15	935.73°	940°
223-242	20	958.58°	960°
243-276	34	974.12°	973° *

* 13° increment

TABLE 5B

NEAR SWATH PRF = 7050

Returning Pulses	Pulses Shifted	Total Actual Phase Shift	Total Using 20° Increments
1-3	3	21.49°	20°
4-6	3	42.74°	40°
7-9	3	63.76°	60°
10-12	3	84.54°	80°
13-15	3	105.07°	100°
16-18	3	125.37°	120°
19-21	3	145.43°	140°
22-24	3	165.25°	160°
25-27	3	184.84°	180°
28-30	3	204.19°	200°
31-33	3	223.29°	220°
34-36	3	242.16°	240°
37-39	3	260.70°	260°
40-42	3	279.19°	280°
43-45	3	297.34°	300°
46-48	3	315.26°	320°
49-52	4	338.77°	340°
53-56	4	361.87°	360°
57-60	4	384.54°	380°
61-64	4	406.78°	400°
65-68	4	428.61°	420°
69-72	4	450.01°	440°
73-76	4	470.98°	460°
77-80	4	491.53°	480°
81-84	4	511.66°	500°
85-88	4	531.36°	520°
89-92	4	550.64°	540°
93-96	4	569.50°	560°
97-100	4	587.93°	580°

NEAR SWATH PRF = 7050 (CONT.)

Returning Pulses	Pulses Shifted	Total Actual Phase Shift	Total Using 20° Increments
101-104	4	605.94°	600°
105-108	4	623.52°	620°
109-112	4	640.69°	640°
113-117	5	661.54°	660°
118-122	5	681.73°	680°
123-127	5	701.27°	700°
128-133	6	723.83°	720°
134-139	6	745.44°	740°
140-145	6	766.10°	760°
146-152	7	788.99°	780°
153-159	7	810.59°	800°
160-166	7	830.89°	820°
167-173	7	849.89°	840°
174-180	7	867.60°	860°
181-188	8	886.24°	880°
189-197	9	905.19°	900°
198-207	10	923.73°	920°
208-222	15	946.57°	940°
223-242	20	967.76°	960°
243-271	29	979.67°	973° *

* 13° increment

TABLE 5C

FAR SWATH PRF = 7200

Returning Pulses	Pulses Shifted	Total Actual Phase Shift	Total Using 20° Increments
1-3	3	20.22°	20°
4-6	3	40.23°	40°
7-9	3	60.04°	60°
10-12	3	79.65°	80°
13-15	3	99.05°	100°
16-18	3	118.24°	120°
19-21	3	137.24°	140°
22-24	3	156.02°	160°
25-27	3	174.60°	180°
28-30	3	192.98°	200°
31-33	3	211.15°	220°
34-36	3	229.12°	240°
37-40	4	252.76°	260°
41-44	4	276.04°	280°
45-48	4	298.95°	300°
49-52	4	321.50°	320°
53-56	4	343.68°	340°
57-60	4	365.50°	360°
61-64	4	386.96°	380°
65-68	4	408.05°	400°
69-72	4	428.78°	420°
73-76	4	449.15°	440°
77-80	4	469.15°	460°
81-84	4	488.79°	480°
85-88	4	508.07°	500°
89-92	4	526.98°	520°
93-96	4	545.53°	540°
97-100	4	563.53	560°
101-104	4	581.53	580°
105-108	4	598.99	600°

FAR SWATH PRF = 7200 (CONT.)

Returning Pulses	Pulses Shifted	Total Actual Phase Shift	Total Using 20° Increments
109-112	4	616.08°	620°
113-117	5	636.94°	640°
118-122	5	657.23°	660°
123-127	5	676.95°	680°
128-133	6	699.86°	700°
134-139	6	721.95°	720°
140-145	6	743.23°	740°
146-151	6	763.71°	760°
152-157	6	783.33°	780°
158-163	6	802.15°	800°
164-169	6	820.15°	820°
170-176	7	840.12°	840°
177-184	8	861.58°	860°
185-192	8	881.58°	880°
193-201	9	902.34°	900°
202-210	9	921.27°	920°
211-220	10	940.14°	940°
221-233	13	961.27°	960°
234-249	16	982.00°	980°
250-297	48	1009.27°	1006° *

* 26° Increment

TABLE 5D

FAR SWATH PRF = 7050

Returning Pulses	Pulses Shifted	Total Actual Phase Shift	Total Using 20° Increments
1-3	3	20.66°	20°
4-6	3	41.11°	40°
7-9	3	61.34°	60°
10-12	3	81.37°	80°
13-15	3	101.17°	100°
16-18	3	120.77°	120°
19-21	3	140.15°	140°
22-24	3	159.32°	160°
25-27	3	178.27°	180°
28-30	3	197.01°	200°
31-33	3	215.54°	220°
34-36	3	233.86°	240°
37-40	4	257.95°	260°
41-44	4	281.66°	280°
45-48	4	304.98°	300°
49-52	4	327.93°	320°
53-56	4	350.50°	340°
57-60	4	372.69°	360°
61-64	4	394.51°	380°
65-68	4	415.94°	400°
69-72	4	436.99°	420°
73-76	4	457.66°	440°
77-80	4	477.96°	460°
81-84	4	497.87°	480°
85-88	4	517.41°	500°
89-92	4	536.56°	520°
93-96	4	555.34°	540°
97-100	4	573.74°	560°
104-108	4	591.76°	580°
109-112	4	609.40°	600°

FAR SWATH PRF = 7050 (CONT.)

Returning Pulses	Pulses Shifted	Total Actual Phase Shift	Total Using 20° Increments
113-116	4	626.65°	620°
117-121	5	647.70°	640°
122-126	5	668.14°	660°
127-131	5	688.00°	680°
132-137	6	711.04°	700°
138-143	6	733.23°	720°
144-149	6	754.57°	740°
150-155	6	775.05°	760°
156-161	6	794.68°	780°
162-167	6	813.46°	800°
168-173	6	831.38°	820°
174-181	7	851.21°	840°
182-189	8	872.46°	860°
190-198	8	892.18°	880°
199-207	9	912.56°	900°
208-217	9	931.01°	920°
218-227	10	949.27°	940°
228-240	13	969.46°	960°
241-256	16	988.80°	980°
257-291	42	1010.71°	1006° *

* 26° Increment

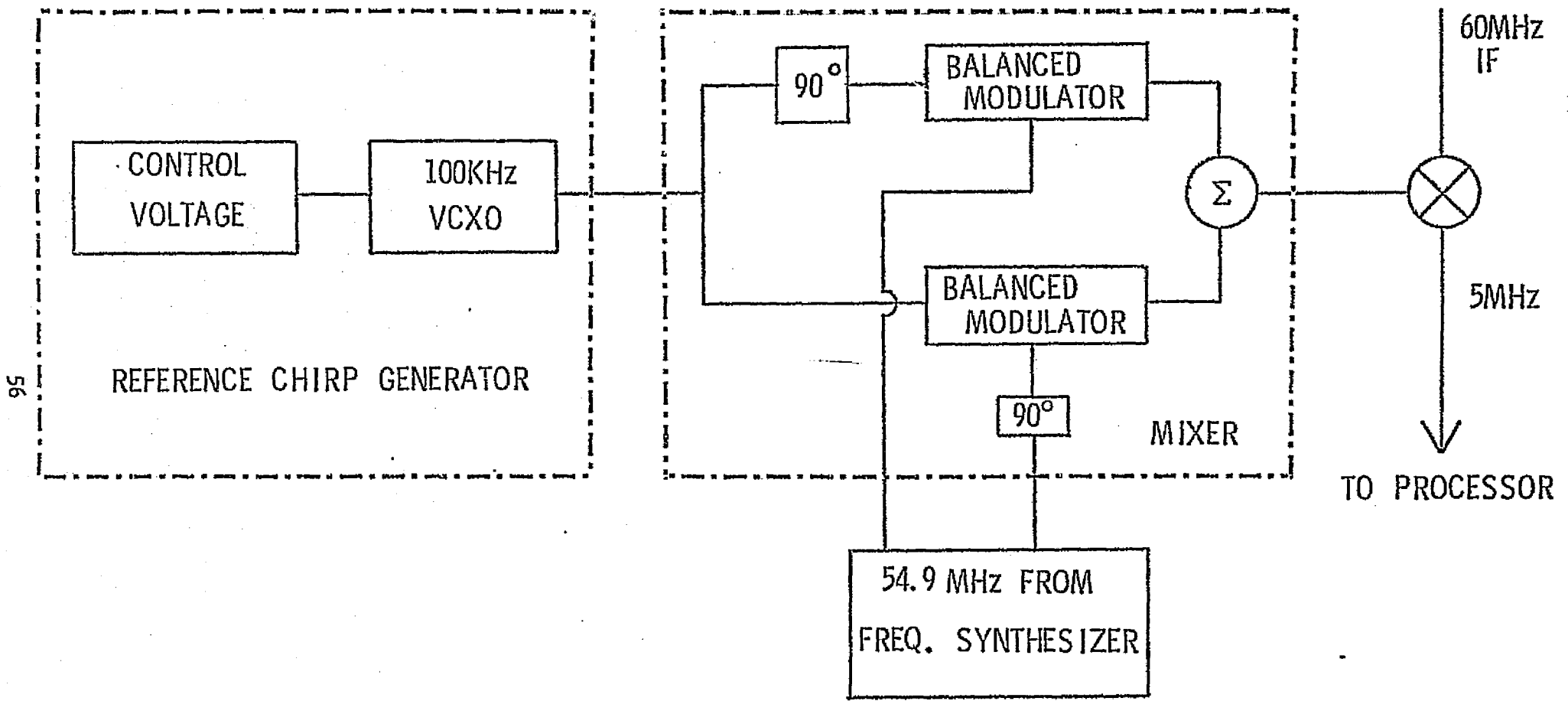


Figure 20. SLO using balanced modulators.

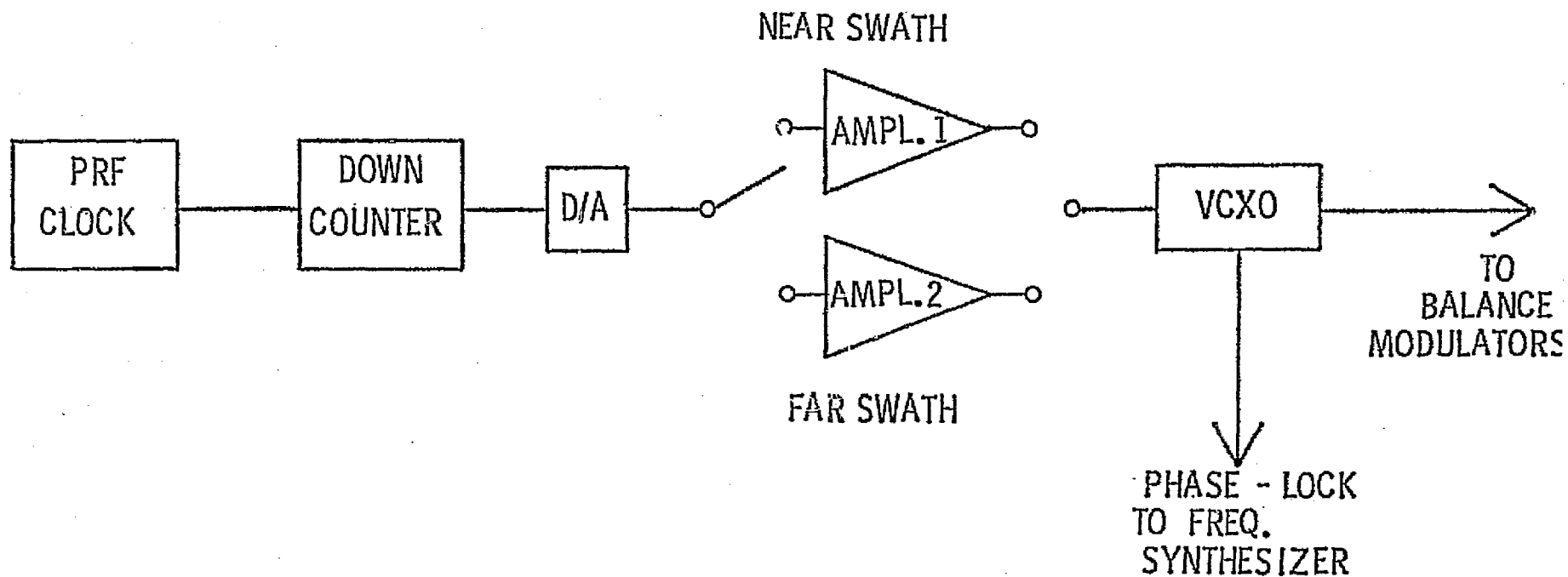


Figure 21. Reference chirp generator.

The reference generator supplies a voltage ramp (which varies proportional to the Doppler shifts from the ground) to the voltage controlled crystal oscillator which provides the chirp to the balanced modulators. The VCXO signal is split into two parts, one of which is phase-shifted by 90° . The VCXO signal is mixed with a 54.9 MHz signal from the frequency synthesizer which is also split with one component undergoing a 90° phase shift. When the mixed signals are recombined at the summing point, the 54.8 MHz component cancels, leaving the chirped 55 MHz component.

The reference function can be generated digitally as in Figure 21. The VCXO requires a control voltage in order to operate. Changing the control voltage in a linear fashion will result in the VCXO generating a chirp. The control voltage is stepped down in the counter on a pulse-by-pulse basis corresponding to the desired rate of frequency change. The amplifiers provide the necessary gain to deliver the proper control voltage to the VCXO for the desired swath.

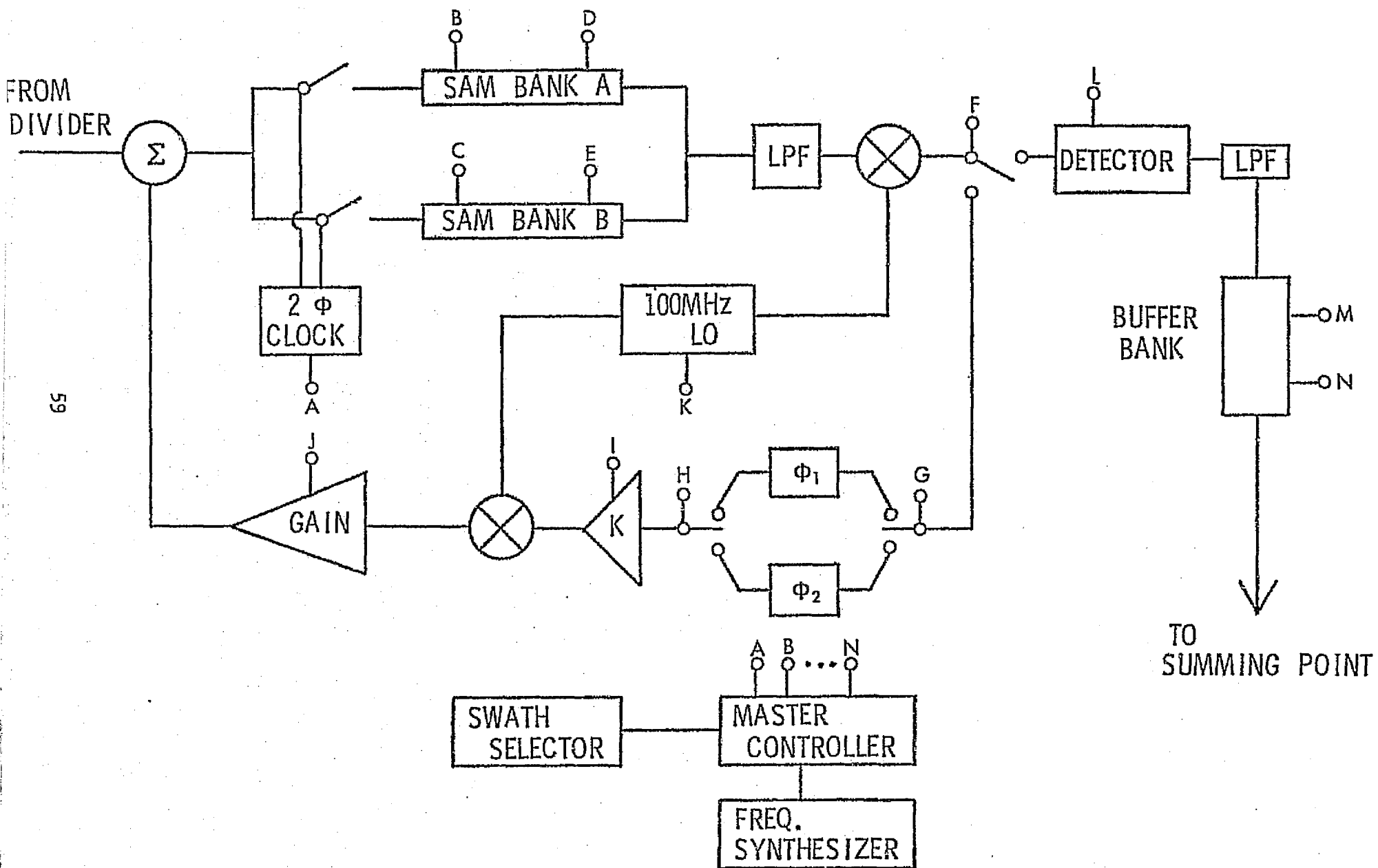
4.4.2 Divider Network

The divider network feeds the SLO mixer output to each filter channel simultaneously. T. E. Sponamore (1976) suggests using passive hybrid networks such as those used in the Bell System L-4 and L-5 carrier systems. However, within the time frame of this report, the author was unable to discern exactly how these networks function and what criteria must be considered in their design. More research must be done in order to find a way to implement a divider network for SCANSAR.

4.4.3 The Filter Channel

A block diagram of a single filter channel is shown in Figure 22. The basic operation of the channel proceeds as follows. The output of the SLO mixer is a set of constant frequencies representing the Doppler shifts from targets on the ground; the frequencies are functions of azimuthal position relative to the spacecraft. The SLO mixer output goes to all 198 (or 185) processor channels simultaneously to be processed for

Figure 22. A comb-filter channel.



range information. Reticon serial analog memories (SAMs) are used to sample and hold the range information for $\frac{1}{\text{PRF}}$ seconds. The maximum clock rate on the Reticon SAM-64 is 12 MHz. Since at least 16.8 MHz is needed to sample the returns, operating two SAM banks in parallel each at 10 MHz will give the desired sampling, plus some oversampling. A 2-phase clock is used to separate the range elements such that SAM bank A handles the odd-numbered elements and bank B the even-numbered elements. After the proper delay, the range elements are recombined, low-pass filtered, and mixed up to 100 MHz to be phase shifted. The channel phase-shifter is selected according to swath, the amount of phase-shift being determined by where the filter is tuned. The comb-filter response is then weighted to reduce sidelobe levels and the signal is mixed down, amplified, and added to the next incoming pulse. After all the pulses for one look have been added, the resulting waveform is demodulated and stored in the buffer bank.

a. Serial Analog Memories

The SAM-64 is a 64 bit analog shift register with independent read-in and read-out clocks. Information read-in and read-out functions cannot occur simultaneously in a storage element, hence one element is left vacant, leaving 63 available for storage for this recursive delay line application. To determine the number of SAMs necessary to process the returns, it is necessary to determine the number of pixels per image (scan) cell. Referring to Figure 2, the slant cell length ΔR is given by,

$$\Delta R = B_h R \tan \theta.$$

This same figure may also be used for a comparable view for a pixel by replacing ΔR with r_s and S with R_r , where r_s is the slant range resolution and R_r is the ground range resolution. r_s is determined by the pulse length τ_p ,

$$r_s = \frac{c\tau_p}{2} = \frac{c}{2B}$$

where

$$B = \text{RF bandwidth} = \frac{1}{\tau_p}.$$

Therefore the number of pixels P , is given by

$$P = \frac{\Delta R}{r_s} = \frac{B_h R \tan \theta}{\frac{c}{2B}} = \frac{2B B_h R \tan \theta}{c}$$

The number of SAM cells SC needed is the round-trip time for each cell divided by the sample time T_s . In the slant cell length equation R is only a one-way length therefore, replacing R with $\frac{2R}{c}$,

$$SC = \frac{2 B_h R \tan \theta}{c} \cdot f_s$$

where

$$f_s = \text{sampling frequency} = \frac{1}{T_s}$$

For a sampling frequency of 20 MHz, near swath B_h of .059 rad and far swath B_h of .026 rad, the number of SAMs needed is given below as a function of angle.

	<u>Near Swath</u>		<u>Far Swath</u>
8.4°	9	22.9°	11
20.8°	23	36.2°	23
22.488° *	25	36.957° *	23

*Farthest look angle due to beamwidth.

Since 25 is the maximum number of SAMs needed to process the returns, the SAM banks referred to earlier can be arranged with 13 SAMs in each bank for a total of 5148 SAMs for all the filter channels.

The SAM banks in Figure 22 actually appear as in Figure 23. SAM's A1 and B1 are activated to sample a return pulse. The counter counts range elements and when all 63 positions are filled, the elements are diverted to A2 and B2, etc. until all the range elements are stored. The buffer bank operates in a similar manner. After 138.9 μ sec or 141.8 μ sec depending on the PRF used, a start pulse from the controller starts the readout clocks and the counter, and the range elements are recombined. It should be noted that this entire process could be implemented digitally.

b. Phase-Shifter

Shifting the center frequency of the filter by an amount less than the spacing of the teeth is accomplished by using a frequency-independent (all pass) phase shift, each channel requiring a different phase shift to tune it to a different doppler frequency. Setting the Doppler filter band

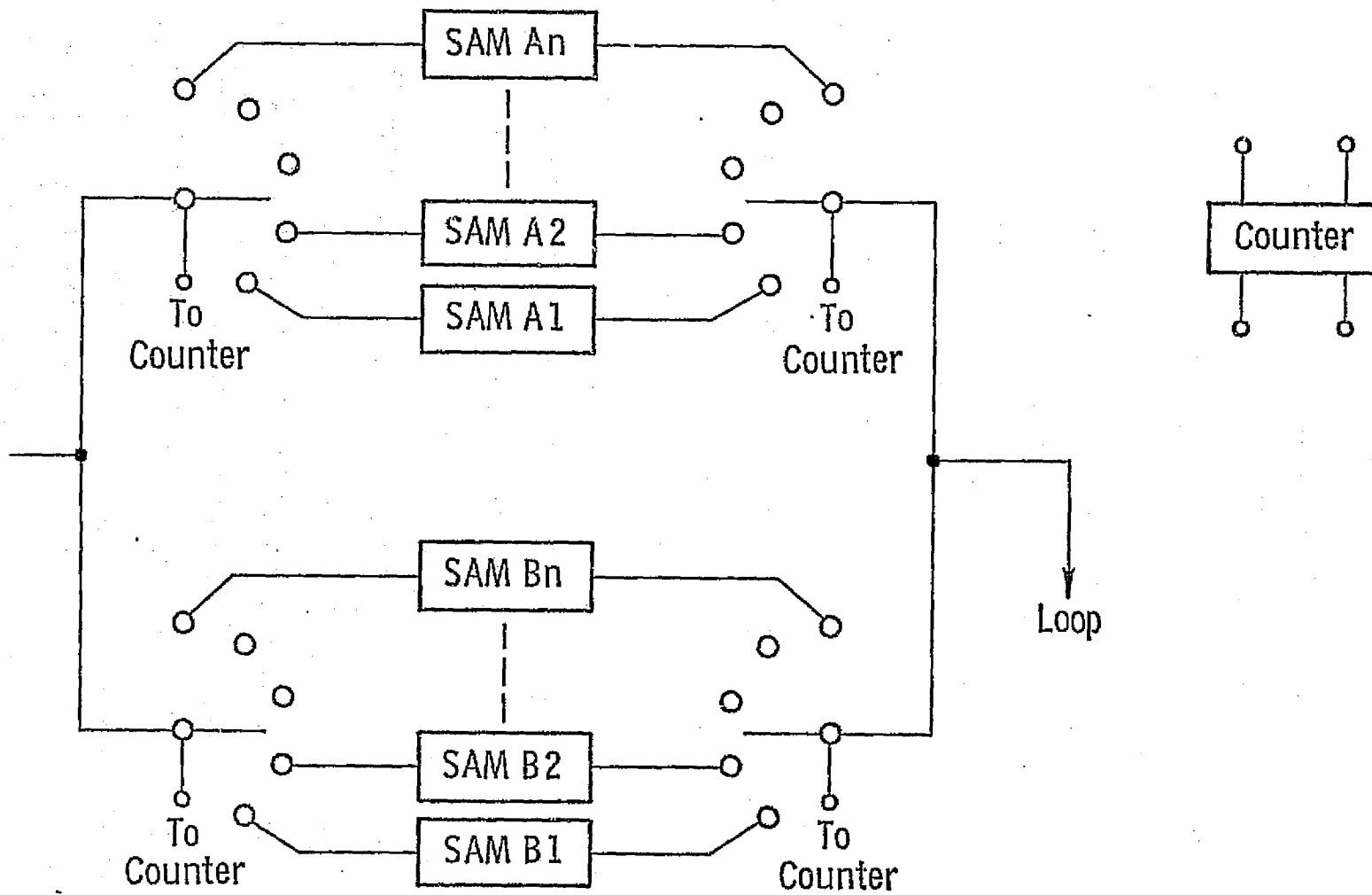


Figure 23. Parallel channel SAM banks.

from 1000 to 5800 Hz (4800 Hz bandwidth) puts the zero Doppler frequency at 3400 Hz. The necessary phase-shift ϕ to tune a channel to a frequency f for a given repetition rate T is

$$\phi = 2\pi f T.$$

The individual filter bandwidths are 26 Hz (near swath) and 24.2 Hz (far swath). Setting the phase shifts for the center at each band would place filters at 13 Hz, 39 Hz, 65 Hz ... for the near swath and 12.1 Hz, 36.3 Hz, 60.5 Hz ... for the far swath.

Some phase-shifts as functions of frequency for the two PRF's are given in Table 6.

All-pass functions have magnitudes constant for all frequencies and are characterized by their poles and zeroes being images with respect to the origin and with respect to the imaginary axis. A network such as in Figure 24 could be employed.

c. Weighting

Amplitude weighting of the frequency comb is used to suppress the sidelobes of the comb response. The first sidelobe resulting from a uniformly weighted comb is approximately 13.2 dB below the peak. By amplitude weighting, the sidelobes may be reduced to any desired level. Unfortunately, reducing the sidelobes results in widening the main lobe thereby degrading the resolution. For the terrain-mapping function of SCANSAR, the sidelobe levels need not be as low as those for identifying hard targets and as a result, the main lobe will not widen as much and the loss in gain is not as severe.

Table 7 shows the sidelobe levels for several basic distributions. The SCANSAR was designed around the relation $B_h = \lambda/H$ (radians) or $57.3 \lambda/H$ (degrees). From the table, it can be seen that this beamwidth can be obtained by using a parabolic weighting with the value for Δ lying between .5 and 0. Using $\Delta = .4$ results in a half power beamwidth of $57.1 \lambda/H$ with sidelobes 18.1 dB below the peak and a gain factor of .952. These values are derived in Appendix D. The weighting can be implemented by using a voltage controlled amplifier (VCA) whose gain K is preprogrammed to weight the response as the pulses circulate through the loop.

TABLE 6

	<u>Near Swath</u>	<u>Far Swath</u>
ϕ (1000)	50.000°	51.064°
ϕ (2000)	100.000°	102.128°
ϕ (3400)	170.000°	173.617°
ϕ (4800)	240.000°	245.106°
ϕ (5800)	290.000°	296.170°

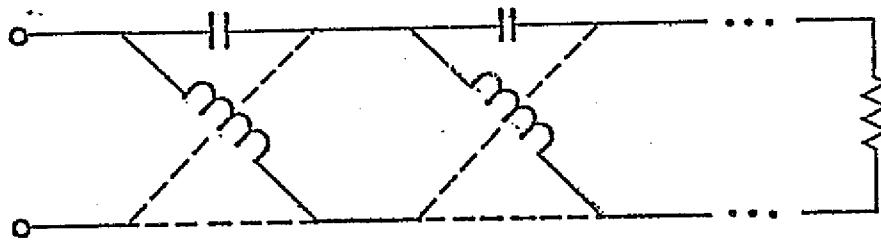


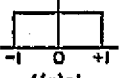
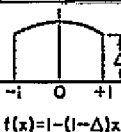
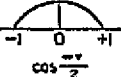
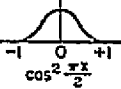
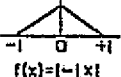


Figure 24. All-pass phase shift network.

the loop; in much the same manner as the SLO balanced modulator reference function generator.

TABLE 7. LINE SOURCE DISTRIBUTIONS *

TYPE OF DISTRIBUTION $-1 \leq x \leq 1$	DIRECTIVITY PATTERN $E(u)$	HALF POWER BEAMWIDTH IN DEGREES 	ANGULAR DISTANCE TO FIRST ZERO 	INTENSITY OF 1st SIDELobe db BELOW MAX.	GAIN FACTOR	
 $f(x)=1$	$\frac{\sin u}{u}$	$50.8 \frac{\lambda}{L}$	$57.3 \frac{\lambda}{L}$	13.2	1.0	
 $f(x)=1-(1-\Delta)x^2$	$\Delta(1+\chi) \frac{\sin u}{u}$ $\chi=(1-\Delta) \frac{d^2}{du^2}$	$\Delta = 1.0$	$50.8 \frac{\lambda}{L}$	$57.3 \frac{\lambda}{L}$	13.2	1.0
		.8	$52.7 \frac{\lambda}{L}$	$60.7 \frac{\lambda}{L}$	15.8	.994
		.5	$55.6 \frac{\lambda}{L}$	$65.3 \frac{\lambda}{L}$	17.1	.970
		0	$65.9 \frac{\lambda}{L}$	$81.9 \frac{\lambda}{L}$	20.6	.833
 $\cos^2 \frac{u}{2}$	$\frac{\pi/2}{2} \frac{\cos u}{(\frac{\pi}{2})^2 - u^2}$	$68.8 \frac{\lambda}{L}$	$85.9 \frac{\lambda}{L}$	23	.810	
 $\cos^2 \frac{\pi x}{2}$	$\frac{\lambda}{2} \frac{\sin u}{u} \frac{\pi^2}{\pi^2 - u^2}$	$83.2 \frac{\lambda}{L}$	$114.6 \frac{\lambda}{L}$	32	.667	
 $f(x)=1- x $	$\frac{\lambda}{2} \left(\frac{\sin \frac{u}{2}}{\frac{u}{2}} \right)^2$	$73.4 \frac{\lambda}{L}$	$114.6 \frac{\lambda}{L}$	26.4	.75	

* From Jasik, H., ed., Antenna Engineering Handbook, McGraw-Hill, 1961, p. 2-26.

d. Gain Stabilization

It may be necessary to guarantee that the gain around the loop stay a constant. This may be done by injecting a signal at a known frequency and voltage as shown in Figure 25, recovering it via a frequency trap and comparing the voltages. The difference voltage may be used to drive the weighting amplifier to restore equilibrium.

e. Channel Summing Point

The channel summing point serves to add an incoming signal to one which has circulated the loop. One unfortunate problem with the SAM is that there is a 92.6% loss in signal amplitude in moving a signal through one, due to the fact that a sample is stored on a 2 pf capacitance but is read out through a 25 pf capacitance. This implies the use of an amplifier to compensate for this loss. A circuit such as in Figure 26 could be used to accomplish both tasks by using a summing-inverter op amp network.

For example, let V_A be an incoming signal and let V_B be a signal which has circulated through the loop and has lost 92.6% of its amplitude. The voltage V_0 at the output of the summing inverter is given by

$$V_0 = R_F \left(\frac{R_A}{V_A} + \frac{R_B}{V_B} \right)$$

where

R_F = feedback resistor

R_A, R_B = input resistances.

Selecting $R_A = NR_B = R_F$,

$$V_0 = R_F \left(\frac{V_A + NV_B}{NR_B} \right) = NV_B + V_A$$

The gain due to the SAMs is $\frac{2}{27}$ or .07407. Therefore,

$$V_B = .07407 \times (\text{SAM input voltage})$$

It is desired to have V_B of the same order as V_A . Let $V_{IN} = .01$ volt.

$$V_B = .0007407.$$

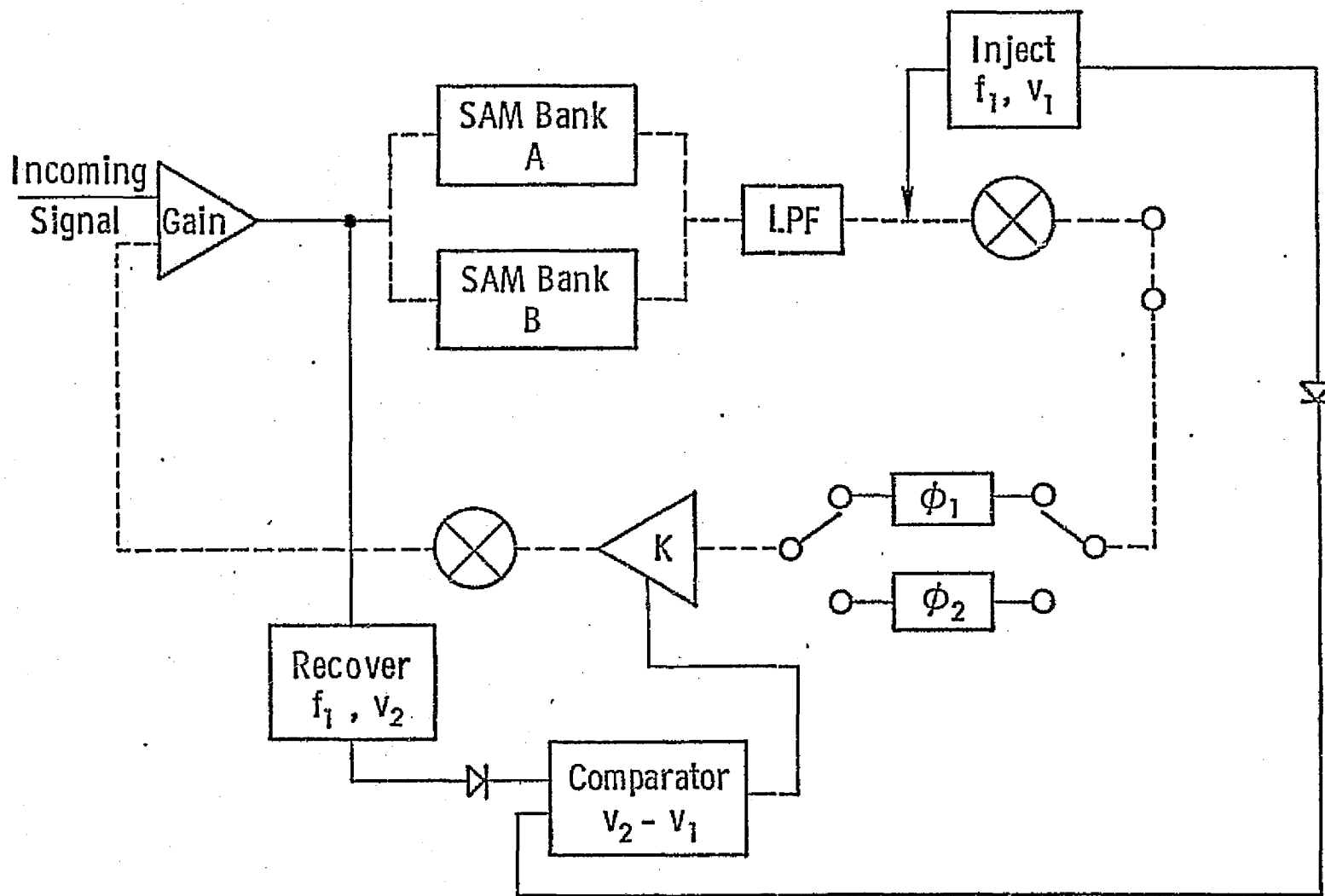


Figure 25. Gain stabilization circuit.

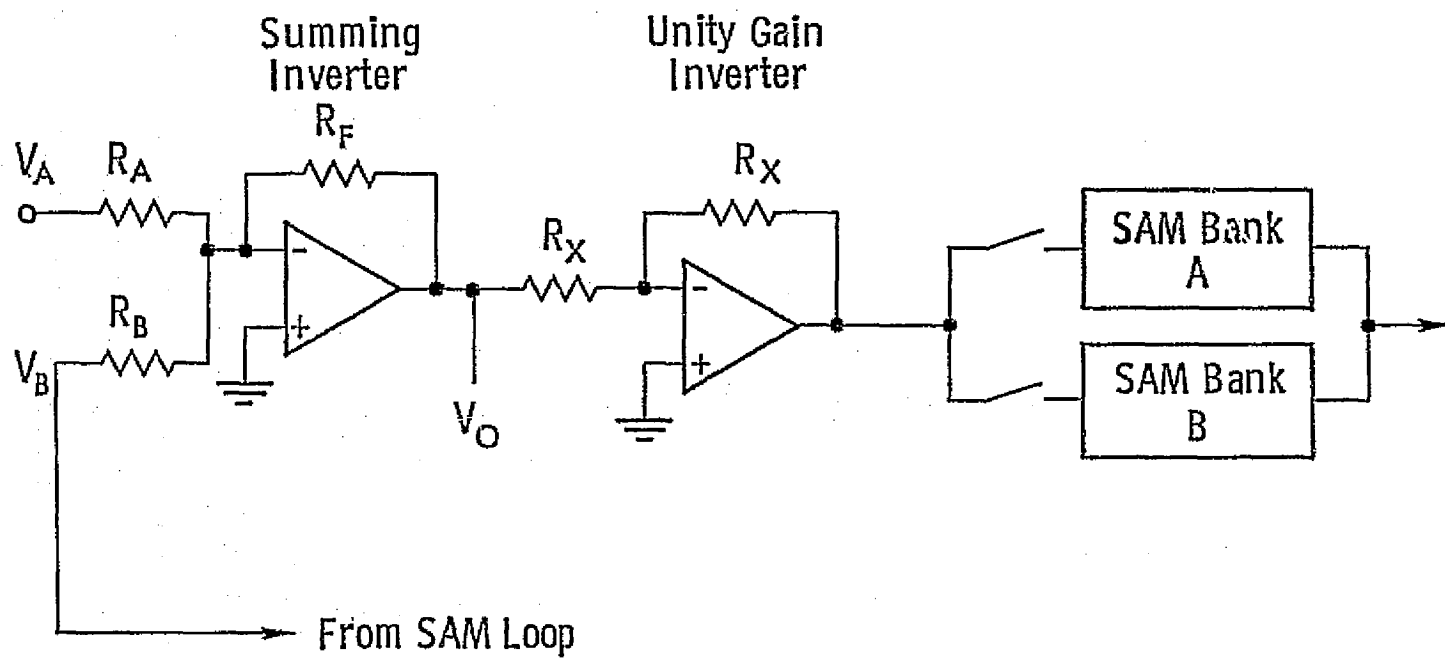


Figure 26. Channel summing point.

Since

$$NV_B = .01$$

$$N = 13.5$$

so

$$V_0 = V_A + 13.5 V_B$$

If V_A is at a level of .01V, the following table traces the signal amplitude.

Pulse	V_A	V_B	V_0	$V_B' (= \frac{2}{27} V_0)$
1	.01 V	0 V	.01 V	.0007407 V
2	.01	.0007407	.02	.0014815
3	.01	.0014815	.03	.0022222
⋮	⋮	⋮	⋮	⋮
297	.01		2.97	

The unity-gain inverter just inverts the output from the summing-inverter with no change in gain. It may be desirable to switch in an amplifier with a gain of 13.5 after the last pulse has been summed in and sent through the SAM to be delivered to the buffer, however its location is not critical and could be placed in the circuit directly preceding the buffer itself.

4.5 DETECTION AND BUFFERING

After all the necessary pulses have been integrated and mixed up to 100 MHz, they are full-wave detected to eliminate the carrier, low-pass filtered to yield a composite waveform and stored in the buffer bank. A detection-filter bank configuration such as that of Figure 27 may be used.

The detection process effectively halves the IF bandwidth, therefore the bandwidths are 3.4 MHz and 3.85 MHz for the two swaths. Running the

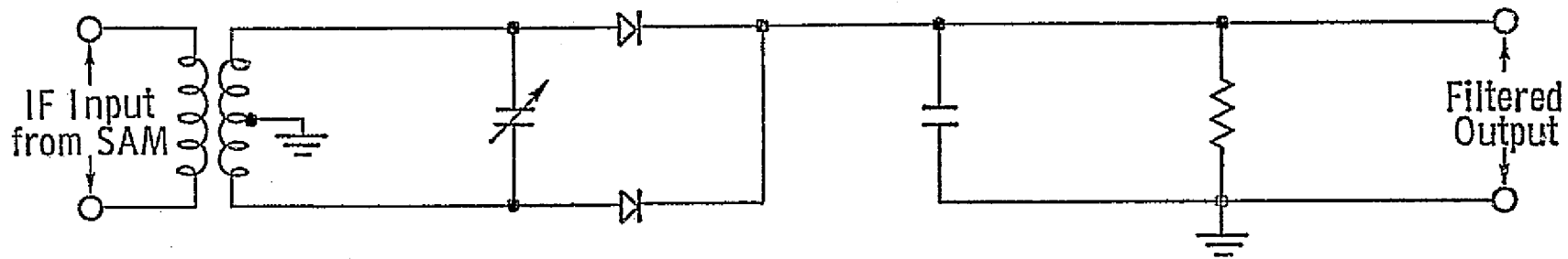


Figure 27. Detector-low pass filter circuit.

71

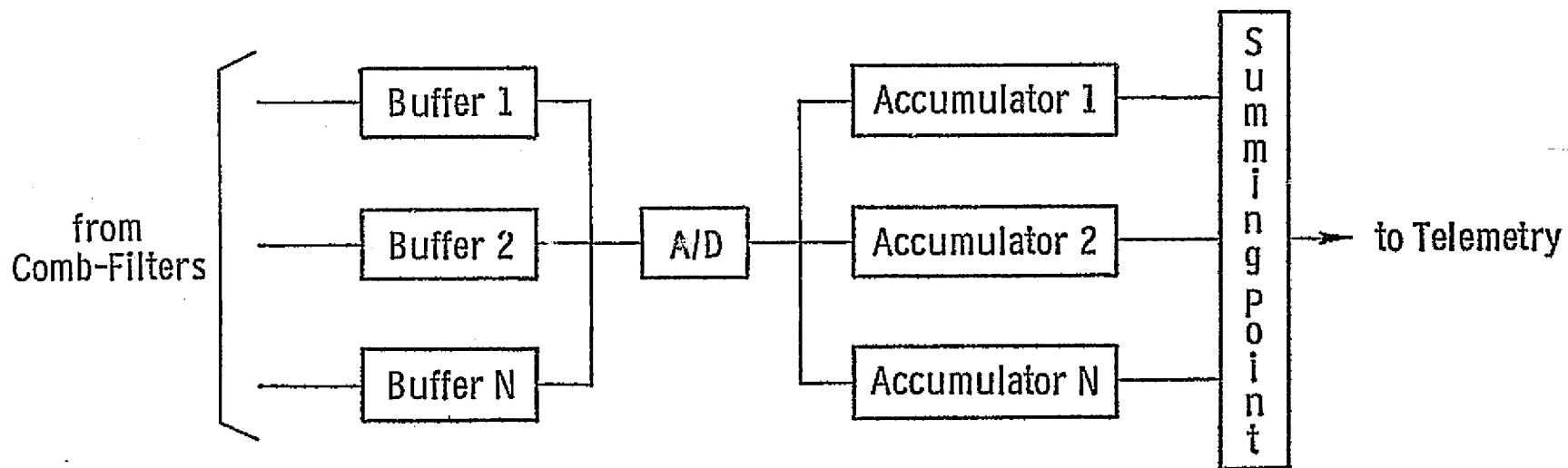


Figure 28. Buffer output system.

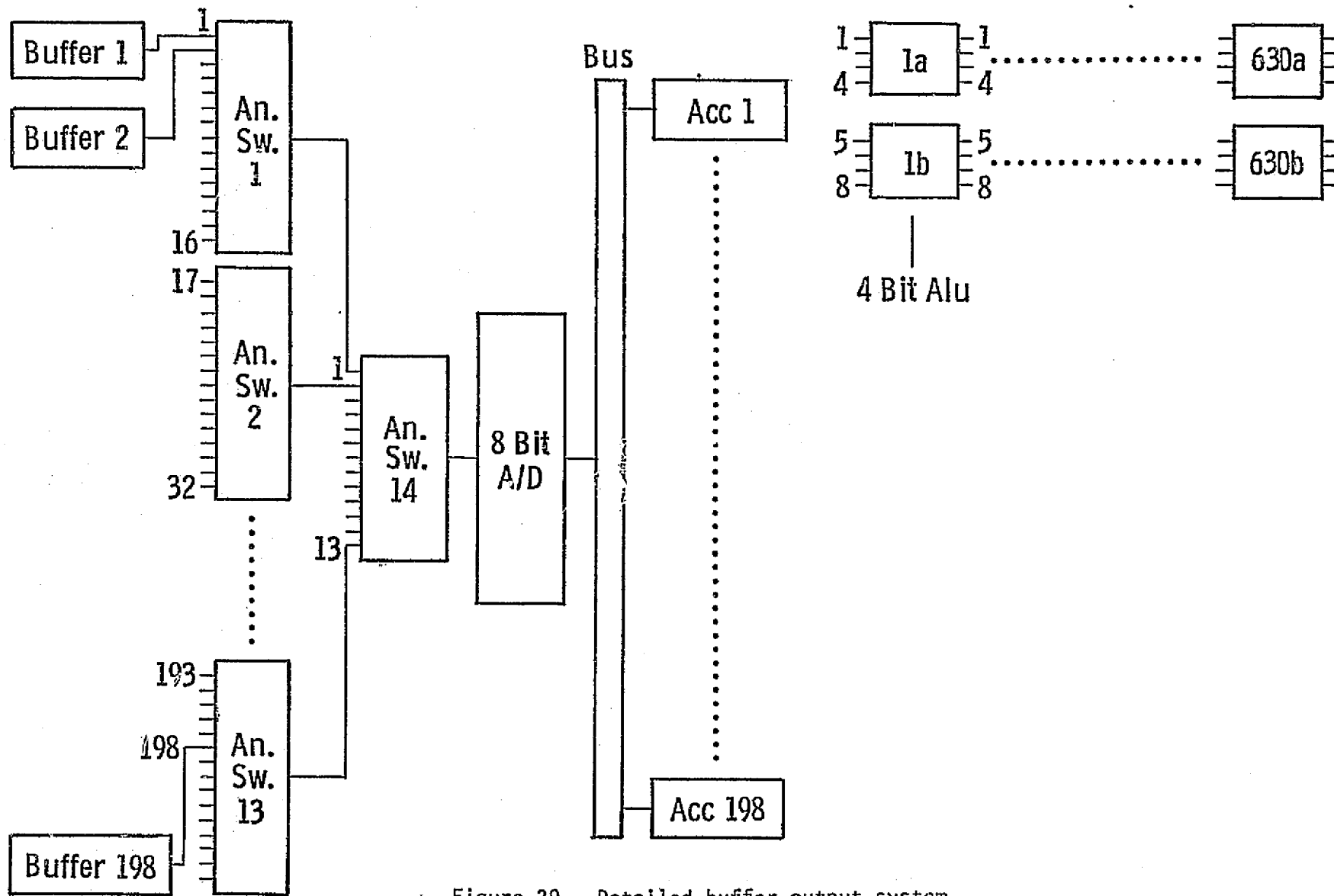


Figure 29. Detailed buffer output system.

buffer SAMs at 8 MHz will sample both swaths. Computing the number of SAMs needed from the expression in the preceding with $f_s = 8$ MHz, 10 SAMs are required for the buffers. The buffers contain the compressed azimuth data observed by each filter.

While the comb filter is summing the returns for one look the range elements in the buffers from the preceding look can be read into the accumulators. The returns for each look are then added to the appropriate addresses in the accumulators.

The basic buffer-accumulator arrangements is shown in Figure 28 and with more detail in Figure 29. The buffers empty into 16-channel analog multiplexing/demultiplexing switches such as the RCA-CD4067B which gate the range samples into an 8-bit A/D converter. From section 1, the number of bits N_b is given by

$$N_b = \frac{\sigma^{\circ}(\text{max}) - \sigma^{\circ}(\text{min})}{3.0103}$$

The maximum number of bits is 7 in the near swath, hence the 8-bit A/D converter.

The conversion time T_c for reading out the buffer samples is given by

$$T_c = \frac{\tau}{N \cdot S}$$

where

τ = time for 1 look (.03846 or .04132 sec)

N = number of channels (185 or 198)

S = total number of samples in each channel buffer bank (640).

T_c is approximately 325 nsec for these values. An A/D converter such as Datel's ADC-UH8B with a 100 nsec conversion time could be employed. The A/D converter output could then be placed on a data bus to be read into the accumulators. RCA-CD4057A 4-bit Arithmetic Logic Units (ALU) could be used to implement the accumulators. These ALUs are capable of performing up to 16 functions although their purpose here is for addition of the looks. Each ALU contains a register and acts as a tri-state device. An enable pulse from the controller can instruct the ALU to

switch into the data bus to retrieve data. The ALUs for accumulators 186-195 could be switched to a high impedance state while the satellite is operating in the near swath. Two ALUs are required to accommodate the 8-bit output from the A/D converter and since there are 640 samples per channel, 1280 ALUs are required for each accumulator.

4.6 TIMING AND CONTROL

There are two major decisions for the master controller. The first decision is which swath the satellite is to observe. From an equipment standpoint, this sets the antenna pointing angle program, the dwell time for each scan cell, and the number of filter channels to be used. It also determines the proper amounts of phase shift (or frequency shift) in the SLO and in the filter channels, and the number of buffer integrations (looks). Once this decision is made, the other is selecting the correct PRF for each scan cell pointing angle. This decision determines the transmit and receive cycles, the read-in and read-out start times on the SAM clocks, and the filter channel delays. Since there is a finite time delay between transmitting a pulse and receiving a return, the transmitter can be shut down after it has sent out the proper number of pulses for all the looks at a scan cell position until all the returns are back. The buffers can then dump their contents into the major summing junction for transmission to earth while the antenna is scanned to its next position.

4.7 ALTERNATIVE PROCESSOR CONFIGURATION

A potential problem exists with the filter channel configuration of Figure 22 in that the dynamic range of the SAMs may not be great enough to accommodate summing 300 pulses. According to Reticon, the spurious level of a SAM is 55 dB below 4 volts or 7 mv. The random noise level is 63 dB below 4 volts or 2.8 mv. This problem can be circumvented by modifying the filter channel arrangement as in Figure 30 and processing the returns in a "pipeline" fashion. A bank of \sqrt{N} filters (where N is the

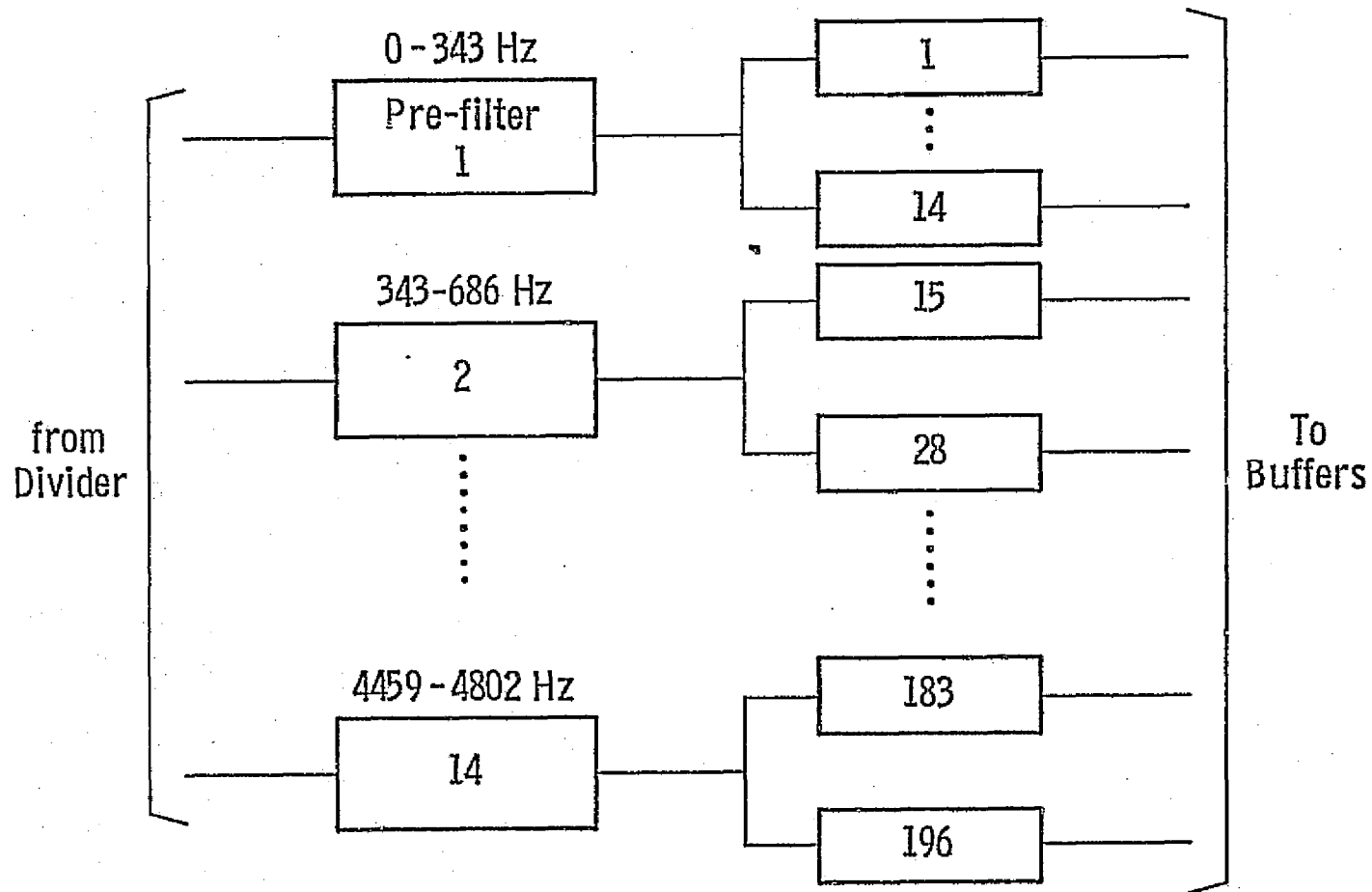


Figure 30. An alternative filter channel arrangement.

total number of filters) pre-filters the returns, summing 20 pulses. This sum is dumped into a secondary bank of filters set up as before but whose delay is 20 times that of the pre-filters. This scheme prevents the total level in any SAM from exceeding 4 volts. For example, let the input voltage level to the pre-filters be .1 volt. After 20 pulses are summed, 2 volts will be in each pre-filter.

Utilizing the 92.6% SAM amplitude loss as a .074 gain factor to set the level to the secondary bank, then .148 volts will be input to these SAMs. In summing 300 pulses, the pre-filter will dump 15 times so that after one look, the total voltage in each secondary filter SAM will be only 2.22 volts.

Other than the two delay times, the only remaining difference between the pre-filters and the secondary filters is that the pre-filter phase shifts are set to the center of their respective 343 Hz bandwidths. The circuit configurations for the filter channels are the same as before and require no basic changes in system hardware either preceding or following them.

4.8 EDGE EFFECTS

According to the system design, the antenna beam will illuminate 9.23 km in azimuth on the ground and the SCANSAR is able to take 6 looks at a scan cell in the near swath. However, since the satellite is moving along-track at 7200 m/sec, the scan cell itself will "slide" along the ground during the time it takes for the 6 looks. Therefore some pixels at the beginning and end of the scan cell will be observed 1 to 5 times instead of the desired 6.

One method of overcoming these "edge effects" would be by broadening the azimuthal beamwidth (B_{θ}) such that the 3 dB point on the antenna pattern would shift down, allowing more coverage. It is also possible to alleviate the problem by making use of the system timing, making the problem one of control.

During each look, the satellite will travel 276 meters and the scan cell will slide by this same amount. After 6 looks, the satellite will

have moved 1656 meters in 0.230 seconds elapsed time. It can be observed from Table 2 that it takes approximately 0.003 seconds (near swath) for the first pulses to return to the radar. Therefore, the amount of time the antenna needs to dwell on any cell is approximately 0.233 seconds (the satellite travelling 1677.6 meters during this time). The SCANSAR computer-design program allows 0.257 seconds of dwell time per cell.

Figure 31 shows a scan cell as it slides along the ground during the six looks. The horizontal lines represent the beginning and end of the scan cell after each look and the number of looks at each area of the cell is given for each position. From the reference point (original beginning edge of the cell), the satellite has moved 10886 meters. Figure 32 shows the breakdown of the 1677.6 meter cell slide. The 21.6 meter number comes from the fact that after the radar has looked at 1 cell and scans to the next, it has moved $.003 \text{ sec} \times 7200 \text{ m/sec}$ (21.6 m) before the first pulses return from the ground. Figure 33 shows a 5 scan-cell swath. Figure 34 shows the starting points of each cell in the swath relative to cell 1. As can be observed, the satellite travels a total of 8388 meters with respect to the reference point so that when the antenna beam returns to position 1, there is an 842 meter overlap on the area observed in the preceding position 1. Therefore those areas on the ground which have been observed less than 6 times from one cell will be seen again on the next antenna scan.

Figure 35 represents the overlap of two superimposed cells at antenna position 1 of adjacent swath scans (see inset). The left cell (1a) was observed in the first scan, the right cell (1b) in the next. The vertical scale is in meters measured from the bottom edge of the left cell. As is apparent from the figure, all ranges except for the 262 meters between the 9506 and 0768 meter marks are seen at least 6 times by 1 cell or the other. The excess looks can be discarded, or may be used to improve gray-level resolution. Since only 5 looks are available in this range from cell 1a, 1 look can be "borrowed" from cell 1b. This should be a relatively simple task for the controller to accomplish.

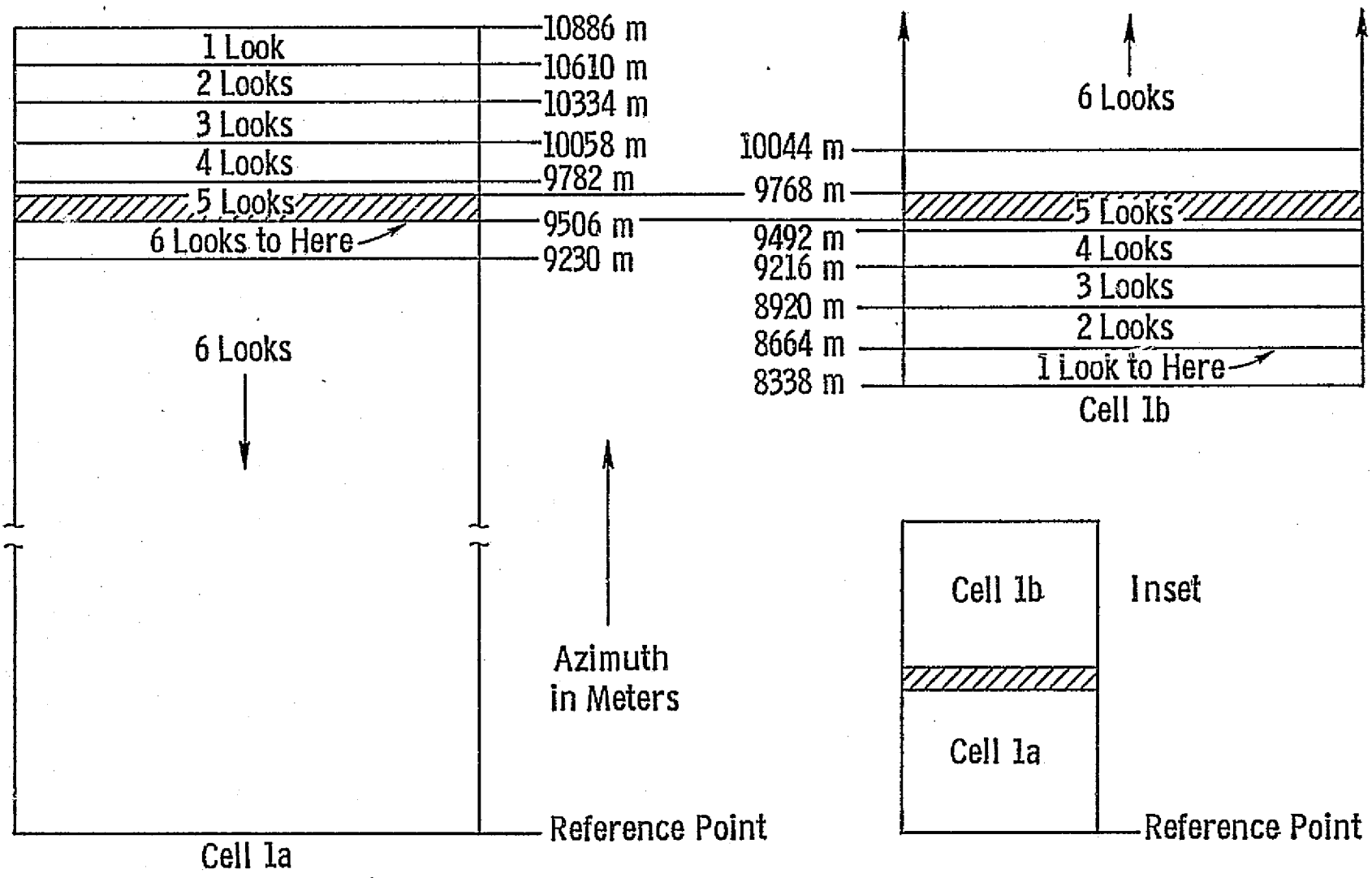


Figure 35. Cell overlap in azimuth.

4.9 SUMMING THE LOOKS

Independent looks can be summed in the accumulators in 2 ways. The first involves resetting the SLO after each look. The satellite moves 276 meters per look. At the end of look 1, filter 1 stores the contents in accumulator 1, filter 2 in accumulator 2, etc. 276 m is 5.52 pixels in azimuth, so at the beginning of look 2, filter 1 is looking a distance 52% of the way into pixel 6 (whose returns are stored in accumulator 6). In order for look 2 to add correctly to look 1, the SLO must have been shifted down from its reset point by $.52 \times 26 \text{ Hz} = 13.52 \text{ Hz}$. Now, filter 1 empties into accumulator 6, filter 2 to accumulator 7, etc. At the beginning of look 3, filter 1 will be at pixel 11.04. Therefore, the SLO must shift down $.04 \times 26 \text{ Hz} = 1.04 \text{ Hz}$. At the end of look 3, filter 1 empties into accumulator 11, filter 2 into 12, etc. This can be performed by the controller.

The other method merely involves letting the SLO run continuously for 6 looks (843.72 Hz) and resetting it only to observe a new scan cell. This way, filter 1 will always empty into accumulator 1, filter 2 to accumulator 2, etc. every look. This can be easily implemented by using 6 of the SLO lumped phase-shift networks or stepping the balanced modulator control voltage ramp for 1656 pulses instead of 276. In either case, 34 extra accumulator banks will be needed to accommodate the cell slide.

5.0 MOTION COMPENSATION

Two kinds of spacecraft motion must be taken into account in the operation of the spacecraft SAR, since both can have the effect of displacing the Doppler band relative to the illumination pattern of the antenna: (1) attitude errors can cause the antenna to point in some direction other than along the zero-Doppler line; and (2) vertical velocity components caused either by non-circularity of the orbit or by the oblateness of the earth cause a net shift in the Doppler frequency and therefore an apparent along-track displacement of the image. Ideally the antenna should be pointed along the zero-Doppler line, but this line is not perpendicular to the orbital plane, since the Doppler frequency is measured in terms of velocity relative to the rotating earth. At the equator a point on the earth has a linear velocity of about 463 m/sec. If the satellite were in a true polar orbit, this would mean that the zero-Doppler line would deviate from perpendicular to the orbit plane by 3.5° at the equator, decreasing to zero at the poles. For other orbits the deviation is less at the equator, but the component along the orbit of the earth-rotation velocity gives a displacement to the image that depends on position in the orbit. With the typical narrow beams, rotation of either the satellite or the antenna to compensate for the rotation of the zero-Doppler line relative to the orbital plane should be included in the design of the satellite-radar system.

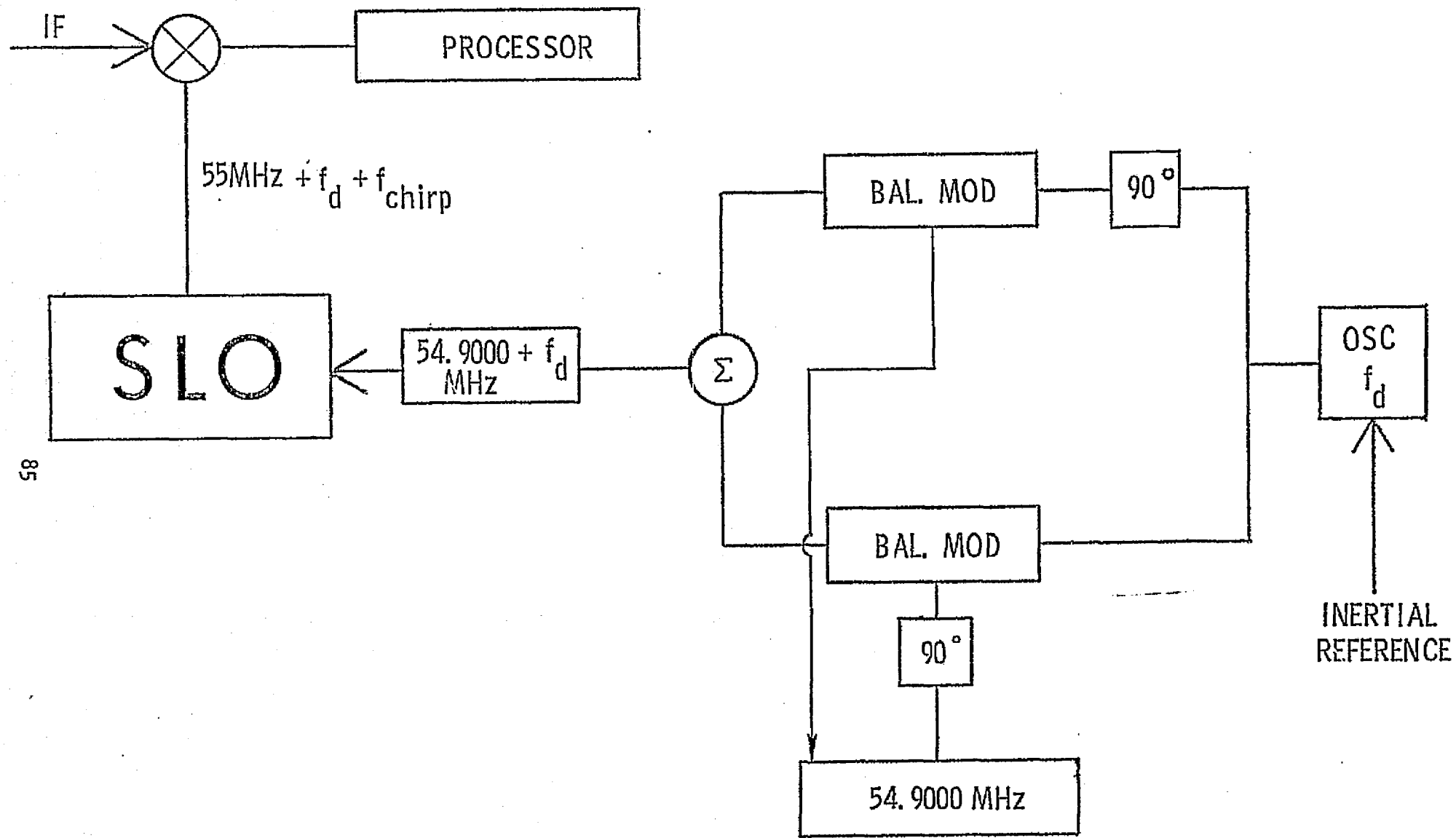
Attitude variations of the satellite can also cause errors in the Doppler shift for which compensation must be provided. Yaw rotates the beam position on the ground; pitch moves the entire pattern ahead of or behind the zero-Doppler line. The satellite attitude control system keeps these variations within relatively firm limits, but additional compensation must be provided unless the attitude limits for the vehicle are kept within very small bounds.

Three methods for compensating for these movements are: (1) controlling the frequency of an oscillator to center the signal spectrum in the processor passband, (2) electronically steering the antenna in azimuth to the desired angle to compensate for yaw and earth's rotation, (3)

physically moving the antenna or spacecraft to correct for earth's rotation and yaw and pitch errors. Roll errors may also cause problems, although these are not usually as severe because of the wider vertical beam of the antenna. In some configurations of the SCANSAR, however, the vertical beam is narrow enough so that roll errors can become a problem. For this situation, stabilization of the antenna (mechanically or electronically) is called for, since Doppler shifting cannot make this type of correction. Furthermore, for some situations involving fine-resolution radars, the curvature of the off-normal isodops must be considered in the processing, but this problem is not believed to be significant for the modest resolution systems discussed here.

Method (1), use of an offset local oscillator frequency, must be used to compensate for vertical velocity variations, and can be used to compensate for earth's rotation and attitude errors. The earth's rotation error correction frequency can be programmed in advance, but attitude errors must be detected by the satellite control system sensors which can then provide a correction voltage to the radar. The output of the error control oscillator can then be mixed in a single-sideband modulator with the 54.9 GHz stable reference from the frequency synthesizer to produce a signal at $54.9 + f_D$ MHz. This signal is then mixed in the scanning local oscillator. A diagram of this method is shown in Figure 36.

In practice, some combination of methods (1), (2), and (3) must be used in the radar-satellite system. Detailed design of this system depends on both orbit and satellite attitude control parameters.



85

Figure 36. Motion compensation circuit using balanced modulations.

6.0 POWER AND SIZE

6.1 POWER CONSUMPTION

The major contributors to the power consumption are the transmitter, the receiver, the frequency synthesizer, the controller, the SAMs and their drivers, and the buffer A/D converter. The average transmitter power is 15 watts but with a 25% efficiency it will use 60 watts. The low noise transistor amplifier used in the receiver can be expected to use 10 watts maximum. Based on presently available units, the frequency synthesizer will use approximately 15 watts continuous power. 25 watts is allotted to the controller on a sheerly intuitive basis. The controller, being the heart of the processor, is an inherently complex device whose specific design was not considered within the context of this report.

The quiescent (DC) power consumption for each SAM is 4 mw. Each filter channel for the single bank configuration contains 36 SAMs (26 in the loop, 10 in the buffer bank) for a 28.51 W DC usage. The DC clock consumption is also 4 mw per SAM, however, only 3 SAMs would be operating in each channel (2 in the loop, 1 in the buffer) for a total of 2.38 W.

The proposed drivers are National Semiconductor MM88C29 CMOS Quad Single-Ended Line Drivers, each package containing 4 drivers. From the National Semiconductor CMOS Data Book, the normalized AC power consumption W_{NAC} for a 10 MHz clock rate at $V_{CC} = 10$ V is 1000 μ W/pf. The power consumption per driver package, W_D , is given by

$$W_D = W_{NAC} (C_{PD} + C_L)$$

where

C_{PD} = no load capacitance. (150 pf for this device).

C_L = load capacitance.

Allowing the absolute maximum power dissipation per package ($W_D = .5$ W), the maximum load capacitance C_L is 350 pf. The SAM clocks are rated at

20 pf, therefore 17 SAMs can be operated by one driver package at 10 MHz. For the 8 MHz buffers, $W_{NAC} = 800 \mu\text{W}/\text{pf}$ and $C_L = 475 \text{ pf}$ resulting in 1 driver package operating 23 SAMs. The final figure for the single channel configuration is 37 W as compared to 33 W for the pipeline approach. See Appendix E for more detail on the power calculations.

The buffer A/D converter uses approximately 10 W. 10 W is allowed for miscellaneous items such as amplifiers, switches, VCOs, and the SLO D/A converter. Included in this total are the 14 analog multiplexers which use 0.2 μW quiescent and 1 mW operating power per unit. Also included are the ALUs. Although 253,440 ALUs are needed, they only use 10 μW apiece quiescent and approximately 1 mW apiece operating power but only 2 operate in each channel at any given time. Power supplies are assumed 85% efficient.

Table 8 shows the power budget for a single-sided SAR with a total power consumption of around 200 watts. One area to be awaited in the near future is the advent of CMOS drivers with lower power consumptions and the ability to accomodate greater load capacitances.

If a longer antenna were used, the number of filter channels would be reduced, although the length of each SAM chain would be increased. Since driver power is proportional to the number of channels, the 37W figure for SAMs and drivers would be less.

Aperture length (AL) and aperture height (AH) are related by

$$AH = \frac{12 V_g R_2 \tan \theta_2 \lambda}{c AL}$$

where

- V_g = satellite ground velocity
- R_2 = slant range at farthest look angle
- θ_2 = farthest look angle in swath
- λ = operating wavelength
- c = speed of light.

For SCANSAR, $V_g = 7.2 \text{ km/sec}$, $R_2 = 465327 \text{ m}$, $\theta_2 = 20.8^\circ$, $\lambda = 0.063 \text{ m}$, and $c = 3 \times 10^8 \text{ m/sec}$ so this relation reduces to

TABLE 8.

	<u>1 side</u>	<u>2 sides</u>
SAMs (and drivers)	- 37 w	74
Transmitter (25% eff.)	- 60	120
Receiver	- 10	20
Frequency Synthesizer	- 15	Shared
Controller	- 25	Shared
Buffer A/D	- 10	20
Miscellaneous	- 10	20
	<hr/>	<hr/>
	167 w	294
Assuming 85% efficient power supplies	- 197	346

$$AH = \frac{3.207}{AL} .$$

Aperture length determines the horizontal beamwidth, the azimuthal scan cell width, and the Doppler bandwidth. The horizontal beamwidth B_ℓ is given by

$$B_\ell = \frac{\lambda}{AL} .$$

The scan cell width GA is given by

$$GA = B_\ell R_1$$

where R_1 = slant range to the scan cell nearest the track.

The Doppler bandwidth F_d is

$$F_d = \frac{2Vg}{AL} .$$

Obviously, when the aperture length decreases, B_ℓ increases and the scan cells become wider. For a given velocity, the Doppler bandwidth becomes larger. The number of filter channels NFLT needed to process the Doppler bandwidth is

$$NFLT = \frac{F_d}{\Delta F_d}$$

where ΔF_d = tracking bandwidth (fixed by the resolution).

Hence NFLT increases as F_d increases. A plot of the number of filters for various aperture lengths is given in Figure 37.

The power consumption is based on requirements for the filter channel and buffer serial analog memories and their associated clock drivers. The number of SAMs required to process the data is given by

$$S = \frac{2 \lambda R_{\max} \tan \theta_{\max} f_s}{63 c AH}$$

where

R_{\max} = slant range at farthest look angle (470800 m)

523

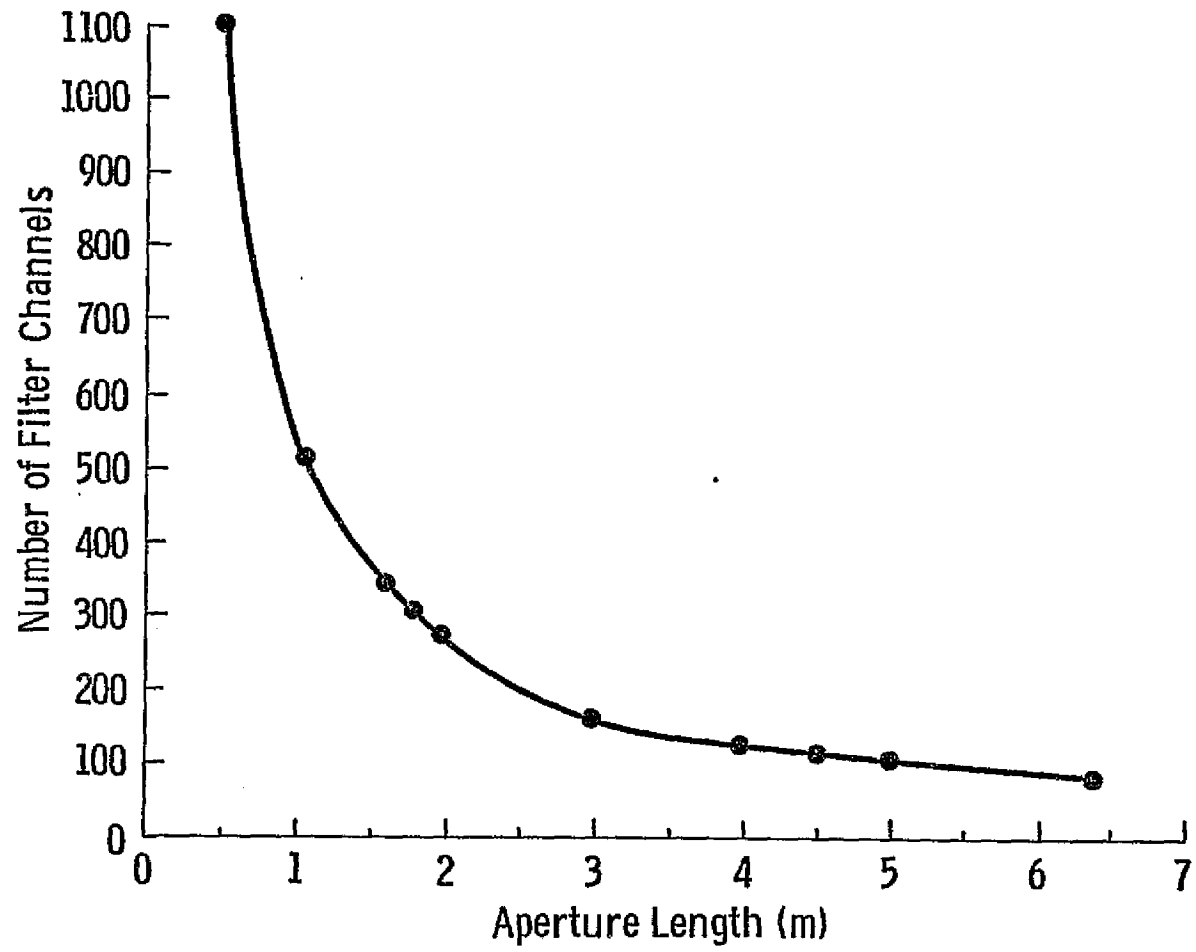


Figure 37. Number of filter channels vs. aperture length.

θ_{\max} = farthest look angle coverage in swath (22.488°)

f_s = SAM sampling frequency.

Using the above constants,

$$S = \frac{1.299 \times 10^{-6}}{AH} f_s$$

where $f_s = 20$ MHz in the filter channels, and $f_s = 8$ MHz for the buffers. Table 9 shows the number of SAMs per channel; the number of channels, and the total number of SAMs per processor as functions of aperture height for the near swath. Figure 38 shows the total channel power consumption considering SAMs and CMOS drivers calculated in the same manner as Appendix E. Although the total number of SAMs fluctuates, their AC power consumption, which depends on the number of SAMs operating at a given time in each channel, will decrease with increasing antenna length. Long, thin antennas give the lowest power consumptions.

6.2 SIZE

The physical size of the radar depends mainly on the layout of the electronic components. It is recommended to mount the components for each channel on the same board in order to minimize propagation delays. The drivers for the SAMs could be located together in order to centralize the large amount of heat they can be expected to generate. Heat can be dissipated by radiation into space. The fixed shapes of many off-the-shelf-items such as the microwave plumbing, transmitter tube, and power supplies must be considered in order to package the hardware for minimum volume. Obviously, high voltage leads should be kept to minimal lengths. It would also be advisable to locate the transmitter tube as far away from the antenna as possible so as to reduce thermal effects. The entire radar system could conceivably be enclosed in a 36" x 36" x 18" volume.

TABLE 9.

<u>Aperture Length</u>	<u>SAMs per Channel</u>	<u>No. of Channels</u>	<u>Total No. of SAMs</u>
0.500	8	1108	8864
1.069	14	518	7252
1.604	19	345	6555
1.791	22	309	6798
2.000	25	277	6925
3.000	36	185	6660
4.000	48	138	6624
4.500	53	123	6519
5.000	59	111	6549
6.414	70	86	6278

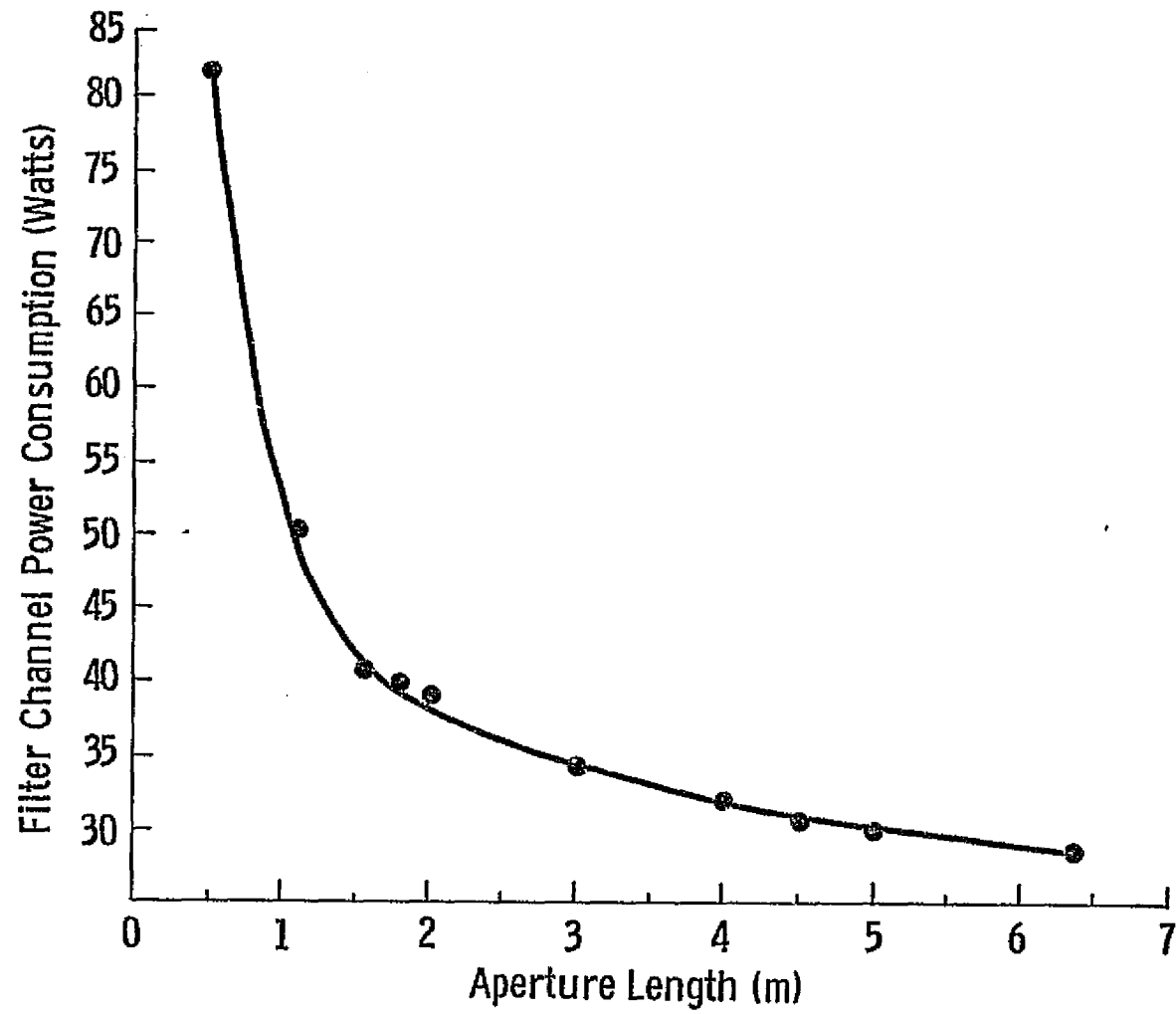


Figure 38. Filter channel power consumption vs. aperture length.

7.0 CONCLUSIONS AND RECOMMENDATIONS

The SCANSAR signal processor can effectively be implemented as an analog system; however, there are a few considerations worth mentioning. The stability of the filter channels is a critical factor and must be examined in detail. Obviously, the more complex a processor is, the more difficult it becomes to operate under a given set of constraints. It is hoped that in the near future, the storage capability of the SAM (or similar devices) will be expanded so that fewer of them will be needed. For example, using 1024-bit analog devices would reduce the number of such devices in each channel to 3 and would eliminate much of the switching circuitry presently required. The effect on the total power consumption is an unresolved issue in that although the number of devices has been decreased, chances are that due to the increased number of bits, the quiescent (DC) power would go up and the clock line capacitance would increase, thereby requiring more drivers.

The width of a comb "tooth" in a comb filter is directly proportional to its tracking bandwidth (Δf_d) and is therefore directly proportional to the azimuth resolution. Decreasing the sidelobe levels results in widening the main lobe and degrading the resolution. It is conceivable that more detailed comb response sidelobe weighting studies may require revision of the resolution requirements.

As was noted in Section 2.2, the SCANSAR computer-design program was written such that the angles used in the design were the pointing angles and inter-cell gaps developed. This was compensated for by changing the angles to account for the beamwidth and increasing the number of cells in the swath by 1. A preferable design would take the beamwidth into account initially when calculating the number of cells, thereby skirting the gap problem entirely.

The ideal way to evaluate system performance and to study possible improvements would be to construct an aircraft version of the processor, which would be considerably less complicated than the satellite version, and fly the system. Perfecting its operation on a small-scale basis would lend itself well to expansion to spacecraft operation.

APPENDIX A

This appendix contains the updated FORTRAN program listing of SCANSAR used in designing the processor for this report. The original version of SCANSAR can be found in Claassen (1975). Final output listings are located in section 2.0.

```

00100SCANSAR      DESIGN OF A SCANNING SAR
00200              THIS PROGRAM WAS PREPARED BY
00300
00400              JOHN P. CLASSEN
00500
00600      DIMENSION THETAD(2), THETAR(2), SIGMAX(2), RA(2),
00700      & RR(2), CC(2), WT(2), TYPE(4), GR(2), GA(2), R(2),
00800      & SIGMIN(2)
00900      REAL NF, KT, LOSS, K
01000      DATA C, DEG, YES, PI, TYPE, THOUS, K, JJ/
01100      & 3.0E08, 0.0174532925, 'YES', 3.141925,
01200      & 'UNFOCU', 'SED', 'SEMI-F', 'DCUSED', 1000.0, 1.38E-23,
01300      & 0177177077040/
01400      ARITHMETIC ASSIGNMENT STATEMENT
01500      TAN(X) = SIN(X)/COS(X)
01600      SPRESS CARRIAGE RETURNS ON READS
01700      CALL FPARAM(3,JJ)
01800      INPUT PARAMETERS(GEOMETRY)
01900  10  WRITE(6,1000)
02000 1000  FORMAT(///1X,'DESIGN OF A SCANNING SAR HAVING',
02100      & ' INPUT DESIGN PARAMETERS AS FOLLOWS: '//
02200      & 'APERTURE LENGTH (M) ')
02300      READ(5,1001) AL
02400 1001  FORMAT(F8.2)
02500      WRITE(6,1002)
02600 1002  FORMAT(1X,'OPERATING WAVELENGTH (M) ')
02700      READ(5,1001) WL
02800      WRITE(6,1003)
02900 1003  FORMAT(1X,'MIN AND MAX VIEW ANGLES (DEG) ')
03000      READ(5,1008) THETAD
03100 1008  FORMAT(2F8.2)
03200      WRITE(6,1004)
03300 1004  FORMAT(1X,'AZIMUTH RESOLUTION (M) ')

03400      READ(5,1001) RA(1)
03500      WRITE(6,1005)
03600 1005  FORMAT(1X,'RANGE RESOLUTION (M) ')
03700      READ(5,1001) RR(1)
03800      WRITE(6,1006)
03900 1006  FORMAT(1X,'GROUND VELOCITY (KM/SEC) ')
04000      READ(5,1001) VGP
04100      WRITE(6,1007)
04200 1007  FORMAT(1X,'SPACECRAFT-ALTITUDE (KM) ')
04300      READ(5,1001) ZP

```

REPRODUCIBILITY OF THE
ORIGINAL PAGE IS POOR

```

0440C          SCALE VARIABLES
0450          VG = VGP*THOUS
0460          Z = ZP*THOUS
0470C          UNFOCUSED PRESUMPTION
0480          ITYPE = 1
0490C          COMPUTE MAX AND MIN RANGE
0500          DO 20 I=1,2
0510          THETAR(I) = THETAD(I)*DEG
0520          R(I) = Z/COS(THETAR(I))
0530    20    CONTINUE
0540C          FULLY FOCUSED LIMITATION
0550          RAFF = AL/2.0
0560          IF(RAFF .LT. RA(1)) GO TO 30
0570          WRITE(6,2000)
0580 2000    FORMAT(1X,'INADEQUATE APERTURE LENGTH TO',
0590    &    'ACHIEVE RESOLUTION. INPUT DATA AGAIN!'/)
0600          GO TO 10
0610C          UNFOCUSED LIMITATION
0620    30    RAUF = SQRT(WL*R(2)/2.0)
0630C          ESTABLISH SYSTEM TYPE
0640          IF(RAUF .LT. RA(1)) GO TO 40
0650C          PARTIALLY OR FULLY FOCUSED SYSTEM REQUIRED
0660          DFD = 2.0*VG*RA(1)/R(1)/WL
0670          RA(2) = DFD*WL*R(2)/2.0*VG
0680          ITYPE = 3
0690          GO TO 45
0700    40    RA(1) = RAUF
0710C          UNFOCUSED SYSTEM REQUIRED
0720          DFD = 2.0*VG*RA(1)/R(1)/WL
0730          RA(2) = DFD*WL*R(2)/2.0*VG
0740C          APERTURE HEIGHT TO SATISFY DOPPLER SAMPLING
0750C          REQUIREMENT
0760    45    FD = 2.0*VG/AL
0770          NFILA = FD/DFD + 0.5
0780          AH = 6.0*FD*R(2)*TAN(THETAR(2))*WL/C
0790C          CHECK WITH DESIGNER
0800          WRITE(6,3000) AH
0810 3000    FORMAT(1X,'THE APERTURE HEIGHT IS',F6.2,' M.',
0820    &    ' DO YOU WISH TO INCREASE THE HEIGHT?')
0830          READ(5,3001) ANS
0840 3001    FORMAT(A3)
0850          IF(ANS .NE. YES) GO TO 70
0860    50    READ(5,1001) AHNEW

```

```

0870      IF (AHNEW .GT. AH) GO TO 60
0880      WRITE(6,3002)
0890 3002  FORMAT(1X,'NEW APERTURE HEIGHT MUST BE LARGER THAN',
0900      & ' THE OLD. TRY AGAIN!'/)
0910      GO TO 50
0920      60  AH = AHNEW
0930      70  BETAH = WL/AH
0940C      COVERAGE PARAMETERS
0950      NCELL = (THETAR(2)-THETAR(1))/BETAH + 0.5
0960      NCELL = NCELL + 1
0970      BETAL = WL/AL
0980      DO 80 I = 1,2
0990      GR(I) = R(I)*BETAL/THOUS
1000      GR(I) = R(I)*BETAH/COS(THETAR(I))/THOUS
1010      80  CONTINUE
1020      SWATH = (R(2)*SIN(THETAR(2))-R(1)*SIN(THETAR(1)))/THOUS +
1030      & (GR(2) + GR(1))/2.0
1040C      TIMING
1050      TSLEW = GR(1)/V6*THOUS
1060      TCELL = TSLEW/NCELL
1070      IF(TCELL .GT. 1.0/DFD) GO TO 85
1080      WRITE(6,3003)
1090 3003  FORMAT(1X,'INSUFFICIENT TIME TO ACHIEVE RESOLUTION!',
1100      & ' TRY AGAIN!'/)
1110      GO TO 10
1120C      PULSE REPETITION FREQUENCY
1130      85  DELR = BETAH*R(2)*TAN(THETAR(2))
1140      PRF = C/(4.0*DELR)
1150C      RANGE RESOLUTION
1160      DR = RR(1)*SIN(THETAR(1))
1170      RR(2) = DR/SIN(THETAR(2))
1180C      BANDWIDTH REQUIRED
1190      BW = C/2.0/DR/THOUS**2
1200C      PROCESSING GAIN
1210      NGP=PRF/DFD
1220C      NO. OF CELLS AVAILABLE FOR AVERAGING
1230      LOOKS = TCELL*DFD
1240C      DEPTH OF FOCUS
1250      RMIN=Z/COS(THETAR(2))-BETAH/2.0)
1260      FACT1 = R(1)*R(1)*WL
1270      FACT2 = 0.6*RA(1)*RA(1)
1280      NFILR = 0
1290      RPLUS = Z/COS(THETAR(2))+BETAH/2.0)

```

```

1300 86   RMINUS = FACT1+RPLUS/(FACT2+RPLUS+FACT1)
1310     NFILR = NFILR+1
1320     IF(RMINUS.LT.RMIN) GO TO 87
1330     RPLUS = RMINUS
1340     GO TO 86
1350C     INPUT POWER PARAMETERS
1360 87   WRITE(6,4000)
1370 4000  FORMAT(1X,'LOSS FACTOR (DB)')
1380     READ(5,1001) LOSS
1390     WRITE(6,4002)
1400 4002  FORMAT(1X,'NOISE FIGURE (DB)')
1410     READ(5,1001) NF
1420     WRITE(6,4003)
1430 4003  FORMAT(1X,'SIGNAL/NOISE (DB)')
1440     READ(5,1001) SN
1450     WRITE(6,4004)
1460 4004  FORMAT(1X,'MAX SCATTERING COEFFICIENTS (DB)')
1470     READ(5,1008) SIGMAX
1480     WRITE(6,4007)
1490 4007  FORMAT(1X,'MIN SCATTERING COEFFICIENTS (DB)')
1500     READ(5,1008) SIGMIN
1510     WRITE(6,4005)
1520 4005  FORMAT(1X,'APERTURE EFF (PERCENT)')
1530     READ(5,1001) AEFF
1540     AEFF = AEFF/100.0
1550     WRITE(6,4006)
1560 4006  FORMAT(1X,'RECEIVER INPUT TEMPERATURE (DEG K)')
1570     READ(5,1001) TEMP
1580C     COMPUTE TRANSMITTER POWER AND CHANNEL CAPACITY
1590     FACTOR = 4.0*PI*WL**2*10.0**((LOSS+NF+SN)/10.0)*PRF*K*TEMP
1600C     NO. OF BITS PER CELL
1610     NBITS = (SIGMAX(1)-SIGMIN(2))/3.0103 + 0.5
1620     DO 90 I = 1,2
1630     WT(I) = 4.0*FACTOR*RR(I)**4/(10.0**((SIGMIN(I)/10.0)*RA(I)*
1640     & RR(I)+NGP*(AL+AH+AEFF)**2)
1650     CC(I) = GR(I)+GA(I)/(RA(I)+RR(I))*NBITS/TCELL
1660 90    CONTINUE
1670C     LIST SYSTEM DESIGN PARAMETERS
1680     WRITE(6,5000) THETA0, WL, AL, RA(1), RR(1),
1690     & VGP, ZP, AEFF*100.0, LOSS, NF, SN, TEMP, SIGMAX, SIGMIN
1700 5000  FORMAT(///20X,'SUMMARY TABLE'///,1X,'RAW DESIGN PARAMETERS'///
1710     & 1X,'PARAMETERS'17X,'VALUES',10X,'UNITS'///
1720     & 1X,'ANGLE SPAN',4X, 2(F10.2,5X),'DEG'//
1730     & 1X,'LAMBDA',8X,F10.3,20X,'M'//

```

```

1740 @ 1X,'APER LENGTH',3X,F10.1,20X,'M'//
1750 @ 1X,'AZ RES',8X,F10.2,20X,'M'//
1760 @ 1X,'RA RES',8X,F10.2,20X,'M'//
1770 @ 1X,'GRD VEL',7X,F10.1,20X,'KM/SEC'//
1780 @ 1X,'ALTITUDE',6X,F10.1,20X,'KM'//
1790 @ 1X,'APER EFF',6X,F10.1,20X,'PERCENT'//
1800 @ 1X,'LOSS FACTOR',3X,F10.1,20X,'DB'//
1810 @ 1X,'NOISE FIG',5X,F10.1,20X,'DB'//
1820 @ 1X,'SIG/NOISE',5X,F10.2,20X,'DB'//
1830 @ 1X,'REC TEMP',6X,F10.1,20X,'DEG K'//
1840 @ 1X,'SIGMAX',8X,2(F10.2,5X),'DB'//
1850 @ 1X,'SIGMIN',8X,2(F10.2,5X),'DB'//
1860C      COMPUTED PARAMETERS
1870      WRITE(6,5001) TYPE(I*TYPE),TYPE(I*TYPE+1),AH, WT,
1880 @ PRF/THOUS, FD/THOUS, BW, NGP, LOOKS, NFILR, NFILA, CC
1890 5001  FORMAT(1X,'COMPUTED SYSTEM PARAMETERS'//
1900 @ 1X,'SYSTEM TYPE:',2X,2A6//
1910 @ 1X,'APER HEIGHT',3X,F10.2,20X,'M'//
1920 @ 1X,'XMIT PWR',6X,2(F10.2,5X),'WATTS'//
1930 @ 1X,'PRF',11X,F10.2,20X,'KHZ'//
1940 @ 1X,'FD',12X,F10.2,20X,'KHZ'//
1950 @ 1X,'RF BW',9X,F10.1,20X,'MHZ'//
1960 @ 1X,'PROC GAIN',5X,I10//
1970 @ 1X,'LOOKS',9X,I10//
1980 @ 1X,'FILTER BANKS',2X,I10//
1990 @ 1X,'FILTERS/BANK',2X,I10//
2000 @ 1X,'CHAN CAP',6X,2(F10.2,5X),'MBITS/SEC'//)
2010      WRITE(6,5002) SWATH, NCELL, GA, GR, TSLEW, TCELL, RA, RR
2020 5002  FORMAT(1X,'COVERAGE AND RESOLUTION'//
2030 @ 1X,'SWATH',9X,F10.2,20X,'KM'//
2040 @ 1X,'CELLS/SCAN',4X,I10//
2050 @ 1X,'CELL WIDTH',4X,2(F10.2,5X),'KM'//
2060 @ 1X,'CELL LENGTH',3X,2(F10.2,5X),'KM'//
2070 @ 1X,'SCAN TIME',5X,F10.2,20X,'SEC'//
2080 @ 1X,'TIME/CELL',5X,F10.3,20X,'SEC'//
2090 @ 1X,'AZ RES',8X,2(F10.2,5X),'M'//
2100 @ 1X,'RA RES',8X,2(F10.2,5X),'M'//
2110 @ 1X,'WANT TO DESIGN ANOTHER ONE'//)
2120      READ(5,3001) ANS
2130      IF(ANS .EQ. YES) GO TO 10
2140      WRITE(6,9000)
2150 9000  FORMAT(1X,'VERY INTERESTING!', ' AUFWIEDERSEHEN'//)
2160      STOP
2170      END

```

APPENDIX B

This appendix contains a program used on a Hewlett-Packard HP-25 scientific calculator to figure the round-trip times to the inner and outer edges of an image cell and the length of the return pulse. The input data required is inner look angle, outer look angle, and altitude. The round-trip time from the inner angle is displayed first, for approximately 4 seconds, followed by the round-trip time from the outer angle for the same display time, followed by the pulse length. In the final design, this must be modified to use spherical-earth geometry.

HP-25 Program To Calculate Round-Trip Times To
The Image Cell Inner and Outer Edges.

<u>STEP</u>	<u>INSTRUCTION</u>	<u>STEP</u>	<u>INSTRUCTION</u>
01	RCL 1	18	COS
02	COS	19	ENTER
03	ENTER	20	RCL 3
04	RCL 3	21	÷
05	÷	22	1/X
06	1/X	23	2
07	2	24	X
08	X	25	RCL 4
09	RCL 4	26	÷
10	÷	27	PAUSE
11	PAUSE	28	PAUSE
12	PAUSE	29	PAUSE
13	PAUSE	30	PAUSE
14	PAUSE	31	PAUSE
15	PAUSE	32	RCL 5
16	STO 5	33	-
17	RCL 2	34	GO TO 00

INPUT

- STO 1 - INNER ANGLE (DEG)
- STO 2 - OUTER ANGLE (DEG)
- STO 3 - ALTITUDE (m)
- STO 4 - 3×10^8 (m/sec)

APPENDIX C

This appendix contains the Fortran program and output listings which generated the incremental phase shifts for the scanning local oscillator discussed in section 4.4.1. Data was input in the following format:

7200. , 7050. , 0. , A, B, NPULSE

where A and B are the swath constants for 7200 Hz and 7050 Hz PRFs (respectively) shown on page 46. NPULSE is the maximum number of pulses per look.

```

0010C      THIS PROGRAM CALCULATES THE INCREMENTAL
0020C      PHASE SHIFTS FOR THE SLO SUBSYSTEM
0030C
0040C      INPUT PARAMETERS
0050C          DPRF(K) = PRF
0060C          A = CONSTANT FOR DPRF(1)
0070C          B = CONSTANT FOR DPRF(2)
0080C          NPULSE = NUMBER OF PULSES PER LOOK
0090C
0100C      OUTPUT PARAMETERS
0110C          I = PULSE NUMBER
0120C          T = TIME (SEC)
0130C          TAVG = AVERAGE TIME (SEC)
0140C          DPHI = INCREMENTAL PHASE SHIFT (DEG)
0150C          PHIT = CUMULATIVE PHASE SHIFT (DEG)
0160C
0170 DIMENSION DPRF(3)
0180 READ(5,1000) (DPRF(K),K=1,3),A,B,NPULSE
0190 1000 FORMAT(3F6.0,2F10.5,I5)
0200 K=1
0210 5 IF(DPRF(K) .EQ. 0.0) GO TO 99
0220 PHIT=0.
0230 WRITE(6,2000) DPRF(K)
0240 2000 FORMAT(2X,'PRF = ',F6.0//4X,'PULSE',4X,'TIME(SEC)',
0250 4X,'AVG TIME(SEC)',4X,'PHASE SHIFT(DEG)',4X,'PHI TOTAL',//)
0260 RR=1.0/DPRF(K)
0270 DEG=8
0280 IF(DPRF(K) .EQ. 7200.) DEG=A
0290 DO 10 I=1,NPULSE
0300 XI=I
0310 T=XI*RR
0320 TAVG=(XI*RR+(XI+1.0)*RR)/2.0
0330 DPHI=DEG*TAVG
0340 PHIT=PHIT+DPHI
0350 WRITE(6,3000) I,T,TAVG,DPHI,PHIT
0360 3000 FORMAT(5X,I3,2(4X,E11.5),9X,F8.5,7X,F9.5)
0370 10 CONTINUE
0380 WRITE(6,4000)
0390 4000 FORMAT(///)
0400 K=K+1
0410 I=1
0420 GO TO 5
0430 99 STOP
0440 END

```

PULSE	TIME(SEC)	AVG TIME(SEC)	PHASE SHIFT(DEG)	PHI TOTAL
1	0.13889E-03	0.20833E-03	0.03809	0.03809
2	0.27778E-03	0.34722E-03	0.06348	0.10157
3	0.41667E-03	0.48611E-03	0.08887	0.19044
4	0.55556E-03	0.62500E-03	0.11426	0.30470
5	0.69444E-03	0.76389E-03	0.13965	0.44435
6	0.83333E-03	0.90278E-03	0.16505	0.60940
7	0.97222E-03	0.10417E-02	0.19044	0.79984
8	0.11111E-02	0.11806E-02	0.21583	1.01566
9	0.12500E-02	0.13194E-02	0.24122	1.25688
10	0.13889E-02	0.14583E-02	0.26661	1.52350
11	0.15278E-02	0.15972E-02	0.29200	1.81550
12	0.16667E-02	0.17361E-02	0.31739	2.13289
13	0.18056E-02	0.18750E-02	0.34279	2.47568
14	0.19444E-02	0.20139E-02	0.36818	2.84386
15	0.20833E-02	0.21528E-02	0.39357	3.23743
16	0.22222E-02	0.22917E-02	0.41896	3.65639
17	0.23611E-02	0.24306E-02	0.44435	4.10074
18	0.25000E-02	0.25694E-02	0.46974	4.57049
19	0.26389E-02	0.27083E-02	0.49514	5.06562
20	0.27778E-02	0.28472E-02	0.52053	5.58615
21	0.29167E-02	0.29861E-02	0.54592	6.13207
22	0.30556E-02	0.31250E-02	0.57131	6.70338
23	0.31944E-02	0.32639E-02	0.59670	7.30008
24	0.33333E-02	0.34028E-02	0.62209	7.92218
25	0.34722E-02	0.35417E-02	0.64749	8.56966
26	0.36111E-02	0.36806E-02	0.67288	9.24254
27	0.37500E-02	0.38194E-02	0.69827	9.94081
28	0.38889E-02	0.39583E-02	0.72366	10.66447
29	0.40278E-02	0.40972E-02	0.74905	11.41352
30	0.41667E-02	0.42361E-02	0.77444	12.18797
31	0.43056E-02	0.43750E-02	0.79984	12.98780
32	0.44444E-02	0.45139E-02	0.82523	13.81303
33	0.45833E-02	0.46528E-02	0.85062	14.66365
34	0.47222E-02	0.47917E-02	0.87601	15.53966
35	0.48611E-02	0.49306E-02	0.90140	16.44106
36	0.50000E-02	0.50694E-02	0.92679	17.36785
37	0.51389E-02	0.52083E-02	0.95218	18.32004
38	0.52778E-02	0.53472E-02	0.97758	19.29761
39	0.54167E-02	0.54861E-02	1.00297	20.30058
40	0.55556E-02	0.56250E-02	1.02836	21.32894
41	0.56944E-02	0.57639E-02	1.05375	22.38269
42	0.58333E-02	0.59028E-02	1.07914	23.46184
43	0.59722E-02	0.60417E-02	1.10453	24.56637
44	0.61111E-02	0.61806E-02	1.12993	25.69630
45	0.62500E-02	0.63194E-02	1.15532	26.85161
46	0.63889E-02	0.64583E-02	1.18071	28.03232
47	0.65278E-02	0.65972E-02	1.20610	29.23842
48	0.66667E-02	0.67361E-02	1.23149	30.46992
49	0.68056E-02	0.68750E-02	1.25688	31.72680
50	0.69444E-02	0.70139E-02	1.28228	33.00908

51	0.70833E-02	0.71523E-02	1.30767	34.31674
52	0.72222E-02	0.72917E-02	1.33306	35.64980
53	0.73611E-02	0.74306E-02	1.35845	37.00825
54	0.75000E-02	0.75694E-02	1.38384	38.39209
55	0.76389E-02	0.77083E-02	1.40923	39.80133
56	0.77778E-02	0.78472E-02	1.43463	41.23595
57	0.79167E-02	0.79861E-02	1.46002	42.69597
58	0.80556E-02	0.81250E-02	1.48541	44.18138
59	0.81944E-02	0.82639E-02	1.51080	45.69218
60	0.83333E-02	0.84028E-02	1.53619	47.22837
61	0.84722E-02	0.85417E-02	1.56158	48.78995
62	0.86111E-02	0.86806E-02	1.58697	50.37693
63	0.87500E-02	0.88194E-02	1.61237	51.98929
64	0.88889E-02	0.89583E-02	1.63776	53.62705
65	0.90278E-02	0.90972E-02	1.66315	55.29020
66	0.91667E-02	0.92361E-02	1.68854	56.97874
67	0.93056E-02	0.93750E-02	1.71393	58.69268
68	0.94444E-02	0.95139E-02	1.73932	60.43200
69	0.95833E-02	0.96528E-02	1.76472	62.19672
70	0.97222E-02	0.97917E-02	1.79011	63.98682
71	0.98611E-02	0.99306E-02	1.81550	65.80232
72	0.10000E-01	0.10000E-01	1.84089	67.64321
73	0.10139E-01	0.10238E-01	1.86628	69.50950
74	0.10278E-01	0.10347E-01	1.89167	71.40117
75	0.10417E-01	0.10456E-01	1.91707	73.31824
76	0.10556E-01	0.10625E-01	1.94246	75.26069
77	0.10694E-01	0.10764E-01	1.96785	77.22854
78	0.10833E-01	0.10903E-01	1.99324	79.22178
79	0.10972E-01	0.11042E-01	2.01863	81.24041
80	0.11111E-01	0.11181E-01	2.04402	83.28444
81	0.11250E-01	0.11319E-01	2.06942	85.35385
82	0.11389E-01	0.11458E-01	2.09481	87.44866
83	0.11528E-01	0.11597E-01	2.12020	89.56886
84	0.11667E-01	0.11736E-01	2.14559	91.71445
85	0.11806E-01	0.11875E-01	2.17098	93.88543
86	0.11944E-01	0.12014E-01	2.19637	96.08180
87	0.12083E-01	0.12153E-01	2.22176	98.30357
88	0.12222E-01	0.12292E-01	2.24716	100.55072
89	0.12361E-01	0.12431E-01	2.27255	102.82327
90	0.12500E-01	0.12569E-01	2.29794	105.12121
91	0.12639E-01	0.12708E-01	2.32333	107.44454
92	0.12778E-01	0.12847E-01	2.34872	109.79326
93	0.12917E-01	0.12986E-01	2.37411	112.16738
94	0.13056E-01	0.13125E-01	2.39951	114.56688
95	0.13194E-01	0.13264E-01	2.42490	116.99178
96	0.13333E-01	0.13403E-01	2.45029	119.44207
97	0.13472E-01	0.13542E-01	2.47568	121.91775
98	0.13611E-01	0.13681E-01	2.50107	124.41882
99	0.13750E-01	0.13819E-01	2.52646	126.94528
100	0.13889E-01	0.13958E-01	2.55186	129.49714

101	0.14028E-01	0.14097E-01	2.57725	132.07439
102	0.14167E-01	0.14236E-01	2.60264	134.67703
103	0.14306E-01	0.14375E-01	2.62803	137.30506
104	0.14444E-01	0.14514E-01	2.65342	139.95848
105	0.14583E-01	0.14653E-01	2.67881	142.63729
106	0.14722E-01	0.14792E-01	2.70421	145.34150
107	0.14861E-01	0.14931E-01	2.72960	148.07109
108	0.15000E-01	0.15069E-01	2.75499	150.82608
109	0.15139E-01	0.15208E-01	2.78038	153.60646
110	0.15278E-01	0.15347E-01	2.80577	156.41223
111	0.15417E-01	0.15486E-01	2.83116	159.24340
112	0.15556E-01	0.15625E-01	2.85655	162.09995
113	0.15694E-01	0.15764E-01	2.88195	164.98190
114	0.15833E-01	0.15903E-01	2.90734	167.88923
115	0.15972E-01	0.16042E-01	2.93273	170.82196
116	0.16111E-01	0.16181E-01	2.95812	173.78008
117	0.16250E-01	0.16319E-01	2.98351	176.76360
118	0.16389E-01	0.16458E-01	3.00890	179.77250
119	0.16528E-01	0.16597E-01	3.03430	182.80680
120	0.16667E-01	0.16736E-01	3.05969	185.86648
121	0.16806E-01	0.16875E-01	3.08508	188.95156
122	0.16944E-01	0.17014E-01	3.11047	192.06203
123	0.17083E-01	0.17153E-01	3.13586	195.19790
124	0.17222E-01	0.17292E-01	3.16125	198.35915
125	0.17361E-01	0.17431E-01	3.18665	201.54579
126	0.17500E-01	0.17569E-01	3.21204	204.75783
127	0.17639E-01	0.17708E-01	3.23743	207.99526
128	0.17778E-01	0.17847E-01	3.26282	211.25808
129	0.17917E-01	0.17986E-01	3.28821	214.54629
130	0.18056E-01	0.18125E-01	3.31360	217.85989
131	0.18194E-01	0.18264E-01	3.33900	221.19889
132	0.18333E-01	0.18403E-01	3.36439	224.56328
133	0.18472E-01	0.18542E-01	3.38978	227.95305
134	0.18611E-01	0.18681E-01	3.41517	231.36823
135	0.18750E-01	0.18819E-01	3.44056	234.80879
136	0.18889E-01	0.18958E-01	3.46595	238.27474
137	0.19028E-01	0.19097E-01	3.49134	241.76608
138	0.19167E-01	0.19236E-01	3.51674	245.28282
139	0.19306E-01	0.19375E-01	3.54213	248.82495
140	0.19444E-01	0.19514E-01	3.56752	252.39247
141	0.19583E-01	0.19653E-01	3.59291	255.98538
142	0.19722E-01	0.19792E-01	3.61830	259.60368
143	0.19861E-01	0.19931E-01	3.64369	263.24738
144	0.20000E-01	0.20069E-01	3.66909	266.91647
145	0.20139E-01	0.20208E-01	3.69448	270.61094
146	0.20278E-01	0.20347E-01	3.71987	274.33081
147	0.20417E-01	0.20486E-01	3.74526	278.07607
148	0.20556E-01	0.20625E-01	3.77065	281.84673
149	0.20694E-01	0.20764E-01	3.79604	285.64277
150	0.20833E-01	0.20903E-01	3.82144	289.46420

151	0.20972E-01	0.21042E-01	3.84683	293.31103
152	0.21111E-01	0.21181E-01	3.87222	297.18325
153	0.21250E-01	0.21319E-01	3.89761	301.08086
154	0.21389E-01	0.21458E-01	3.92300	305.00386
155	0.21528E-01	0.21597E-01	3.94839	308.95226
156	0.21667E-01	0.21736E-01	3.97378	312.92604
157	0.21806E-01	0.21875E-01	3.99918	316.92522
158	0.21944E-01	0.22014E-01	4.02457	320.94978
159	0.22083E-01	0.22153E-01	4.04996	324.99974
160	0.22222E-01	0.22292E-01	4.07535	329.07510
161	0.22361E-01	0.22431E-01	4.10074	333.17584
162	0.22500E-01	0.22569E-01	4.12613	337.30197
163	0.22639E-01	0.22708E-01	4.15153	341.45350
164	0.22778E-01	0.22847E-01	4.17692	345.63042
165	0.22917E-01	0.22986E-01	4.20231	349.83273
166	0.23056E-01	0.23125E-01	4.22770	354.06042
167	0.23194E-01	0.23264E-01	4.25309	358.31352
168	0.23333E-01	0.23403E-01	4.27848	362.59200
169	0.23472E-01	0.23542E-01	4.30388	366.89588
170	0.23611E-01	0.23681E-01	4.32927	371.22514
171	0.23750E-01	0.23819E-01	4.35466	375.57980
172	0.23889E-01	0.23958E-01	4.38005	379.95985
173	0.24028E-01	0.24097E-01	4.40544	384.36530
174	0.24167E-01	0.24236E-01	4.43083	388.79613
175	0.24306E-01	0.24375E-01	4.45623	393.25235
176	0.24444E-01	0.24514E-01	4.48162	397.73397
177	0.24583E-01	0.24653E-01	4.50701	402.24096
178	0.24722E-01	0.24792E-01	4.53240	406.77338
179	0.24861E-01	0.24931E-01	4.55779	411.33117
180	0.25000E-01	0.25069E-01	4.58318	415.91435
181	0.25139E-01	0.25208E-01	4.60857	420.52293
182	0.25278E-01	0.25347E-01	4.63397	425.15689
183	0.25417E-01	0.25486E-01	4.65936	429.81625
184	0.25556E-01	0.25625E-01	4.68475	434.50100
185	0.25694E-01	0.25764E-01	4.71014	439.21114
186	0.25833E-01	0.25903E-01	4.73553	443.94668
187	0.25972E-01	0.26042E-01	4.76092	448.70760
188	0.26111E-01	0.26181E-01	4.78632	453.49392
189	0.26250E-01	0.26319E-01	4.81171	458.30563
190	0.26389E-01	0.26458E-01	4.83710	463.14273
191	0.26528E-01	0.26597E-01	4.86249	468.00522
192	0.26667E-01	0.26736E-01	4.88788	472.89310
193	0.26806E-01	0.26875E-01	4.91327	477.80637
194	0.26944E-01	0.27014E-01	4.93867	482.74594
195	0.27083E-01	0.27153E-01	4.96406	487.70910
196	0.27222E-01	0.27292E-01	4.98945	492.69855
197	0.27361E-01	0.27431E-01	5.01484	497.71339
198	0.27500E-01	0.27569E-01	5.04023	502.75362
199	0.27639E-01	0.27708E-01	5.06562	507.81924
200	0.27778E-01	0.27847E-01	5.09102	512.91026

201	0.27917E-01	0.27936E-01	5.11641	518.02667
202	0.28056E-01	0.28125E-01	5.14180	523.16847
203	0.28194E-01	0.28264E-01	5.16719	528.33566
204	0.28333E-01	0.28403E-01	5.19258	533.52824
205	0.28472E-01	0.28542E-01	5.21797	538.74622
206	0.28611E-01	0.28681E-01	5.24336	543.98958
207	0.28750E-01	0.28819E-01	5.26876	549.25833
208	0.28889E-01	0.28958E-01	5.29415	554.55248
209	0.29028E-01	0.29097E-01	5.31954	559.87202
210	0.29167E-01	0.29236E-01	5.34493	565.21696
211	0.29306E-01	0.29375E-01	5.37032	570.58728
212	0.29444E-01	0.29514E-01	5.39571	575.98299
213	0.29583E-01	0.29653E-01	5.42111	581.40410
214	0.29722E-01	0.29792E-01	5.44650	586.85059
215	0.29861E-01	0.29931E-01	5.47189	592.32248
216	0.30000E-01	0.30069E-01	5.49728	597.81976
217	0.30139E-01	0.30208E-01	5.52267	603.34244
218	0.30278E-01	0.30347E-01	5.54806	608.89050
219	0.30417E-01	0.30486E-01	5.57346	614.46396
220	0.30556E-01	0.30625E-01	5.59885	620.06281
221	0.30694E-01	0.30764E-01	5.62424	625.68704
222	0.30833E-01	0.30903E-01	5.64963	631.33667
223	0.30972E-01	0.31042E-01	5.67502	637.01169
224	0.31111E-01	0.31181E-01	5.70041	642.71210
225	0.31250E-01	0.31319E-01	5.72581	648.43791
226	0.31389E-01	0.31458E-01	5.75120	654.18911
227	0.31528E-01	0.31597E-01	5.77659	659.96570
228	0.31667E-01	0.31736E-01	5.80198	665.76768
229	0.31806E-01	0.31875E-01	5.82737	671.59505
230	0.31944E-01	0.32014E-01	5.85276	677.44781
231	0.32083E-01	0.32153E-01	5.87815	683.32596
232	0.32222E-01	0.32292E-01	5.90355	689.22951
233	0.32361E-01	0.32431E-01	5.92894	695.15845
234	0.32500E-01	0.32569E-01	5.95433	701.11278
235	0.32639E-01	0.32708E-01	5.97972	707.09250
236	0.32778E-01	0.32847E-01	6.00511	713.09761
237	0.32917E-01	0.32986E-01	6.03050	719.12811
238	0.33056E-01	0.33125E-01	6.05590	725.18401

239	0.33194E-01	0.33264E-01	6.08129	731.26530
240	0.33333E-01	0.33403E-01	6.10668	737.37198
241	0.33472E-01	0.33542E-01	6.13207	743.50405
242	0.33611E-01	0.33681E-01	6.15746	749.66151
243	0.33750E-01	0.33819E-01	6.18285	755.84437
244	0.33889E-01	0.33958E-01	6.20825	762.05261
245	0.34028E-01	0.34097E-01	6.23364	768.28625
246	0.34167E-01	0.34236E-01	6.25903	774.54527
247	0.34306E-01	0.34375E-01	6.28442	780.82970
248	0.34444E-01	0.34514E-01	6.30981	787.13951
249	0.34583E-01	0.34653E-01	6.33520	793.47472
250	0.34722E-01	0.34792E-01	6.36060	799.83531
251	0.34861E-01	0.34931E-01	6.38599	806.22130
252	0.35000E-01	0.35069E-01	6.41138	812.63268
253	0.35139E-01	0.35208E-01	6.43677	819.06944
254	0.35278E-01	0.35347E-01	6.46216	825.53160
255	0.35417E-01	0.35486E-01	6.48755	832.01916
256	0.35556E-01	0.35625E-01	6.51294	838.53210
257	0.35694E-01	0.35764E-01	6.53834	845.07044
258	0.35833E-01	0.35903E-01	6.56373	851.63417
259	0.35972E-01	0.36042E-01	6.58912	858.22329
260	0.36111E-01	0.36181E-01	6.61451	864.83780
261	0.36250E-01	0.36319E-01	6.63990	871.47770
262	0.36389E-01	0.36458E-01	6.66529	878.14299
263	0.36528E-01	0.36597E-01	6.69069	884.83368
264	0.36667E-01	0.36736E-01	6.71608	891.54976
265	0.36806E-01	0.36875E-01	6.74147	898.29123
266	0.36944E-01	0.37014E-01	6.76686	905.05809
267	0.37083E-01	0.37153E-01	6.79225	911.85034
268	0.37222E-01	0.37292E-01	6.81764	918.66798
269	0.37361E-01	0.37431E-01	6.84304	925.51102
270	0.37500E-01	0.37569E-01	6.86843	932.37944
271	0.37639E-01	0.37708E-01	6.89382	939.27326
272	0.37778E-01	0.37847E-01	6.91921	946.19247
273	0.37917E-01	0.37986E-01	6.94460	953.13708
274	0.38056E-01	0.38125E-01	6.96999	960.10707
275	0.38194E-01	0.38264E-01	6.99538	967.10246
276	0.38333E-01	0.38403E-01	7.02078	974.12323
277	0.38472E-01	0.38542E-01	7.04617	981.16940

PULSE	TIME(SEC)	AVG TIME(SEC)	PHASE SHIFT(DEG)	PHI TOTAL
1	0.14184E-03	0.21277E-03	0.03973	0.03973
2	0.28369E-03	0.35461E-03	0.06621	0.10593
3	0.42553E-03	0.49645E-03	0.09269	0.19863
4	0.56738E-03	0.63830E-03	0.11918	0.31780
5	0.70922E-03	0.78014E-03	0.14566	0.46346
6	0.85106E-03	0.92199E-03	0.17214	0.63561
7	0.99291E-03	0.10638E-02	0.19863	0.83423
8	0.11348E-02	0.12057E-02	0.22511	1.05934
9	0.12766E-02	0.13475E-02	0.25159	1.31094
10	0.14184E-02	0.14894E-02	0.27808	1.58902
11	0.15603E-02	0.16312E-02	0.30456	1.89258
12	0.17021E-02	0.17730E-02	0.33104	2.22462
13	0.18440E-02	0.19149E-02	0.35753	2.58215
14	0.19858E-02	0.20567E-02	0.38401	2.96616
15	0.21277E-02	0.21986E-02	0.41050	3.37666
16	0.22695E-02	0.23404E-02	0.43698	3.81364
17	0.24113E-02	0.24823E-02	0.46346	4.27710
18	0.25532E-02	0.26241E-02	0.489	4.76705
19	0.26950E-02	0.27660E-02	0.51643	5.28348
20	0.28369E-02	0.29078E-02	0.54291	5.82639
21	0.29787E-02	0.30496E-02	0.56940	6.39579
22	0.31206E-02	0.31915E-02	0.59588	6.99167
23	0.32624E-02	0.33333E-02	0.62236	7.61403
24	0.34043E-02	0.34752E-02	0.64885	8.26288
25	0.35461E-02	0.36170E-02	0.67533	8.93821
26	0.36879E-02	0.37589E-02	0.70182	9.64003
27	0.38298E-02	0.39007E-02	0.72830	10.36832
28	0.39716E-02	0.40426E-02	0.75478	11.12311
29	0.41135E-02	0.41844E-02	0.78127	11.90437
30	0.42553E-02	0.43262E-02	0.80775	12.71212
31	0.43972E-02	0.44681E-02	0.83423	13.54635
32	0.45390E-02	0.46099E-02	0.86072	14.40707
33	0.46809E-02	0.47518E-02	0.88720	15.29427
34	0.48227E-02	0.48936E-02	0.91368	16.20795
35	0.49645E-02	0.50355E-02	0.94017	17.14812
36	0.51064E-02	0.51773E-02	0.96665	18.11477
37	0.52482E-02	0.53191E-02	0.99313	19.10791
38	0.53901E-02	0.54610E-02	1.01962	20.12753
39	0.55319E-02	0.56028E-02	1.04610	21.17363
40	0.56738E-02	0.57447E-02	1.07259	22.24621
41	0.58156E-02	0.58865E-02	1.09907	23.34528
42	0.59574E-02	0.60284E-02	1.12555	24.47083
43	0.60993E-02	0.61702E-02	1.15204	25.62287
44	0.62411E-02	0.63121E-02	1.17852	26.80139
45	0.63830E-02	0.64539E-02	1.20500	28.00639
46	0.65248E-02	0.65957E-02	1.23149	29.23788
47	0.66667E-02	0.67376E-02	1.25797	30.49585
48	0.68085E-02	0.68794E-02	1.28445	31.78030
49	0.69504E-02	0.70213E-02	1.31094	33.09124
50	0.70922E-02	0.71631E-02	1.33742	34.42866

51	0.72349E-02	0.73050E-02	1.36390	35.79257
52	0.73759E-02	0.74468E-02	1.39039	37.16295
53	0.75177E-02	0.75887E-02	1.41687	38.59983
54	0.76596E-02	0.77305E-02	1.44336	40.04318
55	0.78014E-02	0.78723E-02	1.46984	41.51392
56	0.79433E-02	0.80142E-02	1.49632	43.00934
57	0.80851E-02	0.81560E-02	1.52281	44.53215
58	0.82270E-02	0.82979E-02	1.54929	46.08144
59	0.83688E-02	0.84397E-02	1.57577	47.65721
60	0.85106E-02	0.85816E-02	1.60226	49.25947
61	0.86525E-02	0.87234E-02	1.62874	50.88821
62	0.87943E-02	0.88652E-02	1.65522	52.54343
63	0.89362E-02	0.90071E-02	1.68171	54.22514
64	0.90780E-02	0.91489E-02	1.70819	55.93333
65	0.92199E-02	0.92908E-02	1.73467	57.66801
66	0.93617E-02	0.94326E-02	1.76116	59.42917
67	0.95035E-02	0.95745E-02	1.78764	61.21681
68	0.96454E-02	0.97163E-02	1.81413	63.03093
69	0.97872E-02	0.98582E-02	1.84061	64.87154
70	0.99291E-02	0.10000E-01	1.86709	66.73864
71	0.10071E-01	0.10142E-01	1.89358	68.63221
72	0.10213E-01	0.10284E-01	1.92006	70.55227
73	0.10355E-01	0.10426E-01	1.94654	72.49882
74	0.10496E-01	0.10567E-01	1.97303	74.47184
75	0.10638E-01	0.10709E-01	1.99951	76.47136
76	0.10780E-01	0.10851E-01	2.02599	78.49735
77	0.10922E-01	0.10993E-01	2.05248	80.54983
78	0.11064E-01	0.11135E-01	2.07896	82.62879
79	0.11206E-01	0.11277E-01	2.10545	84.73423
80	0.11348E-01	0.11418E-01	2.13193	86.86616
81	0.11489E-01	0.11560E-01	2.15841	89.02457
82	0.11631E-01	0.11702E-01	2.18490	91.20947
83	0.11773E-01	0.11844E-01	2.21138	93.42085
84	0.11915E-01	0.11986E-01	2.23786	95.65871
85	0.12057E-01	0.12128E-01	2.26435	97.92306
86	0.12199E-01	0.12270E-01	2.29083	100.21339
87	0.12340E-01	0.12411E-01	2.31731	102.53120
88	0.12482E-01	0.12553E-01	2.34380	104.87500
89	0.12624E-01	0.12695E-01	2.37028	107.24528
90	0.12766E-01	0.12837E-01	2.39676	109.64205
91	0.12908E-01	0.12979E-01	2.42325	112.06529
92	0.13050E-01	0.13121E-01	2.44973	114.51593
93	0.13191E-01	0.13262E-01	2.47622	116.99124
94	0.13333E-01	0.13404E-01	2.50270	119.49394
95	0.13475E-01	0.13546E-01	2.52918	122.02312
96	0.13617E-01	0.13688E-01	2.55567	124.57879
97	0.13759E-01	0.13830E-01	2.58215	127.16094
98	0.13901E-01	0.13972E-01	2.60863	129.76957
99	0.14043E-01	0.14113E-01	2.63512	132.40469
100	0.14184E-01	0.14255E-01	2.66160	135.06629

REPRODUCIBILITY OF THE
ORIGINAL PAGE IS POOR

101	0.14326E-01	0.14397E-01	2.68808	137.75437
102	0.14468E-01	0.14539E-01	2.71457	140.46894
103	0.14610E-01	0.14681E-01	2.74105	143.20999
104	0.14752E-01	0.14823E-01	2.76753	145.97752
105	0.14894E-01	0.14965E-01	2.79402	148.77154
106	0.15035E-01	0.15106E-01	2.82050	151.59204
107	0.15177E-01	0.15248E-01	2.84699	154.43903
108	0.15319E-01	0.15390E-01	2.87347	157.31250
109	0.15461E-01	0.15532E-01	2.89995	160.21245
110	0.15603E-01	0.15674E-01	2.92644	163.13888
111	0.15745E-01	0.15816E-01	2.95292	166.09180
112	0.15887E-01	0.15957E-01	2.97940	169.07121
113	0.16028E-01	0.16099E-01	3.00589	172.07709
114	0.16170E-01	0.16241E-01	3.03237	175.10946
115	0.16312E-01	0.16383E-01	3.05885	178.16832
116	0.16454E-01	0.16525E-01	3.08534	181.25366
117	0.16596E-01	0.16667E-01	3.11182	184.36548
118	0.16738E-01	0.16809E-01	3.13830	187.50378
119	0.16879E-01	0.16950E-01	3.16479	190.66857
120	0.17021E-01	0.17092E-01	3.19127	193.85985
121	0.17163E-01	0.17234E-01	3.21776	197.07760
122	0.17305E-01	0.17376E-01	3.24424	200.32184
123	0.17447E-01	0.17518E-01	3.27072	203.59257
124	0.17589E-01	0.17660E-01	3.29721	206.88977
125	0.17730E-01	0.17801E-01	3.32369	210.21346
126	0.17872E-01	0.17943E-01	3.35017	213.56364
127	0.18014E-01	0.18085E-01	3.37666	216.94029
128	0.18156E-01	0.18227E-01	3.40314	220.34344
129	0.18298E-01	0.18369E-01	3.42962	223.77306
130	0.18440E-01	0.18511E-01	3.45611	227.22917
131	0.18582E-01	0.18652E-01	3.48259	230.71176
132	0.18723E-01	0.18794E-01	3.50908	234.22083
133	0.18865E-01	0.18936E-01	3.53556	237.75639
134	0.19007E-01	0.19078E-01	3.56204	241.31844
135	0.19149E-01	0.19220E-01	3.58853	244.90696
136	0.19291E-01	0.19362E-01	3.61501	248.52197
137	0.19433E-01	0.19504E-01	3.64149	252.16346
138	0.19574E-01	0.19645E-01	3.66798	255.83144
139	0.19716E-01	0.19787E-01	3.69446	259.52599
140	0.19858E-01	0.19929E-01	3.72094	263.24685
141	0.20000E-01	0.20071E-01	3.74743	266.99427
142	0.20142E-01	0.20213E-01	3.77391	270.76816
143	0.20284E-01	0.20355E-01	3.80039	274.56858
144	0.20426E-01	0.20496E-01	3.82688	278.39546
145	0.20567E-01	0.20638E-01	3.85336	282.24882
146	0.20709E-01	0.20780E-01	3.87985	286.12867
147	0.20851E-01	0.20922E-01	3.90633	290.03500
148	0.20993E-01	0.21064E-01	3.93281	293.96781
149	0.21135E-01	0.21206E-01	3.95930	297.92710
150	0.21277E-01	0.21348E-01	3.98578	301.91288

151	0.21418E-01	0.21489E-01	4.01226	305.92515
152	0.21560E-01	0.21631E-01	4.03875	309.96389
153	0.21702E-01	0.21773E-01	4.06523	314.02913
154	0.21844E-01	0.21915E-01	4.09171	318.12084
155	0.21986E-01	0.22057E-01	4.11820	322.23904
156	0.22128E-01	0.22199E-01	4.14468	326.38372
157	0.22270E-01	0.22341E-01	4.17116	330.55488
158	0.22411E-01	0.22482E-01	4.19765	334.75253
159	0.22553E-01	0.22624E-01	4.22413	338.97666
160	0.22695E-01	0.22766E-01	4.25062	343.22728
161	0.22837E-01	0.22908E-01	4.27710	347.50438
162	0.22979E-01	0.23050E-01	4.30358	351.80796
163	0.23121E-01	0.23191E-01	4.33007	356.13892
164	0.23262E-01	0.23333E-01	4.35655	360.49457
165	0.23404E-01	0.23475E-01	4.38303	364.87761
166	0.23546E-01	0.23617E-01	4.40952	369.28712
167	0.23688E-01	0.23759E-01	4.43600	373.72312
168	0.23830E-01	0.23901E-01	4.46248	378.18560
169	0.23972E-01	0.24043E-01	4.48897	382.67457
170	0.24113E-01	0.24184E-01	4.51545	387.19002
171	0.24255E-01	0.24326E-01	4.54193	391.73196
172	0.24397E-01	0.24468E-01	4.56842	396.30036
173	0.24539E-01	0.24610E-01	4.59490	400.89528
174	0.24681E-01	0.24752E-01	4.62139	405.51667
175	0.24823E-01	0.24894E-01	4.64787	410.16454
176	0.24965E-01	0.25035E-01	4.67435	414.83889
177	0.25106E-01	0.25177E-01	4.70084	419.53973
178	0.25248E-01	0.25319E-01	4.72732	424.26705
179	0.25390E-01	0.25461E-01	4.75380	429.02085
180	0.25532E-01	0.25603E-01	4.78029	433.80114
181	0.25674E-01	0.25745E-01	4.80677	438.60791
182	0.25816E-01	0.25887E-01	4.83325	443.44117
183	0.25957E-01	0.26028E-01	4.85974	448.30090
184	0.26099E-01	0.26170E-01	4.88622	453.18713
185	0.26241E-01	0.26312E-01	4.91271	458.09983
186	0.26383E-01	0.26454E-01	4.93919	463.03902
187	0.26525E-01	0.26596E-01	4.96567	468.00469
188	0.26667E-01	0.26738E-01	4.99216	472.99685
189	0.26809E-01	0.26879E-01	5.01864	478.01549
190	0.26950E-01	0.27021E-01	5.04512	483.06061
191	0.27092E-01	0.27163E-01	5.07161	488.13222
192	0.27234E-01	0.27305E-01	5.09809	493.23031
193	0.27376E-01	0.27447E-01	5.12457	498.35488
194	0.27518E-01	0.27588E-01	5.15106	503.50594
195	0.27660E-01	0.27730E-01	5.17754	508.68348
196	0.27801E-01	0.27872E-01	5.20402	513.88750
197	0.27943E-01	0.28014E-01	5.23051	519.11801
198	0.28085E-01	0.28156E-01	5.25699	524.37500
199	0.28227E-01	0.28298E-01	5.28348	529.65848
200	0.28369E-01	0.28440E-01	5.30996	534.96844

201	0.28511E-01	0.28592E-01	5.33644	540.30488
202	0.28652E-01	0.28723E-01	5.36293	545.66780
203	0.28794E-01	0.28865E-01	5.38941	551.05721
204	0.28936E-01	0.29007E-01	5.41589	556.47311
205	0.29078E-01	0.29149E-01	5.44238	561.91548
206	0.29220E-01	0.29291E-01	5.46886	567.38434
207	0.29362E-01	0.29433E-01	5.49534	572.87968
208	0.29504E-01	0.29574E-01	5.52183	578.40151
209	0.29645E-01	0.29716E-01	5.54831	583.94982
210	0.29787E-01	0.29858E-01	5.57479	589.52462
211	0.29929E-01	0.30000E-01	5.60128	595.12590
212	0.30071E-01	0.30141E-01	5.62776	600.75366
213	0.30213E-01	0.30284E-01	5.65425	606.40791
214	0.30355E-01	0.30426E-01	5.68073	612.08864
215	0.30496E-01	0.30567E-01	5.70721	617.79585
216	0.30638E-01	0.30709E-01	5.73370	623.52955
217	0.30780E-01	0.30851E-01	5.76018	629.28973
218	0.30922E-01	0.30993E-01	5.78666	635.07639
219	0.31064E-01	0.31135E-01	5.81315	640.88954
220	0.31206E-01	0.31277E-01	5.83963	646.72917
221	0.31348E-01	0.31418E-01	5.86611	652.59528
222	0.31489E-01	0.31560E-01	5.89260	658.48788
223	0.31631E-01	0.31702E-01	5.91908	664.40697
224	0.31773E-01	0.31844E-01	5.94556	670.35253
225	0.31915E-01	0.31986E-01	5.97205	676.32458
226	0.32057E-01	0.32128E-01	5.99853	682.32311
227	0.32199E-01	0.32270E-01	6.02502	688.34813
228	0.32340E-01	0.32411E-01	6.05150	694.39963
229	0.32482E-01	0.32553E-01	6.07798	700.47761
230	0.32624E-01	0.32695E-01	6.10447	706.58208
231	0.32766E-01	0.32837E-01	6.13095	712.71303
232	0.32908E-01	0.32979E-01	6.15743	718.87046
233	0.33050E-01	0.33121E-01	6.18392	725.05437
234	0.33191E-01	0.33262E-01	6.21040	731.26478
235	0.33333E-01	0.33404E-01	6.23688	737.50166

236	0.33475E-01	0.33546E-01	6.26337	743.76503
237	0.33617E-01	0.33688E-01	6.28985	750.05488
238	0.33759E-01	0.33830E-01	6.31634	756.37122
239	0.33901E-01	0.33972E-01	6.34282	762.71404
240	0.34043E-01	0.34113E-01	6.36930	769.08334
241	0.34184E-01	0.34255E-01	6.39579	775.47912
242	0.34326E-01	0.34397E-01	6.42227	781.90139
243	0.34468E-01	0.34539E-01	6.44875	788.35014
244	0.34610E-01	0.34681E-01	6.47524	794.82538
245	0.34752E-01	0.34823E-01	6.50172	801.32710
246	0.34894E-01	0.34965E-01	6.52820	807.85530
247	0.35035E-01	0.35106E-01	6.55469	814.40999
248	0.35177E-01	0.35248E-01	6.58117	820.99116
249	0.35319E-01	0.35390E-01	6.60765	827.59882
250	0.35461E-01	0.35532E-01	6.63414	834.23296
251	0.35603E-01	0.35674E-01	6.66062	840.89358
252	0.35745E-01	0.35816E-01	6.68711	847.58068
253	0.35887E-01	0.35957E-01	6.71359	854.29427
254	0.36029E-01	0.36099E-01	6.74007	861.03435
255	0.36170E-01	0.36241E-01	6.76656	867.80099
256	0.36312E-01	0.36383E-01	6.79304	874.59394
257	0.36454E-01	0.36525E-01	6.81952	881.41347
258	0.36596E-01	0.36667E-01	6.84601	888.25948
259	0.36738E-01	0.36809E-01	6.87249	895.13197
260	0.36879E-01	0.36950E-01	6.89897	902.03094
261	0.37021E-01	0.37092E-01	6.92546	908.95640
262	0.37163E-01	0.37234E-01	6.95194	915.90834
263	0.37305E-01	0.37376E-01	6.97842	922.88676
264	0.37447E-01	0.37518E-01	7.00491	929.89167
265	0.37589E-01	0.37660E-01	7.03139	936.92307
266	0.37730E-01	0.37801E-01	7.05788	943.98094
267	0.37872E-01	0.37943E-01	7.08436	951.06530
268	0.38014E-01	0.38085E-01	7.11084	958.17614
269	0.38156E-01	0.38227E-01	7.13732	965.31347
270	0.38298E-01	0.38369E-01	7.16381	972.47728
271	0.38440E-01	0.38511E-01	7.19029	979.66757

7200.,7050.,0.,163.65950,167.14162,00297
 PRF = 7200.

PULSE	TIME<SEC>	R/VG TIME<SEC>	PHASE SHIFT<DEG>	PHI TOTAL
1	0.13889E-03	0.20833E-03	0.03419	0.03419
2	0.27778E-03	0.34722E-03	0.05683	0.09092
3	0.41667E-03	0.48611E-03	0.07956	0.17048
4	0.55556E-03	0.62500E-03	0.10229	0.27277
5	0.69444E-03	0.76389E-03	0.12502	0.39778
6	0.83333E-03	0.90278E-03	0.14775	0.54553
7	0.97222E-03	0.10417E-02	0.17048	0.71601
8	0.11111E-02	0.11806E-02	0.19321	0.90922
9	0.12500E-02	0.13194E-02	0.21594	1.12516
10	0.13889E-02	0.14583E-02	0.23867	1.36383
11	0.15278E-02	0.15972E-02	0.26140	1.62523
12	0.16667E-02	0.17361E-02	0.28413	1.90936
13	0.18056E-02	0.18750E-02	0.30686	2.21622
14	0.19444E-02	0.20139E-02	0.32959	2.54581
15	0.20833E-02	0.21528E-02	0.35232	2.89814
16	0.22222E-02	0.22917E-02	0.37505	3.27319
17	0.23611E-02	0.24306E-02	0.39778	3.67097
18	0.25000E-02	0.25694E-02	0.42051	4.09149
19	0.26389E-02	0.27083E-02	0.44324	4.53473
20	0.27778E-02	0.28472E-02	0.46597	5.00071
21	0.29167E-02	0.29861E-02	0.48871	5.48941
22	0.30556E-02	0.31250E-02	0.51144	6.00085
23	0.31944E-02	0.32639E-02	0.53417	6.53501
24	0.33333E-02	0.34028E-02	0.55690	7.09191
25	0.34722E-02	0.35417E-02	0.57963	7.67154
26	0.36111E-02	0.36806E-02	0.60236	8.27399
27	0.37500E-02	0.38194E-02	0.62509	8.89899
28	0.38889E-02	0.39583E-02	0.64782	9.54680
29	0.40278E-02	0.40972E-02	0.67055	10.21735
30	0.41667E-02	0.42361E-02	0.69328	10.91063
31	0.43056E-02	0.43750E-02	0.71601	11.62664
32	0.44444E-02	0.45139E-02	0.73874	12.36538
33	0.45833E-02	0.46528E-02	0.76147	13.12686
34	0.47222E-02	0.47917E-02	0.78420	13.91106
35	0.48611E-02	0.49306E-02	0.80693	14.71799
36	0.50000E-02	0.50694E-02	0.82966	15.54765
37	0.51389E-02	0.52083E-02	0.85239	16.40005
38	0.52778E-02	0.53472E-02	0.87512	17.27517
39	0.54167E-02	0.54861E-02	0.89785	18.17302
40	0.55556E-02	0.56250E-02	0.92058	19.09361
41	0.56944E-02	0.57639E-02	0.94332	20.03692
42	0.58333E-02	0.59028E-02	0.96605	21.00297
43	0.59722E-02	0.60417E-02	0.98878	21.99175
44	0.61111E-02	0.61806E-02	1.01151	23.00325
45	0.62500E-02	0.63194E-02	1.03424	24.03749
46	0.63889E-02	0.64583E-02	1.05697	25.09446
47	0.65278E-02	0.65972E-02	1.07970	26.17415
48	0.66667E-02	0.67361E-02	1.10243	27.27658
49	0.68056E-02	0.68750E-02	1.12516	28.40174
50	0.69444E-02	0.70139E-02	1.14789	29.54963

51	0.70833E-02	0.71528E-02	1.17962	30.72025
52	0.72222E-02	0.72917E-02	1.19325	31.91360
53	0.73611E-02	0.74306E-02	1.21698	33.12968
54	0.75000E-02	0.75694E-02	1.23881	34.36849
55	0.76389E-02	0.77083E-02	1.26154	35.63004
56	0.77778E-02	0.78472E-02	1.28427	36.91431
57	0.79167E-02	0.79861E-02	1.30700	38.22131
58	0.80556E-02	0.81250E-02	1.32973	39.55105
59	0.81944E-02	0.82639E-02	1.35246	40.90351
60	0.83333E-02	0.84028E-02	1.37519	42.27870
61	0.84722E-02	0.85417E-02	1.39792	43.67663
62	0.86111E-02	0.86806E-02	1.42066	45.09728
63	0.87500E-02	0.88194E-02	1.44339	46.54067
64	0.88889E-02	0.89583E-02	1.46612	48.00679
65	0.90278E-02	0.90972E-02	1.48885	49.49563
66	0.91667E-02	0.92361E-02	1.51158	51.00721
67	0.93056E-02	0.93750E-02	1.53431	52.54152
68	0.94444E-02	0.95139E-02	1.55704	54.09856
69	0.95833E-02	0.96528E-02	1.57977	55.67833
70	0.97222E-02	0.97917E-02	1.60250	57.28083
71	0.98611E-02	0.99306E-02	1.62523	58.90605
72	0.10000E-01	0.10069E-01	1.64796	60.55402
73	0.10139E-01	0.10208E-01	1.67069	62.22471
74	0.10278E-01	0.10347E-01	1.69342	63.91813
75	0.10417E-01	0.10486E-01	1.71615	65.63428
76	0.10556E-01	0.10625E-01	1.73888	67.37316
77	0.10694E-01	0.10764E-01	1.76161	69.13477
78	0.10833E-01	0.10903E-01	1.78434	70.91912
79	0.10972E-01	0.11042E-01	1.80707	72.72619
80	0.11111E-01	0.11181E-01	1.82980	74.55599
81	0.11250E-01	0.11319E-01	1.85253	76.40853
82	0.11389E-01	0.11458E-01	1.87527	78.28379
83	0.11528E-01	0.11597E-01	1.89800	80.18179
84	0.11667E-01	0.11736E-01	1.92073	82.10252
85	0.11806E-01	0.11875E-01	1.94346	84.04597
86	0.11944E-01	0.12014E-01	1.96619	86.01216
87	0.12083E-01	0.12153E-01	1.98892	88.00108
88	0.12222E-01	0.12292E-01	2.01165	90.01272
89	0.12361E-01	0.12431E-01	2.03438	92.04710
90	0.12500E-01	0.12569E-01	2.05711	94.10421
91	0.12639E-01	0.12708E-01	2.07984	96.18405
92	0.12778E-01	0.12847E-01	2.10257	98.28662
93	0.12917E-01	0.12986E-01	2.12530	100.41192
94	0.13056E-01	0.13125E-01	2.14803	102.55995
95	0.13194E-01	0.13264E-01	2.17076	104.73071
96	0.13333E-01	0.13403E-01	2.19349	106.92421
97	0.13472E-01	0.13542E-01	2.21622	109.14043
98	0.13611E-01	0.13681E-01	2.23895	111.37933
99	0.13750E-01	0.13819E-01	2.26168	113.64106
100	0.13889E-01	0.13958E-01	2.28441	115.92548

101	0.14028E-01	0.14097E-01	2.30714	118.23262
102	0.14167E-01	0.14236E-01	2.32987	120.56250
103	0.14306E-01	0.14375E-01	2.35261	122.91510
104	0.14444E-01	0.14514E-01	2.37534	125.29044
105	0.14583E-01	0.14653E-01	2.39807	127.68851
106	0.14722E-01	0.14792E-01	2.42080	130.10930
107	0.14861E-01	0.14931E-01	2.44353	132.55283
108	0.15000E-01	0.15069E-01	2.46626	135.01909
109	0.15139E-01	0.15208E-01	2.48899	137.50808
110	0.15278E-01	0.15347E-01	2.51172	140.01979
111	0.15417E-01	0.15486E-01	2.53445	142.55424
112	0.15556E-01	0.15625E-01	2.55718	145.11142
113	0.15694E-01	0.15764E-01	2.57991	147.69103
114	0.15833E-01	0.15903E-01	2.60264	150.29397
115	0.15972E-01	0.16042E-01	2.62537	152.91935
116	0.16111E-01	0.16181E-01	2.64810	155.56745
117	0.16250E-01	0.16319E-01	2.67083	158.23828
118	0.16389E-01	0.16458E-01	2.69356	160.93184
119	0.16528E-01	0.16597E-01	2.71629	163.64814
120	0.16667E-01	0.16736E-01	2.73902	166.38716
121	0.16806E-01	0.16875E-01	2.76175	169.14891
122	0.16944E-01	0.17014E-01	2.78448	171.93340
123	0.17083E-01	0.17153E-01	2.80722	174.74061
124	0.17222E-01	0.17292E-01	2.82995	177.57056
125	0.17361E-01	0.17431E-01	2.85268	180.42323
126	0.17500E-01	0.17569E-01	2.87541	183.29864
127	0.17639E-01	0.17708E-01	2.89814	186.19678
128	0.17778E-01	0.17847E-01	2.92087	189.11765
129	0.17917E-01	0.17986E-01	2.94360	192.06124
130	0.18056E-01	0.18125E-01	2.96633	195.02757
131	0.18194E-01	0.18264E-01	2.98906	198.01663
132	0.18333E-01	0.18403E-01	3.01179	201.02842
133	0.18472E-01	0.18542E-01	3.03452	204.06294
134	0.18611E-01	0.18681E-01	3.05725	207.12019
135	0.18750E-01	0.18819E-01	3.07998	210.20017
136	0.18889E-01	0.18958E-01	3.10271	213.30288
137	0.19028E-01	0.19097E-01	3.12544	216.42832
138	0.19167E-01	0.19236E-01	3.14817	219.57650
139	0.19306E-01	0.19375E-01	3.17090	222.74740
140	0.19444E-01	0.19514E-01	3.19363	225.94103
141	0.19583E-01	0.19653E-01	3.21636	229.15740
142	0.19722E-01	0.19792E-01	3.23909	232.39649
143	0.19861E-01	0.19931E-01	3.26182	235.65832
144	0.20000E-01	0.20069E-01	3.28456	238.94287
145	0.20139E-01	0.20208E-01	3.30729	242.25016
146	0.20278E-01	0.20347E-01	3.33002	245.58017
147	0.20417E-01	0.20486E-01	3.35275	248.93292
148	0.20556E-01	0.20625E-01	3.37548	252.30840
149	0.20694E-01	0.20764E-01	3.39821	255.70661
150	0.20833E-01	0.20903E-01	3.42094	259.12754

151	0.20972E-01	0.21042E-01	3.44367	262.57121
152	0.21111E-01	0.21181E-01	3.46640	266.03761
153	0.21250E-01	0.21319E-01	3.48913	269.52674
154	0.21389E-01	0.21458E-01	3.51186	273.03860
155	0.21528E-01	0.21597E-01	3.53459	276.57319
156	0.21667E-01	0.21736E-01	3.55732	280.13051
157	0.21806E-01	0.21875E-01	3.58005	283.71056
158	0.21944E-01	0.22014E-01	3.60278	287.31335
159	0.22083E-01	0.22153E-01	3.62551	290.93886
160	0.22222E-01	0.22292E-01	3.64824	294.58710
161	0.22361E-01	0.22431E-01	3.67097	298.25808
162	0.22500E-01	0.22569E-01	3.69370	301.95176
163	0.22639E-01	0.22708E-01	3.71643	305.66821
164	0.22778E-01	0.22847E-01	3.73916	309.40738
165	0.22917E-01	0.22986E-01	3.76190	313.16927
166	0.23056E-01	0.23125E-01	3.78463	316.95390
167	0.23194E-01	0.23264E-01	3.80736	320.76126
168	0.23333E-01	0.23403E-01	3.83009	324.59134
169	0.23472E-01	0.23542E-01	3.85282	328.44416
170	0.23611E-01	0.23681E-01	3.87555	332.31971
171	0.23750E-01	0.23819E-01	3.89828	336.21799
172	0.23889E-01	0.23958E-01	3.92101	340.13900
173	0.24028E-01	0.24097E-01	3.94374	344.08274
174	0.24167E-01	0.24236E-01	3.96647	348.04921
175	0.24306E-01	0.24375E-01	3.98920	352.03841
176	0.24444E-01	0.24514E-01	4.01193	356.05034
177	0.24583E-01	0.24653E-01	4.03466	360.08500
178	0.24722E-01	0.24792E-01	4.05739	364.14239
179	0.24861E-01	0.24931E-01	4.08012	368.22252
180	0.25000E-01	0.25069E-01	4.10285	372.32537
181	0.25139E-01	0.25208E-01	4.12558	376.45095
182	0.25278E-01	0.25347E-01	4.14831	380.59927
183	0.25417E-01	0.25486E-01	4.17104	384.77031
184	0.25556E-01	0.25625E-01	4.19377	388.96408
185	0.25694E-01	0.25764E-01	4.21651	393.18059
186	0.25833E-01	0.25903E-01	4.23924	397.41983
187	0.25972E-01	0.26042E-01	4.26197	401.68179
188	0.26111E-01	0.26181E-01	4.28470	405.96649
189	0.26250E-01	0.26319E-01	4.30743	410.27392
190	0.26389E-01	0.26458E-01	4.33016	414.60408
191	0.26528E-01	0.26597E-01	4.35289	418.95696
192	0.26667E-01	0.26736E-01	4.37562	423.33258
193	0.26806E-01	0.26875E-01	4.39835	427.73093
194	0.26944E-01	0.27014E-01	4.42108	432.15201
195	0.27083E-01	0.27153E-01	4.44381	436.59582
196	0.27222E-01	0.27292E-01	4.46654	441.06236
197	0.27361E-01	0.27431E-01	4.48927	445.55163
198	0.27500E-01	0.27569E-01	4.51200	450.06363
199	0.27639E-01	0.27708E-01	4.53473	454.59836
200	0.27778E-01	0.27847E-01	4.55746	459.15582

201	0.27917E-01	0.27986E-01	4.58019	463.73602
202	0.28056E-01	0.28125E-01	4.60292	468.33894
203	0.28194E-01	0.28264E-01	4.62565	472.96459
204	0.28333E-01	0.28403E-01	4.64838	477.61298
205	0.28472E-01	0.28542E-01	4.67111	482.28499
206	0.28611E-01	0.28681E-01	4.69385	486.97794
207	0.28750E-01	0.28819E-01	4.71658	491.69451
208	0.28889E-01	0.28958E-01	4.73931	496.43382
209	0.29028E-01	0.29097E-01	4.76204	501.19585
210	0.29167E-01	0.29236E-01	4.78477	505.98062
211	0.29306E-01	0.29375E-01	4.80750	510.78812
212	0.29444E-01	0.29514E-01	4.83023	515.61835
213	0.29583E-01	0.29653E-01	4.85296	520.47131
214	0.29722E-01	0.29792E-01	4.87569	525.34699
215	0.29861E-01	0.29931E-01	4.89842	530.24541
216	0.30000E-01	0.30069E-01	4.92115	535.16656
217	0.30139E-01	0.30208E-01	4.94388	540.11044
218	0.30278E-01	0.30347E-01	4.96661	545.07706
219	0.30417E-01	0.30486E-01	4.98934	550.06640
220	0.30556E-01	0.30625E-01	5.01207	555.07847
221	0.30694E-01	0.30764E-01	5.03480	560.11327
222	0.30833E-01	0.30903E-01	5.05753	565.17081
223	0.30972E-01	0.31042E-01	5.08026	570.25107
224	0.31111E-01	0.31181E-01	5.10299	575.35406
225	0.31250E-01	0.31319E-01	5.12572	580.47979
226	0.31389E-01	0.31458E-01	5.14846	585.62824
227	0.31528E-01	0.31597E-01	5.17119	590.79943
228	0.31667E-01	0.31736E-01	5.19392	595.99335
229	0.31806E-01	0.31875E-01	5.21665	601.20999
230	0.31944E-01	0.32014E-01	5.23938	606.44937
231	0.32083E-01	0.32153E-01	5.26211	611.71148
232	0.32222E-01	0.32292E-01	5.28484	616.99632
233	0.32361E-01	0.32431E-01	5.30757	622.30389
234	0.32500E-01	0.32569E-01	5.33030	627.63419
235	0.32639E-01	0.32708E-01	5.35303	632.98721
236	0.32778E-01	0.32847E-01	5.37576	638.36298
237	0.32917E-01	0.32986E-01	5.39849	643.76147
238	0.33056E-01	0.33125E-01	5.42122	649.18269
239	0.33194E-01	0.33264E-01	5.44395	654.62664
240	0.33333E-01	0.33403E-01	5.46668	660.09332
241	0.33472E-01	0.33542E-01	5.48941	665.58273
242	0.33611E-01	0.33681E-01	5.51214	671.09488
243	0.33750E-01	0.33819E-01	5.53487	676.62975
244	0.33889E-01	0.33958E-01	5.55760	682.18736
245	0.34028E-01	0.34097E-01	5.58033	687.76769
246	0.34167E-01	0.34236E-01	5.60306	693.37076
247	0.34306E-01	0.34375E-01	5.62580	698.99655
248	0.34444E-01	0.34514E-01	5.64853	704.64508
249	0.34583E-01	0.34653E-01	5.67126	710.31634
250	0.34722E-01	0.34792E-01	5.69399	716.01032

251	0.34861E-01	0.34931E-01	5.71672	721.72704
252	0.35000E-01	0.35069E-01	5.73945	727.46649
253	0.35139E-01	0.35208E-01	5.76218	733.22867
254	0.35278E-01	0.35347E-01	5.78491	739.01358
255	0.35417E-01	0.35486E-01	5.80764	744.82122
256	0.35556E-01	0.35625E-01	5.83037	750.65159
257	0.35694E-01	0.35764E-01	5.85310	756.50469
258	0.35833E-01	0.35903E-01	5.87583	762.38052
259	0.35972E-01	0.36042E-01	5.89856	768.27938
260	0.36111E-01	0.36181E-01	5.92129	774.20038
261	0.36250E-01	0.36319E-01	5.94402	780.14440
262	0.36389E-01	0.36458E-01	5.96675	786.11115
263	0.36528E-01	0.36597E-01	5.98948	792.10064
264	0.36667E-01	0.36736E-01	6.01221	798.11285
265	0.36806E-01	0.36875E-01	6.03494	804.14780
266	0.36944E-01	0.37014E-01	6.05767	810.20547
267	0.37083E-01	0.37153E-01	6.08040	816.28588
268	0.37222E-01	0.37292E-01	6.10314	822.38902
269	0.37361E-01	0.37431E-01	6.12587	828.51488
270	0.37500E-01	0.37569E-01	6.14860	834.66348
271	0.37639E-01	0.37708E-01	6.17133	840.83481
272	0.37778E-01	0.37847E-01	6.19406	847.02886
273	0.37917E-01	0.37986E-01	6.21679	853.24565
274	0.38056E-01	0.38125E-01	6.23952	859.48517
275	0.38194E-01	0.38264E-01	6.26225	865.74741
276	0.38333E-01	0.38403E-01	6.28498	872.03239
277	0.38472E-01	0.38542E-01	6.30771	878.34010
278	0.38611E-01	0.38681E-01	6.33044	884.67054
279	0.38750E-01	0.38819E-01	6.35317	891.02371
280	0.38889E-01	0.38958E-01	6.37590	897.39961
281	0.39028E-01	0.39097E-01	6.39863	903.79824
282	0.39167E-01	0.39236E-01	6.42136	910.21960
283	0.39306E-01	0.39375E-01	6.44409	916.66370
284	0.39444E-01	0.39514E-01	6.46682	923.13052
285	0.39583E-01	0.39653E-01	6.48955	929.62007
286	0.39722E-01	0.39792E-01	6.51228	936.13235
287	0.39861E-01	0.39931E-01	6.53501	942.66737
288	0.40000E-01	0.40069E-01	6.55775	949.22511
289	0.40139E-01	0.40208E-01	6.58048	955.80559
290	0.40278E-01	0.40347E-01	6.60321	962.40879
291	0.40417E-01	0.40486E-01	6.62594	969.03473
292	0.40556E-01	0.40625E-01	6.64867	975.68340
293	0.40694E-01	0.40764E-01	6.67140	982.35479
294	0.40833E-01	0.40903E-01	6.69413	989.04892
295	0.40972E-01	0.41042E-01	6.71686	995.76578
296	0.41111E-01	0.41181E-01	6.73959	1002.50536
297	0.41250E-01	0.41319E-01	6.76232	1009.26768

PULSE	TIME(SEC)	AVG TIME(SEC)	PHASE SHIFT(DEG)	PHI TOTAL
1	0.14184E-03	0.21277E-03	0.03556	0.03556
2	0.28369E-03	0.35461E-03	0.05927	0.09483
3	0.42553E-03	0.49645E-03	0.08298	0.17781
4	0.56738E-03	0.63830E-03	0.10669	0.28450
5	0.70922E-03	0.78014E-03	0.13039	0.41489
6	0.85106E-03	0.92199E-03	0.15410	0.56699
7	0.99291E-03	0.10638E-02	0.17781	0.74680
8	0.11348E-02	0.12057E-02	0.20152	0.94832
9	0.12766E-02	0.13475E-02	0.22523	1.17355
10	0.14184E-02	0.14894E-02	0.24893	1.42248
11	0.15603E-02	0.16312E-02	0.27264	1.69512
12	0.17021E-02	0.17730E-02	0.29635	1.99147
13	0.18440E-02	0.19149E-02	0.32006	2.31153
14	0.19858E-02	0.20567E-02	0.34377	2.65530
15	0.21277E-02	0.21986E-02	0.36747	3.02277
16	0.22695E-02	0.23404E-02	0.39118	3.41396
17	0.24113E-02	0.24823E-02	0.41489	3.82885
18	0.25532E-02	0.26241E-02	0.43860	4.26745
19	0.26950E-02	0.27660E-02	0.46231	4.72975
20	0.28369E-02	0.29078E-02	0.48601	5.21577
21	0.29787E-02	0.30496E-02	0.50972	5.72549
22	0.31206E-02	0.31915E-02	0.53343	6.25892
23	0.32624E-02	0.33333E-02	0.55714	6.81606
24	0.34043E-02	0.34752E-02	0.58085	7.39691
25	0.35461E-02	0.36170E-02	0.60455	8.00146
26	0.36879E-02	0.37589E-02	0.62826	8.62972
27	0.38298E-02	0.39007E-02	0.65197	9.28169
28	0.39716E-02	0.40426E-02	0.67568	9.95737
29	0.41135E-02	0.41844E-02	0.69939	10.65676
30	0.42553E-02	0.43262E-02	0.72309	11.37986
31	0.43972E-02	0.44681E-02	0.74680	12.12666
32	0.45390E-02	0.46099E-02	0.77051	12.89717
33	0.46809E-02	0.47518E-02	0.79422	13.69139
34	0.48227E-02	0.48936E-02	0.81793	14.50932
35	0.49645E-02	0.50355E-02	0.84164	15.35095
36	0.51064E-02	0.51773E-02	0.86534	16.21629
37	0.52482E-02	0.53191E-02	0.88905	17.10534
38	0.53901E-02	0.54610E-02	0.91276	18.01810
39	0.55319E-02	0.56028E-02	0.93647	18.95457
40	0.56738E-02	0.57447E-02	0.96018	19.91475
41	0.58156E-02	0.58865E-02	0.98388	20.89863
42	0.59574E-02	0.60284E-02	1.00759	21.90622
43	0.60993E-02	0.61702E-02	1.03130	22.93752
44	0.62411E-02	0.63121E-02	1.05501	23.99253
45	0.63830E-02	0.64539E-02	1.07872	25.07124
46	0.65248E-02	0.65957E-02	1.10242	26.17367
47	0.66667E-02	0.67376E-02	1.12613	27.29980
48	0.68085E-02	0.68794E-02	1.14984	28.44964
49	0.69504E-02	0.70213E-02	1.17355	29.62319
50	0.70922E-02	0.71631E-02	1.19726	30.82044

51	0.72340E-02	0.73050E-02	1.22096	32.04140
52	0.73759E-02	0.74463E-02	1.24467	33.28608
53	0.75177E-02	0.75887E-02	1.26838	34.55446
54	0.76596E-02	0.77305E-02	1.29209	35.84654
55	0.78014E-02	0.78723E-02	1.31580	37.16234
56	0.79433E-02	0.80142E-02	1.33950	38.50184
57	0.80851E-02	0.81560E-02	1.36321	39.86505
58	0.82270E-02	0.82979E-02	1.38692	41.25197
59	0.83688E-02	0.84397E-02	1.41063	42.66260
60	0.85106E-02	0.85816E-02	1.43434	44.09694
61	0.86525E-02	0.87234E-02	1.45804	45.55498
62	0.87943E-02	0.88652E-02	1.48175	47.03673
63	0.89362E-02	0.90071E-02	1.50546	48.54219
64	0.90780E-02	0.91489E-02	1.52917	50.07136
65	0.92199E-02	0.92908E-02	1.55288	51.62424
66	0.93617E-02	0.94326E-02	1.57658	53.20082
67	0.95035E-02	0.95745E-02	1.60029	54.80111
68	0.96454E-02	0.97163E-02	1.62400	56.42511
69	0.97872E-02	0.98582E-02	1.64771	58.07282
70	0.99291E-02	0.10000E-01	1.67142	59.74424
71	0.10071E-01	0.10142E-01	1.69512	61.43936
72	0.10213E-01	0.10284E-01	1.71883	63.15820
73	0.10355E-01	0.10426E-01	1.74254	64.90073
74	0.10496E-01	0.10567E-01	1.76625	66.66698
75	0.10638E-01	0.10709E-01	1.78996	68.45624
76	0.10780E-01	0.10851E-01	1.81366	70.27060
77	0.10922E-01	0.10993E-01	1.83737	72.10798
78	0.11064E-01	0.11135E-01	1.86108	73.96906
79	0.11206E-01	0.11277E-01	1.88479	75.85385
80	0.11348E-01	0.11418E-01	1.90850	77.76234
81	0.11489E-01	0.11560E-01	1.93220	79.69455
82	0.11631E-01	0.11702E-01	1.95591	81.65046
83	0.11773E-01	0.11844E-01	1.97962	83.63008
84	0.11915E-01	0.11986E-01	2.00333	85.63341
85	0.12057E-01	0.12128E-01	2.02704	87.66045
86	0.12199E-01	0.12270E-01	2.05074	89.71119
87	0.12340E-01	0.12411E-01	2.07445	91.78564
88	0.12482E-01	0.12553E-01	2.09816	93.88380
89	0.12624E-01	0.12695E-01	2.12187	96.00567
90	0.12766E-01	0.12837E-01	2.14558	98.15125
91	0.12908E-01	0.12979E-01	2.16928	100.32053
92	0.13050E-01	0.13121E-01	2.19299	102.51353
93	0.13191E-01	0.13262E-01	2.21670	104.73023
94	0.13333E-01	0.13404E-01	2.24041	106.97064
95	0.13475E-01	0.13546E-01	2.26412	109.23475
96	0.13617E-01	0.13688E-01	2.28783	111.52258
97	0.13759E-01	0.13830E-01	2.31153	113.83411
98	0.13901E-01	0.13972E-01	2.33524	116.16935
99	0.14043E-01	0.14113E-01	2.35895	118.52830
100	0.14184E-01	0.14255E-01	2.38266	120.91096

101	0.14326E-01	0.14397E-01	2.49637	123.31732
102	0.14468E-01	0.14539E-01	2.43007	125.74740
103	0.14619E-01	0.14681E-01	2.45376	128.29118
104	0.14752E-01	0.14823E-01	2.47749	130.67867
105	0.14894E-01	0.14965E-01	2.50120	133.17986
106	0.15035E-01	0.15106E-01	2.52491	135.79477
107	0.15177E-01	0.15248E-01	2.54861	138.25338
108	0.15319E-01	0.15390E-01	2.57232	140.82570
109	0.15461E-01	0.15532E-01	2.59603	143.42173
110	0.15603E-01	0.15674E-01	2.61974	146.04147
111	0.15745E-01	0.15816E-01	2.64345	148.68492
112	0.15887E-01	0.15957E-01	2.66715	151.35207
113	0.16028E-01	0.16099E-01	2.69086	154.04293
114	0.16170E-01	0.16241E-01	2.71457	156.75750
115	0.16312E-01	0.16383E-01	2.73828	159.49578
116	0.16454E-01	0.16525E-01	2.76199	162.25776
117	0.16596E-01	0.16667E-01	2.78569	165.04346
118	0.16738E-01	0.16809E-01	2.80940	167.85286
119	0.16879E-01	0.16950E-01	2.83311	170.68597
120	0.17021E-01	0.17092E-01	2.85682	173.54279
121	0.17163E-01	0.17234E-01	2.88053	176.42331
122	0.17305E-01	0.17376E-01	2.90423	179.32755
123	0.17447E-01	0.17518E-01	2.92794	182.25549
124	0.17589E-01	0.17660E-01	2.95165	185.20714
125	0.17730E-01	0.17801E-01	2.97536	188.18259
126	0.17872E-01	0.17943E-01	2.99907	191.18156
127	0.18014E-01	0.18085E-01	3.02277	194.20434
128	0.18156E-01	0.18227E-01	3.04648	197.25082
129	0.18298E-01	0.18369E-01	3.07019	200.32101
130	0.18440E-01	0.18511E-01	3.09390	203.41491
131	0.18582E-01	0.18652E-01	3.11761	206.53251
132	0.18723E-01	0.18794E-01	3.14131	209.67383
133	0.18865E-01	0.18936E-01	3.16502	212.83885
134	0.19007E-01	0.19078E-01	3.18873	216.02758
135	0.19149E-01	0.19220E-01	3.21244	219.24002
136	0.19291E-01	0.19362E-01	3.23615	222.47616
137	0.19433E-01	0.19504E-01	3.25985	225.73602
138	0.19574E-01	0.19645E-01	3.28356	229.01958
139	0.19716E-01	0.19787E-01	3.30727	232.32685
140	0.19858E-01	0.19929E-01	3.33098	235.65783
141	0.20000E-01	0.20071E-01	3.35469	239.01251
142	0.20142E-01	0.20213E-01	3.37839	242.39091
143	0.20284E-01	0.20355E-01	3.40210	245.79301
144	0.20426E-01	0.20496E-01	3.42581	249.21882
145	0.20567E-01	0.20638E-01	3.44952	252.66834
146	0.20709E-01	0.20780E-01	3.47323	256.14157
147	0.20851E-01	0.20922E-01	3.49693	259.63859
148	0.20993E-01	0.21064E-01	3.52064	263.15914
149	0.21135E-01	0.21206E-01	3.54435	266.70349
150	0.21277E-01	0.21348E-01	3.56806	270.27155

151	0.21418E-01	0.21489E-01	3.59177	279.86332
152	0.21569E-01	0.21631E-01	3.61547	277.47879
153	0.21702E-01	0.21773E-01	3.63913	281.11797
154	0.21844E-01	0.21915E-01	3.66289	284.76086
155	0.21986E-01	0.22057E-01	3.68660	288.46746
156	0.22128E-01	0.22199E-01	3.71031	292.17777
157	0.22270E-01	0.22340E-01	3.73401	295.91179
158	0.22411E-01	0.22482E-01	3.75772	299.66951
159	0.22553E-01	0.22624E-01	3.78143	303.45094
160	0.22695E-01	0.22766E-01	3.80514	307.25608
161	0.22837E-01	0.22908E-01	3.82885	311.08493
162	0.22979E-01	0.23050E-01	3.85256	314.93748
163	0.23121E-01	0.23191E-01	3.87626	318.81374
164	0.23262E-01	0.23333E-01	3.89997	322.71371
165	0.23404E-01	0.23475E-01	3.92368	326.63739
166	0.23546E-01	0.23617E-01	3.94739	330.58478
167	0.23688E-01	0.23759E-01	3.97110	334.55588
168	0.23830E-01	0.23901E-01	3.99480	338.55068
169	0.23972E-01	0.24043E-01	4.01851	342.56919
170	0.24113E-01	0.24184E-01	4.04222	346.61142
171	0.24255E-01	0.24326E-01	4.06593	350.67734
172	0.24397E-01	0.24468E-01	4.08964	354.76698
173	0.24539E-01	0.24610E-01	4.11334	358.88032
174	0.24681E-01	0.24752E-01	4.13705	363.01737
175	0.24823E-01	0.24894E-01	4.16076	367.17813
176	0.24965E-01	0.25035E-01	4.18447	371.36259
177	0.25106E-01	0.25177E-01	4.20818	375.57077
178	0.25248E-01	0.25319E-01	4.23188	379.80265
179	0.25390E-01	0.25461E-01	4.25559	384.05825
180	0.25532E-01	0.25603E-01	4.27930	388.33755
181	0.25674E-01	0.25745E-01	4.30301	392.64056
182	0.25816E-01	0.25887E-01	4.32672	396.96727
183	0.25957E-01	0.26028E-01	4.35042	401.31770
184	0.26099E-01	0.26170E-01	4.37413	405.69183
185	0.26241E-01	0.26312E-01	4.39784	410.08966
186	0.26383E-01	0.26454E-01	4.42155	414.51121
187	0.26525E-01	0.26596E-01	4.44526	418.95647
188	0.26667E-01	0.26738E-01	4.46896	423.42543
189	0.26809E-01	0.26879E-01	4.49267	427.91810
190	0.26950E-01	0.27021E-01	4.51638	432.43448
191	0.27092E-01	0.27163E-01	4.54009	436.97457
192	0.27234E-01	0.27305E-01	4.56380	441.53837
193	0.27376E-01	0.27447E-01	4.58750	446.12587
194	0.27518E-01	0.27589E-01	4.61121	450.73709
195	0.27660E-01	0.27730E-01	4.63492	455.37201
196	0.27801E-01	0.27872E-01	4.65863	460.03063
197	0.27943E-01	0.28014E-01	4.68234	464.71297
198	0.28085E-01	0.28156E-01	4.70604	469.41901
199	0.28227E-01	0.28298E-01	4.72975	474.14876
200	0.28369E-01	0.28440E-01	4.75346	478.90222

201	0.28511E-01	0.28582E-01	4.77717	483.67939
202	0.28652E-01	0.28723E-01	4.80088	488.48027
203	0.28794E-01	0.28865E-01	4.82458	493.30485
204	0.28936E-01	0.29007E-01	4.84829	498.15314
205	0.29078E-01	0.29149E-01	4.87200	503.02515
206	0.29220E-01	0.29291E-01	4.89571	507.92086
207	0.29362E-01	0.29433E-01	4.91942	512.84027
208	0.29504E-01	0.29574E-01	4.94312	517.78339
209	0.29645E-01	0.29716E-01	4.96683	522.75023
210	0.29787E-01	0.29858E-01	4.99054	527.74077
211	0.29929E-01	0.30000E-01	5.01425	532.75502
212	0.30071E-01	0.30142E-01	5.03796	537.79298
213	0.30213E-01	0.30284E-01	5.06166	542.85464
214	0.30355E-01	0.30426E-01	5.08537	547.94002
215	0.30496E-01	0.30567E-01	5.10908	553.04910
216	0.30638E-01	0.30709E-01	5.13279	558.18188
217	0.30780E-01	0.30851E-01	5.15650	563.33838
218	0.30922E-01	0.30993E-01	5.18020	568.51859
219	0.31064E-01	0.31135E-01	5.20391	573.72250
220	0.31206E-01	0.31277E-01	5.22762	578.95012
221	0.31348E-01	0.31418E-01	5.25133	584.20145
222	0.31490E-01	0.31560E-01	5.27504	589.47649
223	0.31631E-01	0.31702E-01	5.29875	594.77523
224	0.31773E-01	0.31844E-01	5.32245	600.09769
225	0.31915E-01	0.31986E-01	5.34616	605.44385
226	0.32057E-01	0.32128E-01	5.36987	610.81371
227	0.32199E-01	0.32270E-01	5.39358	616.20729
228	0.32340E-01	0.32411E-01	5.41729	621.62457
229	0.32482E-01	0.32553E-01	5.44099	627.06557
230	0.32624E-01	0.32695E-01	5.46470	632.53027
231	0.32766E-01	0.32837E-01	5.48841	638.01868
232	0.32908E-01	0.32979E-01	5.51212	643.53079
233	0.33050E-01	0.33121E-01	5.53583	649.06662
234	0.33191E-01	0.33262E-01	5.55953	654.62615
235	0.33333E-01	0.33404E-01	5.58324	660.20940
236	0.33475E-01	0.33546E-01	5.60695	665.81635
237	0.33617E-01	0.33688E-01	5.63066	671.44701
238	0.33759E-01	0.33830E-01	5.65437	677.10137
239	0.33901E-01	0.33972E-01	5.67807	682.77944
240	0.34043E-01	0.34113E-01	5.70178	688.48122
241	0.34184E-01	0.34255E-01	5.72549	694.20671
242	0.34326E-01	0.34397E-01	5.74920	699.95591
243	0.34468E-01	0.34539E-01	5.77291	705.72881
244	0.34610E-01	0.34681E-01	5.79661	711.52543
245	0.34752E-01	0.34823E-01	5.82032	717.34575
246	0.34894E-01	0.34965E-01	5.84403	723.18978
247	0.35035E-01	0.35106E-01	5.86774	729.05752
248	0.35177E-01	0.35248E-01	5.89145	734.94897
249	0.35319E-01	0.35390E-01	5.91515	740.86412
250	0.35461E-01	0.35532E-01	5.93886	746.80298

251	0.35693E-01	0.35674E-01	5.96257	752.76555
252	0.35745E-01	0.35816E-01	5.98628	758.75182
253	0.35887E-01	0.35957E-01	6.00999	764.76181
254	0.36028E-01	0.36099E-01	6.03369	770.79550
255	0.36170E-01	0.36241E-01	6.05740	776.85291
256	0.36312E-01	0.36383E-01	6.08111	782.93401
257	0.36454E-01	0.36525E-01	6.10482	789.03883
258	0.36596E-01	0.36667E-01	6.12853	795.16736
259	0.36738E-01	0.36809E-01	6.15223	801.31960
260	0.36879E-01	0.36950E-01	6.17594	807.49554
261	0.37021E-01	0.37092E-01	6.19965	813.69519
262	0.37163E-01	0.37234E-01	6.22336	819.91855
263	0.37305E-01	0.37376E-01	6.24707	826.16561
264	0.37447E-01	0.37518E-01	6.27077	832.43639
265	0.37589E-01	0.37660E-01	6.29448	838.73087
266	0.37730E-01	0.37801E-01	6.31819	845.04906
267	0.37872E-01	0.37943E-01	6.34190	851.39095
268	0.38014E-01	0.38085E-01	6.36561	857.75656
269	0.38156E-01	0.38227E-01	6.38931	864.14587
270	0.38298E-01	0.38369E-01	6.41302	870.55890
271	0.38440E-01	0.38511E-01	6.43673	876.99563
272	0.38582E-01	0.38652E-01	6.46044	883.45607
273	0.38723E-01	0.38794E-01	6.48415	889.94022
274	0.38865E-01	0.38936E-01	6.50785	896.44807
275	0.39007E-01	0.39078E-01	6.53156	902.97964
276	0.39149E-01	0.39220E-01	6.55527	909.53490
277	0.39291E-01	0.39362E-01	6.57898	916.11388
278	0.39433E-01	0.39504E-01	6.60269	922.71657
279	0.39574E-01	0.39645E-01	6.62639	929.34296
280	0.39716E-01	0.39787E-01	6.65010	935.99306
281	0.39858E-01	0.39929E-01	6.67381	942.66688
282	0.40000E-01	0.40071E-01	6.69752	949.36440
283	0.40142E-01	0.40213E-01	6.72123	956.08562
284	0.40284E-01	0.40355E-01	6.74493	962.83056
285	0.40426E-01	0.40496E-01	6.76864	969.59921
286	0.40567E-01	0.40638E-01	6.79235	976.39156
287	0.40709E-01	0.40780E-01	6.81606	983.20761
288	0.40851E-01	0.40922E-01	6.83977	990.04738
289	0.40993E-01	0.41064E-01	6.86348	996.91085
290	0.41135E-01	0.41206E-01	6.88718	1003.79893
291	0.41277E-01	0.41348E-01	6.91089	1010.70892

APPENDIX D

This appendix derives the power patterns for the parabolic distribution discussed in section 4.4.3.

According to Silver (1965), the parabolic field distribution is given by

$$f(x) = 1 - (1-\Delta)x^2, \quad |x| < 1.$$

Its directivity pattern is given by

$$g(u) = \frac{a}{2} \int_{-1}^1 f(x) e^{jux} dx$$

where

a = over-all length of the aperture

$$u = \frac{\pi a}{\lambda} \theta$$

θ = angle measured from the normal to the aperture

x = normalized distance along the aperture $-1 \leq x \leq 1$.

Integrating,

$$g(u) = a \left[\frac{\sin u}{u} + (1-\Delta) \frac{d^2}{du^2} \left(\frac{\sin u}{u} \right) \right]$$

where

$$\frac{d^2}{du^2} \left(\frac{\sin u}{u} \right) = \frac{(2 - u^2) \sin u - 2u \cos u}{u^3}$$

The power pattern $g^2(u)$ must be normalized to 1. The limit of the first term as u goes to zero is

$$\lim_{u \rightarrow 0} \frac{\sin u}{u} = \lim_{u \rightarrow 0} \cos u = 1$$

by L'Hospital's rule. Applying the same rule to the second term

$$\begin{aligned}
 (1-\Delta) \lim_{u \rightarrow 0} \left[\frac{(2-u^2) \sin u - 2u \cos u}{u^3} \right] &= (1-\Delta) \lim_{u \rightarrow 0} \left(\frac{-u^2 \cos u}{3u^2} \right) \\
 &= (1-\Delta) \lim_{u \rightarrow 0} \left(\frac{u^2 \sin u - 2u \cos u}{6u} \right) \\
 &= (1-\Delta) \lim_{u \rightarrow 0} \left(\frac{u^2 \cos u + 4u \sin u - 2 \cos u}{6} \right) \\
 &= -\frac{1}{3} (1-\Delta).
 \end{aligned}$$

Therefore, a normalizing factor must be used at each Δ such that the magnitude of $g^2(u=0) = 1$.

$$g^2(u) = 1 = X \left[1 - \frac{1}{3} (1-\Delta) \right]^2$$

where $X =$ normalizing factor.

Then X is given by

$$X = \frac{1}{\left[1 - \frac{1}{3} (1-\Delta) \right]^2}$$

Normalizing factors are listed below for the values of Δ listed in the line source distribution table on page .

Δ	X
1.0	1.0
0.8	1.15
0.5	1.44
0	2.25

At the end of this appendix is an HP-25 calculator program used to plot $g^2(u) X$.

Using $\Delta = 0.4$ results in the distribution falling to its half power point at $U = 89.7^\circ$ (1.566 radians). For $\Delta = 0.4$, the normalizing factor $X = 1.563$. Since

$$u = \frac{\pi a}{\lambda} \theta$$

$$\theta = \frac{u\lambda}{\pi a}$$

$$B_h = 2\theta = \left(\frac{2u}{\pi}\right) \frac{\lambda}{a}$$

Substituting $u = 1.566$ radians,

$$B_h = 0.997 \frac{\lambda}{a}$$

which is quite close to the desired value of $1.0 \lambda/a$. The sidelobes are approximately 18.1 dB below the peak. The gain factor $G(\Delta)$ is given by

$$G(\Delta) = \frac{(2 + \Delta)^2}{9 \left[1 - \frac{2}{3} (1 - \Delta) + \frac{1}{5} (1 - \Delta)^2 \right]}$$

$$G(\Delta=0.4) = 0.952.$$

HP-25 Program To Plot

$$g^2(u) = \left[\frac{\sin u}{u} + (1-\Delta) \left[\frac{(2-u^2) \sin u - 2u \cos u}{u^3} \right] \right]^2$$

<u>STEP</u>	<u>INSTRUCTION</u>	<u>STEP</u>	<u>INSTRUCTION</u>
01	RCL 1	20	RCL 1
02	RCL 2	21	COS
03	X	22	X
04	STO 4	23	CHS
05	ENTER	24	RCL 6
06	3	25	+
07	$\frac{x}{y}$	26	RCL 5
08	STO 5	27	\div
09	2	28	RCL 3
10	RCL 4	29	X
11	x^2	30	STO 7
12	-	31	RCL 1
13	RCL 1	32	SIN
14	SIN	33	RCL 4
15	X	34	\div
16	STO 6	35	RCL 7
17	2	36	+
18	RCL 4	37	x^2
19	X	38	GO TO 00

INPUT:

STO 1 - INPUT ANGLE (DEG)

STO 2 - $\frac{\pi}{180}$ (RAD/DEG)

STO 3 - $1 - \Delta$

APPENDIX E

This appendix shows the power consumption calculations for the two processor configurations discussed in section 6.1.

Duty cycle, D , is defined as

$$D = \frac{\tau}{T}$$

where τ = length of pulse to be sampled

T = how often a pulse arrives at the sampling device (the repetition rate).

From Table 2, the longest pulse is approximately 69.5 μ sec. The repetition rate depends on the actual implementation for each device.

For the loop SAMs in the single channel configuration, the repetition rate is $\frac{1}{7200 \text{ Hz}}$ or 138.9 μ sec. $D = .5$ for this case. The buffers are operated every .03845 sec and the associated duty cycle is .00181.

In the pipeline approach, the pre-filter duty cycle is also .5 and the buffer duty cycle is also .00181. The loop SAMs run 20 times slower than the prefilters, hence, their repetition rate is $\frac{1}{360 \text{ Hz}}$ and their duty cycle is .025.

SINGLE CHANNEL CONFIGURATION

DRIVERS

LOOP SAMs (10 MHz)

$$\frac{2 \text{ SAMs on}}{\text{chan.}} \times 198 \text{ chan} \times \frac{1 \text{ pkg}}{17 \text{ SAMs}} = 24 \text{ drivers}$$

$$24 \text{ drivers @ } .5\text{W ea} = 12 \text{ W} \times \text{D} = \underline{6.00 \text{ W}}$$

BUFFER SAMs (8 MHz)

$$\frac{1 \text{ SAM on}}{\text{chan}} \times 198 \text{ chan} \times \frac{1 \text{ pkg}}{23 \text{ SAMs}} = 9 \text{ drivers}$$

$$9 \text{ drivers @ } .5\text{W ea} = 4.5 \text{ W} \times \text{D} = \underline{.008 \text{ W}}$$

SAMs

$$P_{\text{DC}} = \frac{4\text{mW}}{\text{SAM}} \times \left(\frac{26 \text{ SAMs (loop)} + 10 \text{ SAMs (buffer)}}{\text{chan}} \right) \times 198 \text{ chan}$$
$$= \underline{28.51 \text{ W}}$$

$$P_{\text{DC CLOCK}} = \frac{4\text{mW}}{\text{SAM}} \times \left(\frac{2 \text{ SAMs (loop) on} + 1 \text{ SAM (buffer) on}}{\text{chan}} \right)$$
$$\times 198 \text{ chan}$$
$$= \underline{2.38 \text{ W}}$$

$$P_{\text{TOTAL}} = \underline{36.90 \text{ W}}$$

PIPELINE CONFIGURATION

DRIVERS

LOOP SAMs (10 MHz)

2 SAMs on x 14 chan (pre-filters)

$$\times \frac{1 \text{ pkg}}{17 \text{ SAMs}} = 2 \text{ drivers}$$

$$2 \text{ drivers @ } .5 \text{ W ea} = 1 \text{ W} \times D = \underline{.5 \text{ W}}$$

2 SAMs on x 196 chan (loop)

$$\times \frac{1 \text{ pkg}}{17 \text{ SAMs}} = 24 \text{ drivers}$$

$$24 \text{ drivers @ } .5 \text{ W ea} = 12 \text{ W} \times D = \underline{.3 \text{ W}}$$

BUFFER SAMs (8 MHz)

$$\frac{1 \text{ SAM}}{\text{chan}} \text{ on } x 196 \text{ chan} \times \frac{1 \text{ pkg}}{23 \text{ SAMs}} = 9 \text{ drivers}$$

$$9 \text{ drivers @ } .5 \text{ W ea} = 4.5 \text{ W} \times D = \underline{.008 \text{ W}}$$

SAMs

$$P_{DC} = \frac{4\text{mW}}{\text{SAM}} \times \left(210 \text{ chan} \times \frac{26 \text{ SAMs}}{\text{chan}} + 196 \text{ chan} \times \frac{10 \text{ SAMs}}{\text{chan}} \right) \\ = \underline{29.68 \text{ W}}$$

$$P_{DC \text{ CLOCK}} = \frac{4\text{mW}}{\text{SAM}} \times \left(14 \text{ chan} \times \frac{2 \text{ SAMs}}{\text{chan}} \text{ on} + 196 \text{ chan} \times \frac{3 \text{ SAMs}}{\text{chan}} \text{ on} \right) \\ = \underline{2.46 \text{ W}}$$

$$P_{TOTAL} = \underline{32.95 \text{ W}}$$

REFERENCES

1. Claassen, John P., "A Short Study of a Scanning SAR For Hydrological Monitoring on a Global Basis," RSL Technical Report 295-1, Remote Sensing Laboratory, University of Kansas Center for Research, Inc., Lawrence, KS, September, 1975.
2. Erickson, Rodney L., "State of the Art Radar System Parameters," RSL Technical Memorandum 291-1, Remote Sensing Laboratory, University of Kansas Center for Research, Inc., Lawrence, KS, September, 1975.
3. Fong, Richard K. T., "Methods to Vary Elevation Look Angle Spacecraft SAR," RSL Technical Memorandum 295-4, Remote Sensing Laboratory, University of Kansas Center for Research, Inc., Lawrence, KS, January, 1976.
4. Harger, R. O., "Synthetic Aperture Radar Systems, Theory and Design," Academic Press, New York, 1970.
5. Jasik, Henry, ed., Antenna Engineering Handbook, McGraw-Hill, 1961.
6. Komen, Mark J., "Comb Filter Theory For Use In a Scanning Synthetic Aperture Radar Signal Processor (SCANSAR)," RSL Technical Memorandum 295-7, Remote Sensing Laboratory, University of Kansas Center for Research, Inc., Lawrence, KS, March, 1976.
7. Moore, R. K., "SLAR Image Interpretability - Tradeoffs Between Picture Element Divisions and Non-Coherent Averaging," RSL Technical Report 287-2, Remote Sensing Laboratory, University of Kansas Center for Research, Inc., Lawrence, KS, January, 1976.
8. Nathanson, Fred E., Radar Design Principles, McGraw-Hill, 1969.
9. Silver, S., ed., Microwave Antenna Theory and Design, Dover, 1965.
10. Skolnik, Merril, ed., Radar Handbook, McGraw-Hill, 1970.
11. Sponamore, T. E., Private Communication, Southwestern Bell Telephone Co., Kansas Area Headquarters, Topeka, KS., 1976.
12. Ulaby, F. T. and P. Batlivala, "Optimum Radar Parameters for Mapping Soil Moisture," *Geoscience Electronics*, Vol. GE-14, No. 2, April, 1976.
13. Westinghouse Electric Corporation, "Final Report - Spaceborne SAR Pilot Study," System Development Division, Baltimore, MD, April 11, 1974.

APPENDIX H
RSL TECHNICAL REPORT 295-3
VOLUME IV



THE UNIVERSITY OF KANSAS SPACE TECHNOLOGY CENTER
Raymond Nichols Hall

2291 Irving Hill Drive—Campus West Lawrence, Kansas 66045

Telephone:

A REVIEW OF SWATH-WIDENING TECHNIQUES

RSL Technical Memorandum 295-2
Remote Sensing Laboratory

Stan McMillan

January, 1976

Supported by:

NATIONAL AERONAUTICS AND SPACE ADMINISTRATION
Goddard Space Flight Center
Greenbelt, Maryland 20771

CONTRACT NAS 5-22384



REMOTE SENSING LABORATORY

ABSTRACT

Since snow, surface water and such are extremely changeable quantities, a revisit time of about 6 days is required for the water resources satellite. This short revisit time makes large swath widths necessary, but the swath width, about 400 km, is not attainable using a single antenna because length constraints imposed on a satellite mounted antenna make sufficient ambiguity suppression impossible. Multiple antenna systems are necessary, and the requirement of having non-interfering antenna returns must be considered. Using a technique of implementing a specific sequence of 180° phase shifts of the radar output pulses can effect suppression of ambiguous returns from the terrain adjacent to the imaged terrain, and antenna suppression can now occur in these adjacent regions which allows use of the maximum unambiguous swath, and increases the swath width by about 40%.

A REVIEW OF SWATH-WIDENING TECHNIQUES

Stan McMillan

1.0 Introduction

When considering the necessary parameters of a synthetic aperture radar (SAR) for the water resources mission, we must pay particular attention to the changeableness of the phenomenon we wish to measure, or monitor. Snow, soil moisture, surface water and such are greatly fluctuating quantities, and as such, the imaging of the terrain should be done relatively often.

The requirements of the mission are such that a revisit period of less than or equal to 6 days should be utilized with full coverage of the continental United States and Alaska. This requirement leads to the necessity of using very large swath widths, and this report is concerned with the various techniques of accomplishing large unambiguous swath widths, particularly by using either multiple antennas, an ambiguity suppression technique, or both.

2.0 SAR Theory

It is well known from SAR theory that tradeoffs are required with respect to pulse repetition frequency (PRF), and antenna pattern to minimize range and azimuth ambiguity.

Consider first the difficulty of eliminating ambiguity in the azimuth direction. Figure 1 shows a typical SAR geometry with the half power illumination cell shown. If we assume quadrature detection and processing, then the Nyquist sampling theorem shows that sampling must be done at greater than or equal to the Doppler bandwidth. Hence,

$$PRF \geq \frac{2v}{L}$$

v = satellite velocity (approximately 7 km/sec)

L = length of the physical antenna in the azimuth direction.

where equality would imply a sharp cutoff of the antenna beam at the 3 dB points for no ambiguity. This does not happen, and sampling at a rate of $2v/L$ would cause image degradation because the ambiguous return is only reduced 10 dB. In report GERA-1985 by Goodyear Aerospace Corporation it is maintained that a better selection would be

$$PRF = \frac{2.5 v}{L}$$

2

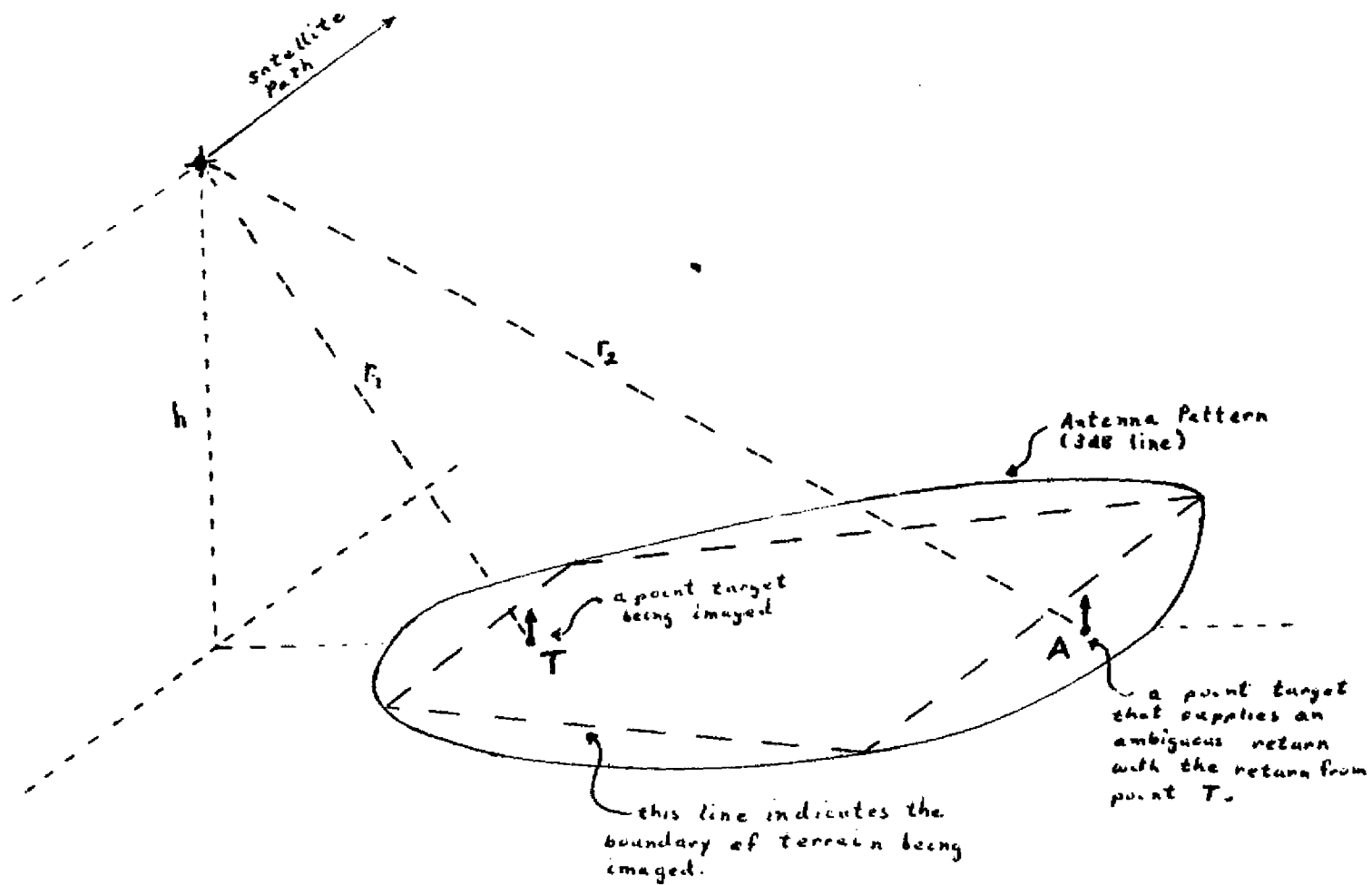


Figure 1.

because the azimuth ambiguity level is reduced about 20 dB after processing. By simply choosing a larger PRF the azimuth ambiguity level is reduced still farther, but unfortunately the sampled nature of azimuth data introduces ambiguity in the range direction.

Clearly, range information is contained in the fact that from a given pulse, different range elements produce returns at different times, but the pulsed nature of the radar signal makes it possible for two different cells sufficiently different radially from the antenna to yield returns at the same time. Hence, the return is ambiguous. The maximum unambiguous slant range that can be imaged is

$$\Delta R_{S\text{MAX}} = \frac{C}{2 \text{ PRF}}$$

but again the antenna pattern will not accommodate such a choice because the ambiguity is not sufficiently reduced. The Goodyear report again is referenced, and

$$\Delta R_S = \frac{.6 c}{2 \text{ PRF}} = \frac{.6 cL}{5 v}$$

An important point is how this slant range converts to unambiguous ground range, but this will be investigated in the next section.

c and v are or can be assumed constants, so that the only variable in the expression for unambiguous slant range is L the length of the antenna. This could be extremely important since by increasing L the swath width can be increased, but in space applications L is also constrained, so other techniques for increasing swath width are required.

3.0 Calculation of Ground Swath Width

Figure 2 is a somewhat distorted but diagrammatical illustration of the geometry for calculating the unambiguous ground range, ΔR_g . It is easily noted that $\Delta R_g = (\alpha_2 - \alpha_1)r$ where α_2 and α_1 are given in radians. Knowledge of the actual radar should allow us to have some idea of θ_1 and h , r is given, and ΔR_S can be calculated. The only unknowns of consequence are R , α_1 , and α_2 . From the law of sines and cosines the following expressions can be derived:

$$R = (r + h) \cos \theta_1 \sqrt{r^2 - (r + h)^2 (1 - \cos^2 \theta_1)}$$

$$\alpha_1 = \sin^{-1} \left[\frac{R \sin \theta_1}{r} \right]$$

$$\alpha_2 = \cos^{-1} \left[\frac{2r^2 + 2rh + h^2 - (R + R_S)^2}{2r(r + h)} \right]$$

The calculation of the ground swath is then completed by substituting into the formula noted earlier, $\Delta R_g = (\alpha_2 - \alpha_1)r$ where α_2 , and α_1 are in radians.

Another important quantity is the 3dB antenna beam width, β , where $\beta = (\theta_2 - \theta_1)$ and is approximately $\frac{\lambda}{H}$ where λ is the radar wavelength, and H is the vertical aperture height. θ_1 is given, and θ_2 can be easily calculated by the law of sines, and

$$\theta_2 = \text{SIN}^{-1} \left[\frac{r \sin \alpha_2}{R + \Delta R_g} \right].$$

Consequently, H can be calculated.

Sometimes the entire unambiguous swath is not required for imaging, and the ground swath is given. By suitable algebraic manipulations the preceding formulae can still be applied.

4.0 Swath Calculations for the Water Resources Mission

Table 1A and Table 1B give parameters of interest to the water resource mission. The altitudes specified are various altitudes that correspond to candidate 6 day coverage orbits ($R = 83, 85, \text{ and } 89$) as advanced in a memo dated January 30, 1975 by Joseph C. King. The other important parameter is θ antenna length in the azimuth direction as this directly affects the unambiguous slant range, and hence the unambiguous ground swath.

An examination of Table 1B gives some interesting information. With a guard band to reduce range ambiguity 20 dB or more we cannot attain a 400+ swath width would require an antenna on the order of 30 meters long in the azimuth dimension. Another interesting point is that for a height of 825 km, and a swath width of 254.3 km, we are covering angles from the nadir of 7° to 23.2° .

The point of these calculations and this memo is that 6 day coverage and reasonable antenna length necessitate the use of some sort of swath widening technique. The remainder of this report will delve into these techniques.

$r = 5500 \text{ km}$ $c = 3 \times 10^5 \text{ km/sec}$ $v = 7.5 \text{ km/sec}$

h (km)	825	725	540
R (km)	832	731	544.5
α_1 (radians)	.0184	.0162	.0121
θ_1 (degrees)	7	7	7

Table 1A: Relevant Parameters for Swath Width Determination at Different altitudes.

Antenna Length (azimuth)	R_S (km)	h = 825 km		h = 725		h = 540	
		α^2 (rad.)	Swath Width (km)	α^2 (rad.)	Swath Width (km)	α^2 (rad.)	Swath Width (km)
4 meters	19.2	.03553	94.2	.0339	92.9	.0281	88 km
8 meters	38.4	.04704	157.5	.04433	153.6	.03808	142.9 km
12 meters	57.6	.0564	209.2	.0531	203	.0462	187.6
16 meters	76.8	.0646	254.3	.0610	246.2	.0533	226.6

Table 1B: Swath Width Versus Antenna Length and Satellite Altitude.

5.0 Swath Width Widening

The problem of extending unambiguous swath width is not one with any easy solution, but any solution must be based on either having more than one radar imaging different terrain so that their respective swath widths are additive, or some technique must be implemented to distinguish between the returns from different pulses. Each technique has advantages and disadvantages which must be considered.

6.0 Multiple Antenna Systems

One possible way to extend the swath width is to use multiple antennas imaging different terrain. It is necessary though to have some way to discriminate between returns that are received by both antennas. Therefore, either the antenna patterns can not overlap or the operating frequencies must be slightly different so that the two terrains can be segregated.

First, consider a satellite radar where two antennas are used to image terrain on either side of the satellite track, between angles of 7° and 22° from the nadir. If the satellite altitude were 825 km and antenna lengths 16 meters, the swath width would be over 500 km. What more, since the antenna patterns are non-overlapping considerable savings in hardware can be accomplished because both antennas can operate at the same frequency. This would allow for only one system to generate pulses of high power microwave energy, where the energy would be divided and fed to the two antennas. The first stages of processing would, of course, need to be duplicated but if digital processing were used this technique would lend itself well to time multiplexing and perhaps a reduction in the required processor hardware.

Another interesting sidelight to this first proposed design is that the optimal range of angles for soil moisture and snow cover detection at X-band appear to be 7° to 22° and the radar would be imaging only within these angles. This may or may not be a considerable advantage, but only further research could answer that question.

Aside from the difficulties of satellite alignment and radar alignment that could be expected in any sidelooking radar system, one major problem opposes the use of imaging on both sides of the satellite track. This problem is satellite orbital considerations related to imaging the terrain.

For purposes of illustration consider Figure 3, which at first sight is pretty but meaningless. Certain facts are also required. The distance on the ground between the antenna patterns at -7° and 7° for a satellite at 825 km is about 220 km, and the unambiguous

swath width for each 16 meter antenna on the same satellite is 254 km. If we consider each strip in Figure 3 as 220 km wide, then a satellite track down the middle of strip B would image strips A and C. Figure 3 now becomes an instrument to illustrate the problems of picking the proper orbits to produce full coverage of the United States.

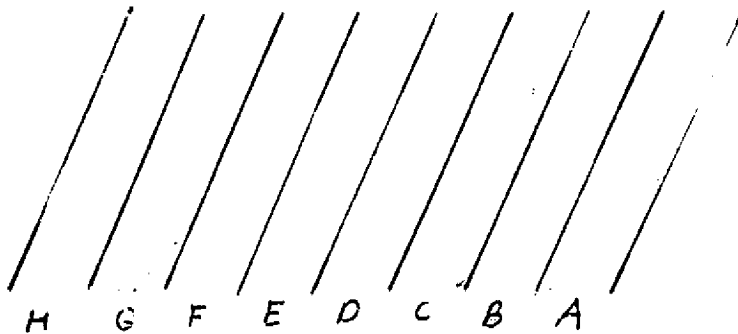


Figure 3. Earth Swathing Patterns.

Perhaps the most preferred orbital selection for earth sensing satellites is a minimum drift sun-synchronous orbit. This choice attempts to form continuous imaging across the terrain and would be realized by imaging A and C the first day and then B and D the next. Then problems arise since C would again be imaged on the third day effectively halving the swath width and eliminating any gain derived from the swath widening attempt. To image the terrain without repetition requires imaging A and C the first day, E and G the second, B and D the fourth, and F and H the fifth. Such an orbit would be possible, but it suffers from the necessity that 3 days separate the imaging of A and B and considerable changes in that general area could transpire in that time.

Another possible configuration for the SAR (Side-looking aerial radar) is to employ two antennas looking on the same side, or one antenna with dual feeds focussed at different terrains at different frequencies. The swath would add and be effectively continuous. This configuration would allow for the usage of a minimum drift orbit selection, which would provide for imaging adjacent strips on adjacent days. Unfortunately considerably more hardware would be needed to produce and amplify pulses at different frequencies. Another consideration is whether the needed information can be gained from the second radar that is focussed from approximately 22° to 35° . Sufficient information does not seem to be available to make an adequate evaluation of this point.

7.0 Ambiguity Suppression Techniques

As seen previously, the unambiguous swath width is directly related to the pulse repetition frequency since ambiguity implies that two different pulses travelling different paths are lending returns to the processor at the same time. Using the antenna beam alone to suppress the ambiguous return has been examined, but this necessitates using only about 60% of the unambiguous swath for imaging and retaining the remaining 40% to effect a guard band for ambiguity suppression. If it were possible to discriminate between the primary return and the first ambiguous return - that is, the return from the terrain adjacent to the unambiguous swath - by coding some sort of information on the radar pulses, then considerably more of the unambiguous swath could be imaged by allowing the antenna suppression bands to be located in the previously ambiguous swath.

Perhaps the simplest technique for effecting this return discrimination is by coding the proper pattern of phase shifts on the sequence of pulses leaving the radar. One workable pattern is as follows:

$$P_i(s, \phi_i) = \text{rect}\left(\frac{s}{S}\right) G \cos(\omega_c s + \phi_i)$$

where

$$\phi_i = \begin{cases} 0^\circ & \text{if } i = 4n \\ 180^\circ & \text{if } i = 4n + 1 \\ 180^\circ & \text{if } i = 4n + 2 \\ 0^\circ & \text{if } i = 4n + 3 \end{cases} \quad \text{where } n = 0, 1, 2, \dots$$

$P_i(s, \phi_i)$ = the i th pulse in the sequence of pulses.

$$\text{rect}\left(\frac{s}{S}\right) = \begin{cases} 1 & \text{if } -\frac{S}{2} \leq s \leq \frac{S}{2} \\ 0 & \text{if } \left|\frac{S}{2}\right| < |s| \end{cases}$$

S = the period of each pulse, a constant.

ω_c = the angular radian frequency of the carrier.

G = amplitude of the pulse, assumed constant.

s = the variable, time

As is easily seen, the only real difference between pulses is the phase function ϕ_i , and this is cyclical, every 4 pulses. It is important to show that this pattern will truly suppress the ambiguous return.

To illustrate the suppression of the ambiguous signal, the greatly simplified case of the two point targets shown in Figure 1 is used. Also, it is assumed that there is no arbitrary phase shift associated with reflection from the targets, that a single aperture of m pulses, where m is a multiple of 8, is processed by the simple processor of Figure 4, and that the synthetic aperture is processed for a uniformly illuminated aperture. Finally, it is assumed that the doppler phase change, θ_i , of a pulse P_i is the same for both targets across the aperture.

The returned voltage, V_R , to the antenna from the two point targets T and A of Figure 1 will be due to pulses P_i and P_{i-1} respectively, and be of the form

$$V_R = T \cos (\omega_c t + \theta_i + \phi_i) + A \cos (\omega_c t + \theta_{i-1} + \phi_{i-1})$$

where

ω_c and ϕ_i are as defined previously, and

θ_i = the doppler phase function associated with a pulse P_i

T, A = the return amplitude associated with the two point targets.

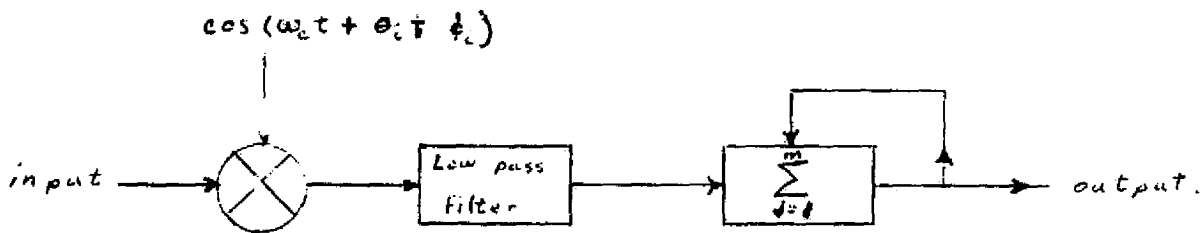


Figure 4.

If the returned voltage becomes the input to the processor of Figure 4, then after performing the multiplications, the low pass filterings, and the additions over the synthetic aperture, the voltage output, V_{out} , is

$$V_{out} = \sum_{i=1}^m T + \sum_{i=1}^m A [\cos (\theta_{i-1} - \theta_i + \phi_{i-1} - \phi_i)].$$

An examination of the function, ϕ_i , shows that there are four different cases for $(\phi_{i-1} - \phi_i)$. These are $(0^\circ - 0^\circ)$, $(0^\circ - 180^\circ)$, $(180^\circ - 180^\circ)$, and $(180^\circ - 0^\circ)$. The facts that $\cos(\alpha \pm 180^\circ) = -\cos \alpha$ and that $\sin(\alpha \pm 180^\circ) = \mp \sin \alpha$ allow us to write

$$V_{\text{out}} = \sum_{i=1}^m T + \sum_{i=1}^{m/2} A [\cos(\theta_{2i-2} - \theta_{2i-1}) - \cos(\theta_{2i-1} - \theta_{2i}) + \sin(\theta_{2i-2} - \theta_{2i-1}) - \sin(\theta_{2i-1} - \theta_{2i})].$$

It is significant that the phase function is very nearly a linear function across the aperture because then $\theta_i - \theta_{i-1} = \Delta\theta = \alpha$ constant. Upon substituting $\Delta\theta$ into the above equation, it is found that

$$V_{\text{out}} = \sum_{i=1}^m T + \sum_{i=1}^{m/2} A (\cos \Delta\theta - \cos \Delta\theta + \sin \Delta\theta - \sin \Delta\theta) = \sum_{i=1}^m T$$

The ambiguous response due to the reflection from point, A, has been suppressed, and only the deviation of the phase function from linearity introduces error in V_{out} due to the point, A.

Using this technique, it is not possible to image more than the calculated maximum unambiguous swath both because returns from imaged terrain would overlap, and because the antenna cannot transmit and receive simultaneously.

The sequence of phase shifts used above is also the simplest sequence possible because a simple alternation of phase gives rise to only negative terms in the summation from the ambiguous terrain rather than alternating terms, and the summation does not tend to zero.

8.0 Conclusions

If sufficiently large antennas could be utilized on a spacecraft, the required 400 km + swath width could be accomplished, but this would require an antenna length of 100 meters or so, which is hardly practical. In fact, an antenna length of about 19 meters is approximately what could be expected.

With an antenna length of 10 meters and using antenna suppression of ambiguous returns alone, 400 km swath widths could not be accomplished even using two antennae, but if a phase shifting ambiguity suppression technique is also implemented, the 10 meter antenna would provide approximately the unambiguous swath width of a 14 meter antenna, and from extrapolation, two antennas would image the desired terrain with a 6 day revisit time. In fact, two 10 meter antennae looking on the same side of the satellite track at different fre-

quencies could be expected to image a swath of approximately 430 km depending on the orbit selected.

It is important to remember that a multiple antenna system must be designed so that the return from one does not add an ambiguous return to the other.

An examination of the problem indicates that the radar would probably consist of two antennae at slightly different frequencies imaging terrain at different depression angles. Also, phase shifting ambiguity suppression would probably be used.

REFERENCES

1. Thompson, C. H., "Orbital Earth Resources Radar Program Definition Study," Goodyear report GERA 1985, NASA Contract NAS 5-21956, January, 1974.
2. Westinghouse Electric Corp., "Final Report Space-borne Synthetic Aperture Radar Pilot Study," NASA Contract NAS 5-21951, April 11, 1974.
3. Gerchberg, Ralph, "Synthetic Aperture Radar and Digital Processing," CRES Technical Report 177-10, University of Kansas Center for Research, Inc., September 1970.
4. King, Joseph C., "Water Resources EOS- Some Orbit Selection Considerations," January 30, 1975.

APPENDIX I

RSL TECHNICAL REPORT 295-3

VOLUME IV



**THE UNIVERSITY OF KANSAS SPACE TECHNOLOGY CENTER
Raymond Nichols Hall**

2291 Irving Hill Drive—Campus West Lawrence, Kansas 66045

Telephone:

SYNTHETIC APERTURE RADAR AND DIGITAL PROCESSING

**RSL Technical Memorandum 295-3
Remote Sensing Laboratory**

Stan McMillan

September, 1975

Supported by:

**NATIONAL AERONAUTICS AND SPACE ADMINISTRATION
Goddard Space Flight Center
Greenbelt, Maryland 20771**

CONTRACT NAS 5-22384

**INTERNAL WORKING PAPER
NOT FOR GENERAL
DISTRIBUTION**

ABSTRACT

On-board processing for spacecraft synthetic-aperture radars is an important goal for any system intended either for a worldwide mission or for a more restricted mission where telemetry bandwidth is not unlimited. Feasibility of constructing an on-board processor for a water-resources mission with 400 km swath has been considered for 1975 components, using the processor scheme proposed by Gerchberg (1970). With 20 m resolution the memory and speed requirements are so high that power consumption of 650 watts is indicated, but with 50 m resolution only 104 watts is calculated, and 100 m resolution only takes 26 watts. No attempt has been made to examine the improvements possible with more efficient algorithms than Gerchberg proposed.

SYNTHETIC APERTURE RADAR AND DIGITAL PROCESSING

Stan McMillan

1.0 Introduction

Imaging radars for space applications like the water resources mission are typically side looking synthetic aperture radars (SAR) because the synthetic aperture radar can achieve resolutions far finer than the actual antenna ground illumination pattern, but the resolution can only be accomplished at the expense of complicated processing of the return signal from the illumination area.

Figure 1 illustrates a typical SAR geometry. The satellite is travelling at a velocity v in the direction indicated, and at an altitude, h . The antenna beam is always perpendicular to the flight path at the satellite location, and the beam coverage area is assumed limited to the half-power points on the pattern. At time, $t = 0$, a point target is located along the line, $x = 0$, and at a radius from the satellite of r_j , and the radar emits high powered, extremely short pulses of radiation at some pulse repetition frequency (PRF), and at times, $t_{-m}, \dots, t_0, \dots, t_m$.

At time, $t = -T/2$, the point target enters the beam coverage area due to the motion of the satellite, and it remains in that area until time, $t = T/2$. That is, the point target contributed to the return to the radar during the period, T , that it was in the beam coverage area. At a time, t_j , a pulse of radiation is emitted; the velocity of light is finite, so the leading edge of the pulse arrives at r_i and starts back considerably before the pulse arrives at $r_j > r_i$, or $r_n > r_j$. We have a response due to all the elements at a varying range that is spread out in time, and hence we can distinguish between or resolve in range by partitioning the return in time, but there is poor resolution in azimuth.

To accomplish resolution in azimuth we must recognize that there is relative motion in the X -direction between the satellite and ground points, and that the relative velocity of this motion changes from positive (motion toward a point) to negative (motion away from the point). The relative velocity gives rise to a Doppler frequency shift which is different for different ground cells depending on their x coordinate respective to the satellite's position. Some sort of filter could then be used to eliminate returns from all but the desired azimuth cell, and resolution in the azimuth dimension could be accomplished.

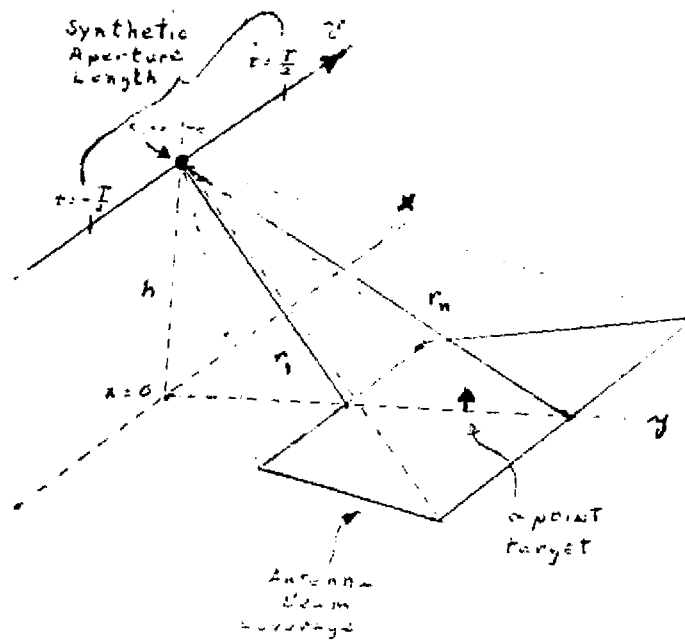


Figure 1 SAR Geometry

The problem of processing is somehow to take the time differences and frequency differences of different cells and obtain a set of numbers proportional to the amplitude of the reflected signal from each cell; or, in a different sense, to somehow effect the time and frequency partitioning.

Gerchberg (1970) approaches the problem of a real-time processor. Real-time implies that terrain can be mapped and images formed at the same rate. Gerchberg concluded that as of 1970 the technology did not exist to construct real-time processors because sufficient memory was not available to process the large amounts of data obtained from a SAR, and that power consumption would be far too great, but he projected that the technology would exist in 1975.

It is now 1975, and this report deals with whether Gerchberg's predictions on the advancement of technology were accurate, and whether his processor is now realizable, and applicable to the water resources mission.

This report deals with:

1. Gerchberg's ideas of a general SAR processor
2. Gerchberg's proposed processor including dimension estimates
3. Sample application of the processor to the water resources mission
4. State of the art assessment as of 1975.

After examining these topics the conclusion is reached that Gerchberg's idea of a truly parallel sub-aperture, non-quadrature processor is realizable using today's components, but that the requirements of the water resources mission are so stringent that power consumption and processor size remain problems for on-board processing. Nevertheless, the power required for a 50-meter-resolution processor is only a little over 100 watts, so such a processor can be used in a spacecraft having only modest available power.

2.0 The Generalized Processor

If noise were not a problem in SAR processing, a single filter looking only at each azimuth cell would suffice to image the terrain, but this is not the case. The information is severely effected by multipath fading, and as such, long integration time, look time, or equivalently many looks are required to remove the signal from the noise.

Figure 2, taken from Gerchberg, is a typical algorithm implemented for digital SAR processing. To illustrate the operation of this processor, suppose, first, that the range cells have already been separated by range gating and, second, that a point target is being imaged such as the point target at range, r_j , in figure 1.

$$S(t) = A \cos (w_c t + kt^2 + \phi)$$

$S(t)$ = return from the point target during the aperture period T

A = amplitude of the response

ϕ = a phase shift associated with reflection

The return during the illumination period from $t = -T/2$ to $t = T/2$ has an angular carrier frequency, the angular frequency from the radar, of w_c and a changing doppler shift, kt , which implies a linear frequency modulation of the carrier frequency. If we restrict the antenna to narrow horizontal beam widths, this is a very good approximation to the actual phase history.

The mixers and low pass filters indicated eliminate the carrier frequency, and the following outputs are found after the correlators:

$$A_1 = A (\overline{cc} \cos \phi - \overline{sc} \sin \phi)$$

$$A_2 = A (\overline{cs} \cos \phi - \overline{ss} \sin \phi)$$

$$B_2 = A (\overline{ss} \cos \phi + \overline{cs} \sin \phi)$$

$$B_1 = A (\overline{sc} \cos \phi + \overline{cc} \sin \phi)$$

where

$$\overline{ss} = \int \sin (kt^2) \sin k (t - \tau)^2 dt$$

$$\overline{cc} = \int \cos (kt^2) \cos k (t - \tau)^2 dt$$

$$\overline{cs} = \overline{sc} = \int \cos (kt^2) \sin k (t - \tau)^2 dt$$

and the integrals are from $-T/2 + \tau$ to $T/2$. Since the returns are not actually continuous but discrete, the integrals should be replaced by summations, and t by t_j $j = \{-m, \dots, m\}$ where m indicates the last return of the aperture and $-m$ the first, but for purposes of illustration the integrals will suffice.

A couple of interesting points are illustrated by the correlation integrals. The variable τ indicates the amount of mismatch between the reference function and the return signal. If the point target is being imaged, then $\tau = 0$, and \overline{ss} and \overline{cc} are maximized while $\overline{cs} = 0$. This corresponds to focusing the aperture on the point target.

Algorithm Employed With Quadrature Detection

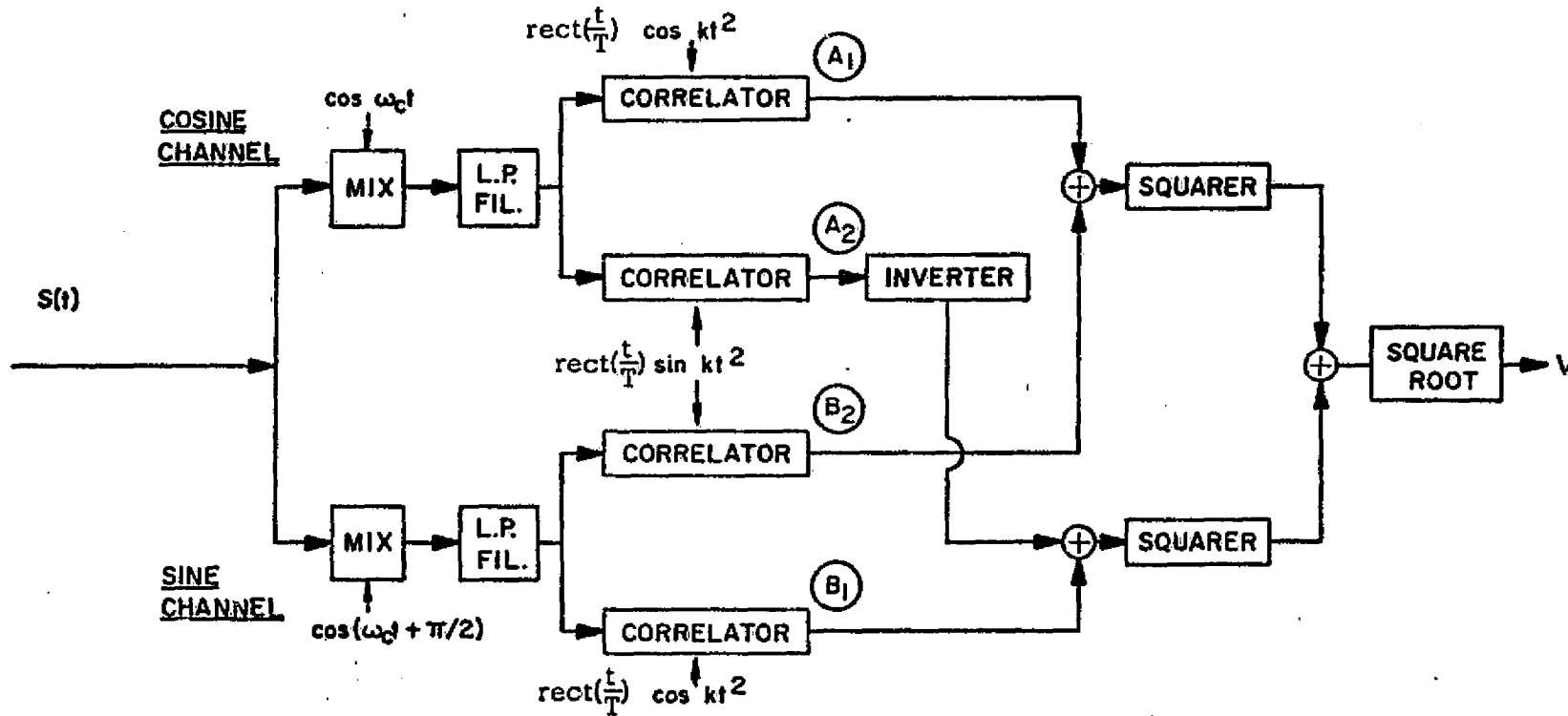


Figure 2

But, if τ is other than zero, then \overline{ss} and \overline{cc} are reduced and go to zero when

$$\cos kt^2 = \sin k(t - \tau)^2.$$

The correlators act in effect like tracking filters.

Finally, the output,

$$V_{\text{out}} = A (\overline{cc} + \overline{ss})$$

is of great significance because the phase angle, ϕ , has been eliminated, and the output is dependent only to the variable τ . Typically this dependence is in a $\frac{\sin x}{x}$ relation. This analysis shows simply that this detection scheme tends to maximize the return from the area of interest, and minimize the effect of targets distant from that area, and noise, since noise will also introduce a mismatch in the correlator. That is the desired effect.

3.0 Gerchberg's processor

The generalized algorithm could be implemented, and an area imaged, but Gerchberg felt that the generalized processor would require too much memory, and too many operations. In a typical space application he envisioned that 2,000 range cells could be required, and also 2,000 returns in an aperture. This would require 4 megacells of memory at the very least, and this would be for azimuth resolutions considerably finer than might be required in a given situation. Gerchberg's next problem was to reduce the amount of memory required while preserving sufficient information for imaging.

First, he considered the effect of just eliminating correlators, A_2 , B_2 , and B_1 without any compensation. It would have a desirable effect; memory would be halved; and the number of operations needed to perform the correlations would be quartered; but a price must be paid. Gerchberg, and later F. Dickey and J. Holtzman (Technical Memorandum 177-29) investigated this problem, and with the hypothesis of a Rayleigh-distributed target, the loss is a 3dB reduction in the mean-to-standard-deviation ratio. This would imply an increase in clutter level of the image and the image would tend to look grainy.

Another consideration is the fact that fully-focused, full-aperture processing resolves the terrain into azimuth cells considerably finer than required in most applications. This finer resolution can be used, and after processor averaging can reduce graininess and reduce the standard deviation by forming larger cells from the small resolution cells, but Gerchberg thought that it would be possible to process for the

TABLE V

Summary of Cycle Times and Storage Capacities for
Sub-Aperture Processing

SYSTEM PARAMETERS:

Doppler Bandwidth of Return Pulse	B
Time for point target in physical antenna beam	T
Radar system velocity	V_0
Finest Along-Track Resolution	V_0/B
Along-Track Resolution Degradation Factor	N
Image M/STD improvement factor due to processor averaging	\sqrt{G}
The largest number of non-overlapping sub-apertures possible in processing	N
Total number of subapertures employed in processing	G
Requantization degradation in M/STD	P (db, negative number)
The square root of the range of differential scattering cross sections to be imaged	R_v
Logarithmic quantum in the averaging stores	$\delta = 1 + 1.82\sqrt{e^{-.23P} - 1}$
Requantization bits	$B = \log_2 \left[\frac{\ln R_v}{\ln \delta} \right]$ raised to the next highest integer
Averaging store counter in bits	$C = \log_2 G$ raised to the next highest integer
Number of bits per word in working stores	L
Number of words in working stores per range bin	TB/N
Number of words in averaging stores per range bin	TBG/N ²
The total number of bits in working stores per range bin	TBL/N

TABLE V (CONT.)

The total number of bits in averaging stores per range bin	$(B+C)TBG/N^2$
The number of bits required in the cumulative summer	$2L + \log_2(TB/N)$
Number of words required in the buffer stores per range bin	N
Number of bits in buffer storage per range bin	NL

FOR SUB-APERTURE PROCESSING WITH SERIAL PROCESSING
IN EACH RANGE BIN:

Working store word maximum cycle time (same as multiplication time)	$N^2/(B^2TG)$
Averaging store word maximum cycle time	N/BG

desired cell size, and still enhance the image. For this purpose he developed a system of sub-aperture processing. The idea was simply to divide the aperture into a group of non-overlapping sub-apertures which could be squinted at each of the resolution cells that contribute to the return in that sub-aperture, and then the outputs of the sub-apertures non-coherently added to form the image of the cell. This would supply resolution to the proper size, and also, due to the non-coherent adding, supply image enhancement.

We now have an idea as to what Gerchberg's processor is like. It is a non-quadrature sub-aperture processor. Figure 3 and Table V taken from Gerchberg show the processor flow diagram and the parameters required for processing.

Referring to Figure 3, after the signal has been range gated, it must be changed to a digital output and stored in buffer storage. The number of bits required in the digital output is highly dependent on the dynamic range of the return. Gerchberg maintains that 5 bits is right for most applications, while John C. Kirk (1975) gives a technique for exactly determining the bit requirements.

When a complete sub-aperture has been entered into buffer memory, it is transferred to active memory and the correlation begins. The elements of the sub-aperture are multiplied by a set of reference functions corresponding to squinting at each of the resolution cells that the sub-aperture will resolve, and the element, reference-function products are summed for each squint angle. This number is then added to a number stored in a slow memory corresponding to the proper resolution cell. The cell is imaged when the proper number of sub-apertures have been added together and the resulting number is output to create the full image.

The logarithmic change is an effort to reduce the storage requirements again by reducing the number of bits required to represent a word. Directly performing the multiplications and sums indicated for this processor algorithm results in word lengths considerably longer than required to maintain the prescribed dynamic range. This was of significance to Gerchberg because a large saving in storage could be realized if fewer bits could be used to represent these words in the slow store. The logarithmic, and antilogarithmic changes illustrated in figure 3 are efforts to accomplish this saving.

A careful examination of Table V gives an idea of the parameters and requirements of the processor. Considerable use of this table will be made in the next section.

4.0 Application of Gerchberg's processor to the water resources problem

It is not immediately evident from Table V, whether a non-quadrature, sub-aperture real time, SAR processor could be constructed using today's technology. An

illustrative example using typical numbers drawn from the requirements of the water resources problem can give more readily understandable information.

Typical satellite and radar parameters are as follows:

altitude - 900 km

velocity - 7 km/sec

antenna configuration - two antennas imaging terrain on both sides of the satellite ground track

antenna length - 8 meters

carrier frequency - 10 GHz

pulse repetition frequency - the Doppler bandwidth - 1750 Hz

swath width/each antenna - 200 km*

azimuth beamwidth - 3.38 km

aperture time, T - .483 sec

resolution cell size - 20m, 50m, 100m

Since this is an example, completely accurate calculations will not be needed. It is assumed that all resolution cells are square and that the number of range resolution cells is just the swath width divided by the resolution cell size. Other important quantities are shown in Table II.

TABLE II

Resolution cell size	20 m	50 m	100 m
No. of azimuth cells across the antenna pattern	169	67	33
No. of range cells/side	10,000	4,000	2,000
No. of sub-apertures, N	5	12.5	25
Pulses per Sub-Aperture, $\frac{TB}{N}$	169	67	33
Sub-Aperture Completion Time	.0966 sec	0.386 sec	.0193 sec

* No attempt is made here to address the radar system problem of achieving this swath width. Ambiguity suppression techniques are the subject of another Technical Memorandum in this series.

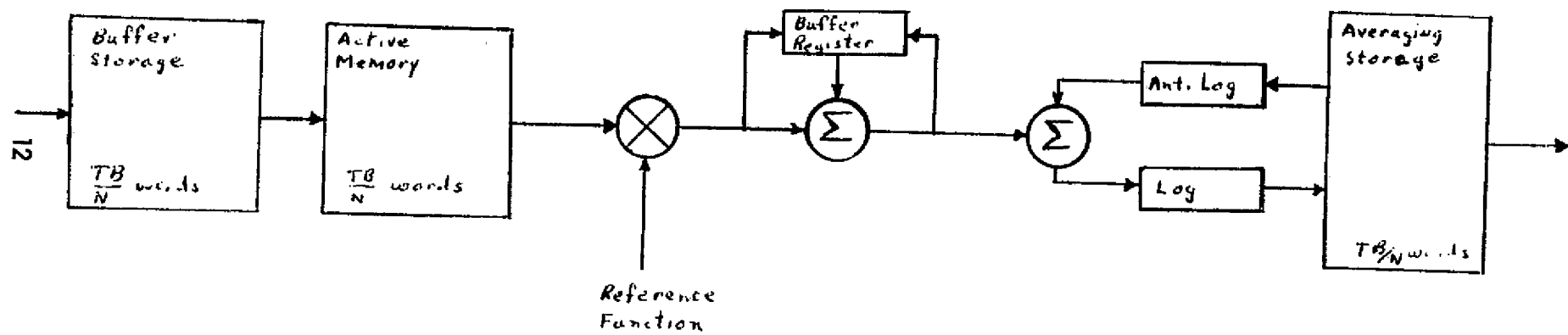


Figure 4

Figure 4 shows the author's conception of Gerchberg's processor as it might be implemented for a single range cell. All range cells are processed in parallel, and each antenna's return is processed separately - effectively here are two separate processors.

Each pulse from the radar gains information on the terrain within the antenna pattern, but each processor like that of Figure 4 can only use a portion of the continuous analog return and the processor must have the information in the form of a digital word. The return from the terrain is partitioned into a group of each signals corresponding to a range element, then converted from analog signals to digital words, and finally each word is assigned to the buffer storage of the processor corresponding to the proper range cell.

When the radar has completed a sub-aperture the buffer storage contains a word for each of the pulses that made up the sub-aperture, and these words are transferred to active storage for processing while another sub-aperture is being completed. From Table V, the number of words in working storage and hence the number of words needed in buffer storage, or the number of pulses per sub-aperture is given as $\frac{TB}{N}$ where T is the period of the complete aperture construction, (the time each ground cell receives illumination by the beam), B is the Doppler bandwidth of the signal, and N is the number of sub-apertures.

Sub-aperture processing requires that the sub-aperture be squinted at each of the azimuth cells within the physical antenna pattern of the sub-aperture, which requires that each word in the active storage be multiplied by a different reference function for each squint, and then that each of the word-reference-function products be summed to obtain a single number for each squint angle. There are $\frac{TB}{N}$ azimuth cells and $\frac{TB}{N}$ squint angles.

Successive sub-apertures are squinted at the same azimuth cell, and the processing of a sub-aperture is completed when the processor word corresponding to squinting at a particular azimuth cell is non-coherently added to a word corresponding to the summation of previous sub-apertures squinted at the same azimuth cell.

The total time, t_T , required to process a sub-aperture is as follows:

$$t_T = \frac{TB}{N} \left[\frac{TB}{N} (t_A + t_M + t_{S1}) + (t_Q + t_X + t_{S2}) \right] + t_B$$

t_A - time to acquire the word from active memory and also the reference function (assumed simultaneously)

t_M - time for a multiplication

t_{S1} - time for each of the first additions

t_Q - acquisition time and storage time

- t_X - time to take the antilog, and the log
- t_{S2} - time for each of the second additions
- t_B - time to move data from buffer to active memory.

In the next section we will investigate the state of the art as applies to these times. It is important to remember that all range cells are processed in parallel so this is the time to process a sub-aperture.

The memory requirements must take into account all the range elements, and also the fact that imaging is performed on both sides of the satellite. The buffer storage, and the active memory have been shown to require $\frac{TB}{N}$ words at L bits per word, and the averaging store needs $\frac{TB}{N}$ words at M bits per word. The total storage S_T is then

$$S_T = 2 \left[\frac{2TB}{N} (L) + \frac{TB}{N} (M) \right]. \text{ (Number of range elements).}$$

Gerchberg shows from his studies that for a 40 dB dynamic range in return $L=5$ is good enough, and that M should then be 9. Table III gives the memory requirements using the different cell sizes.

TABLE III

Res. cell size	20 m	50 m	100 m
Memory size	64 M bits	10.2 M bits	2.5 M bits
Buffer storage	16.9 M bits	2.68 M bits	660 K bits
Active memory	16.9 M bits	2.68 M bits	660 K bits
Averaging Storage	30.2 M bits	4.84 M bits	1.18 M bits

5.0 Device Performance

Gerchberg estimated the requirements for a 4.8 M bit processor in 1970, and decided that the equipment was not yet available to construct a processor but soon would be that would dissipate 10μ watts/bit and perform real time processing. He looked to the semiconductor memory as the most likely candidate and based his estimate on a 4 K RAM that Texas Instrument was developing at the time. 4 K RAM's are now available, and larger RAM's are in the planning stages, but other innovations such as CCD memories are now available which were not even considered in 1970.

One RAM that is available for building memories is a 1 K chip put out by INTERSIL, the IM6508A-1. It is a static RAM using CMOS technology. It has a worst case access time of 100 n sec and typical power dissipation of 9.8 μ watts/bit in the active mode.

On the bulk memory front, INTEL markets a 16 K CCD chip, the INTEL 2416 that has a maximum random access time of 64 microseconds, and power dissipations of 12.2 μ watts/bit, but data can be read in or out serially at a considerably higher rate, approximately 2 M bits/sec.

If we consider multiplication and addition units, then we have a choice of speed, or low power dissipation. From an examination of the requirements low power CMOS components seem to be applicable. As a typical example, the Motorola MC14008AL 4 bit full adder has quiescent power dissipation of 1 microwatt per package, and operation time of 170 n sec, and the Motorola MC14554AL 2 x 2 bit binary multiplier dissipates 100 n watts per package, typically, and performs an operation in 80 n sec.

From an examination of the literature, log and antilog chips do not seem to be available. In fact, they seem little called for, but also there is no doubt that they could be constructed or that memory look-ups could be accomplished if necessary. A conservative estimate of the function time and power dissipation of these chips assuming CMOS construction would be 10 microseconds to perform an operation, and 10 microwatts of power dissipated per package, but simple calculations would show that these times and powers do not greatly affect processor time or power dissipation.

Using these device parameters the total sub-aperture processing time can be calculated, and the processor power consumption estimated.

$$t_A = 100 \text{ n sec}$$

$$t_M = 200 \text{ n sec} \text{ The } 2 \times 2 \text{ bit multipliers must be combined to form a } 5 \times 5.$$

$$t_{S1} = 300 \text{ n sec. The adders must be combined to add 10 bits, but times of execution don't increase proportionately.}$$

$$t_Q = 200 \text{ n sec}$$

$$t_X = 20 \mu \text{ sec}$$

$$t_{S2} = 300 \text{ n sec}$$

$t_B = 70 \mu \text{ sec}$ t_B is the time needed to randomly access one location and serially address the rest. The CCD memory was assumed.

Table IV shows the results of both time calculations and power calculations

TABLE IV

Resolution cell size	20	50	100
Processing time per aperture	20.6 m sec	4.08 m sec	1.4 m sec
Power required	650 watts	104 watts	26 watts

The power calculations were performed assuming that in combining multipliers and adders to perform the computations necessary, about 10 microwatts per adder or multiplier would be dissipated. Also, the complete processor processing the entire 400 km swath width is considered.

6.0 Improvements in, and conclusions about, Gerchberg's processor

As is easily noticed, Gerchberg's processor is basically a brute strength processor using parallel processing to extremes. The times listed are extremely conservative estimates of processing time, but even from these estimates it is shown that time multiplexing to eliminate hardware could be easily accomplished. The savings of time multiplexing would be that, for a slight increase in control complexity, we would decrease the number of required parallel channels with a proportionate decrease in active memory.

An additional point to be considered is whether it is necessary to preserve all the bits available from the multiplication and addition processes. If little or no information is gained from saving these then additional savings might be possible by reducing the necessary averaging memory.

The important point of this report is that Gerchberg's conception of a real time processor appears realizable using today's technology. Main-frame semiconductor memories incorporating 1 k bit chips to form 1 megabit modules have been introduced, and advances are pushing access times and power consumption down.

The problem, as always, with SAR processing is the vast amount of data that must be used to image a terrain. The water resources mission puts some rather stringent requirements on any processor, and the purpose of much of Gerchberg's work was addressed to reducing the memory requirements. To this effect he proposed a non-quadrature sub-aperture processor, plus the idea that imaging does not require all of the sub-apertures for each resolution cell. The author of this report did not address himself to the last possibility. Still, even with an almost minimal memory requirement,

the memory to effect 20 meter resolution was tremendous, 64 megabits. Calculations show that such a processor would be possible but whether it is feasible is a matter for greater consideration. It does not appear feasible for an on board processor both because of size considerations, and because of power dissipation and the difficulty of handling the heat produced. On the other hand, on-board processing for 50 meter resolution seems possible, and it seems completely feasible for a 100 meter resolution cell size.

REFERENCES

1. Gerchberg, Ralph, "Synthetic Aperture Radar and Digital Processing," Technical Report 177-10 of the Center for Research Inc., Engineering Science Division, University of Kansas, September 1970.
2. Dickey, F. and J. Holtzman, "A Comparison of Quadrature and Non-Quadrature Imaging Radar Performance," Technical Memorandum 177-29, Center for Research Inc., University of Kansas, June 1972.
3. Kirk, John C., "A Discussion of Digital Processing in Synthetic Aperture Radar," IEEE Transactions on Aerospace and Electronic Systems, vol. AES-11, no. 3, May 1975.